[redacted]

FINAL REPORT

ARPA ORDER 3386
INTERNAL WAVE MEASUREMENT

Contract No.
N00140-77-C-6670

12 April 1977 - 31 October 1977

30 September 1977

SDL No. 77-6255

Prepared For:

NAVAL UNDERWATER SYSTEMS CENTER
New London, Connecticut 06320

SPECTRON
DEVELOPMENT
LABORATORIES
INC.

FINAL REPORT

ARPA ORDER 3386
INTERNAL WAVE MEASUREMENT

Contract No.
N00140-77-C-6670

12 April 1977 - 31 October 1977

30 September 1977

SDL No. 77-6255

Prepared For:

NAVAL UNDERWATER SYSTEMS CENTER
New London, Connecticut 06320

APPROVED FOR PUBLIC RELEASE
DISTRIBUTION UNLIMITED

SPECTRON DEVELOPMENT LABORATORIES INC.

3303 Harbor Boulevard, Suite G-3
Costa Mesa, California 92626 (714) 549-8477

TABLE OF CONTENTS

TABLE OF CONTENTS (CONT'D)

LIST OF FIGURES

LIST OF TABLES

1.0 INTRODUCTION

A laser velocimeter (LV) is a system which measures the velocity of a fluid by detecting the frequency of sinusoidal variations of laser light scattered by particles suspended in and moving with the fluid. Two types of remote backscatter systems have been developed for laboratory applications. The fringe or dual beam type LV system produces a sinusoidal interference pattern at the intersection of two crossed, focussed, coherent laser beams. A transverse velocity component is measured by the frequency of the particle crossing the projected fringes. A reference beam or optical heterodyne system is also possible in which the Doppler shift due to the axial velocity component of the scatterers is measured. Both types of systems are introduced in more detail with references in an OCEANS '77 paper reproduced in Appendix A. This paper was made possible by a combination of the work reported herein, a concurrent NAVSEA sponsored project (COURAGEOUS), and prior work by SDL in the LV area.

At the 2 September 1976 workshop on laser Doppler velocimetry held at IDA, Washington, D.C., ARPA expressed interest in using laser velocimetry systems for the measurement of internal waves and other small ocean velocity fluctuations. The conclusion of the meeting was that such measurements were probably achievable to the desired accuracy using a fringe LV system, but feasibility should be established by design experiment and analysis. This report describes the results of a study contract conducted by Spectron Development Laoboratories (SDL) during the time period April 13, 1977, to October 31, 1977, to address some of the critical issues. Stated in abbreviated form are work statement objectives:

Task 1

Perform analysis, simulation, and laboratory experiments concerning fringe LV accuracy in the ocean environments as related to small photon noise errors and small errors due to the presence of more than one particle in the probe volume (exclusive of random propagation effects).

Task 2

Develop system concept design and component requirements for optics, mechanics, and data collection electronics for flexible LV system capable of parametric evaluation of the critical design parameters after assembly and sea tests in FY78.

Task 3

Assess the nature of additional instrumentation and procedures which must be used simultaneously during FY78 sea tests of a completed LV system. Also assess the availability of adequate instrumentation at several Navy labs and other sources to determine what instrumentation is available and what should be constructed in FY78 in addition of the LV system itself.

The sections which follow document the work performed in meeting the contract objectives.

2.0 ERROR PREDICTION

The major effort under Task 1 was the development of predictive tools for multiparticle and photon noise errors. We summarize our developments here. The results of using the tools for system design and analysis are presented in a later section.

MULTIPARTICLE ERROR SIMULATION

The Problem

When two sinusoidal waveforms of the same frequency are added together, a third sinusoid of the same frequency results but with a new phase which is a function of the phases and amplitudes of the two component waveforms. When sinusoids with random Gaussian amplitude envelopes are added together randomly in time, the phase of the resulting amplitude modulated signal is also modulated. Variation of phase with time is equivalent to an instantaneous frequency shift which constitutes a velocity error to an electronic signal processor whose function it is to establish the instantaneous frequency (zero-crossing rate) of the signals. The statistics of these multiparticle errors depend on the average number of single-particle signals simultaneously (signal burst width times burst occurrence rate), on the probability distribution of the signal amplitudes and shapes, and on the ratio of system gain to the electronic threshold. These, in turn, depend on the optical and electronic system definition and parameters and the distribution of the backscatter amplitudes and volume number density of ocean scatterers.

It has been found that multiparticle phase errors are most severe at time locations in the composite signal where single-particle components cancel to nearly zero. These are also locations of poorest signal-to-noise ratio. One electronic technique which has been found to reduce velocity measurement errors is to require that the signal crosses an amplitude threshold in between every zero-crossing during a burst frequency measurement. Another technique which is often employed for noise and multiparticle error reduction is to separately measure the frequency from two adjacent or overlapping sections of signal and compare the measurements for agreement to within some small tolerance. Both of these techniques improve the system error statistics by simply rejecting measurements which do not pass the criteria. When one attempts to determine the statistics of the multiparticle errors purely analytically, the situation appears hopeless due to all the nonlinear functional dependence on random processes which are not even Gaussian in nature.

Simulation Software

Our approach to evaluating multiparticle errors is through simulation of the optical system, the physical scattering processes, the electronic burst-counter processor, and the data collection computer, all on a digital computer. A large part of the Task 1 effort consisted of writing and checking out the simulation programs OPTIC, COUNT, and COMP and the display programs HISTO and PLOT. These programs were used with the previously written program SIGNL in the design and evaluation of a 3 meter LV system described later.

The detailed description of all the software written under this contract is provided in Appendices B, C, and D. Appendix B describes the theory for the fringe LV option of the program OPTIC. The program OPTIC has, just at the time of writing of this report, been expanded under concurrent NAVSEA funding (Contract N66604-77-M-8709; Project COURAGEOUS) to include a reference beam option. The pertinent equations for both options are summarized using algebraic expressions but the FORTRAN variable names along with the entire program printout in Appendix C. More details concerning the theory for the reference-beam option is provided in the final report for the COURAGEOUS contract. Appendix D contains a detailed technical description of the simulation programs COUNT and COMP for an electronic burst counter processor and the required data acquisition operations. The appendix also includes brief descriptions of PLOT and HISTO and printouts of all these programs.

PHOTON NOISE PRODUCED ERRORS

Problem

A burst counter operates by measuring the time required for a prescribed number of positive (or negative) going zero crossings of the signal plus noise. The average period thus measured is inverted to obtain a frequency estimate $\hat{f}_i$. Because of the noise, $\hat{f}_i$ does not equal the frequency of the signal alone. There is both a mean error and an apparent turbulence due to the noise.

The reason for the fluctuation errors is easy to visualize. The noise perturbs the location of zero crossings so that for a finite number of cycles of signal, the jitter in time duration computes as a frequency jitter when there is none for the signal alone (or in addition to that of the signals).

The presence of an error in the mean frequency estimate is questionable for high signal-to-noise ratio signals and is quite dependent on the processor and problem definition. To clarify the problem, we refer to Figure 2-1. Adrian, et al[1] have used Rice's classical theory of mean level crossing rate to predict mean bias errors due to additive Gaussian noise. That the noise is Gaussian is a good approximation for high level signals; that it is additive (and stationary) is not necessarily a good approximation for non-stationary photon noise. The main problem, however, is that the Rice theory does not include "error rejection" circuits, so the predicted mean rates include missed and extra zero crossing events. For a long time average, if the noise did not add extra crossing or cause skips occasionally, the mean frequency would not be changed at all. Since we anticipate the use of circuits which reject signals with

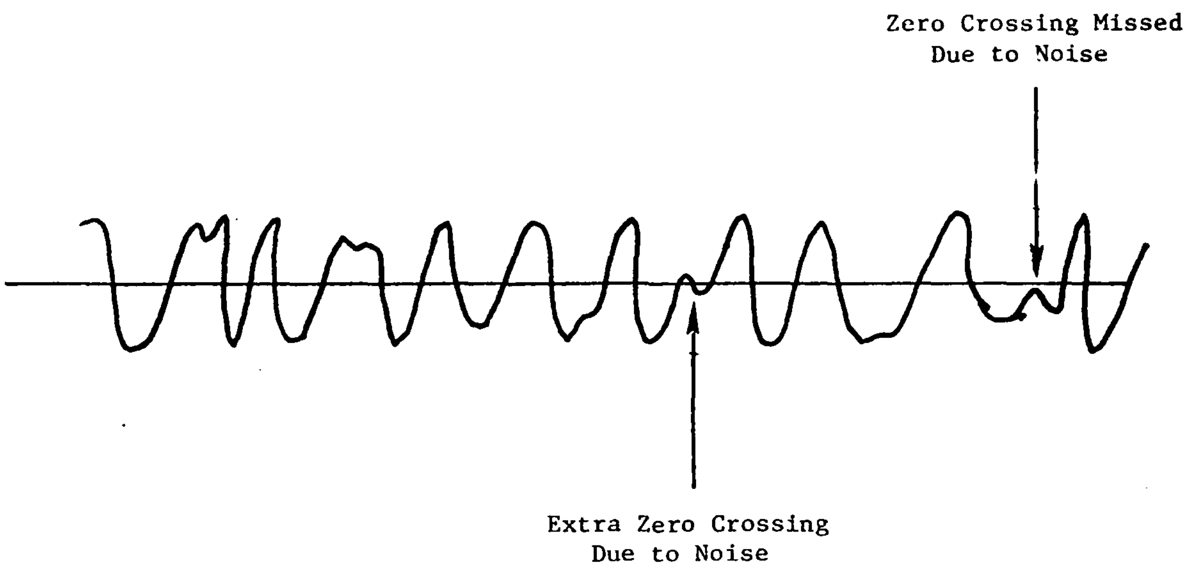

Figure 2-1. Sine Wave Plus Additive Noi~e.

skips and extra crossings, we do not anticipate valid results from the Rice theory quoted by Adrian. Also, he did not provide theory for rms deviation, since in an infinite time average measurement there isn't any deviation.

In another paper, Hösel and Rodi* have empirically studied errors for simulated LV signals with added non-stationary Gaussian noise. Their results are valid only for the counter and counter parameters they used, since no general theory was presented. Their results (see Appendix A) show that there is a noise dependent error in the mean. It would appear from their experiment definition that their counter circuits did not reject data with missed or extra zero crossings.

Dr. William K. George has developed a theory of LDV error rather extensively.** Unfortunately it assumes that there are many scatterers in the probe volume and uses Rice's theory for Gaussian signals. The most basic difficulty is the lack of inclusion of conditional statistics, given that threshold is exceeded.

We may summarize the problem rather simply. There does not appear to be any theory which treats the conditional problem that a high signal-to-noise ratio burst with no glitches is required for

---

* "Errors Occurring in LDA Measurements with Counter Signal Processing," in the Coppenhagen Conference Proceedings, 1975 (see Reference 1).

** The latest of many versions of this theory is reviewed in the Coppenhagen Conference Proceedings, 1975 (see Reference 1).

acceptance. Given these conditions it is not clear that the experimental evidence for mean bias is, in fact, appropriate. No papers have been located which treat the rms deviation both theoretically and experimentally for the conditional case. Thus, we must basically derive such results from the beginning.

Mean Bias

It is simple to demonstrate that interfering signals can alter the zero-crossing rate for signals above a threshold and in a manner which produces no glitches for a short period of time. Consider a "signal" cosine wave and a "noise" cosine wave

$$S(t) = \cos\,[(\omega_c + \Delta\omega)t]$$

$$n(t) = \cos\,[(\omega_c - \Delta\omega)t]$$

Then the sum $r(t) = S(t) + n(t)$ is given by trigonometric identity as (see Figure 2-2)

$$r(t) = 2\cos\Delta\omega t\cos\omega_c t$$

Thus if $\Delta\omega << \omega_c$, $\cos\Delta\omega t$ is an "envelope" amplitude modulation of a high frequency signal whose zero crossings are at a precise rate which is exactly half way between the "signal" frequency and the "noise" frequency.

In the Rice theory, the mean zero-crossing rate is pulled toward the mean crossing rate of the noise alone, slightly higher than the midpoint of the filter pass-band. We have demonstrated with the simple example above that even if glitches (skipped or added crossings)

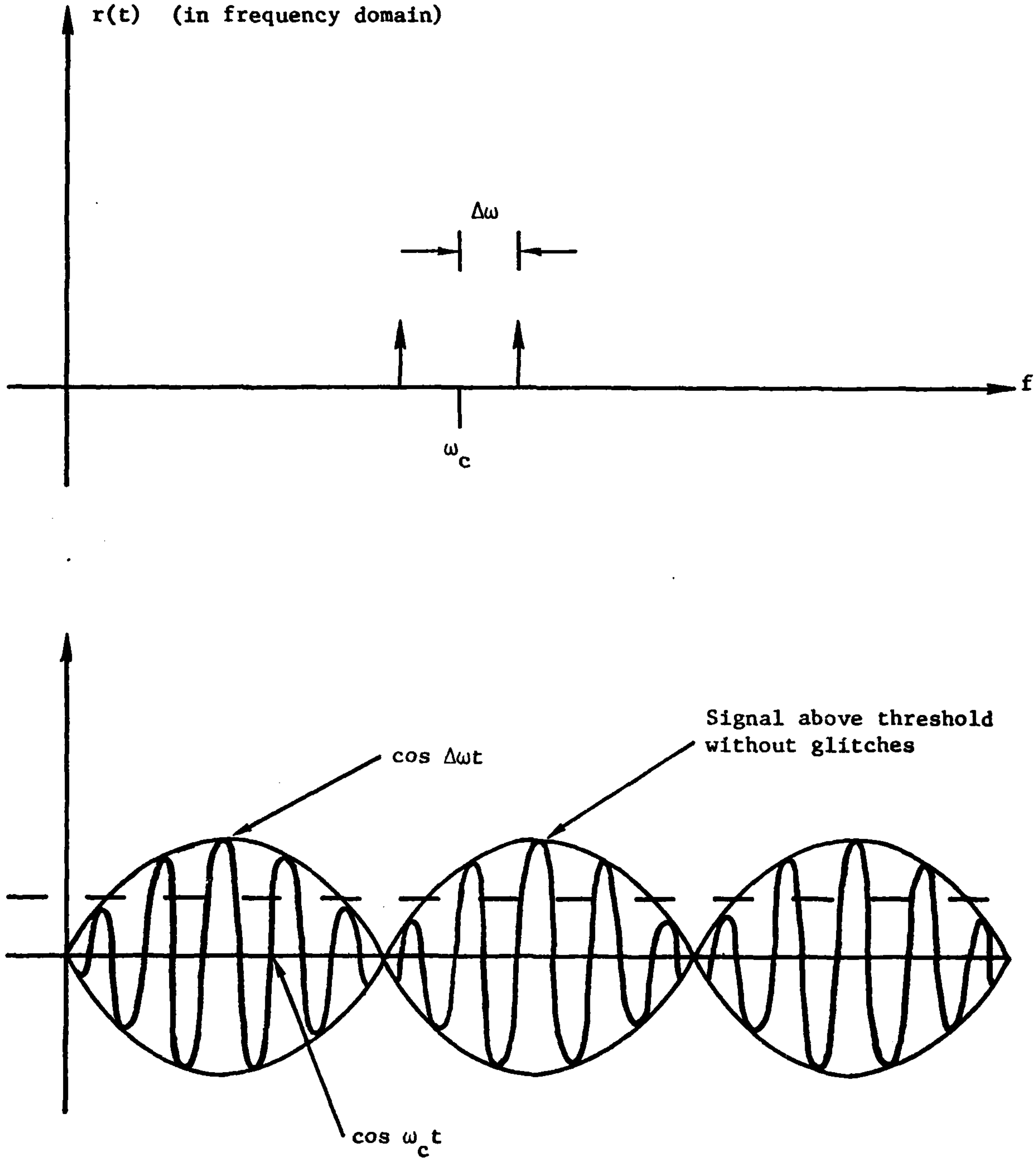

Figure 2-2. Illustration of Frequency "Pulling."

are excluded, the noise can "pull" the mean zero crossing rate. This result supports the Adrian, et al conclusion that a frequency tracker is required so that the noise band pass will always be centered on the signal, except for small deviation, and there will be no "pulling" bias by the noise. We interpret this to mean that the optimum detection system for classical signals must include a tracking filter, but this does not exclude burst-counter detection replacing the presently used phased lock loop techniques.* We conclude that with a properly designed system, mean bias is not a problem. Further study with simulation and/or experiment may be appropriate later.

RMS Fluctuations - Equivalent Turbulence

We have derived a general perturbational model for the fluctuation error which is presented in Appendix E. After many approximations, which are clearly detailed in the appendix, the result reduces to a formula which may be related to radio phase error theory. We obtain for the fractional rms error σ due to noise:

$$\sigma = \frac{1}{2\pi N \sqrt{S/N}}$$

where N = number of signal cycles counted.

$\sqrt{S/N} = \sqrt{a^2/2\langle n^2\rangle}$ = rms signal-to-noise ratio.

$S(t) = a \sin \omega t \Rightarrow a$ = amplitude of signal.

---

* The present techniques utilize analog control loops which could be replaced by digital control loops for increased precision, stability, and data recording reliability.

This formula assumes that the filter bandwidth is wide enough for the number of signal cycles counted so that the errors in zero crossing at the beginning and end are statistically independent. A more exact equation in terms of the autocorrelation function (inverse Fourier transform of frequency power spectrum) of the noise is also presented.

As an example of the order of magnitude of the predicted error, a voltage (rms $\sqrt{S/N}$) SNR of 10 and a 10 cycle average result in an rms error of $\sigma \approx 1/630$. This assumes the given SNR at both ends of the measurement.

Experimental Confirmation

The theory presented above was examined using a Macrodyne burst counter processor and an experimentally-produced simulated signal. The simulated signal consisted of the output of a photomultiplier tube excited by a light emitting diode (LED) that provided sinusoidal intensity modulation driven by a crystal controlled precision oscillator. A steady sinusoidal modulation, which could be removed, and a fixed DC offset level were applied to the LED. The rms value of the filtered output of the photomultiplier was measured with and without the sinusoidal component present. By squaring the results and subtracting to obtain the signal power, the signal-power to noise-power ratio was measured directly. The experiment and the results are described in detail in Appendix F.

It was not possible in the time available to have the processor modified to produce enough output bits to obtain more than three decimal digit precision of the output measurements. However, within the limitations of the dynamic range of the experiment, the simple error theory appears to be validated. There are transient filter effects which may be present for real short burst LV signals due to the non-stationarity of photon shot noise. For the present, however, we will use our simple theory as an upper bound on error due to noise under the assumption that one could do better with a processor that uses the zero crossings in the center of the burst where the "SNR" is higher than at the threshold location of the signal.

During the experiments, the light levels incident on the photo-multiplier tube were measured independently at high levels and reduced parametrically with a calibrated optical filter so that the measured SNR could be compared with that predicted by photomultiplier signal-to-noise ratio theory. The experimental SNR for the photomultiplier tube we were using was eight times less than predicted by simple theory without allowance for fudge factors. A discussion of these factors and the need for caution concerning photomultiplier tubes is also discussed in Appendix F.

MID TERM ACCURACY ASSESSMENT

After completing the checkout and debugging of the simulation software and the error prediction theory, we executed the software for a trial system design based on our best guesses using experience, hand calculator, and available data concerning the distribution of scattering particles. Our purpose in this "mid-term exam" was to provide a thorough demonstration of the software, to see if accuracies of $1:10^4$ could be obtained, and to obtain a baseline system performance before proceeding with a system design.

The particle model used in the mid-term runs assumed a complex index of refraction of 1.03-j0.01 after Brown and Gordon[2] with the intention of using a conservatively low index with small backscatter coefficients. After completion of that sequence of runs, COURAGEOUS computations[3] revealed that Brown and Gordon were using an opposite sign convention on the imaginary part of the index of refraction than is used in our Mie program. This made the backscatter amplitudes used in the mid-term runs approximately the same as would have been computed for mineral particles[3] with $n = 1.15+j0.0$.

Despite the fact that the error in index of refraction model produces better signals than the intended very conservative test case, and despite the fact that we have now added to OPTIC and slightly modified the output format since the mid term runs, we include the mid term results in Appendix G because the figures illustrate aspects of the software and parametric system performance (threshold setting effects) which were not repeated in such detail in later design runs.

Appendix G is a demonstration of the application of the error prediction and system design simulation tools we have developed under this contract for the satisfaction of Task 1. At the end of Appendix G we have added some material to that originally presented in the mid-term calculations. The added material consists of running OPTIC for an additional random set of 1000 particle size realizations to determine how representative the simulations are when only 1000 scatterers are used. The results indicate (as we would expect) that repeatability is not obtained at the largest particle (signal) sizes since there are only a few particles near 10 micrometers in diameter expected according to theory. We expect that our design results in the next section are representative and that uncertainties in the particle index of refraction models are more significant than the statistical stability of the simulations.

3.0 LASER VELOCIMETER DESIGN

This section considers the design of a fringe LV system which, through signal averaging, should be capable of attaining $1:10^4$ velocity accuracy with a range of 3 meters exclusive of any propagation limitations which may be present. We have chosen 3 meters for our design because the 2 meter probable range requirement of the Sept. 1976 ARPA workshop was not at all firm and 3 meters seems like a more conservative objective.

Before proceeding, we point out that although it is somewhat more difficult to attain high single-particle signal-to-noise ratios with a reference beam LV system, the COURAGEOUS program has demonstrated theoretically, by laboratory demonstration, and recently by simulation[3], that reference beam systems are possible for ranges to greater than 3 meters. Such systems measure axial velocity components normal to the direction of those measured by a fringe system and with much more frequency (velocity) sensitivity. The measurement of such additional components could assist in cancellation of vehicle motion or could even provide a better measure of the desired quantities than the fringe system. In light of the recent simulation showing that single-particle reference beam signal amplitudes can, in principle, be made equal to or larger than fringe system signals by increasing the diameter of the transmitter (and equivalent reference) beams, such systems should not be neglected from future considerations once more data concerning backscatter signal amplitudes and propagation limitations are known.

In this section we report three aspects of the design of a 3 meter fringe LV system. These are; first, a set of parametric performance simulation results using the tools developed under Task 1. The second aspect is one specific optical design approach which could be used in the FY78-FY79 sea tests. The last aspect is a set of recommendations regarding optics mechanics, electronics, and data acquisition approaches and components.

OPTICAL SYSTEM PARAMETRIC DESIGN

Many of the general optical system parameters for an LV system are generic and somewhat independent of the practical method of implementation. The parameters include laser power, transmitter beam diameter, beam separation, wavelength, receiver collector area, detector sensitivity, transmission efficiency, and others. It is truly pointless to consider the components for realization of the generic system until some measure of performance assures one that success may be possible; on the other hand, a practical sense of what components and tolerances are reasonably realizable quickly limits the range of parameters to be considered. An iterative design process thus takes place between the limits of practical components and the more unrestrained parametric optimization. The number and complexity of interaction of the parameters has been what kept the business of LV system design a black art. We hope that the simulation software will assist us in turning this art into a science.

We have used calculator computations and experience in establishing the mid-term 2 meter range baseline design reported in the previous section. We have examined the results and selected two trial cases of optical system parameters for a 3 meter system. In order to bracket the performance predictions with respect to the expected variability of the number of scatterers and the unknown scatterer composition (index of refraction), we have selected 2000 and 20,000 particles per cc and indices n = 1.03 and 1.15 as bracketing parameters.

The system parameters are reproduced in Table 3-1. The performance simulation results for these cases are reported in Appendix H. We may summarize the results by saying that if any appreciable fraction of the scatters in the range 5-10 μm are inorganic with index of refraction 1.15-1.20, then we have no signal amplitude related accuracy problems. If all of the scatterers were organic with index ≈ 1.03, the performance would be marginal but could probably be handled with advanced photon counting detection techniques.

Since it is very unlikely that all of the particles would be organic in the 5-10 μm diameter size range, we anticipate that the system is feasible, but the detailed performance cannot be predicted without much better model data.

Table 3-1. Parameters for 3 Meter Design Study.

$V = 10$ m/sec	Velocity
$R = 3$ m	Range
$w_t =$ I: 1.5×10^{-3} m II: 3.75×10^{-3} m	Transmitter beam radius
$\theta = \frac{d}{R} =$ I: 0.015 radians II: 0.03 radians	Beam angle intersection
$d =$ I: 45×10^{-3} II: 90×10^{-3}	Transmitter beam separation (19 fringes) Transmitter beam separation (16 fringes)
$A_c =$ I: $\pi[(0.09)^2-(0.045)^2]$ $= 0.019\ m^2$ II: $\pi[(0.09)^2-(0.055)^2]$ $= 0.016\ m^2$	Receiver collecting area (≈7.5 inch diameter)
$T = 0.5$	Transceiver transmission efficiency
$P_o = 1.0$ watt	2.0 watt laser split to form two 1.0 watt sections
$\phi =$ I: 0.015 rad II: 0.018 rad	Off axis view angle of receiver due to observation disc
$\lambda_o = 0.488\times10^{-6}$	Free-space wavelength of laser
$\eta = 0.2$	Effective quantum efficiency
$C = 0.1/m$	Water attenuation coefficient

Table 3-1. Parameters for 3 Meter Design Study (Cont'd).

n_o = 1: 1.03+j0.0 2: 1.15+j0.0	Relative index of refraction of particles
$n = 1.33$	Index of refraction of water
N = A: 2000×10^6 B: $20{,}000 \times 10^6$	Number of particles*/m^3 greater in diameter than y_o
$y_o = 1.0 \times 10^{-6}$ m	Lower cutoff of size distribution
$b = 3.65$	Negative slope of particle diameter probability density
$y_{max} = 20 \times 10^{-6}$ m	

---

* Cumulative:

$$N > y = 2000 \left(\frac{y}{1.0 \times 10^{-6}}\right)^{-2.65} \times 10^6/m^3 \quad , \quad 1.0 \times 10^{-6} \leq y \leq 20\ \mu m$$

LV SYSTEM DESIGN

Figure 3-1 is a concept drawing of a backscatter fringe velocimeter suited for the ARPA project with remotely adjustable range (1 and 3 meters), beam separation (4.5 cm and 9.0 cm), and beam radius (1.5 and 3.75 mm). The price for this flexibility will be the need for fine tuning the alignment with remotely controlled servos. The system components are discussed in greater detail below.

We wish to emphasize here that due to the accuracy requirements of this system, the remote nature of the experiment, and due to the possibility of also using the forward-scattered light for simultaneous particle sizing, there will be several unique considerations for this laser velocimeter system. The final design will require laboratory checkout in a water trough with all interface electronics, data acquisition equipment, and software. The final selection and purchase of the glass components will be minimal in cost in comparison with the mechanical, electronic, and software design, assembly, and debugging costs.

LV COMPONENT RECOMMENDATIONS

This section includes recommendations concerning the detailed optical, mechanical, and electronic design of the LV system.

The laser used for the experiments should be capable of producing a stable reliable output TEM_{oo} beam with over 1 watt for

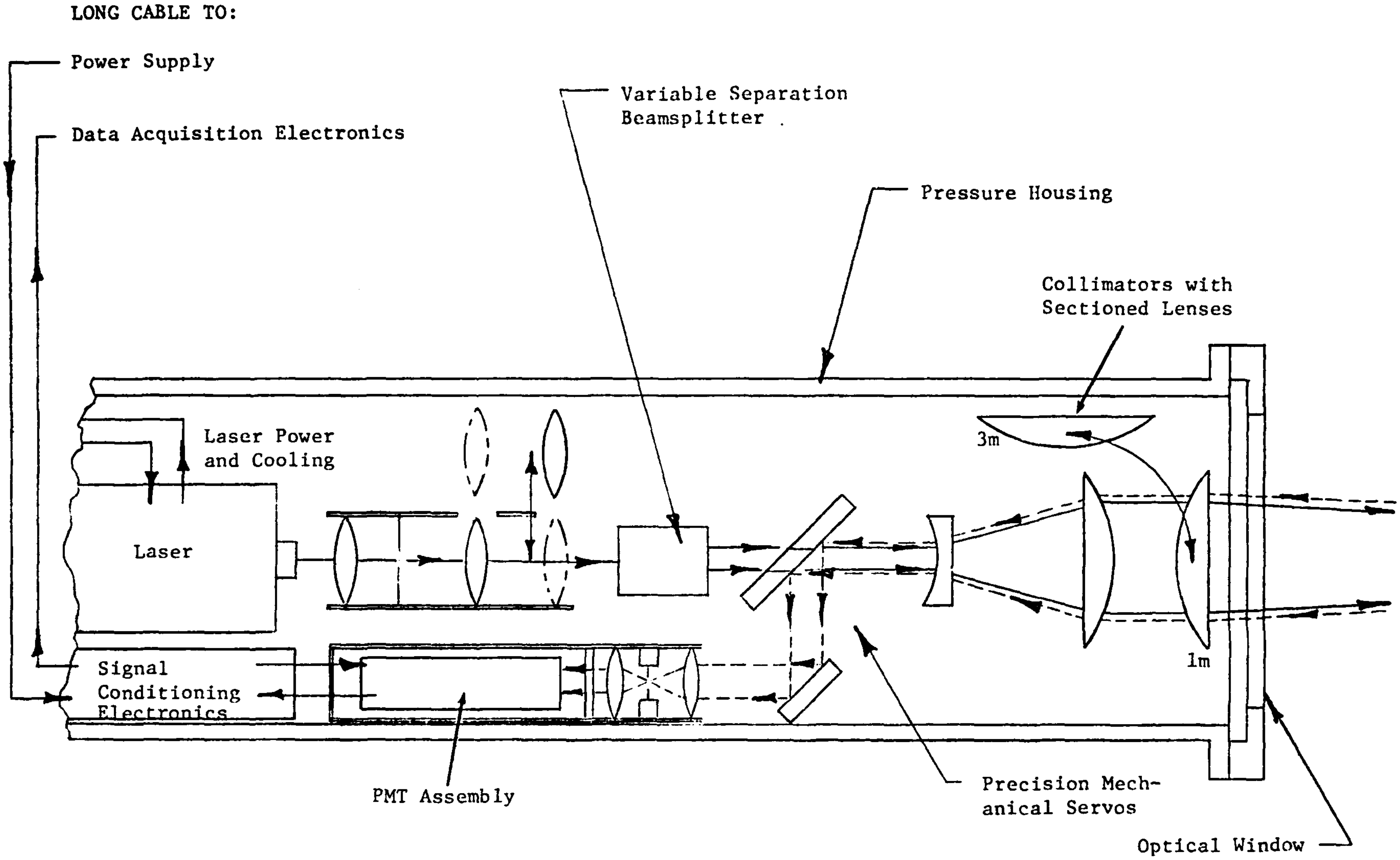

Figure 3-1. System Drawing of a Backscatter Fringe Velocimeter.

each of the wavelengths, λ = 4880 Å and λ = 5145 Å. This laser should have reliability and features equal or equivalent to a new Spectra-Physics Model 165. (This could include a Spectra-Physics or CRL argon ion laser with a new plasma tube and mirrors, or some other equivalent laser.)

Two selections of output beam diameter can be realized by using a specially designed lens-pinhole collimator with two output objectives which are alternately clicked in place by a servo system. This must be a precision assembly with high-quality lenses with hard dielectric antireflection coating to avoid multiple output beams and excessive scattered light.

The beam splitter element should be a combination of two or more sets of splitter elements precisely aligned so that servo translation of the assembly in and out of the plane of the illustration results in selection of different beam separations while maintaining parallelism, beam direction, and centeredness.

A telescope with roughly a 2:1 expansion ratio will assist in matching the desired output transmitter/receiver dimensions to those more convenient for the other elements. The lenses should be sectioned to separate scattered light from the transmitted beams and the return weak signal light.

Two output ranges may be obtained without affecting alignment or introducing abberations by rotating in and out reversed collimators optimized for the glass water interface and the range to focus in the water. The output window flatness should optimally be less than 1/10 wavelength over the maximum transmitter beam diameter of 0.75 cm.

Precision servomechanisms must be included to allow remote fine tuning of the optical alignment. This may include precision focus perturbation of the lens-pinhole collimator output lens, precision focus perturbation of the 2X telescope, or even, if necessary, the inclusion of a precision differential beam-direction prism pair with servo drives.

The photomultiplier tube for this application should be a low gain tube (6-9 stages) so that it may be operated at rated voltage without producing dynode fatigue or signal saturation from the high-level signals of interest in this application. Also, a significant amount of care should be taken with tube selection* and low-noise preamplifier design to assure wide linear dynamic range (4-5 orders of magnitudes are desirable for diagnostics of backscatter signal distributions). (We have encountered similar requirements in our present particle sizing work.) It is not a simple matter to obtain 10 μvolt to 1 volt noise-free linear signal range even without the requirements of a 300 foot cable for transmission to data collection electronics.

Generally in the design of LV optical component holders and positioners, there are always tradeoffs between flexibility and general purposeness and rigidity and stability of alignment. The more degrees of freedom of adjustment that are allowed, the more

---

* For example, EMI 9846 with high voltage above rated value (1200-1500 V).

difficult it is to obtain correct alignment and have it stay there. This means that if general purpose components such as those provided by TSI and DISA are to be used for an environmentally remote and difficult application, one may risk misalignment and/or vibration problems unless the mechanical design of each component as a part of the entire system is reviewed. The proposed sea tests are going to be so operationally difficult that we are recommending simplicity above all: a one component system, without Bragg cells, with all optical components rigidly mounted in a compact small space with a minimum of alignment adjustments possible.

The pressure housing design is a nontrivial item. It must include a heat exchanger cooling coil and pump for the laser water cooling. It must have appropriate power and signal cable feedthroughs or connectors and internal mechanical support for the laser and optics. These issues have already been addressed at NUSC with the laser MTF/LV fringe experiment pressure housing and window. The clear aperture of this system is 10 inches in diameter.

The data acquisition system problems primarily focus in the signal conditioning and transmission electronics. There is not room for extensive electronics in the pressure housing. There is room for a tape recorder, an oscilloscope, and a burst-counter processor in the NUSC instrumentation van. The difficulties concern dynamic range, accuracy, and ease of real time data analysis. In order to send the signals up the 300 foot cable without introducing noise over the desired range may require compression with logrithmic amplifiers or even analog-to-digital conversion. It is certain that even if the data is tape recorded in analog form, a burst-counter velocity processor and a histogram generator and display should be available along with the oscilloscope for real time operator assistance in checking the system alignment and performance. The details of the electronics are just as important as those of the optics and should be given considerable attention by the hardware system contractor.

Any of the newest burst-frequency processors by TSI, DISA, and Macrodyne would be adequate for use with the sea test equipment if modified properly to read out enough bits to obtain 4 decimal place precision. All three manufacturers have high-speed stable digital counting systems which are adequate. We have had the most experience with the Macrodyne units (see Appendix F) and find the Macrodyne bipolar threshold test to be significantly useful in rejecting undesirable signal glitches. None of these units will be useful on board in real time unless a minicomputer, microcomputer, or special-purpose histogram generator, recorder and display unit are available to further process the single-particle period measurements. If a computer or microcomputer is used, software will be required. If not, then only a special higher precision interface to a high-precision histogram generator may be needed.

4.0 IN SITU INSTRUMENTATION

In this section we address the issues of concern under Task 3. We begin by making certain program recommendations concerning the conduct of possible sea tests. Following that we discuss desirable test instrumentation, available test instrumentation, and finally recommendations for a compromise instrumentation package which includes immediate development of missing initial components.

PROGRAM RECOMMENDATIONS

There are several Navy laboratories, private firms, and university laboratories that, given sufficient time and money, could do an excellent job of designing and conducting tests of laser velocimeters in the ocean, particularly with consulting assistance from SDL and/or W. Stachnik of the Naval Underwater Systems Center concerning prior experience. However, there are already existing plans and NAVSEA funding for assembly of laser velocimeter sea test equipment in FY78 and preexisting relevant NUSC COURAGEOUS experience and equipment development. If ARPA is willing to conduct a joint, simultaneous, sea test with the COURAGEOUS program on a mutually agreed upon schedule, it is very unlikely that any other Navy laboratory, firm, or university could conduct comparable tests in the same time frame without much higher costs. For this reason, we recommend that NUSC, New London, be made responsible for the sea test in cooperation with the COURAGEOUS tests to be held at the end of FY78 or beginning of FY79.

DESIRED IN SITU MEASUREMENTS

Velocity Verification

There are several considerations about measurements that could be made simultaneously with a test of an LV system in the sea. The first is that a separate physical measurement of water velocity in the vicinity of the optical probe volume is desirable to verify directly the accuracy of the LV system down to the limits of the physical probe.

The first consideration implys that a rigid structure which holds the laser velocimeter and the physical probe is needed. This structure should be lightweight and stiff, so that fundamental resonant flexures occur at a frequency much higher than the velocity fluctuations of interest. Thus, averaging velocity samples over intervals short compared with velocity changes will remove both bias errors due to particle sample rate and structural vibration and flexure components. The structure should also be designed to minimize turbulent flow in the probe volume due to the structure. If the test is to be at say* 0.1% turbulence levels, then a thorough mechanical and fluid dynamic evaluation and design may be required instead of simply placing everything on an I beam. This requirement could be eased somewhat by assuming that the desired internal wave measurements would be relatively slow with averages to remove turbulence effects. However, 10,000

* Dr. Reichman at NOSC has indicated that 0.1% is obtainable with a hot film probe.

measurements with independent turbulence components at 1% rms turbulence would be required to reduce the rms variation to 0.01%.

Standard Oceanographic Data

Most optical oceanographic measurements are not directly applicable to performance prediction for LV systems without further assumptions and model manipulations. However, a lot of data is available and it would be very useful to be able to globally relate such data to LV performance even if only to order of magnitude approximation. Thus, such standard measures should, if possible, all be made at the same time and location as the LV data is collected. These include Coulter counter particle size data, microscope samples, transmissometer measurements, volume scattering function measurements, narrow angle beam spread function measurements, and mean temperature, salinity, and velocity profiles versus depth.

Presently Available Specialized Oceanographic Instrumentation

None of the standard oceanographic data is adequate with present models to be used for optimization and performance predictions for a high accuracy LV system. We actually need single-particle backscattering cross-sections and number density data from about 1.0 μm diameter upwards to greater than 100 μm; and we need characterization of propagation effects down to a few microradians instead of down to a few milliradians.*

---

* A formulation of the effects of propagation is provided in Reference 3.

There are several different instruments which are either under construction or completed at various labs for measurements in the milliradian angles near the forward or the 180° directions. There are also instruments becoming available for measurements of localized thermal and salinity microstructure. Although theoretical modeling is being performed, we do not yet have models for detailed performance prediction in terms of microstructure measurements.

Desired In Situ Data

This section discusses measurements which if made at the same time the LV system were operating (in test or in practice), should allow computer optimization of the system and prediction of the available accuracy.

In order to statistically predict multiparticle errors and optimum signal processor threshold settings, we may use the probability density function for the amplitudes of the single-particle backscatter signals and the total number of particles per unit volume (see previous discussion on conditional density). We are presently calculating such distributions based on assumed particle shape (spherical), index of refraction, and size distribution. The validity of such an approach should be checked by performing the same type of simulations with real time size data taken simultaneously with actual backscatter amplitude distribution data.

The simplest way to get backscatter distribution data is from the LDV signals themselves. This approach will be limited on the small particle end of the distribution. Optimum design for detecting small-particle backscatter amplitudes would require a short-range, low f/no instrument with a very small probe volume to separately resolve individual particles at possibly high number density. It might be possible to include an alternate beam path through shorter focal length optics in the design of the LDV instrument so that these high-resolution backscatter amplitude measurements would be included.*

A second category of tests concerns some form of measurement of the random refractive effects due to temperature and salinity which bridges the gap between predictions based on point measurements of thermal and salinity microstructure and the actual beam wander and fringe deformation which results. Candidates for this type of measurement are shearing interferometry, laser schlieren, MTF, and holographic interferometry. Of these, holographic interferometry has the most potential since quantitative measurements of many kinds can be performed later with laboratory reconstructions. This technique would also be far more expensive than a low-power laser schlieren or shearing interferometry experiment.

Test Instrumentation

There is a category of measurements which should be made during testing of the LDV system which would not be made as backup during system utilization for its intended purpose. This category includes

---

* This has been provided by the 1 meter, large beam, large separation option of our LV design.

the hot film velocity verification mentioned previously, and any optical forward scatter measurements beyond the LDV probe volume. There are at least three such optical measurements which may all be made with the use of the same equipment and test structure which will hold the hot film probe. These are actual beam wander, fringe deformation, and multiparticle scatter background light in the microradian range in and near the scattered focussed beams. These measurements can be made with a microscope objective imaging the transmitted beams at the probe volume onto a motion picture film plane and/or television camera sensor with a set of calibrated attenuators remotely available. Remote video monitoring during the experiment would be controllable.

The desired types of in situ instrumentation are summarized in Figure 4-1.

ASSESSMENT OF AVAILABLE CAPABILITY

Conversations have been held with SAI, La Jolla, NUSC, New London, NOSC, San Diego, and NRL, Washington, personnel concerning available underwater instrumentation at these locations and at Scripps, San Diego. Certain possibilities have been raised and eliminated.

The Scripps ALSCAT system reportedly has the capability to measure small-angle scatter at 3, 6, and 12 mrad angles. This sensitivity is inadequate for small-angle measurements on the order of 10 microradians and is thus inappropriate for measuring the primary beam degradation effects.

LDV SYSTEM INSTRUMENTATION

- HYDROMECHANICALLY DESIGNED SUPPORT STRUCTURE
- HOT FILM PROBE NEAR LV PROBE
- ATTENUATED MICRO MOTION PICTURE AND/OR TELEVISION RECORDING OF:
  - BEAM WANDER
  - BACKGROUND LIGHT
  - FRINGE DEFORMATION

PREDICTIVE MODEL VERIFICATION (OPTIONS)

- THERMAL AND SALINITY MICROSTRUCTURE
- OPTICAL SPATIAL COHERENCE MEASUREMENTS
  - AVERAGE
  - "INSTANTANEOUS"

  } MTF, SCHLIEREN, SHEARING INTERFEROM. HOLOG. INTERFEROM.
- LOW F/NO, SHORT RANGE PARTICLE BACKSCATTER CROSS-SECTION DISTRIBUTION

"STANDARD" OCEANOGRAPHIC MEASUREMENTS

- MEAN TEMPERATURE AND SALINITY
- TRANSMISSIVITY
- VOLUME SCATTER FUNCTIONS
- BEAM/POINT SPREAD FUNCTIONS
- COULTER COUNTER DATA + MICROSCOPE SAMPLES

Figure 4-1. Summary of Desired Test Instrumentation.

The preliminary discussions with Dr. Vince Del Grosso at NRL concerning the MTF equipment being constructed there indicates that this equipment may be useful at the level of precision required. Further efforts are required to ascertain if the required sensitivity will actually be available. The results of sea tests scheduled for October 1977 should be reviewed.

Mr. Bill Stachnik has provided a list of facilities available through the NUSC, New London, laboratory. Due to previous related work and the equipment and experience developed under the COURAGEOUS program, NUSC has a considerable amount of underwater optical facilities which are quite relevant to the needs of this program.

Dr. Mike Reichman of NOSC has provided information concerning relevant facilities and experience at NOSC. A primary relevant facility and experience seems to be the water tunnel and hot film measurement capability coupled with extensive LV lab experiences of Dr. Reichman. Other significant facilities include the NOSC tower* which could provide a location close to shore for initial equipment shakedown tests, and FLIP.

Abbreviated copies of the description material provided by NUSC, NOSC, and NRL are included in this report as Appendix I.

---

* Unfortunately, the particulate content of the near-shore water of the NOSC tower is expected to be too high and to be non-representative. We thus would recommend tank tests followed by open ocean tests. A stable water tunnel would be very useful for lab tests of the optical and electronics subsystems.

DEFINITION OF IN SITU INSTRUMENTATION

Figure 4-1 was a summary of our preliminary suggestions for the in situ instrumentation. Figure 4-2 illustrates schematically the results of tradeoffs between money, available equipment, and desired equipment. We now discuss the items on Figure 4-1 item by item.

LV System Instrumentation

According to Dr. Michael Reichman, NOSC, the structure produced turbulence should not produce turbulence for currents less than 1 meter per second, and hot film probes should be capable of 0.1 percent fluctuating velocity measurements. These points imply that the shape of the optical bench should not be an issue, and that the achievement of 0.01 percent precision will most likely be achieved by averaging in both the hot film and the LV measurements. No methods of direct probe verification of LV precision to $1:10^4$ is known.

Figure 4-2 indicates the presence of an ambient light meter for separate measurement of background (sunlight) level. An NUSC 35 mm "Fringe Camera" will be further modified to magnify and photograph the fringe pattern in the forward direction. This will provide instantaneous (1/1000 sec) recordings.

There are two deficiencies which we see from the ideal. First, there appears to be no way to measure the correlated beam wander*

---

* "ee Reference 3 for discussion of propagation effects.

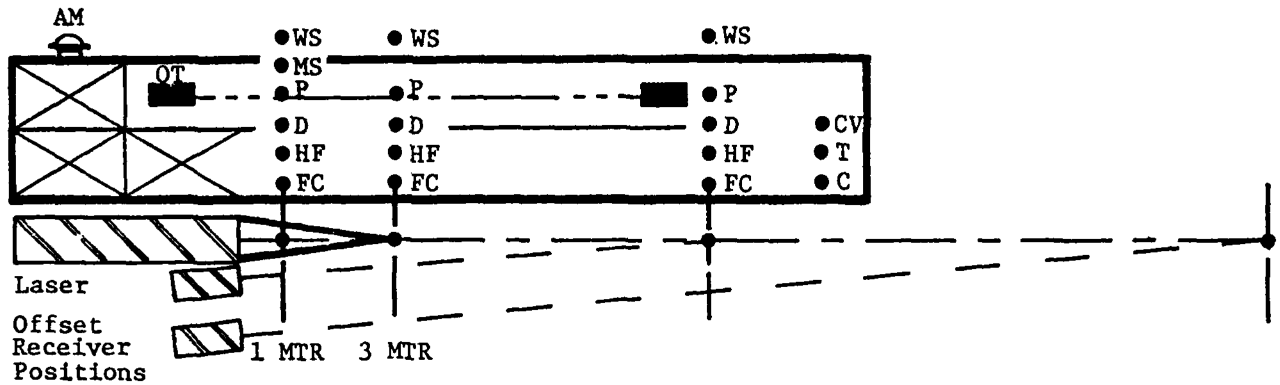

MS	=	Microstructure Instrument	T	=	Temperature Sensor
P	=	Flow Generating Pump	S	=	Conductivity Sensor
D	=	Constant Speed Disk	WS	=	Water Sampler
HF	=	Hot Film Probe	OT	=	Optical Transmissometer
FC	=	Fringe Camera/T.V. Camera/ Fiber Optic Probe/FS Receiver	AM	=	Ambient Light Meter
CV	=	Current Velocity Sensor			• Coulter Counter, • Index Estimations } Deck Equipment

Figure 4-2. Underwater Optical Bench (Configured for Both ARPA and NAVSEA Programs).

without expensive additional items due to the flexure of the optical bench. A way to do the measurement exists. A separate collimated laser beam could be transmitted to a precision corner cube, returned to a Fourier transform lens, and the location of the focused spot monitored electronically with a photo diode array, filter optic array, or other position sensor.

A second deficiency is the lack of measurement of scintillation (time effects) to complement the spatial effects recorded on film. The TV camera will not be expected to be fast enough and have dynamic range enough for this task. We anticipate the investigation of the possibility of adding a fiber optic probe in the fringe camera to allow photomultiplier tube monitoring of scintillation of the beams. (The transmissometer will also record scintillation effects.)

Predictive Model Verification

Thermal and salinity microstructure will be measured by the Triadic and Neil Brown microstructure instruments available at NUSC.

Optical spatial coherence will be measured from the analysis of microdensitometer scans of the calibrated fringe camera transparencies. Unless additional steps are taken, correlated (two beam) wavefront tilt will not be measurable due to masking by bench flexure.

The simulation studies have shown that knowledge of particle size distribution alone is totally inadequate to predict LV performance.

Index of refraction and possible particulate structure will be significantly important. Argonne National Laboratories is currently funding SDL for the further development of a forward scatter real time particle-sizing system based on the M. Farmer signal visibility technique and the forward scatter ratio technique. This development, which will be completed in January 1978, is being followed by additional ERDA-sponsored development contracts. We anticipate that by the time the laboratory tests are conducted, a forward scatter particle sizing model for ocean applications could be refined from the ERDA instrument system. The short range backscatter LV transmitter/receiver would then simultaneously measure particle size independent of index in the forward scatter direction while measuring backscatter cross section with the LV optics. This is a very critical link with available Coulter counter data which could be made to provide future design confidence.

Standard Oceanographic Instruments

The NUSC data acquisition van, Xerox computer, and instrument set provide all the necessary "standard" instrumentation. This includes precision mean temperature and salinity and narrow beam transmissivity. Narrow-beam spread functions are to be provided by the fringe camera.

5.0 CONCLUSIONS AND RECOMMENDATIONS

All of the work statement tasks summarized in the introduction have been accomplished. This report is organized so that all the detailed work is reported in the Appendices. The body of the report is also the summary, both of the contractual work and of the report itself.

In addition to the single-particle Fringe LV simulation software developed under this contract, we have also just completed Reference Beam LV simulation software for the NAVSEA COURAGEOUS program. The results of running that program[3] indicate that there could still be advantages for using a reference beam system for internal wave measurement. However, that conclusion makes propagation assumptions which are more severe than those for the fringe velocimeter. We recommend that more realistic comparative simulations be performed next year after single-particle scattering amplitude data and propagation coherence diameter measurements are available.

The basic fundamental nature of photodetection at visibile wavelengths is digital, i.e., photo-electron emission quanta. Photon counting detection systems are presently limited to applications with less severe accuracy requirements than internal wave measurements. However, the signal frequencies for such applications are very low with respect to the state-of-the-art photon counting rates of over 100×10^6 Hz. This means that the potential exists for the later development of very high accuracy, single-particle photon counting detection techniques which are much more efficient with available laser power. We recommend that these notions be reviewed after the sea test data is available.

Three final conclusions of this report are: first, simulations using available data and models indicate that a fringe LV system which we have designed could produce the data rate and accuracy desired for internal wave measurements; second, sea tests with adequate in situ instrumentation should be performed to verify design techniques, establish a more detailed data base for the models, and determine the nature of any operational problems which might arise; and third, additional simulation modeling of random refractive propagation effects should be undertaken.

6.0 REFERENCES

1. Adrian, Humphrey, and Whitelaw, "Frequency Measurement Errors Due to Noise in LDV Signals," in The Accuracy of Flow Measurements by Laser Doppler Methods, published by the Proceedings LDA-Symposium Coppenhagen, 1975.

2. O. B. Brown and H. R. Gordon, "Size-Refractive Index Distribution of Clear Coastal Water Particulates from Light Scattering," Applied Optics, 13, 2874 (December 1974).

3. W. T. Mayo, Jr., "Support of Project COURAGEOUS Optics," Final Report on Contract N66604-77-M-8709, SDL Report No. 77-6251, 30 September 1977 (CONFIDENTIAL).

APPENDIX A

OPTICAL VELOCIMETERS FOR USE IN SEAWATER

A paper to be presented at OCEANS '77
Los Angeles, California
October 18, 1977

OPTICAL VELOCIMETERS FOR USE IN SEAWATER

W. J. Stachnik
Naval Underwater Systems Center
New London, Connecticut 06320

W. T. Mayo, Jr.
Spectron Development Laboratories, Inc.
3303 Harbor Boulevard, Suite G-3
Costa Mesa, California 92626

Summary

Laser velocimeters are versatile instruments in controlled liquid flows, wind tunnels, and atmospheric environments. The first steps are now being taken to bring the versatility of these instruments to use into the more difficult ocean environment. In this environment optical clarity and particulate concentrations are not adjustable and this presents significant constraints in the design of such systems. This paper describes the investigative work that is presently being performed to make the transition. The analysis considers natural waterborne particulate concentrations, optical propagation phenomena, and signal processor behavior. Preliminary conclusions are that optical velocimeter devices are likely to be employed in the study of ocean wave action, in the study of turbulence and material transport, in the study of advective and convective currents, in the study of structure-generated flow fields, in the study of particulate microdynamics, in the more detailed analysis of particulate size distributions, and even in the optical detection of sound transmission in water.

The data base which was used in performance calculations thus far seems adequate for our present optimism, but not conclusive without experimental demonstration and additional performance model verification. Experiments for these purposes are planned for 1978.

Introduction

Laser velocimeters (LV) are versatile instruments in the laboratory.[1,2] They possess extremely small sensing volumes, often less than a cubic millimeter, can measure velocities remotely without themselves disturbing the flow, and possess inherently high accuracies and stabilities that do not require recalibration. These characteristics arise from the fact that the short wavelength of coherent laser radiation allows this form of energy to be focussed to very small sensing volumes and the high frequency stability of laser sources allow optically interfering beams to form stable interference patterns in space and in time. In addition, LV systems provide high data rates even at low flow velocities; and, for those familiar with the behavior of mechanical current meters, LV systems do not stall.

If practical LV systems are developed, then they may be used with significant advantage in the study of ocean wave action, in the study of turbulence and material transport, in the study of advective and convective currents, in the study of structure-generated flow fields, in the study of particulate microdynamics, in the more detailed analysis of particulate size distributions, and even in the optical detection of sound transmission in water.

With all of the above advantages, the application of LV systems to the oceans is quite desirable, but there are some important, and even basic, questions that must be considered before confident, widespread usage can be expected to come about. These questions are concerned with the fluid medium itself and with the particulates that are contained in it.

Before becoming involved with such questions, one should refer to the four basic laser velocimeter configurations shown in Figure 1. Each type depends upon the scattering of source light with particulates entrained in the moving fluid. LV systems are classified by the location of the receiver collection

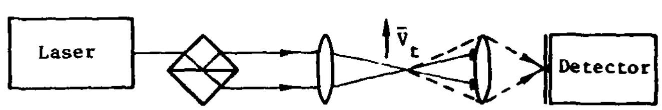

(a) Forward Scatter Dual Beam (Fringe) Velocimeter: Transverse Velocity.

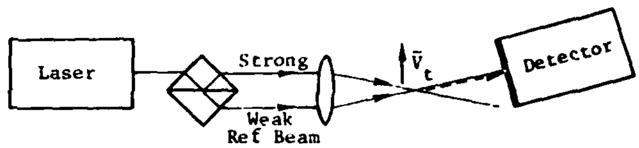

(b) Forward Scatter Reference Beam (Heterodyne) Velocimeter: Transverse Velocity.

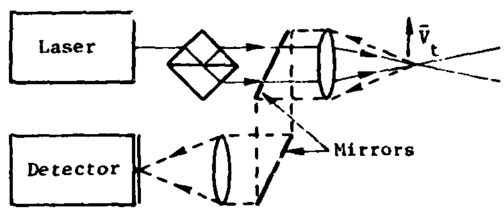

(c) Backscatter Dual Beam (Fringe) Velocimeter: Transverse Velocity

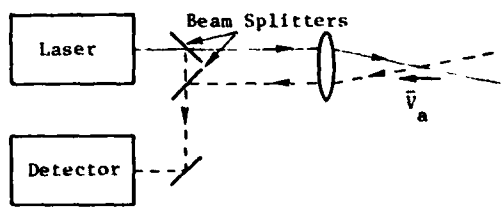

(d) Backscatter Reference Beam (Heterodyne) Velocimeter: AXIAL Velocity

Figure 1. Four Types of Laser Velocimeters

optics relative to the transmitter and scattering intersection volume as forward scatter or backscatter systems. These basic configurations can be further classified according to whether the combining wave fronts in each of the configurations produce interference patterns distributed spatially (known as dual beam or fringe systems) or temporally (known as heterodyne or reference beam systems). Only the backscatter reference beam system measures axial velocity components. It is important to make these distinctions because the analysis, although similar, is different in several important details including signal-to-noise ratio behavior.[3]

What we shall do in the material that follows is discuss phenomena that affect each of the four basic configurations. These fluid phenomenologies for ocean water fall into the important and familiar categories of marine biology and physical oceanography. In a later section, the effects of scattering particle models on error performance are shown via computer simulation for the backscatter dual-beam system.

Propagation Effects

The first consideration to be made concerning the part that seawater plays in the velocimetry process is concerned with water itself. It is, of course, the primary constituent of the optical pathway through ocean water. In pure form, water has what appears to be unrivaled optical properties among liquids, having very low absorption ($0.017m^{-1}$) and, because of polymerization-like molecular linkages, very low scattering properties.[4]

The propagation velocity of any particular wavelength of light in water has long been known to depend upon the temperature, dissolved mineral content and pressure existing in the medium. In fact, such behavior has been reported with great accuracy.[5] Such values are for bulk samples that are homogeneous in these three common characteristics. The oceans, however, possess spatial distributions of such values that change with time. As a consequence, other approaches have had to be taken to describe such phenomena in relationship to optical propagation behavior. The detailed treatment of such behavior is both complicated and incomplete at this time.

In order to obtain some understanding of the refractive limitations for fringe velocimeter systems, we refer to the theoretical results of Babak, et al.[6] reproduced in Figure 2. In this treatment, one can consider the angular fringe separation (fringes per unit angle) as a particular spatial frequency in the modulation transfer function response of the medium, and the response (vertical axis), as the reduced average contrast of the interference pattern as a function of range, path refractive variations, and dominant refractive scale size. For example, 10,000 fringes/m in a dual-beam probe volume located at a range of 0.5 meters is an angular frequency of 5000 lines/radian. If the parameters of the Babak figure were typical, higher spatial frequencies than this could pose difficulties in some LV applications.

In coastal water where optical paths of the order of a particulate scattering length or longer would be typical, modulation transfer functions that include particulate effects must be considered. Fortunately, or unfortunately, the time-averaged nature of such MTF results will be inadequate for a complete analysis of a single-particle LV system which depends on instantaneous refractive and scattering effects. Good instantaneous signals may be obtained (with fading) while the average fringe contrast is low. Our present theoretical investigations address the signal fading problem from the point of view of short-term beam wander with loss of signal when the focussed beams do not cross and with the assumption of independence of the two beams. Further advances in theory of correlated two-beam wander and defocussing and experimental measurements are needed to complete our understanding of the refractive limitations in the ocean.

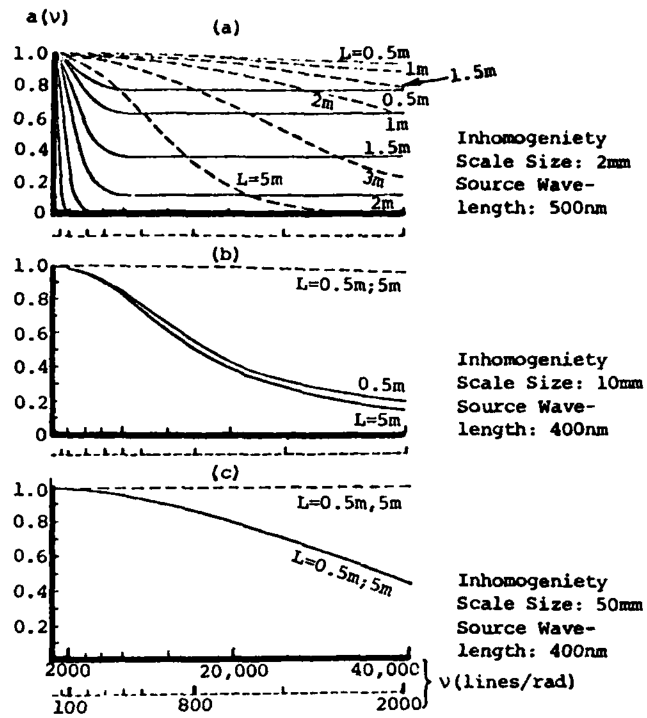

Refractive variations for all of the above response curves $\Delta N = 2x10^{-5}$

Figure 2. The Effect of Refractive Inhomogeniety Scale Size Upon the Modulation Transfer Function of Water.

(from Babak, et al.[6])

Scattering Particulate Models

Attention is now directed to the particulate content of seawater. Kullenberg reports the range of such suspensions from 0.005 mg/l in the deep Central Pacific to 2.5 mg/l in North Atlantic surface waters.[7] Narrow beam attenuation coefficients range from 0.05 m^{-1} in deep clear ocean waters to 0.2 m^{-1} in surface waters and significantly higher in coastal waters. The attenuation coefficient c is used in calculating one-way power loss according to e^{-cR} where R is range.

Although the above weight values serve to quantify the amount of particulates present, the values are insufficient for calculation of single-particle signal magnitudes due to backscatter from the beam-cross probe volume. What is necessary in calculating signal scattering strengths is an equivalent spherical particle size and relative refractive index distribution that is predictive of the waterborne particulate optical behavior. Such generalizations are necessary because of the highly varied shapes of plankton, detritus, and clays.

A number of individuals have provided size distributions of ocean particulates and have made reasonable assumptions concerning the average index of refraction of these particles.[7,8,9] Hyperbolic distributions (commonly called Jung's distributions) are of the form:

$$N(d>y) = ky^{-m} \quad (1)$$

where: $N(d>y)$ = cumulative number of particulates per cubic centimeter greater in diameter than y,

m = characteristic slope of the distribution, and

k = numbers of particulates per cubic centimeter greater than one micrometer diameter.

An example set of number distribution data provided by Kullenberg[7] is reproduced in Figure 3.

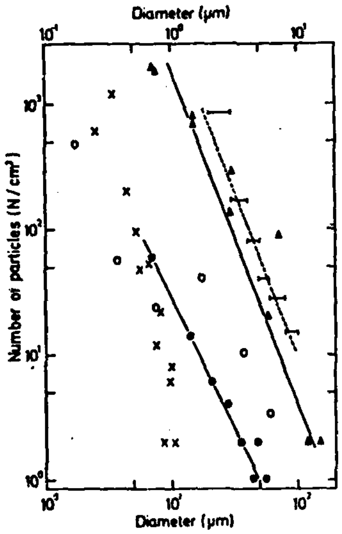

Fig. 5. Examples of particles size distributions:

Upper scale:

△ Kullenberg, Pacific deep, 1953;
|—| Brun-Cottan, Coulter counter, 500 m depth, Mediterranean, 1971.

Lower scale:

● Gordon D.C., microscope, organic matter, surface Atlantic, 1970;
× Carder *et al.*, Coulter counter, Pacific surface, 1971;
▲ Jerlov, microscope, fiord, 1955;
○ Ochakovsky, microscope, Mediterranean, 1966a.

Figure 3. Kullenberg's Figure 5 on Particle Size Distrubutions.[7]

Typical clear ocean water has values of k between 2000 and 20,000/cc. Typical slopes are m = 2.7 for the 1 - 10 μm diameter range. Conservation of volume (partial volume due to particulates) shows that $|m|$ must exceed 3 for larger particles.

The above type of size data is generally obtained by either Coulter counter measurements of small samples or microscope inspection of small samples. Both procedures are inadequate for determining the distribution of the larger particles (greater than 10 μm in diameter) due to the small sample sizes. This is unfortunate, since calculations show that in some situations, particles in the 10 - 100 μm size range are known to exist, but little data is available. The referenced paper by McCave indicates the power law distribution may extend to 50 μm, but more measurements are needed in the large particle regime.

Some of the most thorough index of refraction modeling efforts have been made by Gordon and his associates. In a fairly recent paper, Brown and Gordon provide clear coastal water models with a small-fraction index of refraction, a mid-fraction pair of indices of refraction (with relative occurrence probability) and a large-fraction index of refraction. The deduction of the effective values of the indices was based on trial and error fits of average Mie scattering computations to measured angular volume scattering functions (VSF). The size distributions used were piecewise linear fits on a log-log plot of Coulter counter size distributions with the small-fraction number densities selected somewhat arbitrarily to satisfy the VSF data. The procedure in such modeling attempts is to use a priori assumptions that organic components have indices in the 1.01 to 1.05 range and mineral components fall in the 1.15 to 1.20 range. The resulting fits of the predicted VSFs agree reasonably well with measured data, except at very small forward-scatter angles (indicating lack of correct large particle number data) and backscatter angles near 180° (where no scattering data was measured).

The sensitivity of Mie scattering calculations at 180° backscatter to the refractive index has been demonstrated in some of the computations we have performed. In fact, the computations show that available models are inadequate for precise performance computations for backscatter velocimeter systems because the signal levels that result from as small as a 10 percent change in refractive index (1.05 to 1.15) produce decades of difference in backscatter signal levels. This is graphically illustrated in Figure 4 which is described in the next section.

Performance Simulation Codes

When a single scattering particle passes through a sinusoidal optical interference pattern, the intensity of the scattered light varys sinusoidally in time with a frequency proportional to the velocity of the particle. A burst-counter processor is one which "arms" when the signal exceeds a threshold and then measures the time required for a fixed number of signal zero crossings. This short time average period measurement will include small errors for a variety of reasons even when the signal-to-noise ratio is large and electronic jitter and optical component abberations are negligible. First, there are small noise perturbations of the location of the zero-crossings, which we have studied theoretically and experimentally, but which we will not discuss here. Second, there are propagation-induced distortions of the fringe pattern as previously mentioned. Finally, there are phase shifts which occur when more than one particle is crossing the interference pattern at the same time. These multiparticle phase shifts need not be of concern when one very large signal is present with many other much smaller ones. Thus, processor threshold selection offers the possibility of reducing multiparticle errors at the expense of data rate when the dynamic range of signal amplitudes is sufficiently large.

The relative error effects of the random signal amplitudes is a nonlinear statistical process not presently amenable to closed form analysis. Thus, the multiparticle phase errors have been studied by direct simulation in which individual scattering signals are summed and then detected with a burst counter processor model. To do this we have expanded computer simulation

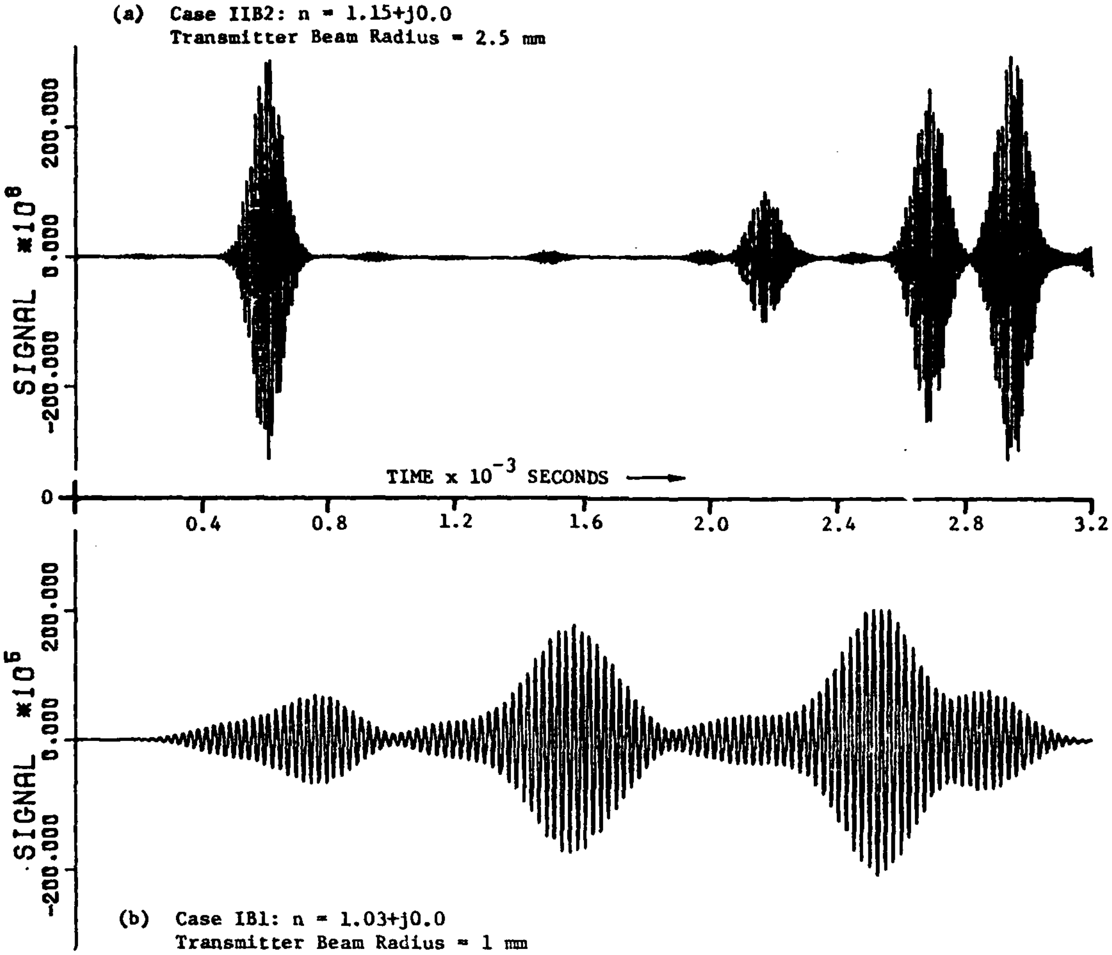

Figure 4. Example Signals (Expressed in Photoelectron Rate) Vs. Time for Two Selections of Particle Index and Transmitter Geometry. (Assumes 20,000 Particles/cc Greater than 1.0 μm Diameter with Cumulative Slope of -2.65.)

programs previously developed by W. T. Mayo, Jr., for NASA.[10] Examples of simulated signals are reproduced in Figure 4. These examples demonstrate the critical dependence of the nature of the signal on the assured index of refraction and the optical geometry. An example of normalized error histogram for a burst counter processor with bipolar arming thresholds of a specific value is illustrated in Figure 5. Parametric

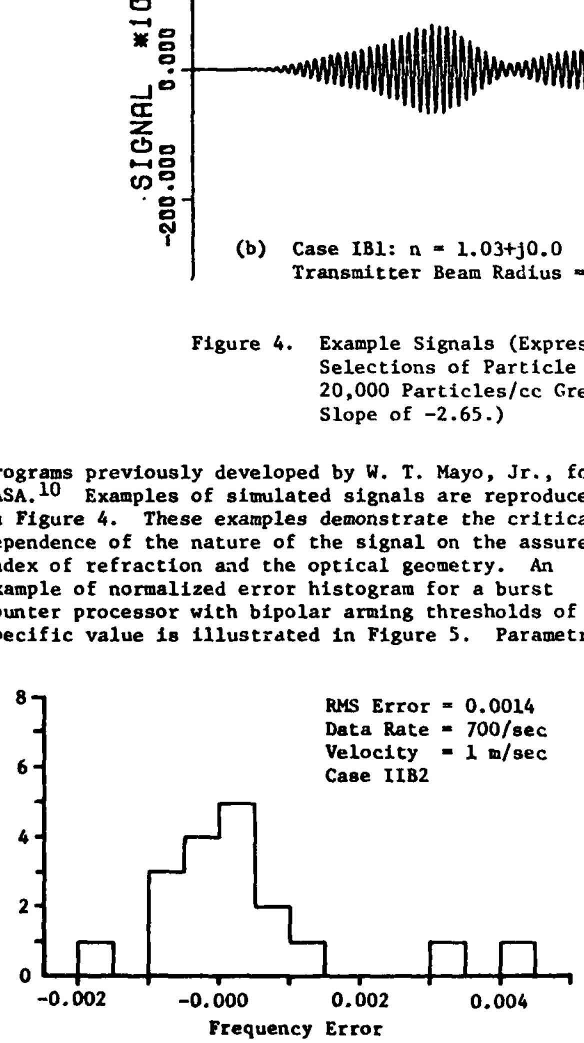

Figure 5. A Typical Multiparticle Phase Error Histogram.

variation of these thresholds indicated that multiparticle phase error can be reduced adequately in many cases by increasing the threshold. The simulation programs are now described in more detail.

OPTIC: This program randomly realizes particle diameters according to input number density, slope, and minimum size; computes the Mie differential scattering cross section for the random diameters according to the input laser wavelength and the relative index of refraction; computes the peak optical power received by an LV receiver photodetector (expressed in photoelectrons/sec) in terms of the input LV system geometry, laser power, and medium attenuation coefficient; computes the LV probe volume, the mean occurrence rate of single-particle signals, the signal frequency and duration, the fringe period in space; computes other quantities; and has other options for reference beam geometries. The output is a printout of constants and a disc file of the single-particle mean peak photoelectron rates (multiplied by random probe volume entry location factors to account for the Gaussian beam profile).

HISTO: This program sorts the particle diameter realizations, the single-particle signal amplitudes, or any other disc file, into linear or logarithmic histograms or cumulative histograms. Thus, in conjunction with PLOT, a general purpose plotter program, we verified the minus 2.65 slope and straight line nature of the simulated random particle size distribution when plotted as a log-log cumulative histogram. Also, the slope of the log-log cumulative histogram of the resulting signal amplitudes has been found to be significant in burst counter processor error studies.

SIGNAL: This program generates Poisson random occurrence times for the single-particle signals at the mean rate input to the program; the single-particle signals are realized on uniformly spaced sample points selected automatically as a small fraction of the mean signal frequency; the signals are summed in an overlapping manner with selectable truncation width of the single particle signals; the amplitudes, frequencies, signal visibilities, and number of cycles are all input selectable as a constant, a random variable with input mean, rms deviation and probability density function, or as an input disc file from OPTIC. Figure 4 illustrates two examples of plotting sections of two SIGNAL output files.

COUNT/COMP: These two programs together allow simulation of a burst counter processor (assumes signal has been detected and bandpass filtered). A variety of options are included, but in Figure 5 a Macrodyne processor was modeled which has a threshold equally spaced on each side of the zero level and requires that the ac signal magnitude sequentially exceed these thresholds in between each zero crossing; the counter then measures the time required for 8 such zero crossings to achieve an 8-cycle average single-particle period measurement which is inverted to obtain frequency and then scaled to obtain velocity; these programs include interpolation between the sample points for very accurate zero-crossing calculations; the simulated measured frequencies are subtracted from the original input frequency to SIGNAL and normalized by division. The resulting normalized errors due to multiparticle phase addition and processor threshold are displayed as in Figure 5 via the PLOT program.

In addition to the above subprograms which were utilized in parametric runs exemplified by Figures 4 and 5, there are also several other program modules existing or under present development for NASA which could be used in later developments of LV applications in the sea. These are as follows:

PMT: This program simulates the physical processes in photo-multiplier detection with inhomogeneous Poisson occurrence of single photoelectron emission events according to any input time-varying classical optical power; it further allows random single photoelectron pulse charge gain according to input selected probability density function, and provides convolution of these impulses with a selectable-width low-pass impulse response; this program thus simulates directly both photon-resolved and higher density "classical" signals with photon shot noise.

FILTER: This is a digital filter program which requires expansion for general purpose use between PMT and COUNT.

CORRELATE: This program counts single photoelectron pulses on uniformly spaced short intervals, computes photon correlation functions,[10,11] and is presently being expanded for NASA to include digital data processing algorithms for velocity extraction from the photon correlograms.

Conclusions

Using the simulation software, and both theory and experiments for noise which were not described in this paper, we have concluded that the multiparticle and photon noise errors do not exclude the use of practical LV systems even under a worse case assumption of all organic ($n \simeq 1.03$) particles limited in diameter to the range ($1.0 \leq d \leq 10$ μm). Both types of error will be reduced by the presence of even a small amount of quartz or other mineral particles ($n \simeq 1.15$), by the existence of larger particles and by adaptive threshold techniques.

Refractive variations of the propagation path will degrade the performance of laser velocimeter systems. However, initial study indicates that systems having separations of 1 meter between the probe volume and the instrument will perform adequately in most ocean environments.

The work up to this point has placed primary emphasis on backscatter fringe velocimeter systems and has revealed where gaps lie in our understanding of the effects of ocean particulates and of refractive effects for velocimeter systems of this type. Ocean measurements presently being prepared are intended to verify modeling that has already been performed and provide an extended data base for future modeling. In the course of our work, we expect to model and analyze each of the four basic system configurations and perform experiments with the most promising.

Acknowledgements

We gratefully acknowledge the support of the Advanced Research Projects Agency and the Naval Sea Systems Command.

References

1. J. D. Trolinger, Laser Instrumentation for Flow Field Diagnositcs, AGARDograph No. 186, National Technical Information Service, Springfield, VA (1974). Also available from Spectron Development Laboratories, 3303 Harbor Blvd., G-3, Costa Mesa, CA 92626.

2. Buchhave, Delhay, Durst, George, Refslund, Whitelaw (Editors), The Accuracy of Flow Measurements by Laser Doppler Methods, published by Proceedings LDA-Symposium Copenhagen 1975, P.O. Box 70, DK-2740, Skovlunde, Denmark.

3. A. J. Hughes, and E. R. Pike, "Remote Measurement of Wind Speed by Laser Doppler Systems," Applied Optics, 12, 597 (March 1973).

4. M. Kerker, The Scattering of Light and Other Electromagnetic Radiation, page 487, Academic Press, N.Y., 1969.

5. R. W. Austin, N. G. Halikas, "The Index of Refraction of Seawater," Visibility Lab, Scripps Institute of Oceanography, La Jolla, CA 92093, SIO Technical Report, Reference No. 76-1 (January 1976).

6. Babak et al., as reported O. A. Sokolov in "Underwater Visibility," Gidrometeoizdat Publishing House, Leningrad (1974).

7. G. Kullenberg, Optical Aspects of Oceanography, edited by N. G. Jerlov & E. S. Nielsen, Academic Press, N.Y., 1974.

8. O. B. Brown and H. R. Gordon, "Size-Refractive Index Distribution of Clear Coastal Water Particulates from Light Scattering," Applied Optics, 13, No. 12, 2874 (December 1974).

9. I. N. McCave, "Vertical Flux of Particulates in the Ocean," Deep Sea Research, 1975, Vol. 22, pg 491.

10. W. T. Mayo, Jr., "Study of Photon Correlation Techniques for Processing of Laser Velocimeter Signals," NASA Langley Contractor Report No. CR-2780, Feb 1977.

11. W. T. Mayo, Jr., "Photon Counting Discriminator for LDV Systems," in Photon Correlation Spectroscopy and Velocimetry, H. Z. Cummins and E. R. Pike Eds., Plenum Press, N.Y., 1977.

APPENDIX B
METHOD OF APPROACH: SIMULATION PROGRAM OPTIC

SCATTERING THEORY MODELS

When we look closely at the scattering theory models which have been used for laser velocimetry calculations in the past, we see that a great many assumptions are used which may not be valid for long propagation distance and large f/no systems when many scatterers are present. This discussion reviews what the assumptions are which will be used here so that a basis for further investigation is established.

Perturbational Approach

Generally, we have assumed that the beam diameter is much, much larger than any scatterers at all points between the transmitter and including the probe volume; that the scatterers are sparse; that the wavefield incident on the probe volume is negligibly affected, except for possible attenuation by the scattering during propagation; and that the multiply scattered light reaching the probe volume is incoherent. These assumptions may be valid even when a considerable amount of the light has been removed from the transmitted beam by narrow angle forward scatter; because even the "narrow angle" scatter less than 10 mili-radians is not in the same angular space with the 10 micro radian transmitter beams. (There could be 10^6 more power in the multiple-scattered component to have the unscattered and multiple-scattered light equal in intensity within the probe volume.)

Plane Wave Approximation

In computing the scattered fields, it is typically assumed that a uniform plane wave is incident on the scattering center. This is based on a second assumption that the scatterer is located within a Gaussian beam waist with plane phase fronts and small change in amplitude over the diameter of the particle. A more exact solution would be obtained by superposition of the results over a spectrum of plane waves (a Fourier synthesis of the Gaussian beam waist), but this is generally unnecessary*.

The Single Scatter Approximation

Let $\bar{u}(\bar{r},\bar{p})$ represent in complex notation a normalized vector electric field at a point $\bar{r}$ on the photodetector surface due to a scatterer at vector location $\bar{p}$ in the scattering volume. The normalization is the square root of the intrinsic impedance of the medium so that for paraxial propagation, the mean power density on the PMT surface at $\bar{r}$ is

$$I(\bar{r}) = \bar{u} \cdot \bar{u}^* = |\bar{u}|^2 \tag{1}$$

where the dot is the vector dot product and the asterisk denotes complex conjugate. If the cathode quantum efficiency is given as a function of $\bar{r}$ as $\eta(\bar{r})$, and the photon energy is $h\nu$, then the expected value of the photocurrent at the cathode is an integral over the cathode area as

$$i = \frac{e}{h\nu} \int_A \eta(\bar{r}) I(\bar{r}) \, dA \tag{2}$$

---

* See Casperson, et al for a discussion of the limitations and additional references: "Single Particle Scattering with Focussed Laser Beams," Applied Optics, 16, p. 1104 (April 1977).

Now for a collection of scatterers with number density high enough to have many scatterers in the probe volume at once, we obtain

$$\bar{u}(\bar{r}) = \sum_{i=1}^{N} \bar{u}_i(\bar{r},\bar{p}_i) \tag{3}$$

where N is the instantaneous number of scatterers present and $\bar{p}_i$ is the location of the ith scatterer. Substitution of (3) into (1) and expansion gives a double summation of self and cross terms:

$$I(\bar{r}) = \sum_i \sum_j \bar{u}_j(\bar{r},\bar{p}_j)\cdot\bar{u}_i{}^*(\bar{r},\bar{p}_i) = \sum_i \sum_j I_{ij}(\bar{r}) \tag{4}$$

The summation of terms I_{ii} is the incoherently added optical power from each scatterer. The cross terms are effects of the coherence of the illumination and scattering process.

Now, this is a subtle point. As long as the collecting lens is much larger than the transmitter beam diameter, then the diffraction limited resolution of the receiver is a much smaller spot at the probe volume than the incident beams. In a diffraction limited system, this would mean that scatterers separated by more than the receiving lens resolution would be imaged to separate locations on the PMT surface. Under these conditions, the I_{ij} terms vanish because only one of the illuminated scatterers is imaged to point $\bar{r}$ on the photocathode. Conservation of energy arguments show that the result must be the same if the receiver is slightly defocussed, or otherwise aberrated by the lens or the propagation medium, since the total power reaching the photocathode is unchanged.

The conclusion of this thought process is that the coherent mixing terms may be neglected as long as the mean distance between scatterers in the image plane exceeds the diffraction limited Airy disc diameter. This condition will generally be satisfied by short range, low f/no systems and will not be satisfied for long range, large f/no systems. This is not a statement about better or worse performance; it is a statement about the validity of the computational models.

The Mie Scattering Approximation - The Field Approach

Generally speaking, the computation of even the single-scatter fields is very complicated and beyond the present day state-of-the-art except for very restrictive assumptions on the scatterer composition and geometry. For a homogenous spherical particle immersed in a lossless medium with a uniform plane wave incident, the well publicized Mie theory provided formulas which may be used for somewhat lengthy calculations of the scattered electric fields. Even in this case, the detailed behavior of the fields is quite complicated for particles larger than a wavelength in diameter. For a fringe LV system we are concerned with a summation of two scattered fields, one from each incident beam, for each scatterer. Thus in the single scatter approximation discussed above, the field $\bar{u}(\bar{r},\bar{p}_i)$ becomes the summation of two fields.

When the intricate details of the field variation are included in a computation of the integral given in (2) with a numerical approximation of the Mie scattering approximation from two beams, then some rather strange behavior is predicted. According to the recent calculations of Ron Adrian* there are cases where the signal "visibility" goes to zero due to cancellation of the sinusoidal component of the signal as a result of changes of phase of the Mie scattering functions across the receiver collecting solid angle. The implications are that the desired sinusoidal signal may sometimes be less than would be predicted using the Mie calculation for single-beam scattered power and assuming the signal "visibility" was unity. We note, however, that this effect is generally not significant when the scatterers are small compared with the fringe spacing. We will neglect such details at the present level of computation but remain aware of the considerations.

Mie Scattering - Integrated Intensity

Significant scatterers in the ocean may be 10 micrometers in diameter or larger. Also refractive perturbations will be minimized by the use of small angles between the transmitted beams and hence large fringe spacing. These considerations suggest the use of fringes which are significantly larger than those typical of low-speed water channel and low-speed air-flow measurements. Fringe spacings of 10-50 micrometers with corresponding beam angles to 0.5 deg (8 mrad) may be appropriate if probe volume size may be adequately reduced to avoid unacceptable multiparticle effects. The lobe structure of the Mie

---

* "Laser Anemometer Signals: Visibility Characteristics and Application to Particle Sizing," Applied Optics, 16, 677 (March 1977).

patterns has characteristic width on the order of λ/d radians. For particles up to 10 μmeter in diameter, this is greater than or equal to about 35 mrad. Thus, for the present, we take the point of view that the relative variations between the two scattered fields and the resulting visibility reduction can be ignored.

The variation of the Mie function over the total solid angle of the collecting lens connot be so easily ignored. At a range of 2 meters, a 15 cm collecting lens subtends a half angle from the beam axis of

$$\mathrm{Tan}^{-1}(7.5/200) = 37.5 \text{ m radian.}$$

An even larger 20 cm diameter lens could be useful, and/or larger particles could be of concern; and significant variation occurs for angles which are a fraction of the full λ/d lobe width. Thus for careful calculations of signal power at a given size and geoemtry, we will have to ultimately resort to integrating the differential scattering cross section over the collecting aperture, or even going to the more complete E field integrations like those of Adrian.

Mie Scattering - Multiparticle Noise Approximation

For the present calculations we intend to totally neglect all of the variations of the differential scattering cross sections with angle. Inclusion of this second-order effect would so greatly increase the complexity of the analysis that a quick parametric study would become impossible (because all of the distributions of scattering amplitudes would then be f/no dependent). Thus, the program OPTIC will generate a realization of signal amplitudes as follows:

a) Realize a set of 1000 particle sizes according to a specified power law distribution (see discussion below).

b) Assign an index of refraction and compute the 1000 associated Mie backscatter coefficients.

c) Separately calculate 1000 random probe volume entry factors. (Assume uniform probability of entry between $1/e^2$ beam power points and obtain profile multipliers.)

d) Use sequential values of scattering coefficients multiplied by sequential values of beam profile factor as the effective scattering coefficients.

e) Multiply by the laser power - optical gain constant to obtain equivalent signal amplitudes.

f) Store amplitudes in a file for use with SIGNL.

g) When running SIGNL, input the effect of absolute number density - probe volume factor computed by OPTIC.

A Mie scattering subroutine is already available. The realization of the power law probability density will be accomplished as a functional mapping of uniform random variable realizations as discussed below.

DEFINITION OF SIZE/INDEX MODEL

Several sources of particle size data have been obtained both by W. T. Mayo, Jr., SDL, and William Stachnik, NUSC, New London. These include unpublished Scripps Coulter counter data from off the coast of Southern California which was provided to Dr. Mayo via Dr. Reichman from Dr. Tom Lang, NOSC. Dr. Lang also sent Dr. Mayo a copy of Techmate TR 74-03-01, "The Nature and Concentration of Ocean Particulate as Related to the Performance of Boundary Layer Suction Slots," by Charles A. Atkinson, which was prepared in 1975 for Autonetics under ARPA-sponsored contract. Mr. Stachnik is presently reviewing new data by Pak, et al. Reviews of the data by Dr. Mayo and Mr. Stachnik will continue under Project COURAGEOUS.

The particle size data that is available has been obtained with a variety of techniques. Much of the data comes from Coulter counters which produce histograms of the total count in each of a sequence of "bins." There is a procedure for converting from the data in this form to the form of a cumulative size distribution.

The cumulative size distribution, $N(d>y)$, is typically given in units of number particles per c.c. with diameter d greater than y. Since all particles have diameter greater than zero, we observe that

$$N(d>y) = N_0 P(d>y)$$

where N_0 is the total number of particles per c.c. and $P(d>y)$ is the probability that a particle sampled from the collection has diameter greater than y. Unfortunately, real instruments cannot measure the total number of particles because of the low size cutoff of the instrument capability. Thus, generally we must replace the definition of N_0 as the number of particles greater than some size y_0 and the probability becomes the conditional probability that $d \geq y$ given that $d > y_0$.

Thus far, our review of the data indicates that in most cases the data may be modeled by an inverse power law in the range 1 to 10 μm diameter as

$$N(d>y) = N_0\left(\frac{y}{y_0}\right)^{-c} \quad , \quad y > y_0 = 1\ \mu m$$

$$= 0 \quad , \quad \text{otherwise}$$

where N_0 is the number of particles per c.c. greater in diameter than y_0, and c is a positive number in the neighborhood of magnitudes 2 to 3. We feel certain that arbitrary extension of this type of model outside the limits 1.0 μm to 10 μm diameter without data would be quite unwise. Physically meaningless garbage can result from singularities at zero and infinite particle diameter.

With the above thoughts in mind and while still reviewing existing models, we have derived a computer simulation procedure for realizing sample particle diameters randomly with a specified power law cumulative distribution function N(d>y). The way this is done is by realizing samples with the correct conditional probability density function $f_y(y)$ as described in detail in the next subsection and using the following relationships to relate the conditional density and the required cumulative distributions. The procedure for using the present simulation model is to pick the values of y_0 and c and the index of refraction to best fit the data for the simulation problem. In the future, more elaborate realization procedures may be desirable for a better fit to a more extensive set of data*.

The steps which relate the given cumulative power law model to the conditional probability density form are as follows. In this discussion, the word "conditional" will be dropped for convenience, although it is a very significant word**. The usual probability distribution function $P_{d<y}$ is given by

$$P_{d<y} = 1 - P_{d \geq y}$$

---

* Or if actual measurements of single-particle backscatter amplitudes are available, these could be stored in a table for direct use in simulations of different number densities.

** A large number of particles in the 0.1 to 1.0 μm diameter range could possibly affect an LDV signal from particles in the 1.0 to 10 μm range whether the model says they are there or not.

$$f_y(y) = \frac{d\left(P_{d<y}\right)}{dy} = -\frac{d\left(P_{d\geq y}\right)}{dy} \quad , \quad y > y_0$$

$$= \frac{c}{y_0}\left(\frac{y}{y_0}\right)^{-(c+1)} \quad , \quad y > y_0$$

$$= 0 \quad , \quad \text{otherwise}$$

In a simulation, the rate of generating the particle diameters is determined by N_0, the total number per c.c.

This very simple procedure will be slightly complicated when the value of y_0 is not 1.0 μm. For example, if the model is extended down to y_0 = 0.2 μm, then N_0, the way we just defined it, is the number of particles greater than 0.2 μm. However, much of the literature defines N as the number of particles greater than 1 μm in diameter. When using such models

$$N_{d>y} = N\left(\frac{y}{1.0\ \mu m}\right)^{-c} \quad , \quad y > y_0 \quad ,$$

but this equates to

$$N_{d>y} = N_0\left(\frac{y}{y_0}\right)^{-c}$$

from which we would obtain

$$N_0 = \left(\frac{y_0}{1.0\ \mu m}\right)^{-c} N$$

as the correct value of N_0 in our approach.

PARTICLE SIZE REALIZATION

Our objective is a subroutine that randomly generates realizations of particle diameter according to a given probability distribution. Subroutines are already available for realizing a uniform random variable. Realization of exponential, Rayleigh, and Gaussian random variables are available also. In this section we discuss realization of a negative power law distribution such that the probability density $f_y(y)$ is

$$f_y(y) = Ky^{-b} \quad , \quad y > y_0 \tag{5}$$

$$= 0 \quad , \quad \text{otherwise}$$

where $b > 1.0$.

The cumulative probability* that $y \geq y_1$ is

$$F(y_1) = \int_{y_1}^{\infty} Ky^{-b}\, dy \quad , \quad y_1 \geq y_0 \tag{6}$$

$$= \frac{Ky_1^{(1-b)}}{b-1}$$

$$= 1 \quad , \quad y_1 \leq y_0$$

From this it follows that

$$K = \frac{b-1}{y_0^{1-b}} \tag{7}$$

---

* The cumulative number density $N > y_1$ is given by $N_0F(y_1)$ where N_0 is the total number of scatterers per unit volume.

Figure B-1 illustrates the transformation of the uniform probability density

$$f_x(x) = 1 \quad , \quad (0 \leq x \leq 1) \qquad (8)$$

$$= 0 \quad , \quad \text{elsewhere}$$

to the desired density $f_y(y)$ via a functional dependence*

$$y = g(x) \qquad (9)$$

with g(x) given by a negative power law function, it is easy to see graphically that

$$y_o = g(x=1) \qquad (10)$$

since $f_x(x) = 0$ for $x > 1$.

Now given $y = g(x)$ the *positive real root* $x_1 = g^{-1}(y)$ is unique for this exercise. From Papoulis* we have, with g'(x), the derivative of $g(x_1)$,

$$f_y(y) = \frac{f_x(x_1)}{|g'(x_1)|} . \qquad (11)$$

We will assume that g(x) is a power law function of the form

$$g(x) = cx^{-a} \quad , \quad a > 0; \qquad (12)$$

---

* For complete discussion of determination of the probability density for a function of a random variable, see Papoulis, Probability, Random Variables, and Stochastic Processes, McGraw Hill, 1965, page 126.

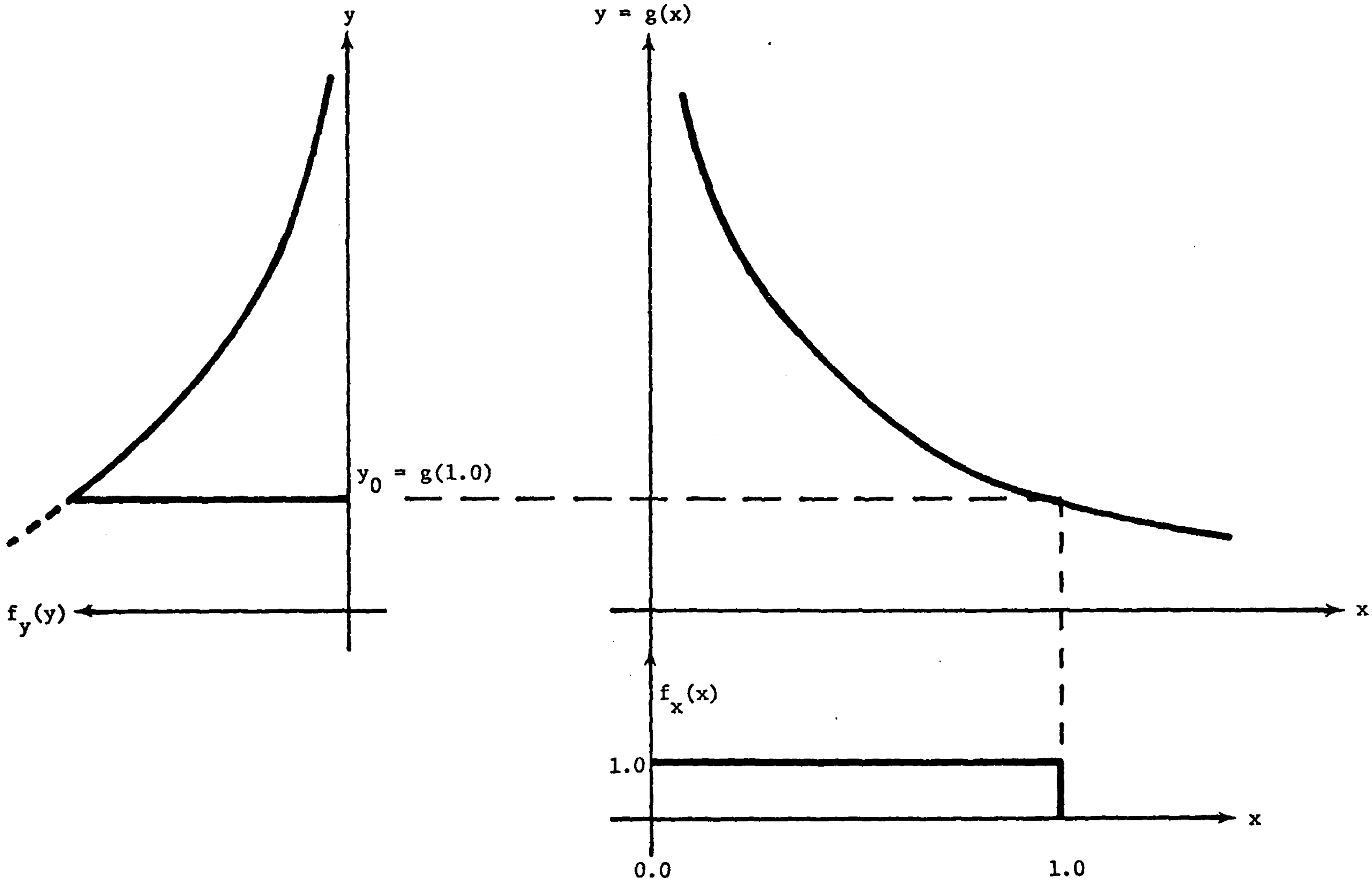

Figure B-1. Probability Density Function Mapping.

and since $g(x=1) = y_0$, we obtain

$$C = y_0 \tag{13}$$

$$g(x) = y_0 \; x^{-a}$$

$$x_1 = \left(\frac{y}{y_0}\right)^{-\frac{1}{a}}$$

with the derivative

$$g'(x) = -a \; y_0 \; x^{-(a+1)} \tag{14}$$

Now, if we picked a functional form for $g(x)$ correctly by hindsight, then when we equate (5), with K substituted from (7), to (11) with $g'(x_1)$ and x_1 from (14) and (13), we should get a simple equation for the functional power law a in terms of the desired power law b. Carrying out these steps leads to equating the powers of y and obtaining

$$a = \left(\frac{1}{b-1}\right). \tag{15}$$

When this is inserted back into the coefficients of the equation, equality is also obtained. Thus, we have the desired result.

To summarize, if we wish to realize random variables with a power law probability density of the form

$$f_y(y) = (b-1)y_0^{(b-1)} \; y^{-b} \quad , \quad y \geq y_0 \tag{16}$$

$$= 0 \;\; \text{elsewhere,}$$

we may do this by realizing random variables x which are uniformly distributed on (0,1) and then computing

$$y = y_0 \, x^{-\left(\frac{1}{b-1}\right)} \tag{17}$$

As an example, let us generate random particle sizes in the range $y \geq 10^{-6}$ m with y^{-4} probability density and a cumulative y^{-3} law. Then

$$y_0 = 10^{-6} \quad , \quad b = 4 \quad , \quad a = \frac{1}{3}$$

$$g(x) = 10^{-6} \, x^{-\frac{1}{3}}$$

OPTIC - FRINGE MODE

The objective of this program is to accept the system parameters as inputs and generate the inputs required by SIGNL. This program assumes that the scatterers are spherical with a negative power law size distribution truncated at a minimum diameter y_0.

The key inputs for SIGNL that OPTIC must calculate are:

1. Mean burst rate.
2. Optical gain factor.
3. Realization of Mie scattering cross section.
4. The number of cycles between the $1/e^2$ value of the signals.
5. Signal visibility factor (unity for now).

Other required inputs for SIGNL include the sampling interval DT and the total simulated signal duration.

We will assume that the mean transverse velocity V is perpendicular to the fringes. Any *random* velocity fluctuation which is assumed due to probe volume gradients or small scale turbulence will be assigned as a fraction of the mean. The program will compute the mean frequency as

$$f_m = \frac{2nV}{\lambda_0} \sin\left(\frac{\theta}{2}\right)$$

where n = index of refraction

λ_0 = free-space wavelength of laser

θ = angle between the beams in the medium at the probe volume.

The number of stationary cycles between the $1/e^2$ points on the fringe pattern is determined by the ratio of the transmitter beam separation to the beam radius at the transmitter output lens as

$$N_f = \frac{4\ R \sin\left(\frac{\theta}{2}\right)}{\pi\, w_t \cos\left(\frac{\theta}{2}\right)} \approx \frac{2d}{\pi w_t}$$

where $\tan\frac{\theta}{2} \approx \frac{d}{2R}$, θ = small angle

R = range to beam crossover

w_t = $1/e^2$ beam radius at the transmitter

d = separation between the beams at the transmitter.

The program will use the exact form for N_f with the tan $\left(\frac{\theta}{2}\right)$. For small turbulence levels, N_f is also the number of signal cycles.

The realization of the Mie scattering coefficients will be performed by the program as follows. The particle inputs are lower cutoff size, slope, and total number per cubic meter* and the relative index of refraction. The procedure previously discussed will be used to realize a set of particle diameters for use in computing the differential scattering cross section σ. The only other required factor is the optical gain constant which is the amplitude of a signal from a particle with unit scattering cross-section passing through the center of the probe volume.

The optical gain constant will be defined in such a way for the fringe mode that the output values will be peak mean photo-electron rate λ_p at the photocathode given by

$$\lambda_p = \frac{P\eta}{h\nu}$$

where P = peak optical signal power collected, averaged over a Doppler cycle (peak pedestal exclusive of any constant background)

η = the cathode quantum efficiency

$h\nu$ = the photon energy.

---

* Previous discussion concerning literature gives N_0 per cc. Such values must be multiplied by 10^6 for input to OPTIC.

In order to relate the signals thus produced by SIGNL to the processor current thresholds in COUNT, the input scale factor of COUNT must be

$$SCALE = GRe$$

where G is the dynode current gain,

R is the effective load resistor (including any preamp gain)

e = electronic charge in coulombs.

The collected peak optical signal power is given by

$$P_{sj} = \left(I_{inc}\right)\left(\sigma_j\right)\left(\Omega\right) e^{-cR} \text{ (FACT)}$$

$$= \left(\frac{2P_0T}{\pi r_0^2}\right)\left(\sigma_j\right)\left(\frac{A_c}{R^2}\right) e^{-2cR} \text{ (FACT)}$$

where FACT = random probe volume entry factor

Ω = collection solid angle

I_{inc} is the peak intensity in center of probe volume

P_0 = laser power

T = transmission efficiency of transmitter-receiver optics

$r_0 = \frac{\lambda R}{\pi w_t} = 1/e^2$ width in probe volume

σ_j = differential Mie scattering cross section for $\theta = 180°$

λ_0 = free-space wavelength

n = index of refraction of the propagation medium

A_c = receiver collection area

R = range

c = attenuation coefficient.

The σ_j quantity will be realized randomly as previously discussed. The remaining factors constitute the optical gain and the laser power. Thus, the optical gain constant is defined by

$$P_{sj} = P_0 \; G_0 \; \sigma_j \; FACT$$

$$G_0 = \frac{2t \; A_c}{\pi \; r_0^2 \; R^2} \; e^{-2cR}$$

The rate of Poisson occurrence of the signal bursts is given by

$$\lambda_b = N_0 \; V \; A_p$$

where N_0 = total number of particles greater than y_0 in diameter per cubic meter

A_p = cross sectional area of probe volume in direction of mean velocity.

We have decided to limit the width of the probe volume observed by the receiver with a slit at the image of the probe volume which is equal to the image of the $1/e^2$ diameter, $2r_0$. The probe volume length will be restricted by the same slit in conjunction with a small off-axis viewing angle ϕ to $\approx 2r_0/\phi$. The off-axis viewing effect will be created by annular collection or a separate off-axis collecting lens. Thus, the probe volume cross-sectioned area is

$$A_p \approx \left(2r_0\right)^2/\phi \quad .$$

APPENDIX C

OPTIC: A SIMULATION PROGRAM FOR FRINGE AND REFERENCE BEAM LV SIGNALS

The program OPTIC described in the Oceans '77 paper by Stachnik and Mayo was developed by Spectron Development Laboratories for ARPA under NUSC Contract No. N00140-77-C-6670. As part of a concurrent COURAGEOUS Support Contract NUSC No. N66604-77-M-8709, we have expanded the program to include an option for calculation of single-particle reference beam LV signal parameters. In order that both sponsors may benefit from all of the work, a printout of the expanded version of OPTIC is herewith included in both contract final reports. The theory for the fringe system equations is discussed in the ARPA report and that for the reference beam is discussed in the COURAGEOUS report.

A list of the input variables for the program OPTIC is given in Table C-1. The equations used in OPTIC are provided algebraicly in Tables C-2, C-3, and C-4 using the variable names from OPTIC to assist a reader in relating the theory discussions to the FORTRAN IV software language. Table C-2 is a list of output quantities common to both fringe and reference beam options. The quantities specific to the fringe and reference beam options are listed in Tables C-3 and C-4.

Values for the input variables in OPTIC may be read in either from an interactive terminal or from a previously prepared disc file specified by the user. In order to save execution time by avoiding repetitious calculations, there also exists the option to read the differential Mie scattering cross sections from a previously generated table stored on disc. If this option is not selected, the Mie scattering cross sections are calculated and stored in a table on disc in order to be available for future runs of OPTIC. If this option is selected and the end of the *table of Mie* values is reached before the specified number of amplitudes is generated, then control returns to the beginning of the file and the values are used again.

Table C-1. OPTIC Input Variables.

N	=	Index of refraction of particle (complex)
NZERO	=	Index of refraction of medium (real)
LAMBZ	=	Free-space wavelength
THETA	=	Angle between beams
R	=	Range to beam crossover
WT	=	e^{-2} beam radius at transmitter
YZERO	=	Lower cutoff particle diameter
DMAX	=	Upper cutoff particle diameter
NPART	=	Total number of particles/m^3
PHI	=	Off-axis viewing angle
T	=	Transmission efficiency of optics
RCA	=	Receiver collection area
V	=	Transverse particle velocity
C	=	Attenuation coefficient of medium
PZERO	=	Laser power
ETA	=	Cathode quantum efficiency
B	=	Coefficient in negative power law distribution
LIMIT	=	Number of burst amplitudes to generate
MODE	=	{ 1 = fringe option 2 = reference beam option
MIELM	=	Maximum number of Mie Iterations to be performed

Additional Inputs for Reference Beam Option:

PR	=	Reference beam power
VZ	=	Axial velocity

Table C-2. OPTIC Outputs Common to Both Fringe and Reference Beam Options.

FM = Fringe signal frequency = $\frac{2 \cdot NZERO \cdot V}{LAMBZ} \cdot \sin\left(\frac{THETA}{2}\right)$

SIGP = Fringe signal period = $\frac{1}{FM}$

BSTWD = e^{-2} burst width = NF•SIGP

BANDW = Bandwidth* = $\frac{1}{BSTWD}$

RZERO = Focal beam radius = $\frac{LAMBZ \cdot R}{NZERO \cdot \pi \cdot WT}$

AP = Cross sectional area of probe volume (in direction of transverse velocity) = $\frac{(2 \cdot RZERO)^2}{PHI}$

LAMBB = Burst rate = NPART•AP•V

SEPAR = Burst separation = $\frac{1}{LAMBB}$

BRATE = Number of particles in probe volume = $\frac{BSTWD}{SEPAR}$

FSRS = Axial velocity sensitivity (Hertz/m/sec) = $\frac{2 \cdot NZERO}{LAMBZ}$

T = Total simulation time estimate (for input into SIGNL program = LIMIT•SEPAR

---

* This bandwidth is $\pi/4$ times the e^{-2} width of the signal power spectrum due to transit time only and is thus probably the smallest that could ever be realized even with a tracking filter.

Table C-3. OPTIC Outputs for Fringe Option.

GZERO = Gain constant = $\frac{2 \cdot T \cdot RCA}{\pi \cdot RZERO^2 \cdot R^2} e^{-2 \cdot C \cdot R}$

DT = Signal sampling interval (for input into SIGNL program) = $\frac{1}{17.314159 \cdot FM}$

NF = Number of fringes = $\frac{4 \cdot R}{\pi \cdot WT} \tan\left(\frac{THETA}{2}\right)$

Output Files of Randomly Realized Burst Values

Table File:

DIAM = Random particle diameter (meters)

SIGMA = Differential Mie scattering cross section ($meter^2$)

FACT = Random probe volume entry factor (dimensionless)

PC = Collected optical power at detector (watts) = PZERO•GZERO•SIGMA•FACT

SNR = Peak signal-to-noise power ratio = $\frac{AMPL}{4 \cdot BANDW}$

Amplitude File:

AMPL = Peak photoelectron rate = $PC \cdot \left(\frac{ETA}{HV}\right)$

Table C-4. OPTIC Outputs for Reference Beam Option.

RBPR = DC cathode photon rate due to reference beam = $\frac{ETA}{HV} \cdot PR$

IDC = Cathode DC current = $RBPR \cdot 1.6x10^{-19}$

REFRQ = Reference system signal frequency = FSRS•VZ

DT = Signal sampling interval (for input into SIGNL program) = $\frac{1}{17.314159 \cdot REFRQ}$

AC = Effective receiver collection area = $\pi \cdot (WT)^2$

GR = Gain constant = $\left(4\pi\right)\left(\frac{ETA \cdot 1.6x10^{-19}}{HV}\right)\left(\frac{WT^2 \cdot NZERO}{R^2 \cdot LAMBZ}\right)\left(\sqrt{T}\right)e^{-C \cdot R}$

NFREF = Number of fringes (for input into SIGNL program) = $\frac{4\ R}{\pi \cdot WT} \tan\left(\frac{THETA}{2}\right) \cdot \left(\frac{REFRQ}{FM}\right)$

Output Files of Randomly Realized Burst Values

Table File:

DIAM = Random particle diameter (meters)

SIGMA = Differential scattering cross section

FACT = Random probe volume entry factor = e^{-2X^2}, X is a random variable uniformly distributed on (0,1)

SNR = Peak signal-to-noise power ratio = $\frac{AMPI^2}{4 \cdot (1.6x10^{-19}) \cdot IDC \cdot BANDW}$

AMPI = Peak cathode signal current = $\left(\sqrt{PR \cdot PZERO}\right)\left(GR\right)\left(\sqrt{SIGMA}\right)\left(FACT\right)$

Table C-4. OPTIC Outputs for Reference Beam Option (Cont'd)

Amplitude File for SIGNL:

AMPL = Peak cathode signal current expressed as a photoelectron rate = $\frac{AMPI}{1.6 \times 10^{-19}}$

```
FTN4,L
      PROGRAM OPTIC
C
C     THIS PROGRAM ACCEPTS THE SYSTEM PARAMETERS AS INPUTS AND
C     GENERATES THE INPUTS REQUIRED BY SIGNL.  IT IS ASSUMED THAT
C     THE SCATTERERS ARE SPHERICAL WITH A NEGATIVE POWER LAW SIZE
C     DISTRIBUTION TRUNCATED AT A MINIMUM AND MAXIMUM DIAMETER.
C
C     OPTIC GENERATES UP TO 3 SEPARATE FILES--ONE CONTAINS THE INPUT
C     AMPLITUDES FOR SIGNL, ONE CONTAINS A TABLE OF VALUES
C     INCLUDING SUCH INFORMATION AS THE PARTICLE DIAMETERS AND FACTORS
C     GENERATED, AND THE THIRD (POSSIBLE) FILE CONTAINS A TABLE OF
C     DIAMETERS AND MIE COEFFICIENTS TO BE USED IN FUTURE RUNS IN
C     ORDER TO SAVE EXECUTION TIME
C
      REAL LAMB,LAMBB,LAMBZ,NPART,NF,KL,NZERO,IDC,NFREF
      COMPLEX N
      DIMENSION ITIME(5),IYEAR(1),IPRAM(5),ID9(144),IB9(40),NAM9(3),
     +NAM2(3),IB2(40),ID2(144)
      COMMON NAM7(3),NAM8(3),IOPT7,IOPT8,ID7(144),
     +ID8(1296),IB7(40),IB8(40),LU
      CALL RMPAR(IPRAM)
      RN=47594118.0
      PI=3.14159265
      LU=IPRAM(1)
      IF(LU.EQ.0)LU=1
      WRITE(LU,21)
   21 FORMAT(" DO YOU WANT THE MIE VALUES READ FROM AN INPUT TABLE?")
      READ(LU,22)ITAB
   22 FORMAT(A2)
      IF(ITAB.EQ.2HYE)GO TO 25
      WRITE(LU,3)
    3 FORMAT(" ENTER FILE NAME FOR OUTPUT MIE VALUES")
      READ(LU,4)(NAM9(I),I=1,3)
    4 FORMAT(3A2)
      IOPT9=100
      CALL CREAT(ID9,IERR,NAM9,IOPT9,3,0,12,144)
      CALL CODE
      WRITE(IB9,6)
    6 FORMAT(" TABLE OF MIE SCATTERING COEFFICIENTS")
      CALL WRITF(ID9,IERR,IB9,40)
      NHEAD=2
      CALL CODE
      WRITE(IB9,7)NHEAD
    7 FORMAT(I5," LINES OF HEADER INFORMATION",5X)
      CALL WRITF(ID9,IERR,IB9,40)
      GO TO 9
   25 WRITE(LU,5)
    5 FORMAT(" ENTER INPUT FILE NAME OF MIE VALUES")
      READ(LU,4)(NAM9(I),I=1,3)
      CALL OPEN(ID9,IERR,NAM9,3,0,12,144)
      DO 114 I=1,4
  114 CALL READF(ID9,IERR,IB9,40)
    9 CALL NAME
      WRITE(LU,35)
```

```
  35  FORMAT(" DO YOU WANT SYSTEM INPUT VALUES READ FROM A FILE?")
      READ(LU,22)IN
      IF(IN.EQ.2HYE)GO TO 38
      WRITE(LU,10)
  10  FORMAT(" INPUT THE FOLLOWING:"/
     +      "     (1) INDEX OF REFRACTION OF PARTICLE(REAL,IMAG)"/
     +      "     (2) INDEX OF REFRACTION OF MEDIUM"/
     +      "     (3) FREE-SPACE WAVELENGTH"/
     +      "     (4) ANGLE BETWEEN BEAMS"/
     +      "     (5) RANGE TO BEAM CROSS OVER"/
     +      "     (6) 1/E**2 BEAM RADIUS AT TRANSMITTER")
      READ(LU,*)N,NZERO,LAMBZ,THETA,R,WT
      WRITE(LU,20)
  20  FORMAT(" INPUT THE FOLLOWING:"/
     +      "     (1) LOWER CUTOFF PARTICLE DIAMETER"/
     +      "     (2) UPPER CUTOFF PARTICLE DIAMETER"/
     +      "     (3) TOTAL # OF PARTICLES/M**3"/
     +      "     (4) OFF-AXIS VIEWING ANGLE"/
     +      "     (5) TRANSMISSION EFFICIENCY OF OPTICS"/
     +      "     (6) RECEIVER COLLECTION AREA"/
     +      "     (7) TRANSVERSE PARTICLE VELOCITY")
      READ(LU,*)YZERO,DMAX,NPART,PHI,T,RCA,V
      WRITE(LU,30)
  30  FORMAT(" INPUT THE FOLLOWING:"/
     +      "     (1) ATTENUATION COEFFICIENT OF MEDIUM"/
     +      "     (2) LASER POWER"/
     +      "     (3) CATHODE QUANTUM EFFICIENCY"/
     +      "     (4) B COEFFICIENT IN NEGATIVE POWER LAW PROB DIST"/
     +      "     (5) INTEGER NUMBER OF AMPLITUDES TO GENERATE"/
     +      "     (6) MODE OPTION: 1=FRINGE  2=REFERENCE BEAM"/
     +      "     (7) UPPER LIMIT OF MIE ITERATIONS")
      READ(LU,*)C,PZERO,ETA,B,LIMIT,MODE,MIELM
      GO TO 39
  38  WRITE(LU,400)
 400  FORMAT(" ENTER FILE NAME")
      READ(LU,4)(NAM2(I),I=1,3)
      CALL OPEN(ID2,IERR,NAM2,3,0,12,144)
      CALL READF(ID2,IERR,IB2,40)
      CALL CODE
      READ(IB2,410)N,NZERO,LAMBZ,THETA
 410  FORMAT(5E16.8)
      CALL READF(ID2,IERR,IB2,40)
      CALL CODE
      READ(IB2,410)R,WT,YZERO,DMAX,NPART
      CALL READF(ID2,IERR,IB2,40)
      CALL CODE
      READ(IB2,411)PHI,T,RCA,V
 411  FORMAT(4E16.8)
      CALL READF(ID2,IERR,IB2,40)
      CALL CODE
      READ(IB2,411)C,PZERO,ETA,B
      CALL READF(ID2,IERR,IB2,40)
      CALL CODE
      READ(IB2,420)LIMIT,MODE,MIELM
 420  FORMAT(3I5)
```

```
39   HV=1.987E-25/LAMBZ
     TERM=ETA/HV
     LAMB=LAMBZ/NZERO
     FSRS=2.0/LAMB
     IF(MODE.EQ.1)GO TO 41
     WRITE(LU,42)
42   FORMAT(" INPUT REFERENCE BEAM POWER")
     READ(LU,*)PR
     RBPR=TERM*PR
     IDC=RBPR*(1.6E-19)
     WRITE(LU,43)
43   FORMAT(" INPUT AXIAL VELOCITY")
     READ(LU,*)VZ
     REFRQ=FSRS*VZ
     AC=PI*WT*WT
41   CALL CREAT(ID8,IERR,NAM8,IOPT8,3,0,12,1296)
     CALL CREAT(ID7,IERR,NAM7,IOPT7,3,0,12,144)
C
C    GET TIME OF DAY (TO STORE IN HEADERS OF CREATED FILES).
C
     CALL EXEC(11,ITIME,IYEAR)
C
C    COMPUTE MEAN FREQUENCY AND SIGNAL PERIOD
C
     FM=2.*NZERO/LAMBZ*SIN(THETA/2.)*V
     SIGP=1.0/FM
C
C    COMPUTE THE BURST WIDTH (# OF FRINGES) AND
C    THE 1/E**2 BURST WIDTH
C
50   NF=4*R/(PI*WT)*TAN(THETA/2.)
     IF(MODE.EQ.2)NFREF=NF*REFRQ/FM
     BSTWD=NF*SIGP
     BANDW=1.0/BSTWD
     RZERO=LAMB*R/(PI*WT)
C
C    COMPUTE CROSS SECTIONAL AREA OF PROBE VOLUME IN DIRECTION OF
C    MEAN VELOCITY
C
     AP=(2.*RZERO)**2.0/PHI
     LAMBB=NPART*AP*V
C
C    COMPUTE BURST SEPARATION AND ESTIMATES FOR T AND DT (TO BE USED
C    IN SIGNL).  ALSO COMPUTE 'BRATE' = THE # OF PARTICLES IN 1/E**2
C    PROBE VOLUME AT ONCE
C
     SEPAR=1./LAMBB
     BRATE=BSTWD/SEPAR
     TOTDT=LIMIT*SEPAR
     IF(MODE.EQ.1)DT=1.0/(17.314159*FM)
     IF(MODE.EQ.2)DT=1.0/(17.314159*REFRQ)
C
C    OUTPUT HEADER INFORMATION TO FILES
C
     CALL CODE
```

```
      WRITE(IB8,59)
   59 FORMAT("  OPTIC OUTPUT")
      CALL WRITF(ID8,IERR,IB8,40)
      NHEAD=21
      IF(MODE.EQ.1)NHEAD=19
      CALL CODE
      WRITE(IB8,33)NHEAD
   33 FORMAT(I5,"  LINES OF HEADER INFORMATION")
      CALL WRITF(ID8,IERR,IB8,40)
      CALL CODE
      WRITE(IB8,31)ITIME(5),IYEAR(1),ITIME(4),ITIME(3),ITIME(2)
   31 FORMAT(" CREATION DATE: ",I5,1X,I5,"          TIME: ",3I5)
      CALL WRITF(ID8,IERR,IB8,40)
      CALL CODE
      WRITE(IB7,32)
   32 FORMAT(" OPTIC OUTPUT--TABLE OF VALUES")
      CALL WRITF(ID7,IERR,IB7,40)
      CALL CODE
      WRITE(IB7,31)ITIME(5),IYEAR(1),ITIME(4),ITIME(3),ITIME(2)
      CALL WRITF(ID7,IERR,IB7,40)
      IF(MODE.EQ.1)GO TO 508
      CALL CODE
      WRITE(IB7,509)
  509 FORMAT("     DIAMETER   SIGMA          FACT           SNR",8X,"AMPI")
      CALL WRITF(ID7,IERR,IB7,40)
      GO TO 507
  508 CALL CODE
      WRITE(IB7,610)
  610 FORMAT("     DIAMETER    SIGMA          FACT           PC",9X,"SNR")
      CALL WRITF(ID7,IERR,IB7,40)
  507 CALL CODE
      WRITE(IB8,60)N,NZERO
   60 FORMAT(" N(PARTICLE)=",2F8.4," N(MEDIUM)=",F8.4,10X)
      CALL WRITF(ID8,IERR,IB8,40)
      CALL CODE
      WRITE(IB8,62)LAMBZ,THETA
   62 FORMAT(" FREE SPACE WAVELENGTH=",E10.4,
     +"   ANGLE BETWEEN BEAMS=",E10.4)
      CALL WRITF(ID8,IERR,IB8,40)
      CALL CODE
      WRITE(IB8,64)R,WT
   64 FORMAT(" RANGE TO BEAM CROSS OVER=",E10.4,
     +"   1/E**2 BEAM RADIUS=",E10.4)
      CALL WRITF(ID8,IERR,IB8,40)
      CALL CODE
      WRITE(IB8,66)YZERO,DMAX
   66 FORMAT(" LOWER CUTOFF SIZE=",E10.4,
     +"       UPPER CUTOFF SIZE=",E10.4,10X)
      CALL WRITF(ID8,IERR,IB8,40)
      CALL CODE
      WRITE(IB8,81)PHI,T
   81 FORMAT(" OFF AXIS VIEWING ANG=",E10.4,
     +"  TRANSMISSION EFFICIENCY=",E10.4)
      CALL WRITF(ID8,IERR,IB8,40)
      IF(MODE.EQ.1)GO TO 89
```

```
      CALL CODE
      WRITE(IB8,82)AC,NFREF
82    FORMAT(" EFFECTIVE RECEIVER COLLECTION AREA=",E10.4,
     +"  # FRINGES(REF)=",E10.4,20X)
      CALL WRITF(ID8,IERR,IB8,40)
      GO TO 79
89    CALL CODE
      WRITE(IB8,78)RCA
78    FORMAT(" RECEIVER COLLECTION AREA=",E10.4,40X)
      CALL WRITF(ID8,IERR,IB8,40)
79    CALL CODE
      WRITE(IB8,83)C,PZERO
83    FORMAT(" ATTENUATION COEFF=",E10.4,"    LASER POWER=",E10.4,20X)
      CALL WRITF(ID8,IERR,IB8,40)
      CALL CODE
      WRITE(IB8,84)ETA
84    FORMAT(" CATHODE QUANTUM EFFIC.=",E10.4,30X)
     +"       BRAGG CELL OFFSET FREQ=",E10.4)
      CALL WRITF(ID8,IERR,IB8,40)
      CALL CODE
      WRITE(IB8,85)B,LIMIT
85    FORMAT(" B COEFF. IN NEG. POWER LAW DIST.=",E10.4,
     +" # OF AMP.'S GENERATED=",I5)
      CALL WRITF(ID8,IERR,IB8,40)
      CALL CODE
      WRITE(IB8,86)V,NPART
86    FORMAT(" VELOCITY=",E10.4,"    TOTAL # OF PARTICLES=",E10.4,25X)
      CALL WRITF(ID8,IERR,IB8,40)
      CALL CODE
      WRITE(IB8,68)FM,SIGP
68    FORMAT(" FREQ(FRINGE)=",E16.8,"    SIGNAL PERIOD(FRINGE)=",
     +E16.8,15X)
      CALL WRITF(ID8,IERR,IB8,40)
      CALL CODE
      WRITE(IB8,88)MODE,MIELM
88    FORMAT(" MODE=",I1," (1=FRINGE,2=REF.BEAM)",
     +"     MIE LOOP LIMIT=",I5,22X)
      CALL WRITF(ID8,IERR,IB8,40)
      DO 80 I=1,40
80    IB8(I)=2H
C
C     COMPUTE 1/E**2 WIDTH IN PROBE VOLUME AND COMPUTE OPTICAL
C     GAIN CONSTANT
C
      IF(MODE.EQ.1)GO TO 47
      EXPCR=EXP(-C*R)
      GR=4.0*PI*TERM*(1.6E-19)*(WT**2.0)*NZERO*SQRT(T)*EXP(-C*R)
     +/(R**2.0*LAMBZ)
      PG=PZERO*GR
      GO TO 48
47    EXPCR=EXP(-2.*C*R)
      GZERO=((2.0*T*RCA)/(PI*RZERO**2.0*R**2.0))*EXPCR
      PG=PZERO*GZERO
48    CALL CODE
      WRITE(IB8,90)SEPAR,LAMBB
```

```
   90 FORMAT(" BURST SEPARATION=",E16.8,"     BURST RATE=",E16.8)
      CALL WRITF(ID8,IERR,IB8,40)
      CALL CODE
      WRITE(IB8,91)BSTWD,BANDW
   91 FORMAT(" 1/E**2 BURST WIDTH=",E10.4,"    BANDWIDTH=",E10.4,15X)
      CALL WRITF(ID8,IERR,IB8,40)
      IF(MODE.EQ.1)GO TO 105
      CALL CODE
      WRITE(IB8,94)GR,EXPCR
   94 FORMAT(" GR=GAIN CONSTANT(INCLUDES EXP(-CR))=",E10.4,
     +"    EXP(-CR)=",E10.4,10X)
      CALL WRITF(ID8,IERR,IB8,40)
      GO TO 106
  105 CALL CODE
      WRITE(IB8,92)GZERO,EXPCR
   92 FORMAT(" GAIN CONSTANT(INCLUDES EXP(-2CR))=",E10.4,
     +" EXP(-2CR)=",E10.4,10X)
      CALL WRITF(ID8,IERR,IB8,40)
  106 CALL CODE
      WRITE(IB8,93)PG,BRATE
   93 FORMAT(" P*G=",E10.4,"    # OF PARTICLES IN PROBE VOLUME=",
     +E10.4,23X)
      CALL WRITF(ID8,IERR,IB8,40)
      IF(MODE.EQ.1)GO TO 98
      CALL CODE
      WRITE(IB8,95)PR,RBPR
   95 FORMAT(" REF BEAM POWER=",E10.4,"    REF BEAM PHOTON RATE=",
     +E10.4,10X)
      CALL WRITF(ID8,IERR,IB8,40)
      SIGP=1.0/REFRQ
      CALL CODE
      WRITE(IB8,97)REFRQ,SIGP
   97 FORMAT(" REFERENCE FREQUENCY=",E16.8,"  REF.SIGNAL PERIOD=",
     +E10.4)
      CALL WRITF(ID8,IERR,IB8,40)
      CALL CODE
      WRITE(IB8,220)VZ,IDC
  220 FORMAT(" AXIAL VELOCITY=",E10.4,"     IDC=",E10.4,25X)
      CALL WRITF(ID8,IERR,IB8,40)
      GO TO 96
   98 CALL CODE
      WRITE(IB8,99)NF
   99 FORMAT(" # OF FRINGES=",E16.8,35X)
      CALL WRITF(ID8,IERR,IB8,40)
   96 CALL CODE
      WRITE(IB8,46)TOTDT,DT
   46 FORMAT(" T=",E16.8,"      DT=",E16.8,30X)
      CALL WRITF(ID8,IERR,IB8,40)
C
C     'TTIME' AND 'DTIME' ARE USED TO PUT THE OUTPUT FILE IN A FORMAT
C     SUITABLE FOR INPUT INTO THE HISTOGRAM PROGRAM OR THE PLOT PROGRAM
C
      TTIME=FLOAT(LIMIT)
      DTIME=1.0
      CALL CODE
```

```
      WRITE(IB8,71)TTIME,DTIME
   71 FORMAT(2E16.8,30X)
      CALL WRITF(ID8,IERR,IB8,40)
      CN1=REAL(N)
      CN2=AIMAG(N)
      KL=2.*PI/LAMB
      IF(ITAB.EQ.2HYE)GO TO 72
      CALL CODE
      WRITE(IB9,73)CN1,CN2
   73 FORMAT(" CN1=",E10.4," CN2=",E10.4," THETA= 180 DEGREES")
      CALL WRITF(ID9,IERR,IB9,40)
      CALL CODE
      WRITE(IB9,74)
   74 FORMAT("    DIAMETER      I-PERPENDICULAR      I-PARALLEL ")
      CALL WRITF(ID9,IERR,IB9,40)
C
C     GENERATE REALIZATIONS OF PARTICLE DIAMETER ACCORDING TO NEGATIVE
C     POWER LAW DISTRIBUTION
C
   72 DO 100 I=1,LIMIT
      IF(ITAB.NE.2HYE)GO TO 110
      CALL READF(ID9,IERR,IB9,24,LEN)
      IF(LEN.NE.-1)GO TO 117
      CALL RWNDF(ID9,IERR)
      DO 116 K=1,5
  116 CALL READF(ID9,IERR,IB9,40)
  117 CALL CODE
      READ(IB9,111)PSIZE,COEF1
  111 FORMAT(2E16.8,16X)
      X=RAND(4,RN,0.)
      GO TO 112
  110 X=RAND(4,RN,0.)
      PSIZE=YZERO*X**(-(1/(B-1)))
      IF(PSIZE.GE.DMAX)GO TO 110
      PSIZE=PSIZE*(KL/2.0)
C
C     GENERATE MIE SCATTERING COEFFICIENTS
C
      CALL MIE(PSIZE,CN1,CN2,180.,MIELM,COEF1,COEF1)
      CALL CODE
      WRITE(IB9,113)PSIZE,COEF1,COEF1
  113 FORMAT(3E16.8,5X)
      CALL WRITF(ID9,IERR,IB9,24)
  112 SIGMA=COEF1/KL**2.0
C
C     GENERATE RANDOM PROBE VOLUME ENTRY FACTORS
C
      X=RAND(4,RN,0.)
      X=(X-.5)*2.
      FACT=EXP(-2.*ABS(X)**2.0)
C
C     COMPUTE EFFECTIVE SCATTERING COEFFICIENTS THEN OBTAIN EQUIVALENT
C     SIGNAL AMPLITUDES
C
      PC=FACT*PO*SIGMA
```

```
      AMPL=PC*TERM
      IF(MODE.EQ.2)AMPI=SQRT(PR*PZERO)*GR*SQRT(SIGMA)*FACT
      IF(MODE.EQ.2)AMPL=AMPI/(1.6E-19)
      CALL CODE
      WRITE(IB8,500)AMPL
500   FORMAT(E16.8,60X)
      CALL WRITF(ID8,IERR,IB8,8)
      PSIZE=PSIZE/(KL/2.0)
      IF(MODE.EQ.1)GO TO 101
      SNR=AMPI**2.0/(4.0*(1.6E-19)*IDC*BANDW)
      CALL CODE
      WRITE(IB7,510)PSIZE,SIGMA,FACT,SNR,AMPI
      CALL WRITF(ID7,IERR,IB7,40)
      GO TO 100
101   SNR=AMPL/(4.0*BANDW)
      CALL CODE
      WRITE(IB7,510)PSIZE,SIGMA,FACT,PC,SNR
510   FORMAT(5E12.4)
      CALL WRITF(ID7,IERR,IB7,40)
100   CONTINUE
      CALL LOCF(ID7,IERR,IREC,IRB,IOFF,JSEC)
      ITRUN=JSEC/2-IRB-1
      CALL CLOSE(ID7,IERR,ITRUN)
      IF(IERR.LT.0)CALL CLOSE(ID7)
      CALL LOCF(ID8,IERR,IREC,IRB,IOFF,JSEC)
      ITRUN=JSEC/2-IRB-1
      CALL CLOSE(ID8,IERR,ITRUN)
      IF(IERR.LT.0)CALL CLOSE(ID8)
      IF(ITAB.EQ.2HYE)GOTO 250
      CALL LOCF(ID9,IERR,IREC,IRB,IOFF,JSEC)
      ITRUN=JSEC/2-IRB-1
      CALL CLOSE(ID9,IERR,ITRUN)
      IF(IERR.LT.0)CALL CLOSE(ID9)
      GOTO 270
250   CALL CLOSE(ID9)
270   STOP
      END
```

FTN4 COMPILER: HP92060-16092 REV. 1726

** NO WARNINGS ** NO ERRORS ** PROGRAM = 04098 COMMON = 01529

```
      FUNCTION RAND(I,Q,G)
C- THIS ROUTINE COMPUTES A RANDOM VARIABLE ACCORDING TO I
C-    I=1,CALCULATE AN EXPONENTIAL R.V., MEAN=1
C-    I=2,CALCULATE A  RAYLIEGH  R.V.,   MEAN=1
C-    I=3,CALCULATE A  GAUSSIAN  R.V.,   MEAN=1 NORM.S.D.=G
C-    I=4,CALCULATE A  UNIFORM   R.V., RANGE 0 TO 1
      Q=23.0*Q
      Q=AMOD(Q,100000001.0)
      X=Q/100000001.0
      GO TO (1,2,2,4),I+0.0
    4 RAND=X
      RETURN
    1 RAND=ALOG(1.0/X)
      RETURN
    2 RAND=SQRT(-2*ALOG(X))*SQRT(2/3.14159265)
      IF(I.EQ.2)RETURN
      RAY=RAND
      Q=23.0*Q
      Q=AMOD(Q,100000001.0)
      X=Q/100000001.0
      RAND=G*(RAY*COS(6.2831853*X))/SQRT(2/3.14159265)+1
      RETURN
      END
```

FTN4 COMPILER: HP92060-16092 REV. 1726

** NO WARNINGS ** NO ERRORS ** PROGRAM = 00167 COMMON = 00000

```
      SUBROUTINE NAME
C
C     THIS IS A MODIFIED VERSION OF THE 'NAME' SUBROUTINE USED IN
C     OTHER PROGRAMS IN THIS SIMULATION
C
      COMMON NAM7(3),NAM8(3),IOPT7,IOPT8,ID7(144),
     +ID8(1296),IB7(40),IB8(40),LU
      WRITE(LU,1)
    1 FORMAT(" PLEASE ENTER THE OUTPUT TABLE FILE NAME")
      READ(LU,2)(NAM7(I),I=1,3)
      IOPT7=100
      WRITE(LU,3)
    3 FORMAT(" NOW THE AMPLITUDE FILE NAME")
      READ(LU,2)(NAM8(I),I=1,3)
    2 FORMAT(3A2)
      IOPT8=100
      DO 10 I=1,40
      IB7(I)=2H
   10 IB8(I)=2H
      RETURN
      END

FTN4 COMPILER: HP92060-16092 REV. 1726

**  NO WARNINGS **  NO ERRORS **   PROGRAM = 00130       COMMON = 01529
```

```
      SUBROUTINE MIE(Q,CN1,CN2,STA,MIELM,AIPAR,AIPER)
      COMPLEX CN,TERM1,TERM2,SUM1,SUM2,Z1,Z2,AIE,AIL,CS1A,CS11A,PHIA,
     +       PHI1A,CS1B,CS11B,PHIB,PHI1B,CA1,CA2,BL1,BL2,CC1,CS1,
     +CC2,CS2,FJ01,FJ11,FJ1,FY01,FY11,FY1,FJ02,FJ12,FJ2,FY02,FY12,FY2
C     - THIS IS A MODIFIED VERSION OF THE MIE SCATTERING
C     - PROGRAM WRITTEN FOR LOCKHEED BY T.R. LAWRENCE.
C     - THIS VERSION IS IN SUBROUTINE FORM AND ALSO HAS MANY
C     - OF THE REPETITIOUS CALCULATIONS REMOVED TO PROVIDE
C     - OPTIMUM RUN-TIME USAGE.
C     - INPUT PARAMETERS ARE:
C     - Q=     SIZE PARAMETER=2*PI*RADIUS/WAVELENGTH
C     - CN1=  REAL PART OF COMPLEX REFRACTIVE INDEX
C     - CN2=  IMAGINARY PART OF COMPLEX REFRACTIVE INDEX
C     - STA=  THE SCATTERING ANGLE IN DEGREES
C     - OUTPUT PARAMETERS ARE:
C     - AIPAR=MIE SCATTERING COEFFICIENT I1
C     - AIPER=MIE SCATTERING COEFFICIENT I2
      CN=CMPLX(CN1,CN2)
      Z1=CMPLX(Q,0.0)
      Z2=Z1*CN
      THETA=STA
      THETA=THETA/57.2957795
      AIE=(0.0,1.0)
      AIL=(1.0,0.0)
      SUM1=(0.0,0.0)
      SUM2=(0.0,0.0)
      SUM5=0.0
      C=COS(THETA)
C
C     DUE TO FAILURE OF HP FUNCTIONS FOR COMPLEX SINE AND COMPLEX
C     COMPLEX COSINE, THE FOLLOWING 4 STATEMENTS WERE MODIFIED TO
C     COMPUTE THESE FUNCTIONS.
C
      CC1=(CEXP(AIE*Z1)+CEXP(-AIE*Z1))/2.0
      CS1=(CEXP(AIE*Z1)-CEXP(-AIE*Z1))/(2.0*AIE)
      CC2=(CEXP(AIE*Z2)+CEXP(-AIE*Z2))/2.0
      CS2=(CEXP(AIE*Z2)-CEXP(-AIE*Z2))/(2.0*AIE)
C
C     **NOTE** IF THE UPPER LIMIT OF THE FOLLOWING LOOP IS EXCEEDED,
C     THE RESULTING DATA WILL BE MISLEADING, SO TO INFORM THE USER
C     OF SUCH A SITUATION, 10.0**36 IS OUTPUT AS THE COEFFICIENT WHEN
C     THIS OCCURS....
C
      DO 56 L=1,MIELM
      AL=L
      AIE=AIE*(0.0,1.0)
      FL=(2.0*AL+1.0)/(AL*(AL+1.0))
      CALL PNXX(L,THETA,PNMX,DPNMX,C,P1,P2)
      CALL JBESL(L,Z1,CS1A,CS11A,CC1,CS1,FJ01,FJ11,FJ1)
      CALL YBESL(L,Z1,PHIA,PHI1A,CC1,CS1,FY01,FY11,FY1)
      CALL JBESL(L,Z2,CS1B,CS11B,CC2,CS2,FJ02,FJ12,FJ2)
      CALL YBESL(L,Z2,PHIB,PHI1B,CC2,CS2,FY02,FY12,FY2)
      CA1=CS1A-(0.0,1.0)*PHIA
      CA2=CS11A-(0.0,1.0)*PHI1A
      BL1=AIE*FL*(CN*CS11A*CS1B-CS1A*CS11B)/(CN*CS1B*CA2-CA1*CS11B)
```

```
      BL2=AIE*FL*(CN*CS1A*CS11B-CS11A*CS1B)/(CN*CS11B*CA1-CA2*CS1B)
      AIL=AIL*(0.0,-1.0)
      TERM1=AIL*(BL1*DPNMX-BL2*PNMX)
      TERM2=AIL*(BL1*PNMX-BL2*DPNMX)
      SU=(AL*(AL+1.0))**2/(2.0*AL+1.0)*(CABS(BL1)**2+CABS(BL2)**2)
      SUM5=SUM5+SU
      SUM1=SUM1+TERM1
      SUM2=SUM2+TERM2
      IF(CABS(TERM1).LT.0.0001.AND.CABS(TERM2).LT.0.0001)GO TO 36
56    CONTINUE
36    SUM3=CABS(SUM1)
      SUM4=CABS(SUM2)
      AIPAR=SUM3*SUM3
      AIPER=SUM4*SUM4
      IF(L.GT.MIELM)AIPAR=10.0E+36
      IF(L.GT.MIELM)AIPER=10.0E+36
      RETURN
      END
```

FTN4 COMPILER: HP92060-16092 REV. 1726

** NO WARNINGS ** NO ERRORS ** PROGRAM = 00900 COMMON = 00000

```
      SUBROUTINE PNXX(N,THETA,PNMX,DPNMX,C,P1,P2)
      AN=N
      I=N-1
      IF(N.EQ.1)GO TO 131
      IF(N.EQ.2)GO TO 132
      B=P2
      AM=I
      PNMX=(2.0*AM+1.0)/AM*C*P2-P1*(AM+1.0)/AM
      P1=P2
      P2=PNMX
      DPNMX=-AN*C*PNMX+(AN+1.0)*B
      GO TO 911
  131 PNMX=1.0
      DPNMX=-C
      GO TO 911
  132 PNMX=3.0*C
      DPNMX=-3.0*COS(2.0*THETA)
      P1=1.0
      P2=3.0*C
  911 RETURN
      END
```

FTN4 COMPILER: HP92060-16092 REV. 1726

** NO WARNINGS ** NO ERRORS ** PROGRAM = 00158 COMMON = 00000

```
      SUBROUTINE YBESL(N,Z,CS1,CS11,CC,CS,F0,F1,F)
      COMPLEX Z,CS1,CS11,F0,F1,F,X,CC,CS
      AN=N
      IF(N.EQ.1)GO TO 63
      IF(N.EQ.2)GO TO 64
      IR=N-1
      AJ=IR
      X=F
      F0=F1
      F1=F
      F=(2.0*AJ+1.0)*F1/Z-F0
      CS1=-Z*F
      CS11=-Z*(X-(AN+1.0)/Z*F)-F
      GO TO 81
63    F0=-CC/Z
      F1=-CC/Z**2-CS/Z
      F=3.0*F1/Z-F0
      CS1=-Z*F1
      CS11=-CS/Z-CC/Z**2+CC
      GO TO 81
64    CS1=(3.0/(Z**2)-1.0)*CC+3.0/Z*CS
      CS11=-6.0/(Z**3)*CC-(3.0/(Z**2)-1.0)*CS
      CS11=CS11+3.0/Z*CC-3.0/(Z**2)*CS
81    RETURN
      END
```

FTN4 COMPILER: HP92060-16092 REV. 1726

** NO WARNINGS ** NO ERRORS ** PROGRAM = 00420 COMMON = 00000

```
      SUBROUTINE JBESL(N,Z,PH1,PH11,CC,CS,F0,F1,F)
      COMPLEX Z,PH1,PH11,F0,F1,F,X,CC,CS
      AN=N
      IF(N.EQ.1)GO TO 63
      IF(N.EQ.2)GO TO 64
      IR=N-1
      AJ=IR
      X=F
      F0=F1
      F1=F
      F=(2.0*AJ+1.0)*F1/Z-F0
      PH1=Z*F
      PH11=Z*(X-(AN+1.0)/Z*F)+F
      GO TO 81
   63 F0=CS/Z
      F1=CS/Z**2-CC/Z
      F=3.0*F1/Z-F0
      PH1=Z*F1
      PH11=CC/Z-CS/Z**2+CS
      GO TO 81
   64 PH1=(3.0/(Z**2)-1.0)*CS-3.0/Z*CC
      PH11=-6.0/(Z**3)*CS+(3.0/(Z**2)-1.0)*CC
      PH11=PH11+3.0/Z*CS+3.0/(Z**2)*CC
   81 RETURN
      END
```

APPENDIX D

PROCESSOR SIMULATION

INTRODUCTION

The software we have written under this contract allows us to predict, by simulation, the data rates and level of error due to multiparticle effects for several available burst-counter processors. The data rates and rms single-burst errors may be provided as graphic functions of the system input parameters by plotting the results of many parametrically varied system simulation runs.

The new software consists of program modules which are compatible with other modules previously written under NASA contract. Figure D-1 illustrates the previously available program modules. In addition, an efficient (and proven) Mie scattering program was available which is not shown on the figure. The PLOT program shown was for a CALCOMP plotter. We have written a new PLOT program for the HP plotter. The photon correlation programs were not used for this contract. In fact, only the Mie program and the SIGNL program were used since photon noise was not considered via direct simulation. The modules SIMU, PMT, and FILTR could be used later.

An objective of the present work was to develop the other modules which were needed. These modules are: OPTIC, which, as already discussed, calculates factors due to optical geometry and scatterer

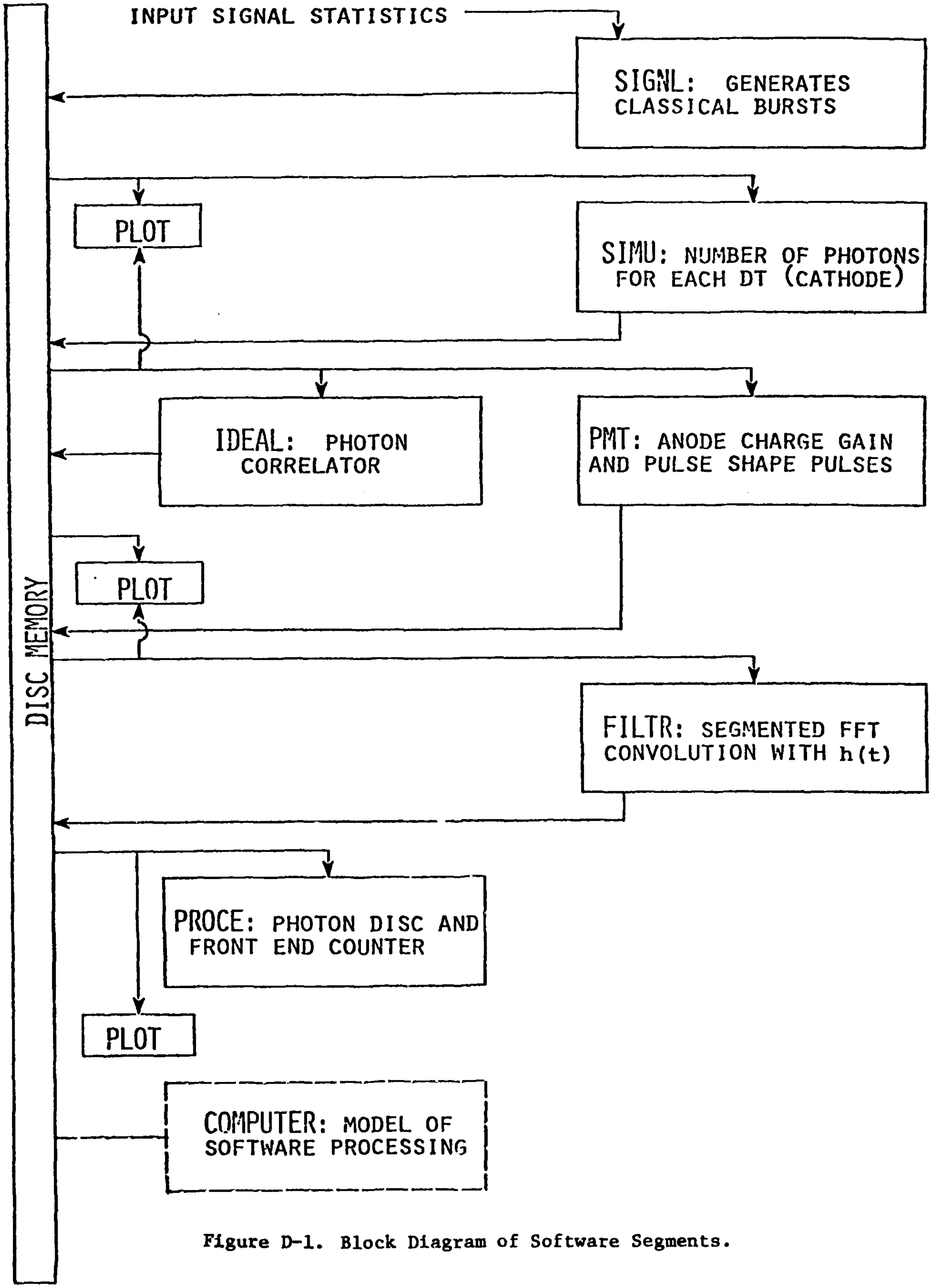

Figure D-1. Block Diagram of Software Segments.

parameters and then produces random realizations of the signal amplitudes and other parameters for table lookup by SIGNAL; COUNT, which allows simulation of DISA, TSI, MACRODYNE, and other counter processors by different combinations of error detection logic and other processor parameters; and COMP, which simulates a couple of the counter processor functions after the fact (to assist in the way parametric studies are done efficiently) and the post detection processing which might be performed by a computer after the counter data was obtained. Because these are simulation programs, COMP is able to assess error by direct comparison with assumed velocity inputs. This, of course, cannot be done with the post detection computations in real flow experiments.

In addition to the simulation programs, we have also developed a diagnostic program for use with PLOT which forms histograms or cumulative log histograms. This allows us to check the simulated particle size distributions, to display the resulting signal amplitudes and single-particle signal-to-noise data available from OPTIC, and to display histograms of the simulated electronic processor errors.

We have documented in the following pages the algorithms for the required software, the inputs and outputs for each program, and a printout of the software. The program COUNT has been described in great detail because it is more a logical algorithm than an algebraic program.

MODIFICATIONS OF SIGNL

This program simulates the classical signal without photon noise as though it had been perfectly bandpass filtered to remove the DC level and the pedestal (low-pass) portions of the signal. We have done this by simply omitting the DC level and the pedestals at the point of formation of the signals in the SIGNL programs.

A separate concern is the width in SIGNL where the infinite width of the Gaussian envelope is truncated to zero values. In previous use of the SIGNL program for NASA, the bursts were truncated at the point where the envelope was down by a factor of $e^{-4.5}$ by selecting the cutoff at 1.5 x the $1/e^2$ width. This is equivalent to truncation at a value approximately 1 percent of the maximum burst amplitude. This was reduced to 0.034 percent by extending the truncation value to twice the $1/e^2$ width as $\exp [2(2W_o/W_o)^2] = \exp [-8] = 0.00034$. Higher extensions of this are possible so long as the product of burst width and sample frequency remains less than the double buffer array length in SIGNL. The double buffer arrays allow the data read from and to the disc to be very long with no apparent interruption due to the reading and writing to and from core.

An additional input variable THRES, which specifies a threshold value for amplitude, has been created. If an amplitude is retrieved which is less than this threshold, then it is skipped and the next burst occurrence time is computed. This may be used to save time in executing SIGNL and succeeding programs in certain cases.

PLOT

This program uses the HP plotter support software to scale, plot axes and tick numbers, label, and plot sample segments of the simulated signals, processor outputs, histograms, etc. It is set up so that a given number of data points may be extracted from the different types of files produced by all the other programs. It assumes that everything to be plotted is on disc and not being simultaneously generated. Thus, batch runs may be made on the computer overnight with the output stored on disc. This output may then be plotted at a later time.

This program has several options as described now. First, the scales may be operator selected or automatic. Selected means the extreme ranges are specified and the program simply replaces the data with the scale maxima if the data goes off scale. Automatic scale means the program scans the entire data set to be plotted and normalizes to the extrema of the data. (This generally results in a difficult-to-read scale.) Generally, unknown data will be plotted on automatic for inspection, then replotted with an appropriate easy-to-read scale selected.

The program provides options for linear plots, semilog plots, log-log plots, and histogram plots. When linear plots are selected, the origin may be located anywhere on the paper. When logrithmic plots are requested, all data less than or equal to 0.0 is flagged by being set equal to an extreme negative value (-10^{36}). When linear histograms are requested, the option to normalize the data to the maximum value is available.

Two data compression options are included to allow long segments of data to be compressed by some factor to fit on a given page. The first one is the skipping option. In this case, only every NSKIP'th point is plotted and the others are simply omitted. If instead the averaging option is used, then consecutive groups of NAVG points are averaged and the average of the group is plotted.

Line and symbol options are included as follows: Data points are connected by no lines at all or straight lines. Data points may be plotted as a circle, a square, or a triangle, or any of several other symbols. More than one graph may be plotted on the same set of axes using combinations of symbols and line types to distinguish.

HISTO

This programs takes data from an input file and creates an output file containing either linear histogram or cumulative histogram values. Histograms are plotted by using the output file of HISTO as the input file to PLOT.

If a linear histogram is desired, the following input variables are required:

- LOWER - lower limit of sort bins.
- UPPER - upper limit of sort bins.
- NBINS - total number of bins

If a cumulative histogram sort is desired, the following input variables are required:

- A - constant multiplier.
- B - base.
- NBINS - total number of bins.

The value of a cumulative histogram at $x = A$ is then calculated as the number of elements greater than A, at $x = B \cdot A$ the value is the number of elements greater than $B \cdot A$, and so on for $x = B^2 \cdot A$, $x = B^3 \cdot A$, ..., $x = B^{NBINS} \cdot A$. When a cumulative histogram file is used as input to PLOT, it is automatically plotted on a log-log scale.

HISTO adds two bins to the end of the output file (regardless of the type of sort used). The first of these contains the number of elements less than the first bin; the other contains the number of elements greater than the last bin.

COUNT: BURST COUNTER SIMULATION

This program is designed to simulate a burst counter processor with the assumption that the signal is a bandpass function. (Pedestals and DC components have been removed by prior filtering.)

<u>Inputs</u>

The data for the program is a long disc file of periodically taken samples of the simulated bandpass signal (standard 32 bit FORTRAN REAL). The input parameters and options are selected with interactive programming similar to that in other programs. These options are:

- SCALE - A REAL number which converts the input data to voltage. (Includes PMT and preamp gains if not already included.)
- TREST - Maximum burst width time allowed before automatic reset.
- VMAX - Maximum signal voltage.
- NC - Integer number of cycles during which time is measured.
- MC - Integer number of cycles during which check time is measured.
- ZERO - Threshold used for zero crossing (usually zero) $\leq$ VA.
- VA, VB, VC - Threshold voltages used for signal amplitude verification and end of burst detection: VB > VA, both positive; VC is negative. Example: $VB = 20\times10^{-3}$ V, $VA = 10\times10^{-3}$ V, $VC = -10\times10^{-3}$ V.
- AR2 - Two-sided arming (true, false).
- ARB - Burst arming (true, false).
- EOB - End of burst reset (true, false).
- IDEG - Degree of interpolation desired (0 = none, 1 = linear).
- DEAD - Number of cycles to wait after a reset before testing for arm condition.
- DT - Sampling interval (automatically read from output file of SIGNL).

Note: A real processor would have a given clock frequency and time between burst clock frequency. The effects of these selections can best be simulated in a later program so that separate checks of the effectiveness of these choices may be made without rerunning the entire simulation. Thus, this program measures the occurrence times and burst periods as precise REAL numbers even though actual processors do not do this. The effects of clock error are included in COMP.

Outputs

- At the beginning of execution of program, all the selections of the program input parameters and options are written to the output file.
- The data output file consists of 4 real numbers (see Figure D-2) and an integer message word.
  - TA - End of burst or reset time.
  - TB - Time of first positive going zero-crossing after arming (the zeroth crossing).
  - TM - Time of Mth crossing after the zeroth crossing, TB.
  - TN - Time of Nth crossing after the zeroth (note: TN > TM).

Note: TB is measured as the difference between the last TB occurrence and the present so that each time the sequence starts, the measurement of time is re-zeroed. The 5th word is an integer

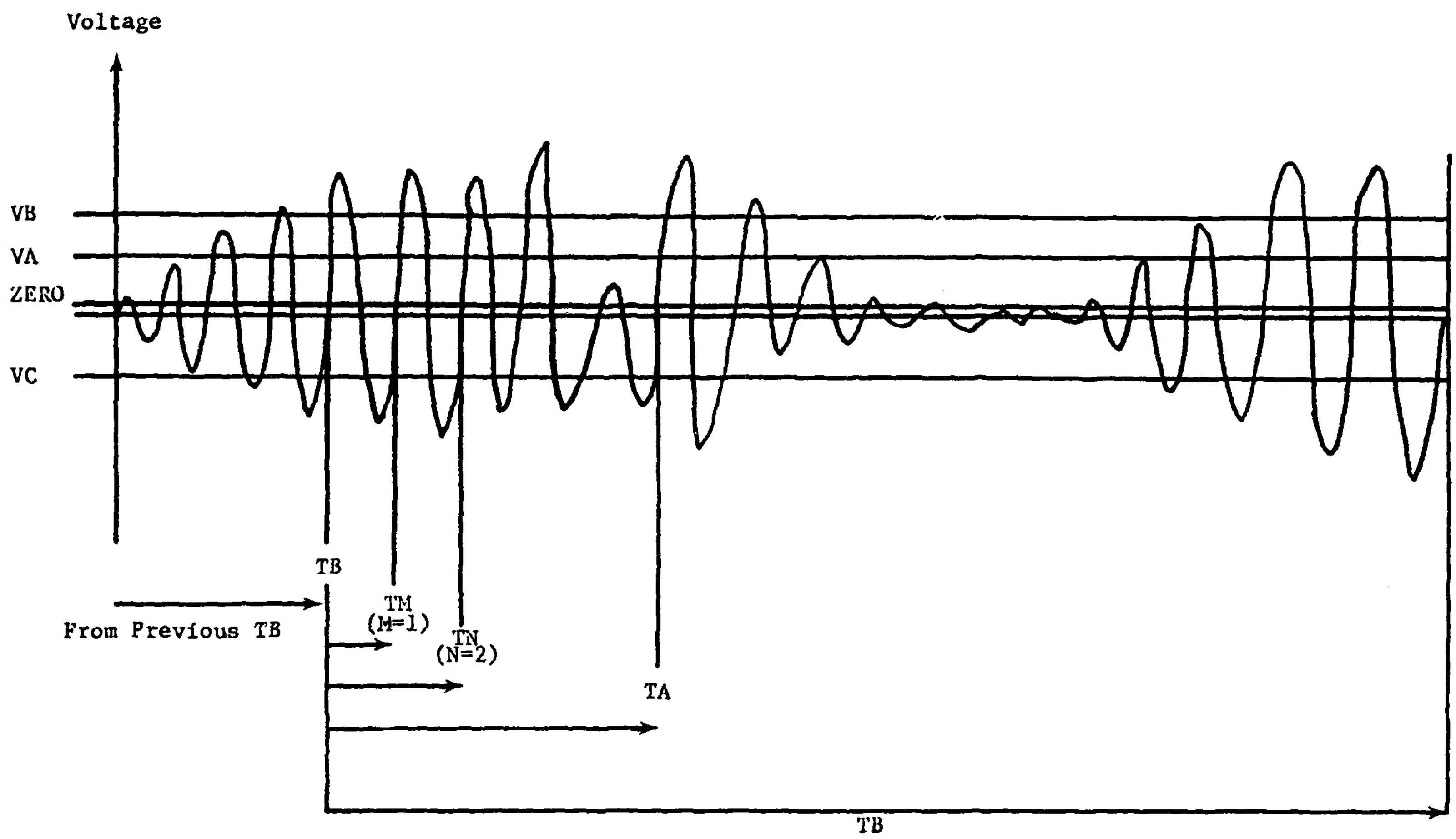

Figure D-2. Definition of Processor Time Intervals and Threshold Levels.

word which contains the following information in the 10^4 and 10^5 digits. For example:

0 Reset on NCth zero.

1 Reset due to failure of bipolar threshold test prior to TN. ⇒ TA = reset time.

2 End of burst reset.

3 End of burst without exceeding VA.

4 VMAX exceeded, reset.

5-30 See Table D-1 for complete list. See Table D-2 also.

<u>Operation</u>

An arming condition is established according to the logical input variables. When this arming condition is met, the next positive going zero crossing is to be interpolated for TB and the beginning of all other timing operations for the burst (TM, TN, TA). All zero crossing times are measured on positive-going crossings (abbreviated zero+). Any reset causes a string of data words to be generated: TA,TB,TM,TN,MESS, where MESS is the integer message word, and the other words are time data in 32 bit REAL format. MESSAGES describe what type of reset occurred and the number of cycles of signal between TB = 0 and the reset time. (The three least significant digits are for this.)

MESS	Message
00XXX	NC cycles completed and reset. (Use test [MESS/1000] = 0? to avoid the table lookup on "standard" runs.)
01XXX	Failure of bipolar threshold test prior to NC cycles ⇒TA = reset time*.
02XXX	End of burst prior to NC cycles (VA but not VB).
03XXX	End of burst prior to NC cycles; both VB and VA skipped between ZERO+ and ZERO-.
04XXX	Reset due to VMAX exceeded.
05XXX	Reset due to TREST exceeded.
06XXX	Reset due to end of input file.
07XXX-15XXX	Reserved for other error resets.
16XXX	Data OK: N $\geq$ NC. Reset on end of burst. (VA and VB both missed.)
17XXX	Data OK:** N $\geq$ NC. Reset on end of burst (VA but not VB).
18XXX-31XXX	Other messages.

* Reset time is the ZERO+ following the occurrence of the reset condition; TA = reset time on all resets other than an NC reset.

** For count to NC modes, MESS = 0 is the only validation test needed in the post processing; for total burst modes, MESS > 15 (test only one bit in binary) is a valid test and so is MESS > 16 wherein the double level drop is excluded. For more detailed failure analysis, table lookup of MESS will be required.

Table D-1. Error Messages.

EOB / N ≥ NC AT RESET	TRUE	FALSE
TRUE	MESS = 16 OR 17 OR 04 OR 05 OR 06	MESS = 0 N = NC
FALSE	MESS = 02 OR 03 OR 05 OR 04 OR 06	MESS = 01 OR 05 OR 04 OR 06

Table D-2. Truth Table for Possible Message Conditions

Arm Conditions

If both AR2 and ARB are input false, then the arm condition is met when the signal exceeds VA. The signal should not be tested unless a reset just occurred.

If ARB is input true, but not AR2, then the arm condition is met when the signal exceeds VB. The signal should not be tested unless a reset just occurred.

If AR2 is input true, then all other arm modes are ignored* and the following applies. We will designate the event of signal exceeding VA as VA+, signal going more negative than VC as VC-, and the positive and negative going transitions through the level ZERO as ZERO+ and ZERO-. Then the logic is as follows: The only acceptable sequence is ... VA+, ZERO-, VC-, ZERO+, VA+, ZERO-, VC-, ... and the ZERO+ transitions are the zero crossings which are counted. Anytime a ZERO+ or ZERO- follows each other without the appropriate VA+ or VC- in between, a reset occurs and is accompanied by a data sequence output with appropriate message word. When VA+ was missed, no arming occurs until VA+ is exceeded by the signal again and the pattern takes back up as VA+, ZERO-, VC-, ZERO+, etc., and the ZERO+ is the time for TB. When the reset occurred because VC- was missed, then an arming does not occur until the signal goes less than VC. After this VC-,

---

* Addition: If ARB is also true, then VB must be exceeded to start the ARM process (followed by VC-, ZERO+, VA+, ZERO-, etc.).

the sequence continues VC-, ZERO+, etc. with that ZERO+ being the TB time. If it happens that arming occurs by VA+ being exceeded, and the sequence should be VA+, ZERO-, ZERO+, this would cause a reset due to the missing VC-, but the ZERO+ would still be used for the TB zero crossing since a value for TB should be output for every reset, even if no other zero crossings are valid.

Other Reset Conditions

Once TB has been measured and a new zero time is established, the next value of TB will be (see next section) the product of the sample interval and the number of samples plus the interpolated fractions of a sample time between TB = 0 and the next beginning ZERO+. If the count of samples exceeds TREST/DT before TN or TA is measured, then reset; output data with message 5. However, do not reset this count until the next TB is measured.

Unless the EOB variable is true, then a reset should occur immediately after the NC zero crossing, with a message of "0" if no other reset occurs first.

If the EOB variable is true, then the following test is included. Set VBP true when signal exceeds VB, and reset VBP when signal crosses VA going down (this is a VA-). If VA- occurs and VBP is not set true, that means that the present cycle exceeded VA, but not VB, and an EOB reset occurs after the next ZERO+ transition is interpolated to determine TA, and the message is 2 or 17. If, in this mode, the sequence occurs as ... ZERO+, ZERO- ... without either VB or VA being crossed in between the positive and negative going ZERO transition, then also end on next ZERO+ (and measure TA), but put out MESS = 3 or 16.

Zero Crossing Interpolation

Once the arming condition has been met, then the times TB, TM, TN, and TA are to be determined unless a reset occurs and causes some of these not to be obtained. (TB is always obtained.) TM and TN are the interpolated Mth and Nth ZERO crossings after the one at the TB measurement. TA is the one which follows the EOB reset described above.

Time will be measured internally by an integer number of sample increments plus the beginning and ending fractions of an increment which are obtained by interpolation. The interpolation (IDEG) choices are zeroth order (use the next discrete sample time following the crossing) and first order (linear interpolation between the values on either side of ZERO level).

The interpolation procedures are described now in more detail. We assume that S(K) is the sample data set and that these numbers are available sequentially from an array in memory. The test is:

"Is S(K) $\geq$ ZERO and S(K-1) $\leq$ ZERO?"

When this test is true, then the following is done:

- Add one to NCYC counter.
- Interpolate if NCYC=MC, NCYC=NC, or TB or TA are needed at this point.

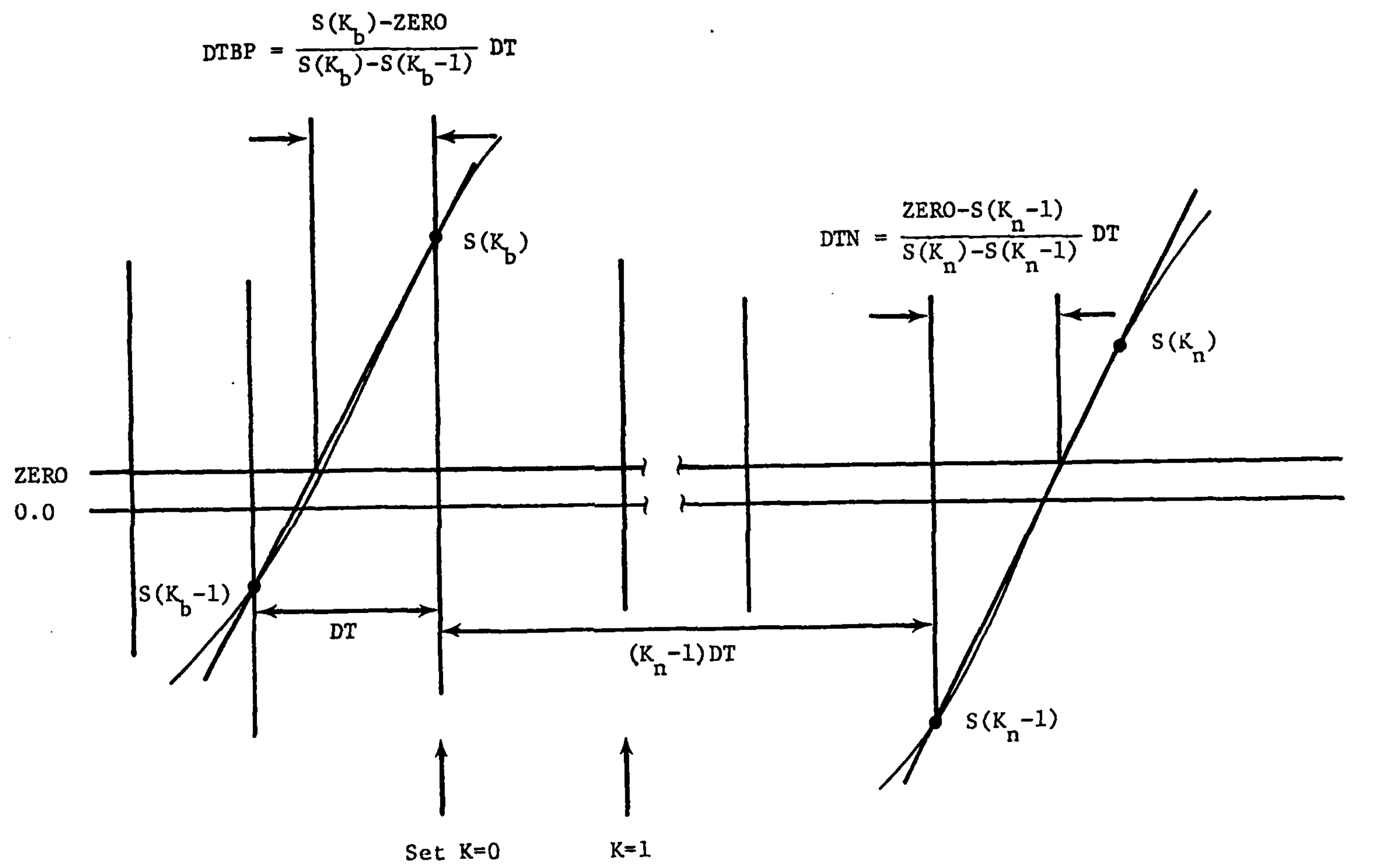

Figure D-3. Linear Interpolation of the Zero Crossings.

If IDEG = 0, then

$$T = K*DELT$$

where K = count of data since the last TB was measured (the number of intervening samples).

If IDEG = 1, then

$$T = DTBP + (K_n-1)DT + DTN$$

where
$$DTBP = \frac{(S(K_b)-ZERO)}{S(K_b)-S(K_b-1)} DT$$

and
$$DTN = \frac{(-S(K_n-1)+ZERO)}{S(K_n)-S(K_n-1)} DT$$

as illustrated in Figure D-3.

Note that the zero crossings are about the input level ZERO which is not necessarily numerically 0.0. In particular, the old single-level counters may be simulated with ZERO = VA and AR2 = ARB = False.

POST DETECTION PROCESSING: COMP

<u>Present Time</u>

The error that the processor makes is the difference between the estimated frequency at total time TBTOT=ΣTB and the instantaneous mean frequency assumed at the same time in SIGNL. In order to determine this error, the same input function used to generate frequencies in SIGNL must be evaluated at TBTOT=ΣTB to produce an error set. In the simplest case, a constant mean frequency will be assumed but other more complicated velocity time functions may be desired later. For this reason, this program computes the present time TBTOT as the summation of all the particle interarrival times TB.

RMS Error

We not let T[n] represent the occurrence time of the nth occasion of an arming and a measurement being initiated. COMP generates an output file consisting of the errors normalized to the instantaneous mean frequency. Thus, with F(N) as the nth frequency estimate and FT(N) = true instantaneous mean frequency,

$$ER(N) = \frac{F(N)-FT(N)}{FT(N)}$$

This output file of COMP may be used as input to the program HISTO to generate a histogram of these errors. (Histogram data is also stored on a disc file which is in turn used by the PLOT program.) If desired, the histogram may be plotted symmetrically about zero with total number of bins in the 10-100 range on a scale selectable from $\approx \pm$ EPS, where EPS is 0.0001, 0.001, 0.01, 0.10, 1.0. Also, the option exists to normalize the presentation to the peak value of the histogram as illustrated in Figure D-4.

The rms deviation of the normalized frequency error will also be computed directly from the estimates as:

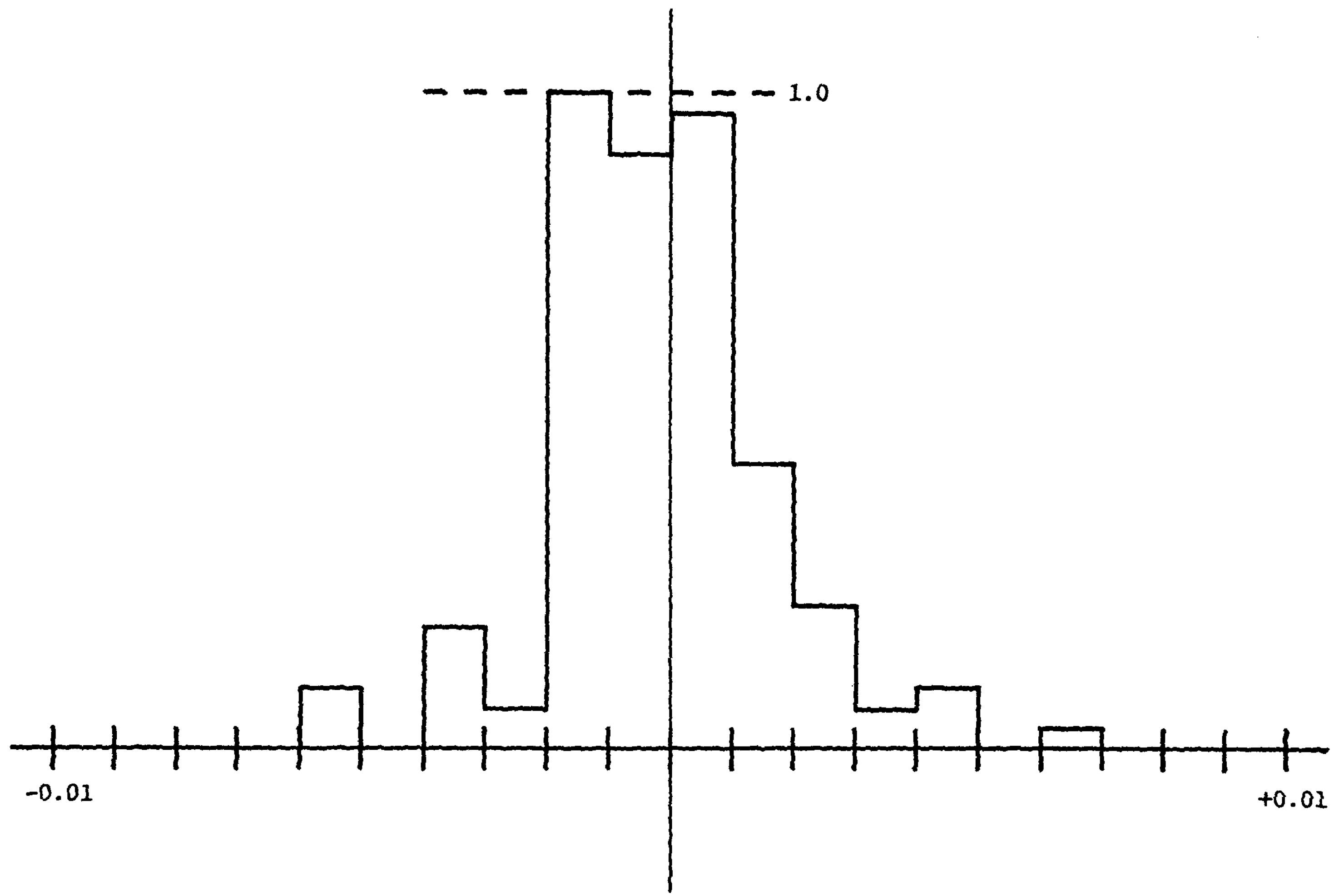

Figure D-4. Example of Histogram for Normalized Measurement Errors.

$$\text{RMSE} = \left(\frac{1}{N}\sum_{n=1}^{N}\left(\frac{F(n)-FT(n)}{FT(n)}\right)^2\right)^{\frac{1}{2}}$$

The histograms and normalized rms error figures allow the effects of various processor ARMING and RESET algorithms and levels to be parametrically studied along with clock errors, etc.

Error Check Circuit

Before computing the histograms and rms errors described above, the raw data set is "thinned" by removing (for the present execution only) the data which does not satisfy certain error checks. Any or all of the following conditions may be required by logical input selections to the present program.

- NXM at X percent level check.

  Frequency estimate based on two time lengths TN and TM must agree within X percent, i.e.,

  f_n = NC/TN

  f_m = MC/TM

  $\left|\frac{f_n - f_m}{f_n}\right| \leq$ MXNTL (condition satisfied or reject)

  MXNTL = Input on order of 0.01 or other choice of MXN tolerance.

  MESS = 0 or $\geq$ 16 or 17 required.

- *Total Burst Mode:* $f_n = N/TA$, where N is the number of zero crossings between TB and TA recorded in three least significant message digits. Requires MESS = 16, 17 or $\geq$ 16.
- NC check.

  Throw out all data reset before NC counts are obtained. $f_n = NC/TN$. (This is automatically included in NXM; it is an option alone or in addition to other tests.)
- Stopping option.

  An option exists to either stop processing after a specified amount of time has elapsed or to stop processing after a specified number of valid data samples have been collected.

Clock Resolution Effects

In practice the times TB, TM, TN, and TA are measured as an integer number of cycles of a stable high-frequency oscillator (called the clock). Generally speaking, the clock for measurement of TB would be either 100 KHz or 1 MHz, while for the other three quantities 100-500 MHz is now typical. Here it is assumed that the measurement of TB is error free, since for all practical purposes this is easy to accomplish electronically with a 1 MHz clock.

We now give the procedure for simulating the clock digitization error. With reference to Figure D-5, assume that δ_b is known from the previous set of data (TB, TM, TN, TA). Then

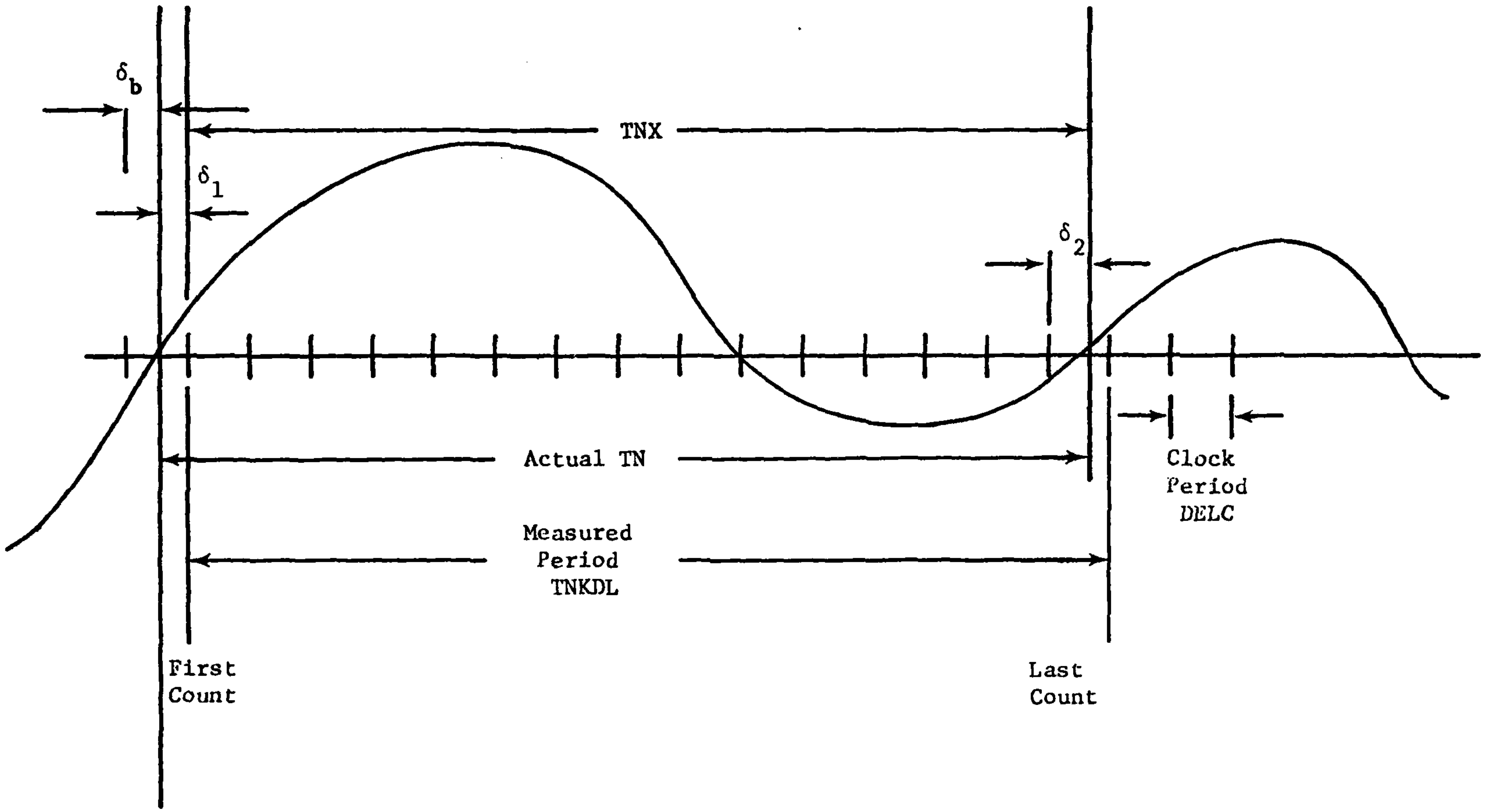

Figure D-5. Simulation of Processor Clock Discretization Error.

$$\delta_1 = DELC-\delta_b$$

Then compute TMX, TNX, TAX, TBX as

$$TX = T-\delta_1$$

where T is the simulated exact interval. Then compute

$$K-1 = \left[\frac{TX}{DELC}\right]$$

where [] is the greatest integer function.

The simulated processor measurement is then

$$TNKDL = K*DELC$$

and the δ_2 value to store for the next set is obtained as

$$\delta_2 = TX - (TNKDL-DELC)$$

This is only needed for the δ_b for the next iteration. The δ_2 quantity is not needed for the TM, TN, and TA results.

In order to initialize the above procedure, we simply set $\delta_b = 0$ for the first data point. Generally speaking, this procedure is not simultaneously applicable to studying effects of the time between burst clock which would be operating at a much lower frequency. We have included the effects on the TB measurement here, simply to correctly keep the starting phase random in the TM, TN, and TA measurements. The effect of using a synchronous subharmonic of the high speed clock (obtained straightforwardly by down counting) as the inter burst clock can be simulated correctly by a further discretization of TNKDL.

Accuracy Figure of Merit

The rms deviation of individual measurements is reduced by increasing the detection threshold level. However, the number of measurements obtained per second is also reduced in that case. Now if a short-time average frequency is measured during some interval which is small compared with the intervals over which the velocity changes, then the accuracy is improved if the measurement errors are independent. Clock, photon noise, multiparticle, and flow gradient errors are all independent of the velocity field. Therefore, short-time averages are desired. We do not know without doing the simulation where the optimum threshold for any given experiment is and what the precision obtainable for that threshold setting is.

We will assume that the "good" data, which passes the processor error checks, is collected in short-time averages as illustrated in the timing diagram of Figure D-6. (Short-time averaging as described here is included in COMP, however, the accuracy of these measurements has not been tested.) The duration of each short-time average is TSAMP, and it includes however many signal bursts occur in each such interval. Thus we have for each such interval:

$$FSAMP[J] = \frac{1}{NTB} \sum F(n)$$

An appropriate figure of merit is the rms error of this quantity. Therefore, we compute

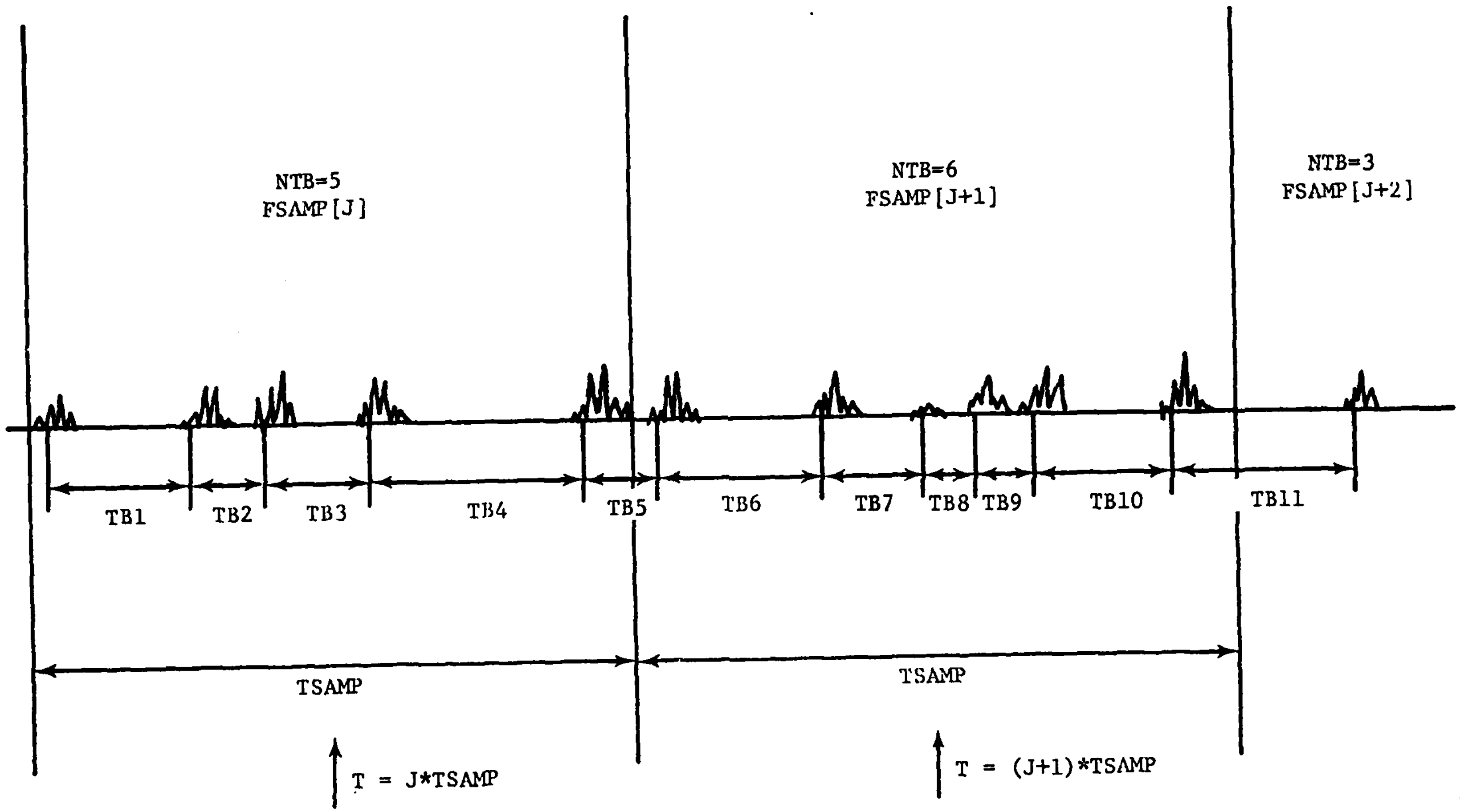

Figure D-6. Illustration of Short Time Sample Averaging.

$$SIG = \left(\frac{1}{SAMPL-1} \sum_{J=1}^{SAMPL} \left(FT(J*TSAMP)-FSAMP[J]\right)^2\right)^{\frac{1}{2}}$$

where FT(J*TSAMP) is the known input frequency used in SIGNL for the time located at the middle of the Jth interval of length TSAMP.

The deviations FT(J*TSAMP)-FSAMP[J] are stored in a second output file which can also be plotted in a histogram. The behavior of the rms deviations and histograms at this final level of processing will ultimately determine the precision limitations of the LDV system with post-detection short term averaging.

```
FTN4,L
      PROGRAM COUNT
C
C     A PROGRAM TO SIMULATE A BURST COUNTER PROCESSOR WITH THE
C     ASSUMPTION THAT THE SIGNAL IS A BANDPASS FUNCTION. (PEDESTALS
C     AND DC COMPONENTS HAVE BEEN REMOVED BY PRIOR FILTERING.)
C     COUNT TAKES THE OUTPUT OF SIGNL AS INPUT AND PRODUCES ONE
C     OUTPUT FILE CONSISTING OF ONE LINE OF INFORMATION FOR EVERY
C     RESET WHICH OCCURS.
C
      REAL INTRP
      INTEGER RESET,TOTDT,TBN
      DIMENSION ITIME(5),IYEAR(1),IPRAM(5)
      LOGICAL EOF,ARB,AR2,EOB,CROSS,VBP,VCM,VAP,ZP,ZM,PROPR,FOUND,
     +DELAY
      COMMON NAM7(3),NAM8(3),IOPT7,IOPT8,ID7(576),ID8(144),IB7(40),
     +IB8(40),J,TOTDT,TBN,SIG1(500),SIG2(500),SAVEJ(2),DT,DTBP,DTN,
     +ZERO,NDT,VA,VB,VC,VAP,ZP,VBP,VCM,ZM,VARM,LU
      CALL RMPAR(IPRAM)
      LU=IPRAM(1)
      IF(LU.EQ.0)LU=1
      DELAY=.FALSE.
      CALL NAME
      WRITE(LU,6)
    6 FORMAT(" INPUT THE FOLLOWING:"/
     +  "(1)  SCALE (TO CONVERT INPUT TO VOLTAGE)"/
     +  "(2)  MAXIMUM BURST WIDTH TIME BEFORE AUTOMATIC RESET"/
     +  "(3)  MAXIMUM SIGNAL VOLTAGE"/
     +  "(4)  NC--NUMBER OF CYCLES DURING WHICH TIME IS MEASURED"/
     +  "(5)  MC--NUMBER OF CYCLES DURING WHICH CHECK TIME IS MEASURED")

      READ(LU,*)SCALE,TREST,VMAX,NC,MC
      WRITE(LU,7)
    7 FORMAT(" INPUT THRESHOLD FOR ZERO CROSSING")
      READ(LU,*)ZERO
      WRITE(LU,8)
    8 FORMAT(" INPUT VA, VB, AND VC (THRESHOLD VOLTAGES)")
      READ(LU,*)VA,VB,VC
      WRITE(LU,9)
    9 FORMAT(" TWO-SIDED ARMING?  (TRUE OR FALSE)")
      READ(LU,72)AR2
   72 FORMAT(L1)
      WRITE(LU,3)
    3 FORMAT(" BURST ARMING?  (TRUE OR FALSE)")
      READ(LU,72)ARB
      WRITE(LU,70)
   70 FORMAT(" END OF BURST RESET?  (TRUE OR FALSE)")
      READ(LU,72)EOB
      WRITE(LU,71)
   71 FORMAT(" INPUT INTERPOLATION CHOICE(0=NONE, 1=LINEAR)")
      READ(LU,*)IDEG
      WRITE(LU,80)
   80 FORMAT(" INPUT DELAY TIME (# OF CYCLES)")
      READ(LU,*)DEAD
```

```
C
C     (DELAY TIME IS THE # OF CYCLES TO WAIT AFTER A RESET BEFORE
C     ARMING AGAIN.)
C
  82  CALL OPEN(ID7,IERR,NAM7,IOPT7,0,12)
      CALL CREAT(ID8,IERR,NAM8,IOPT8,3,0,12,144)
C
C     GET TIME OF DAY (TO STORE IN HEADER OF CREATED FILE).
C
      CALL EXEC(11,ITIME,IYEAR)
      CALL READF(ID7,IERR,IB7,40)
      CALL READF(ID7,IERR,IB7,40)
      CALL CODE
      READ(IB7,79)NHEAD
 79   FORMAT(I5)
      DO 73 I=1,NHEAD-1
 73   CALL READF(ID7,IERR,IB7,40)
      CALL READF(ID7,IERR,IB7,40)
      CALL CODE
      READ(IB7,160)FT
 160  FORMAT(E16.8)
      DTDLY=DEAD*(1.0/FT)
      CALL READF(ID7,IERR,IB7,40)
      CALL CODE
      READ(IB7,2)T,DT
   2  FORMAT(2E16.8)
C
C     WRITE HEADER INFORMATION TO OUTPUT FILE
C
      CALL CODE
      WRITE(IB8,150)
 150  FORMAT("  COUNT OUTPUT")
      CALL WRITF(ID8,IERR,IB8,40)
      NHEAD=4
      CALL CODE
      WRITE(IB8,153)NHEAD
 153  FORMAT(I5," LINES OF HEADER INFORMATION")
      CALL WRITF(ID8,IERR,IB8,40)
      CALL CODE
      WRITE(IB8,151)ITIME(5),IYEAR(1),ITIME(4),ITIME(3),ITIME(2)
 151  FORMAT(" CREATION DATE: ",I5,1X,I5," TIME:",3I5)
      CALL WRITF(ID8,IERR,IB8,40)
      CALL CODE
      WRITE(IB8,154)SCALE,TREST,VMAX
 154  FORMAT(" SCALE=",E10.4," TREST=",E10.4," VMAX=",E10.4)
      CALL WRITF(ID8,IERR,IB8,40)
      CALL CODE
      WRITE(IB8,156)ZERO,VA,VB,VC
 156  FORMAT(" ZERO=",E10.4," VA=",E10.4," VB=",E10.4," VC=",E10.4)
      CALL WRITF(ID8,IERR,IB8,40)
      CALL CODE
      WRITE(IB8,158)AR2,ARB,EOB,IDEG
 158  FORMAT(" AR2=",L1," ARB=",L1," EOB=",L1," IDEG=",I1,40X)
```

```
      CALL WRITF(ID8,IERR,IB8,40)
      CALL CODE
      WRITE(IB8,162)T,DT
  162 FORMAT(2E16.8)
      CALL WRITF(ID8,IERR,IB8,40)
      CALL CODE
      WRITE(IB8,164)FT
  164 FORMAT(E16.8,20X)
      CALL WRITF(ID8,IERR,IB8,40)
      CALL CODE
      WRITE(IB8,152)NC,MC
  152 FORMAT(2I3,30X)
      CALL WRITF(ID8,IERR,IB8,40)
      NDT=T/DT
      TREST=TREST/DT
      TBN=0
      ZP=.FALSE.
      VBP=.FALSE.
      ZM=.FALSE.
      VCM=.FALSE.
      VAP=.FALSE.
      TOTDT=0
      DTBP=0.0
      J=0
      IF(.NOT.ARB)VARM=VA
      IF(ARB)VARM=VB
C
C     DO INITIAL READS TO GET SIGNALS FROM DISC FILE
C
      DO 22 I=1,500
      SIG2(I)=0.0
      CALL READF(ID7,IERR,IB7,8,LEN)
      IF(LEN.NE.-1)GO TO 21
      SIG1(I)=0.0
      GO TO 22
   21 CALL CODE
      READ(IB7,4)SIG1(I)
    4 FORMAT(E16.8)
   22 CONTINUE
C
C     SHIFT SIGNALS TO SECOND ARRAY (SIG2) AND ISSUE NEW READ TO
C     FIRST ARRAY (SIG1)
C
      CALL SHIFT
   50 CALL NEXTS(EOF)
      IF(EOF) GO TO 999
      IF(.NOT.DELAY)GO TO 51
      DEADT=DEADT+DT
      IF(DEADT.LT.DTDLY)GO TO 50
   51 IF(VARM.GE.ZERO)GO TO 10
      IF(SIG2(J).GE.VARM) GO TO 50
      VCM=.TRUE.
      GO TO 300
```

```
 10   IF(SIG2(J).LT.VARM)GO TO 50
      VAP=.TRUE.
C
C     ARM CONDITION WAS MET; SET TB AT NEXT ZERO+ CROSSING
C
 300  CALL FINDZ(TB,IIERR,IDEG)
      IF(IIERR.EQ.1) GO TO 999
      DTBP=DT-DTN
      TBN=0
      NCYC=0
      TA=0.0
      TN=0.0
      TM=0.0
      IF((IIERR.EQ.2).AND.AR2) GO TO 807
 350  CALL NEXTS(EOF)
      IF(EOF) GO TO 999
      IF(TBN.LE.TREST)GO TO 400
      CALL FINDZ(TA,IIERR,IDEG)
      IF(IIERR.EQ.1) GO TO 999
C
C     RESET DUE TO TREST EXCEEDED
C
      RESET=5
      GO TO 500
 400  CALL CHKZE(CROSS)
      IF(.NOT.CROSS)GO TO 410
C
C     JUST CROSSED ZERO+ ---INCREMENT COUNTER AND SET TM AND TN
C     IF APPROPRIATE
C
      NCYC=NCYC+1
      IF(NCYC.EQ.MC)TM=INTRP(IDEG)
      IF(NCYC.EQ.NC)TN=INTRP(IDEG)
 410  IF(EOB)GO TO 420
      IF(NCYC.NE.NC) GO TO 700
C
C     RESET DUE TO NC CYCLES COMPLETED
C
      TA=INTRP(IDEG)
      RESET=0
      DELAY=.TRUE.
      DEADT=0.0
      GO TO 500
C
C     END OF BURST CHECK--DID VA- OCCUR WITHOUT BEING PRECEDED BY VB?
C
 420  IF(J.NE.1)GO TO 421
      IF((SAVEJ(1).GT.VA.AND.SIG2(1).LE.VA).AND.(VBP))GO TO 502
 421  IF((SIG2(J-1).GT.VA.AND.SIG2(J).LE.VA).AND.(VBP))GO TO 502
 427  CALL FINDZ(TA,IIERR,IDEG)
      IF(IIERR.EQ.1) GO TO 999
      IF(NCYC.GE.NC)GO TO 501
C
```

```
C     RESET DUE TO END OF BURST PRIOR TO NC CYCLES  (VB MISSED)
C
      RESET=2
      GO TO 500
C
C     RESET DUE TO END OF BURST AFTER NC CYCLES  (VB MISSED)
C
 501  RESET=17
      GO TO 500
 502  IF(J.NE.1) GO TO 101
      IF((SAVEJ(1).GT.ZERO.AND.SIG2(1).LE.ZERO).AND.
     +(VBP.OR.VAP))GO TO 700
 101  IF((SIG2(J-1).GT.ZERO.AND.SIG2(J).LE.ZERO).AND.
     +(VBP.OR.VAP))GO TO 700
      CALL FINDZ(TA,IIERR,IDEG)
      IF(IIERR.EQ.1) GO TO 999
      IF(NCYC.GE.NC)GO TO 710
C
C     RESET DUE TO END OF BURST PRIOR TO NC CYCLES (VA AND VB MISSED)
C
      RESET=3
      GO TO 500
C
C     RESET DUE TO END OF BURST AFTER NC CYCLES (VA AND VB MISSED)
C
 710  RESET=16
      GO TO 500
 700  IF(AR2) GO TO 800
 705  IF(SIG2(J).LE.VMAX)GO TO 350
C
C     RESET DUE TO VMAX EXCEEDED
C
      CALL FINDZ(TA,IIERR,IDEG)
      IF(IIERR.EQ.1) GO TO 999
      RESET=4
      GO TO 500
C
C     BIPOLAR TEST--CHECK FOR PROPER SEQUENCE
C
 800  CALL CHKSQ(PROPR,ARB)
      IF(PROPR) GO TO 705
      IF(VARM.NE.VC)GO TO 806
      TA=INTRP(IDEG)
      GO TO 807
 806  CALL FINDZ(TA,IIERR,IDEG)
      IF(IIERR.EQ.1) GO TO 999
C
C     RESET DUE TO FAILURE OF BIPOLAR THRESHOLD TEST PRIOR TO NC CYCLES
C
 807  RESET=1
C
C     RESET ROUTINE--GENERATE MESSAGE WORD AND OUTPUT 5 WORDS OF INFO
C     (TA,TB,TM,TN,MESS) TO DISC
```

```
C
 500  MESS=RESET*1000+NCYC
      CALL CODE
      WRITE(IB8,54)TA,TB,TM,TN,MESS
  54  FORMAT(4E16.8,I5)
      CALL WRITF(ID8,IERR,IB8,40)
      GO TO 50
C
C     A MESSAGE ERROR OF '6' WAS ADDED TO INDICATE WHAT HAPPENED
C     WHEN THE END OF THE INPUT FILE WAS REACHED
C
 999  MESS=6000+NCYC
      CALL CODE
      WRITE(IB8,54)TA,TB,TM,TN,MESS
      CALL WRITF(ID8,IERR,IB8,40)
      CALL CLOSE(ID7)
      CALL LOCF(ID8,IERR,IREC,IRB,IOFF,JSEC)
      ITRUN=JSEC/2-IRB-1
      CALL CLOSE(ID8,IERR,ITRUN)
      IF(IERR.LT.0)CALL CLOSE(ID8)
      STOP
      END



      SUBROUTINE FINDZ(VAR,IIERR,IDEG)
C
C     THIS ROUTINE FINDS THE NEXT POSITIVE-GOING ZERO CROSSING
C     AND RETURNS THE INTERPOLATED VALUE IN THE VARIABLE SPECIFIED
C     BY 'VAR'.  IF END-OF-FILE IS ENCOUNTERED BEFORE CROSSING IS FOUND
C     THEN IIERR=1 IS RETURNED (OTHERWISE, IIERR=0).
C
      REAL INTRP
      INTEGER TOTDT,TBN
      LOGICAL CROSS,EOF,INSEQ,VBP,VCM,VAP,ZP,ZM
      COMMON NAM7(3),NAM8(3),IOPT7,IOPT8,ID7(576),ID8(144),IB7(40),
     +IB8(40),J,TOTDT,TBN,SIG1(500),SIG2(500),SAVEJ(2),DT,DTBP,DTN,
     +ZERO,NDT,VA,VB,VC,VAP,ZP,VBP,VCM,ZM,VARM,LU
      IIERR=0
  20  CALL NEXTS(EOF)
      IF(EOF) GO TO 10
      CALL CHKSQ(INSEQ,ARB)
      IF(.NOT.INSEQ)IIERR=2
      CALL CHKZE(CROSS)
      IF(.NOT.CROSS) GO TO 20
      VAR=INTRP(IDEG)
      GO TO 30
  10  IIERR=1
  30  RETURN
      END
```

```
      SUBROUTINE CHKZE(CROSS)
C
C     THIS ROUTINE DETERMINES WHETHER A POSITIVE-GOING ZERO CROSSING
C     JUST OCCURRED
C
      INTEGER TOTDT,TBN
      LOGICAL CROSS,VAP,ZP,VBP,VCM,ZM
      COMMON NAM7(3),NAM8(3),IOPT7,IOPT8,ID7(576),ID8(144),IB7(40),
     +IB8(40),J,TOTDT,TBN,SIG1(500),SIG2(500),SAVEJ(2),DT,DTBP,DTN,
     +ZERO,NDT,VA,VB,VC,VAP,ZP,VBP,VCM,ZM,VARM,LU
      IF(J.NE.1) GO TO 10
      IF(SAVEJ(1).LE.ZERO.AND.SIG2(J).GT.ZERO)30,20
   10 IF(SIG2(J-1).LE.ZERO.AND.SIG2(J).GT.ZERO) GO TO 30
   20 CROSS=.FALSE.
      RETURN
   30 CROSS=.TRUE.
      RETURN
      END



      SUBROUTINE SHIFT
C
C     DOES MANIPULATION OF I/O ARRAYS; THAT IS, IT SHIFTS INFORMATION
C     FROM SIG1 TO SIG2 AND ISSUES A NEW READ TO SIG1.
C
      INTEGER TOTDT,TBN
      LOGICAL VAP,ZP,VBP,VCM,ZM
      COMMON NAM7(3),NAM8(3),IOPT7,IOPT8,ID7(576),ID8(144),IB7(40),
     +IB8(40),J,TOTDT,TBN,SIG1(500),SIG2(500),SAVEJ(2),DT,DTBP,DTN,
     +ZERO,NDT,VA,VB,VC,VAP,ZP,VBP,VCM,ZM,VARM,LU
C
C     SAVE SIGNALS WHICH MAY BE NEEDED FOR INTERPOLATION
C
      SAVEJ(1)=SIG2(500)
      SAVEJ(2)=SIG2(499)
      DO 10 I=1,500
      SIG2(I)=SIG1(I)
   10 SIG1(I)=0.0
      DO 20 I=1,500
      CALL READF(ID7,IERR,IB7,8,LEN)
      IF(LEN.NE.-1)GO TO 22
      SIG1(I)=0.0
      GO TO 20
   22 CALL CODE
      READ(IB7,30)SIG1(I)
   30 FORMAT(E16.8)
   20 CONTINUE
      J=0
      RETURN
      END
```

```
      SUBROUTINE NEXTS(EOF)
C
C     GETS NEXT SIGNAL, CHECKS FOR END-OF-FILE (OF INPUT SIGNALS)
C     AND END-OF-ARRAY (INDICATING THAT I/O ARRAY MANIPULATION NEEDS
C     TO BE DONE), AND ALSO INCREMENTS NECESSARY COUNTERS.
C
      INTEGER TOTDT,TBN
      LOGICAL EOF,VAP,ZP,VBP,VCM,ZM
      COMMON NAM7(3),NAM8(3),IOPT7,IOPT8,ID7(576),ID8(144),IB7(40),
     +IB8(40),J,TOTDT,TBN,SIG1(500),SIG2(500),SAVEJ(2),DT,DTBP,DTN,
     +ZERO,NDT,VA,VB,VC,VAP,ZP,VBP,VCM,ZM,VARM,LU
      TOTDT=TOTDT+1
      IF(TOTDT.LE.NDT) GO TO 100
      EOF=.TRUE.
      RETURN
  100 J=J+1
      IF(J.LE.500) GO TO 200
      CALL SHIFT
      J=1
  200 TBN=TBN+1
      EOF=.FALSE.
      RETURN
      END
```

```
      SUBROUTINE NAME
      INTEGER TOTDT,TBN
      LOGICAL VAP,ZP,VBP,VCM,ZM
      COMMON NAM7(3),NAM8(3),IOPT7,IOPT8,ID7(576),ID8(144),IB7(40),
     +IB8(40),J,TOTDT,TBN,SIG1(500),SIG2(500),SAVEJ(2),DT,DTBP,DTN,
     +ZERO,NDT,VA,VB,VC,VAP,ZP,VBP,VCM,ZM,VARM,LU
      WRITE(LU,1)
    1 FORMAT(" PLEASE ENTER THE INPUT FILE NAME")
      READ(LU,2)(NAM7(I),I=1,3)
      IOPT7=1
      WRITE(LU,3)
    3 FORMAT(" NOW THE OUTPUT FILE NAME")
      READ(LU,2)(NAM8(I),I=1,3)
    2 FORMAT(3A2)
      IOPT8=200
      DO 10 I=1,40
      IB7(I)=2H
   10 IB8(I)=2H
      RETURN
      END
```

```
      REAL FUNCTION INTRP(IDEG)
C
C     INTERPOLATION ROUTINE
C       OPTIONS:   IDEG=
C                        ZERO--NO INTERPOLATION
C                        ONE---LINEAR INTERPOLATION
C
      INTEGER TOTDT,TBN
      LOGICAL VAP,ZP,VBP,VCM,ZM
      COMMON NAM7(3),NAM8(3),IOPT7,IOPT8,ID7(576),ID8(144),IB7(40),
     +IB8(40),J,TOTDT,TBN,SIG1(500),SIG2(500),SAVEJ(2),DT,DTBP,DTN,
     +ZERO,NDT,VA,VB,VC,VAP,ZP,VBP,VCM,ZM,VARM,LU
      IF(IDEG.EQ.0) GO TO 10
      IF(J.NE.1) GO TO 20
      SIGA=SAVEJ(1)
      GOTO 30
   20 SIGA=SIG2(J-1)
   30 DTN=(-SIGA+ZERO)*DT/(SIG2(J)-SIGA)
      INTRP=DTBP+(TBN-1)*DT+DTN
      RETURN
   10 INTRP=TBN*DT
      RETURN
      END



      SUBROUTINE CHKSQ(PROPR,ARB)
C
C     THIS ROUTINE CHECKS THE SEQUENCE OF THE SIGNALS AS THEY'RE
C     ACCESSED AND SETS THE APPROPRIATE LOGICAL VARIABLES.  ALSO, IT
C     CHANGES 'VARM' IF A SIGNAL IS MISSED.
C
      INTEGER TOTDT,TBN
      LOGICAL PROPR,VAP,ZP,VBP,VCM,ZM,ARB
      COMMON NAM7(3),NAM8(3),IOPT7,IOPT8,ID7(576),ID8(144),IB7(40),
     +IB8(40),J,TOTDT,TBN,SIG1(500),SIG2(500),SAVEJ(2),DT,DTBP,DTN,
     +ZERO,NDT,VA,VB,VC,VAP,ZP,VBP,VCM,ZM,VARM,LU
      IF(J.NE.1) GO TO 11
      SIGA=SAVEJ(1)
      GO TO 12
   11 SIGA=SIG2(J-1)
   12 IF(SIGA.LE.VA.AND.SIG2(J).GT.VA) GO TO 20
      IF(SIGA.LE.VB.AND.SIG2(J).GT.VB) GO TO 33
      IF(SIGA.GT.VC.AND.SIG2(J).LE.VC) GO TO 40
      IF(SIGA.LE.ZERO.AND.SIG2(J).GT.ZERO) GO TO 55
      IF(SIGA.GT.ZERO.AND.SIG2(J).LE.ZERO) GO TO 60
      GO TO 705
   20 VAP=.TRUE.
      ZP=.FALSE.
      GO TO 705
```

```
 33   VBP=.TRUE.
      GO TO 705
 40   VCM=.TRUE.
      ZM=.FALSE.
      GO TO 705
 55   IF(VCM) GO TO 28
      VARM=VC
      GO TO 805
 28   ZP=.TRUE.
      VCM=.FALSE.
      GO TO 705
 60   IF(VAP) GO TO 29
      VARM=VA
      IF(ARB)VARM=VB
      GO TO 805
 29   ZM=.TRUE.
      VAP=.FALSE.
      VBP=.FALSE.
705   PROPR=.TRUE.
      GO TO 710
805   PROPR=.FALSE.
710   RETURN
      END
```

```
FTN4,L
      PROGRAM COMP
C
C     THIS PROGRAM TAKES THE OUTPUT OF COUNT AS INPUT, PERFORMS
C     COMPUTATIONS ON THIS INFORMATION, AND OUTPUTS TWO FILES.  ONE
C     FILE CONSISTS OF THE NORMALIZED FREQUENCY ERRORS  THE OTHER
C     FILE CONSISTS OF THE FREQUENCY ERRORS FOR SHORT-TIME SAMPLES.
C     ALSO, THE RMS ERRORS ARE COMPUTED AND STORED IN THE HEADER
C     OF THE APPROPRIATE FILE
C
      DIMENSION FREQ(1000),ER(1000),IPRAM(5),FSAMP(1000)
      INTEGER SAMPL,ITIME(5),IYEAR(1)
      REAL MXNTL
      COMMON NAM7(3),NAM8(3),IOPT7,IOPT8,ID7(144),ID8(144),ID9(144),
     +IB7(40),IB8(40),IB9(40),NAM9(3),LU
      CALL RMPAR(IPRAM)
      LU=IPRAM(1)
      IF(LU.EQ.0)LU=1
      IOPT7=1
C
C     THERE ARE 3 ERROR CHECK OPTIONS WHICH CAN BE USED TO 'THIN'
C     THE RAW DATA SET.
C          OPTION 1:  FREQUENCY ESTIMATES MUST AGREE WITHIN X PERCENT
C                     --IGNORE ALL RESETS BEFORE NC COUNTS WERE OBTAINED
C
C          OPTION 2:  USE ONLY RESETS DUE TO END OF BURST
C          OPTION 3:  IGNORE ALL RESETS BEFORE NC COUNTS WERE OBTAINED
C                     (SAME AS OPTION 1 EXCEPT NO REQUIREMENT FOR
C                     AGREEMENT BETWEEN FREQUENCY ESTIMATES)
C     ---SO FAR, ONLY OPTION 3 HAS BEEN TESTED---
C
      WRITE(LU,10)
   10 FORMAT(" INPUT ERROR CHECK OPTION:"/
     +      "         1= MXN AT X PERCENT LEVEL CHECK"/
     +      "         2= TOTAL BURST MODE CHECK"/
     +      "         3= NC COUNT CHECK")
      READ(LU,*)ICHCK
      CALL NAME
      WRITE(LU,50)
   50 FORMAT(" INPUT DATA DIGITIZATION OPTION:"/
     +      "         0= DO NOT DIGITIZE DATA"/
     +      "         1= DIGITIZE DATA")
C
C     THE OPTION TO DIGITIZE THE DATA IS PROVIDED IN ORDER TO SIMULATE
C     THE CLOCK DIGITIZATION ERROR (BUT THIS OPTION HAS NOT YET BEEN
C     TESTED)
C
      READ(LU,*)IDIG
      IF(IDIG.EQ.0)GO TO 70
      WRITE(LU,60)
   60 FORMAT(" ENTER VALUE FOR INTERVAL SIZE (DELC)")
      READ(LU,*)DELC
      DELT1=DELC
      DELT2=0.0
C
C     NS=NUMBER OF VALID SAMPLES OBTAINED
C     NTB=NUMBER OF TB'S THAT HAVE BEEN PROCESSED
C     TBTOT=CURRENT TIME
```

```
C       TNEXT=END TIME FOR CURRENT SHORT-TIME AVERAGE
C
   70   NS=0
        NTB=0
        TBTOT=0.0
        FRQSM=0.0
        TNEXT=TSAMP
        SAMPL=0
        CALL CREAT(ID8,IERR,NAM8,IOPT8,3,0,12,144)
        CALL CREAT(ID9,IERR,NAM9,IOPT8,3,0,12,144)
C
C       GET TIME OF DAY TO STORE IN HEADER OF CREATED FILE
C
        CALL EXEC(11,ITIME,IYEAR)
        CALL OPEN(ID7,IERR,NAM7,IOPT7)
        CALL READF(ID7,IERR,IB7,40)
        CALL READF(ID7,IERR,IB7,40)
        CALL CODE
        READ(IB7,126)NHEAD
  126   FORMAT(I5)
        DO 127 I=1,NHEAD
  127   CALL READF(ID7,IERR,IB7,40)
        CALL READF(ID7,IERR,IB7,40)
        CALL CODE
        READ(IB7,130)T,DT
  130   FORMAT(2E16.8)
        CALL READF(ID7,IERR,IB7,40)
        CALL CODE
        READ(IB7,135)FT
  135   FORMAT(E16.8)
        CALL READF(ID7,IERR,IB7,40)
        CALL CODE
        READ(IB7,137)NC,MC
  137   FORMAT(2I3)
        WRITE(LU,80)
   80   FORMAT(" INPUT STOPPING OPTION:"/
     +  "          1=STOP AFTER GIVEN AMOUNT OF TIME"/
     +  "          2=STOP AFTER GIVEN AMOUNT OF VALID DATA"/
     +  "             HAS BEEN COLLECTED")
        READ(LU,*)ISTOP
        IF(ISTOP.EQ.1)GO TO 100
        WRITE(LU,90)
   90   FORMAT(" ENTER AMOUNT (OF VALID DATA SAMPLES)")
        READ(LU,*)NSAMP
        GO TO 120
  100   WRITE(LU,110)
  110   FORMAT(" ENTER TIME")
        READ(LU,*)FTIME
        IF(FTIME.LE.T)GO TO 120
        WRITE(LU,115)
  115   FORMAT(" TIME INPUT IS GREATER THAN TOTAL SIMULATION TIME"/
     +  "--VALUE IS ADJUSTED TO EQUAL TOTAL SIMULATION TIME"/)
```

```
      FTIME=T
 120  WRITE(LU,125)
 125  FORMAT(" INPUT DURATION TIME FOR SHORT-TIME AVERAGE")
      READ(LU,*)TSAMP
      IF(TSAMP.GT.T)TSAMP=T
      GO TO (1,2,3)ICHCK
C
C     M X N TOLERANCE LEVEL CHECK
C
 1    WRITE(LU,200)
 200  FORMAT(" INPUT MXN TOLERANCE LEVEL")
      READ(LU,*)MXNTL
 205  IF(TBTOT.LT.TNEXT) GO TO 207
C
C     END OF SHORT-TIME AVERAGE REACHED, COMPUTE SAMPLE FREQUENCY AND
C     UPDATE COUNTERS
C
      SAMPL=SAMPL+1
      FSAMP(SAMPL)=1.0/NTB*FRQSM
      NTB=0
      TNEXT=TNEXT+TSAMP
      FRQSM=0.0
 207  IF((ISTOP.EQ.1).AND.(TBTOT.GE.FTIME)) GOTO 500
      CALL READF(ID7,IERR,IB7,40)
      CALL CODE
      READ(IB7,210)TA,TB,TM,TN,MESS
 210  FORMAT(4E16.8,I5)
      TBTOT=TBTOT+TB
      NTB=NTB+1
C
C     IMESS IS THE REASON A RESET OCCURRED
C
      IMESS=MESS/1000
      IF((IMESS.GE.1).AND.(IMESS.LE.5))GO TO 250
      IF(IDIG.EQ.0)GO TO 230
      TM=DIGTZ(TM,DELTI,DELC)
      TN=DIGTZ(TN,DELTI,DELC)
      CALL TBDIG(TB,DELTI,DELC,DELTI)
 230  FN=NC/TN
      FM=MC/TM
      IF(ABS((FN-FM)/FN).GT.MXNTL) GO TO 205
      NS=NS+1
      FREQ(NS)=FN
      FRQSM=FRQSM+FREQ(NS)
      IF((ISTOP.EQ.2).AND.(NS.GE.NSAMP))GO TO 500
      GO TO 205
 250  IF(IDIG.EQ.1) CALL TBDIG(TB,DELTI,DELC,DELTI)
      GO TO 205
C
C     TOTAL BURST MODE CHECK
C
 2    IF(TBTOT.LT.TNEXT) GO TO 290
      SAMPL=SAMPL+1
```

```
      FSAMP(SAMPL)=1.0/NTB*FRQSM
      NTB=0
      TNEXT=TNEXT+TSAMP
      FRQSM=0.0
  290 IF((ISTOP.EQ.1).AND.(TBTOT.GE.FTIME))GO TO 500
      CALL READF(ID7,IERR,IB7,40)
      CALL CODE
      READ(IB7,300)TA,TB,TM,TN,MESS
  300 FORMAT(4E16.8,I5)
      TBTOT=TBTOT+TB
      NTB=NTB+1
      IMESS=MESS/1000
      IF(IMESS.LT.16) GO TO 310
      IF(IDIG.EQ.0) GO TO 305
      TA=DIGTZ(TA,DELTI,DELC)
      CALL TBDIG(TB,DELTI,DELC,DELTI)
  305 NS=NS+1
      FREQ(NS)=(MESS-1000*IMESS)/TA
      FRQSM=FRQSM+FREQ(NS)
      IF((ISTOP.EQ.2).AND.(NS.GE.NSAMP)) GO TO 500
      GO TO 2
  310 IF(IDIG.EQ.1) CALL TBDIG(TB,DELTI,DELC,DELTI)
      GO TO 2
C
C     NC COUNT CHECK
C
    3 IF(TBTOT.LT.TNEXT) GO TO 390
      SAMPL=SAMPL+1
      FSAMP(SAMPL)=1.0/NTB*FRQSM
      NTB=0
      TNEXT=TNEXT+TSAMP
      FRQSM=0.0
  390 IF((ISTOP.EQ.1).AND.(TBTOT.GE.FTIME)) GO TO 500
      CALL READF(ID7,IERR,IB7,40)
      CALL CODE
      READ(IB7,400)TA,TB,TM,TN,MESS
  400 FORMAT(4E16.8,I5)
      TBTOT=TBTOT+TB
      NTB=NTB+1
      IMESS=MESS/1000
      IF((IMESS.GE.1).AND.(IMESS.LE.6)) GO TO 420
      IF(IDIG.EQ.0) GO TO 410
      TN=DIGTZ(TN,DELTI,DELC)
      CALL TBDIG(TB,DELTI,DELC,DELTI)
  410 NS=NS+1
      FREQ(NS)=NC/TN
      FRQSM=FRQSM+FREQ(NS)
      IF((ISTOP.EQ.2).AND.(NS.GE.NSAMP))GO TO 500
      GO TO 3
  420 IF(IDIG.EQ.1) CALL TBDIG(TB,DELTI,DELC,DELTI)
      GO TO 3
C
C     STOPPING CRITERION WAS MET--COMPUTE FREQUENCY ERROR AND RMSE
C
```

```
500 SUMSQ=0.0
    SUMER=0.0
    DO 550 I=1,NS
    ER(I)=(FREQ(I)-FT)/FT
    SUMER=SUMER+ER(I)
550 SUMSQ=SUMSQ+ER(I)*ER(I)
    EMEAN=1.0/NS*SUMER
    RMSE=SQRT(1.0/NS*SUMSQ)
    SUMSQ=0.0
    DO 600 I=1,SAMPL
600 SUMSQ=SUMSQ+(FT-FSAMP(I))**2
    SIG=SQRT(1.0/(SAMPL-1)*SUMSQ)
    WRITE(LU,702)RMSE,SIG
702 FORMAT(" RMSE=",E16.8,"    SIG=",E16.8,5X)
C
C     WRITE HEADER INFORMATION TO OUTPUT FILE
C
    CALL CODE
    WRITE(IB8,610)
610 FORMAT(" COMP OUTPUT")
    CALL WRITF(ID8,IERR,IB8,40)
    NHEDR=7
    CALL CODE
    WRITE(IB8,620)NHEDR
620 FORMAT(I5," LINES OF HEADER INFORMATION")
    CALL WRITF(ID8,IERR,IB8,40)
    CALL CODE
    WRITE(IB8,625)ITIME(5),IYEAR(1),ITIME(4),ITIME(3),ITIME(2)
625 FORMAT(" CREATION DATE:",I5,1X,I5," TIME:",3I5)
    CALL WRITF(ID8,IERR,IB8,40)
    CALL CODE
    WRITE(IB8,630)ICHCK,IDIG,DELC
630 FORMAT(" ERROR CHECK OPTION=",I1,"  DIG. OPTION=",I1,
   +"  INTERVAL SIZE=",E10.4)
    CALL WRITF(ID8,IERR,IB8,40)
    CALL CODE
    WRITE(IB8,640)ISTOP,NSAMP,FTIME
640 FORMAT(" STOPPING OPTION=",I2,"   # OF VALID SAMPLES=",I5,
   +"   TIME=",E10.4)
    CALL WRITF(ID8,IERR,IB8,40)
    CALL CODE
    WRITE(IB8,650)TSAMP,MXNTL
650 FORMAT(" TIME FOR SHORT-TIME AVG.=",E10.4,"   M X N TOLERANCE=",
   +E10.4)
    CALL WRITF(ID8,IERR,IB8,40)
    CALL CODE
    WRITE(IB8,660)(NAM7(I),I=1,3),(NAM8(I),I=1,3)
660 FORMAT(" INPUT FILE="3A2,"    OUTPUT FILE="3A2,25X)
    CALL WRITF(ID8,IERR,IB8,40)
    CALL CODE
    WRITE(IB8,701)EMEAN
701 FORMAT(" MEAN ERROR=",E16.8,25X)
    CALL WRITF(ID8,IERR,IB8,40)
```

```
      CALL CODE
      WRITE(IB8,705)RMSE
705   FORMAT(" RMSE=",E16.8,25X)
      CALL WRITF(ID8,IERR,IB8,40)
      CALL CODE
      WRITE(IB8,670)NS
670   FORMAT(E16.8,50X)
      CALL WRITF(ID8,IERR,IB8,40)
      DO 700 I=1,NS
      CALL CODE
      WRITE(IB8,710)ER(I)
710   FORMAT(E16.8)
700   CALL WRITF(ID8,IERR,IB8,8)
      CALL CODE
      WRITE(IB9,800)
800   FORMAT(" COMP SHORT-TIME AVERAGING OUTPUT")
      CALL WRITF(ID9,IERR,IB9,40)
      NHEDR=3
      CALL CODE
      WRITE(IB9,620)NHEDR
      CALL WRITF(ID9,IERR,IB9,40)
      CALL CODE
      WRITE(IB9,625)ITIME(5),IYEAR(1),ITIME(4),ITIME(3),ITIME(2)
      CALL WRITF(ID9,IERR,IB9,40)
      CALL CODE
      WRITE(IB9,810)TSAMP,SIG
810   FORMAT(" TIME FOR SHORT-TIME AVG.=",E10.4,
     +"  SIG(RMS ERROR)=",E16.8)
      CALL WRITF(ID9,IERR,IB9,40)
      CALL CODE
      WRITE(IB9,840)(NAM8(I),I=1,3)
840   FORMAT(" CORRESPONDING NORMALIZED FREQ. ERROR FILE = ",3A2,25X)
      CALL WRITF(ID9,IERR,IB9,40)
      CALL CODE
      WRITE(IB9,670)SAMPL
      CALL WRITF(ID9,IERR,IB9,40)
      DO 820 I=1,SAMPL
      FSAMP(I)=FT-FSAMP(I)
      CALL CODE
      WRITE(IB9,830)FSAMP(I)
830   FORMAT(E16.8)
820   CALL WRITF(ID9,IERR,IB9,8)
      CALL LOCF(ID8,IERR,IREC,IRB,IOFF,JSEC)
      ITRUN=JSEC/2-IRB-1
      CALL CLOSE(ID8,IERR,ITRUN)
      IF(IERR.LT.0)CALL CLOSE(ID8)
      CALL LOCF(ID9,IER,IREC,IRB,IOFF,JSEC)
      ITRUN=JSEC/2-IRB-1
      CALL CLOSE(ID9,IERR,ITRUN)
      IF(IERR.LT.0)CALL CLOSE(ID9)
      CALL CLOSE(ID7)
      STOP
      END
```

```
      FUNCTION DIGTZ(TX,DELTI,DELC)
C
C     THIS FUNCTION COMPUTES THE SIMULATED PROCESSOR MEASUREMENT OF TX.
C
      TXX=TX-DELTI
      KX=INT(TXX/DELC)+1
      DIGTZ=KX*DELC
      RETURN
      END


      SUBROUTINE TBDIG(TB,DELTI,DELC,DELTB)
C
C     THIS SUBROUTINE COMPUTES THE SIMULATED PROCESSOR MEASUREMENT OF TB
C     AND COMPUTES THE FRACTIONAL VALUE OF INTERVAL TIME TO BE STORED
C     FOR THE NEXT SET
C
      TBN=DIGTZ(TB,DELTI,DELC)
      DELTB=(TB-DELTI)-(TBN-DELC)
      RETURN
      END


      SUBROUTINE NAME
      COMMON NAM7(3),NAM8(3),IOPT7,IOPT8,ID7(144),ID8(144),ID9(144),
     +IB7(40),IB8(40),IB9(40),NAM9(3),LU
      WRITE(LU,1)
    1 FORMAT(" PLEASE ENTER THE INPUT FILE NAME")
      READ(LU,2)(NAM7(I),I=1,3)
      IOPT7=1
      WRITE(LU,3)
    3 FORMAT(" NOW THE NORMALIZED FREQUENCY ERROR OUTPUT FILE NAME")
      READ(LU,2)(NAM8(I),I=1,3)
    2 FORMAT(3A2)
      WRITE(LU,4)
    4 FORMAT(" NOW ENTER THE SHORT-TIME AVERAGING OUTPUT FILE NAME")
      READ(LU,5)(NAM9(I),I=1,3)
    5 FORMAT(3A2)
      IOPT8=100
      DO 10 I=1,40
      IB7(I)=2H
      IB8(I)=2H
   10 IB9(I)=2H
      RETURN
      END
```

```
FTN4,L
      PROGRAM HISTO
C
C     THIS PROGRAM TAKES DATA FROM AN INPUT FILE AND, GIVEN THE
C     LOWER BOUND, THE UPPER BOUND, AND THE NUMBER OF BINS, CREATES
C     AN OUTPUT FILE CONTAINING HISTOGRAM VALUES.  EITHER A LINEAR OR
C     A LOG-LOG SORT MAY BE DONE.
C
      REAL LOWER
      DIMENSION X(2000),XNUM(100),IPRAM(5),V(100)
      COMMON NAM7(3),NAM8(3),IOPT7,IOPT8,ID7(144),ID8(144),
     +IB7(40),IB8(40),LU
      CALL RMPAR(IPRAM)
      LU=IPRAM(1)
      IF(LU.EQ.0)LU=1
      CALL NAME
      CALL CREAT(ID8,IERR,NAM8,IOPT8,3,0,12,144)
      CALL OPEN(ID7,IERR,NAM7,IOPT7,12)
      CALL READF(ID7,IERR,IB7,40)
      CALL READF(ID7,IERR,IB7,40)
C
C     READ THE # OF ELEMENTS IN THE FILE
C
      CALL CODE
      READ(IB7,12)NHEAD
   12 FORMAT(I5)
      DO 13 I=1,NHEAD
   13 CALL READF(ID7,IERR,IB7,40)
      CALL READF(ID7,IERR,IB7,40)
      CALL CODE
      READ(IB7,10)XN
   10 FORMAT(E16.8)
      N=XN
      WRITE(LU,15)
   15 FORMAT(" ENTER INPUT SCALE FACTOR (1.0 IF NOT DESIRED)")
      READ(LU,*)SCALR
      WRITE(LU,70)
   70 FORMAT(" ENTER OUTPUT SCALE FACTOR (1.0 IF NOT DESIRED)")
      READ(LU,*)SCAL1
      IF(SCAL1.NE.1.0)SCAL1=SCAL1/N
      DO 100 I=1,N
      CALL READF(ID7,IERR,IB7,8)
      CALL CODE
      READ(IB7,20)X(I)
   20 FORMAT(E16.8)
  100 X(I)=X(I)*SCALR
      CALL CODE
      WRITE(IB8,40)
   40 FORMAT("HISTOGRAM DATA")
      CALL WRITF(ID8,IERR,IB8,40)
      WRITE(LU,16)
   16 FORMAT(" INPUT DESIRED TYPE OF HISTOGRAM SORT:"/
     +      "  0=LINEAR      1=LOG-LOG")
```

```
      READ(LU,*)LOG
      IF(LOG.NE.1)GO TO 17
C
C     LOG-LOG SORT OPTION
C
      WRITE(LU,300)
 300  FORMAT(" INPUT CONSTANT MULTIPLIER,BASE,AND NUMBER OF INTERVALS")

      READ(1,*)A,B,NBINS
      V(1)=A
      DO 310 I=2,NBINS+1
 310  V(I)=V(I-1)*B
      DO 315 I=1,NBINS+1
 315  XNUM(I)=0
      DO 320 I=1,NBINS+1
      DO 320 J=1,N
 320  IF(X(J).GE.V(I))XNUM(I)=XNUM(I)+1
      CALL CODE
      WRITE(IB8,330)A,B,NBINS,LOG,SCALR
 330  FORMAT(2E10.4,1X,I3,I2,E10.4)
      CALL WRITF(ID8,IERR,IB8,40)
      NBINS=NBINS-1
      GO TO 115
C
C     LINEAR SORT OPTION
C
 17   WRITE(LU,30)
 30   FORMAT(" INPUT LOWER AND UPPER LIMIT AND TOTAL # OF BINS")
      READ(LU,*)LOWER,UPPER,NBINS
      CALL CODE
      WRITE(IB8,50)LOWER,UPPER,NBINS,LOG,SCALR
 50   FORMAT(2E10.4,1X,I3,I2,E10.4)
      CALL WRITF(ID8,IERR,IB8,40)
      XINC=(UPPER-LOWER)/NBINS
      DO 105 I=1,NBINS+2
 105  XNUM(I)=0.0
      DO 110 I=1,N
      INDX=(X(I)-LOWER)/XINC+1
C
C     TWO EXTRA BINS ARE APPENDED.  THE FIRST CONTAINS THE NUMBER OF
C     VALUES < THE LOWER BOUND; THE SECOND CONTAINS THE NUMBER OF VALUES

C     > THE UPPER BOUND
C
      IF(X(I).LT.LOWER)INDX=NBINS+1
      IF(X(I).GE.UPPER)INDX=NBINS+2
 110  XNUM(INDX)=XNUM(INDX)+1
 115  CONTINUE
      DO 150 I=1,40
 150  IB8(I)=2H
      DO 200 I=1,NBINS+2
      XNUM(I)=XNUM(I)*SCAL1
      IF(LOG.NE.1)GO TO 151
      CALL CODE
      WRITE(IB8,61)V(I),XNUM(I)
```

```
51    FORMAT(2E16.8)
      CALL WRITF(ID8,IERR,IB8,16)
      GO TO 200
151   CALL CODE
      WRITE(IB8,60)XNUM(I)
60    FORMAT(E16.8)
      CALL WRITF(ID8,IERR,IB8,40)
200   CONTINUE
      CALL CLOSE(ID7)
      CALL LOCF(ID8,IERR,IREC,IRB,IOFF,JSEC)
      ITRUN=JSEC/2-IRB-1
      CALL CLOSE(ID8,IERR,ITRUN)
      IF(IERR.LT.0)CALL CLOSE(ID8)
      STOP
      END


      SUBROUTINE NAME
      COMMON NAM7(3),NAM8(3),IOPT7,IOPT8,ID7(144),
     +ID8(144),IB7(40),IB8(40),LU
      WRITE(LU,1)
1     FORMAT(" PLEASE ENTER THE INPUT FILE NAME")
      READ(LU,2)(NAM7(I),I=1,3)
      IOPT7=1
      WRITE(LU,3)
3     FORMAT(" NOW THE OUTPUT FILE NANE")
      READ(LU,2)(NAM8(I),I=1,3)
2     FORMAT(3A2)
      IOPT8=100
      DO 10 I=1,40
      IB7(I)=2H
10    IB8(I)=2H
      RETURN
      END
```

```
FTN4,L
      PROGRAM PLOT
C
C     THIS PROGRAM ALLOWS SEVERAL TYPES OF PLOTS TO BE PRODUCED FROM
C     DATA READ FROM AN INPUT FILE.  THERE ARE TWO POSSIBLE TYPES OF
C     INPUT FILES:
C
C          1.  A FILE CONTAINING HISTOGRAM DATA (THE FIRST LINE OF
C              SUCH A FILE MUST BE A TITLE STARTING WITH THE
C              LETTERS 'HI')
C          2.  A FILE CONTAINING A SINGLE LIST OF NUMBERS REPRESENTED
C              AS A FUNCTION OF TIME (THESE NUMBERS ARE PRECEDED BY
C              HEADER INFORMATION FOLLOWED BY 'T' AND 'DT', WHICH ARE
C              THE TOTAL TIME AND THE TIME INCREMENT)
C
C     OPTIONS ARE INCLUDED FOR:
C          1.  LINEAR VS. LOGARITHMIC PLOTS
C          2.  OPERATOR SELECTED VS. AUTOMATIC SCALING OF AXES
C          3.  LABELING OF AXES
C          4.  SKIPPING EVERY 'N' POINTS VS. AVERAGING EVERY 'N' POINTS
C          5.  NORMALIZATION OF HISTOGRAMS TO MAXIMUM VALUE
C          6.  SELECTION OF SYMBOL TYPE AND FREQUENCY OF PLOTTED SYMBOL:
C
      DIMENSION X(1500),Y(1500),NAM7(3),ID7(576),IB7(40)
      INTEGER XNAME(16),YNAME(16),NEG(3),POS(3),IPRAM(5),IMAX(3)
      REAL LOWER,MAX,NUM(100)
      DATA NEG/4,2HNE,2HG=/
      DATA POS/4,2HPO,2HS=/
      DATA IMAX/4,2HMA,2HX=/
      CALL RMPAR(IPRAM)
      LU=IPRAM(1)
      IF(LU.EQ.0)LU=1
      IRUN=0
      LOG2=0
      CALL PLTLU(10)
      WRITE(LU,40)
 40   FORMAT(" DO YOU WANT 8 INCREMENTS OR 10 ON X-AXIS?")
      READ(LU,*)LEN
      IF(LEN.EQ.10)GO TO 42
      CALL SFACT(11.,8.5)
      XLEN=-8.
      YLEN=6.
      GO TO 1
 42   CALL SFACT(13.,10.)
      XLEN=-10.
      YLEN=8.
 1    WRITE(LU,14)
 14   FORMAT(" PLEASE TYPE IN THE DATA FILE NAME AND CARTRIDGE #")
      READ(LU,15)(NAM7(I),I=1,3),ICR
 15   FORMAT(3A2,1X,I2)
      IF(IRUN.NE.0)GO TO 49
      WRITE(LU,12)
 12   FORMAT(" INPUT X AND Y AXIS LABELS")
```

```
      READ(LU,13)(XNAME(I),I=2,16),(YNAME(J),J=2,16)
13    FORMAT(15A2,1X,15A2)
      XNAME(1)=30
      YNAME(1)=30
      IOPT7=1
49    CALL LLEFT
      DO 10 I=1,40
10    IB7(I)=2H
      CALL OPEN(ID7,IERR,NAM7,IOPT7,ICR)
C
C     THE FIRST LINE OF THE INPUT FILE (THE TITLE) DETERMINES WHAT TYPE
C     OF PLOT IS DESIRED.  SPECIFICALLY, IF THE FIRST 2 CHARACTERS ARE
C     'HI', IT IS ASSUMED TO BE HISTOGRAM DATA.
C
      CALL READF(ID7,IERR,IB7,40)
      CALL CODE
      READ(IB7,30)ITYPE
30    FORMAT(A2)
      IF(ITYPE.EQ.2HHI)GO TO 800
C
C     FILE IS NOT HISTOGRAM DATA. SKIP OVER HEADER LINES AND READ T AND
C     DT TO DETERMINE THE NUMBER OF VALUES IN THE FILE.
C
      CALL READF(ID7,IERR,IB7,40)
      CALL CODE
      READ(IB7,31)NHEAD
31    FORMAT(I5)
      DO 32 I=1,NHEAD
32    CALL READF(ID7,IERR,IB7,40)
      CALL READF(ID7,IERR,IB7,40)
      CALL CODE
      READ(IB7,20)T,DT
20    FORMAT(2E16.8)
      TSUM=-DT
      NDT=T/DT
21    WRITE(LU,4)
4     FORMAT(" INPUT TYPE OF PLOT (0=LINEAR,1=LOG)")
      READ(LU,*)LOG
      WRITE(LU,5)
5     FORMAT(" INPUT SKIP INTERVAL (I.E.'3' PLOTS EVERY 3RD POINT "/
     +       "                                BEGINNING WITH THE FIRST POINT;"/
     +       "                                '0' SELECTS AVERAGING OPTION)")
      READ(LU,*)NSKIP
      IF(NSKIP.NE.0) GO TO 9
C
C     IF SKIP INTERVAL IS SPECIFIED AS '0' THEN GIVE OPTION TO AVERAGE
C
      WRITE(LU,6)
6     FORMAT(" INPUT # OF CONSECUTIVE POINTS TO AVERAGE")
      READ(LU,*)NAVG
      NDT=NDT/NAVG
      GO TO 11
9     NDT=NDT/NSKIP
```

```
 11  WRITE(LU,16)
 16  FORMAT(" INPUT SCALING OPTION--0=OPERATOR SELECTED"/
    +     "                                  1=AUTOMATIC")
     READ(LU,*)ISCAL
C
C    IF AUTO SCALING IS SELECTED AND THIS IS A LINEAR HISTOGRAM PLOT,
C    DON'T GIVE OPTION OF TYPE OF LINE TO DRAW (SO WILL AUTOMATICALLY
C    PLOT CONTINUOUS LINE)
C
     IF((ISCAL.EQ.1).AND.(ITYPE.EQ.2HHI).AND.(LOG2.NE.1))GO TO 855
     IF(ISCAL.EQ.1) GO TO 600
C
C    IF OPERATOR SCALED, ACCEPT SCALE VALUES
C
     WRITE(LU,17)
 17  FORMAT(" INPUT MINIMUM AND INCREMENT FOR X-AXIS")
     READ(LU,*)XMIN,XINC
     WRITE(LU,18)
 18  FORMAT(" INPUT MINIMUM AND INCREMENT FOR Y-AXIS")
     READ(LU,*)YMIN,YINC
     X(NDT+1)=XMIN
     X(NDT+2)=XINC
     Y(NDT+1)=YMIN
     Y(NDT+2)=YINC
C
C    IF LINEAR HISTOGRAM ,A CONTINUOUS LINE WILL AUTOMATICALLY BE DRAWI
C    SO SKIP NEXT OPTION
C
     IF((ITYPE.EQ.2HHI).AND.(LOG2.NE.1))GO TO 855
 600 WRITE(LU,19)
 19  FORMAT(" INPUT CONTROL VALUE AND SYMBOL NUMBER"/
    +     "          (SEE PLOT MANUAL--ROUTINE 'LINES')")
     READ(LU,*)NCNTR,SYM
     IF(LOG2.EQ.1)GO TO 500
C
C    IF NOT HISTOGRAM PLOT, SET UP SKIPPING OR AVERAGING DATA
C
     IF(NSKIP.EQ.0) GO TO 22
C
C    SKIPPING OPTION
C
     CALL READF(ID7,IERR,IB7,8)
     CALL CODE
     READ(IB7,35)Y(1)
     X(1)=0.0
     DO 100 I=2,NDT
     X(I)=X(I-1)+NSKIP*DT
     DO 200 J=1,NSKIP
 200 CALL READF(ID7,IERR,IB7,8)
     CALL CODE
     READ(IB7,35)Y(I)
     IF(LOG.NE.1)GO TO 100
     IF(Y(I).LE.0)Y(I)=-1.0E+36
```

```
      IF(Y(I).GT.0)Y(I)=ALOGT(Y(I))
  100 CONTINUE
      IF(LOG.NE.1)GO TO 500
      IF(Y(I).LE.0)Y(I)=-1.0E+36
      IF(Y(I).GT.0)Y(I)=ALOGT(Y(I))
      GO TO 500
C
C     AVERAGING OPTION
C
   22 DO 400 I=1,NDT
      SUM=0.0
      SUMT=0.0
      DO 300 J=1,NAVG
      CALL READF(ID7,IERR,IB7,8)
      CALL CODE
      READ(IB7,35)SGNAL
      TSUM=TSUM+DT
      SUMT=SUMT+TSUM
  300 SUM=SUM+SGNAL
      X(I)=SUMT/NAVG
      Y(I)=SUM/NAVG
      IF(LOG.NE.1) GO TO 400
C
C     IF LOG PLOT DESIRED, TAKE LOG--IF VALUE IS <=1, SET VALUE TO
C     MINIMUM NUMBER (AS A FLAG)
C
      IF(Y(I).LE.0)Y(I)=-1.0E+36
      IF(Y(I).GT.0)Y(I)=ALOGT(Y(I))
  400 CONTINUE
      GO TO 500
C
C     HISTOGRAM ROUTINE
C
  800 CALL READF(ID7,IERR,IB7,40)
      CALL CODE
      READ(IB7,810)LOWER,UPPER,NBINS,LOG2,SCALR
  810 FORMAT(2E10.4,1X,I3,I2,E10.4)
      WRITE(LU,808)
  808 FORMAT(" NORMALIZE TO MAXIMUM VALUE? (0=NO, 1=YES)")
      READ(LU,*)NORM
      IF(LOG2.EQ.1)NBINS=NBINS-1
      MAX=0.0
      DO 825 I=1,NBINS+2
      IF(LOG2.NE.1)GOTO 827
C
C     IF LOG-LOG HISTOGRAM, READ X AND Y VALUES FROM FILE
C
      CALL READF(ID7,IERR,IB7,16)
      CALL CODE
      READ(IB7,826)X(I),NUM(I)
  826 FORMAT(2E16.8)
      GO TO 828
C
```

```
C      IF LINEAR HISTOGRAM, READ JUST Y VALUES FROM FILE
C
  827 CALL READF(ID7,IERR,IB7,8)
      CALL CODE
      READ(IB7,830)NUM(I)
  830 FORMAT(E16.8)
      IF((NORM.NE.1).OR.(I.GE.NBINS+1))GO TO 825
  828  IF(NUM(I).GT.MAX)MAX=NUM(I)
  825  CONTINUE
      IF(LOG2.NE.1)GO TO 815
C
C      IF LOG-LOG HISTOGRAM ,TAKE LOG--IF VALUE IS <=1, SET VALUE TO
C      MINIMUM NUMBER (AS A FLAG)
C
      NBINS=NBINS+2
      DO 900 I=1,NBINS
      IF(NUM(I).LE.0.0)Y(I)=-1.0E+36
      IF(NUM(I).GT.0.0)Y(I)=ALOGT(NUM(I))
      IF(X(I).LE.0.0)X(I)=-1.0E+36
      IF(X(I).GT.0.0)X(I)=ALOGT(X(I))
  900 IF(NORM.EQ.1)Y(I)=Y(I)/MAX
      NDT=NBINS
      GO TO 11
C
C      IF LINEAR HISTOGRAM, DO THE FOLLOWING ROUTINE TO SQUARE OFF
C      CORNERS OF PLOT
C
  815 XINC=(UPPER-LOWER)/NBINS
      Y(1)=NUM(1)
      IF(NORM.EQ.1)Y(1)=Y(1)/MAX
      X(1)=LOWER
      I=1
      DO 850 J=2,NBINS
      I=I+1
      Y(I)=NUM(J)
      IF(NORM.EQ.1)Y(I)=Y(I)/MAX
      X(I)=X(I-1)+XINC
      IF(Y(I).EQ Y(I-1))GO TO 850
      Y(I+1)=Y(I)
      Y(I)=Y(I-1)
      X(I+1)=X(I)
      I=I+1
  850 CONTINUE
      NDT=I+1
      Y(NDT)=Y(NDT-1)
      X(NDT)=X(NDT-1)+XINC
      GO TO 11
  855  NCNTR=0
      SYM=0.0
  500 CALL PLOT(0.,0.,-3)
C
C      IF THIS IS THE FIRST RUN, CHECK FOR SCALING OPTION
C
```

```
      IF(IRUN.NE.0)GO TO 705
      IF(ISCAL.NE.1) GO TO 700
      CALL SCALE(X(1),ABS(XLEN),NDT,1)
      CALL SCALE(Y(1),YLEN,NDT,1)
  700 CALL AXIS(1.0,1.0,XNAME,XLEN,0.,X(NDT+1),X(NDT+2))
      CALL AXIS(1.0,1.0,YNAME,YLEN,90.,Y(NDT+1),Y(NDT+2))
  705 CALL PLOT(1.,1.,-3)
C
C     COMPUTE MAXIMUN VALUES OF X AND Y.  DROP OFF ANY X VALUES WHICH
C     GO OFF SCALE.  SET ANY OFF-SCALE Y VALUES TO MAXIMUM Y VALUE.
C
  701 YMAX=Y(NDT+1)+YLEN*Y(NDT+2)
      XMAX=X(NDT+1)+ABS(XLEN)*X(NDT+2)
      IDROP=0
      DO 706 I=1,NDT
      IF(Y(I).LT.Y(NDT+1))Y(I)=Y(NDT+1)
      IF(X(I).LT.X(NDT+1))X(I)=X(NDT+1)
      IF(X(I).GT.XMAX)IDROP=IDROP+1
  706 IF(Y(I).GT.YMAX)Y(I)=YMAX
      IF(IDROP.EQ.0)GO TO 707
      X(NDT-IDROP+1)=X(NDT+1)
      X(NDT-IDROP+2)=X(NDT+2)
      Y(NDT-IDROP+1)=Y(NDT+1)
      Y(NDT-IDROP+2)=Y(NDT+2)
      NDT=NDT-IDROP
      WRITE(LU,98)IDROP
   98 FORMAT(" IDROP=",I5)
  707 CALL LINES(X(1),Y(1),NDT,1,NCNTR,SYM)
      IF((ITYPE.NE.2HHI).OR.(LOG2.EQ.1).OR.(IRUN.NE.0))GO TO 715
C
C     ON FIRST RUN, IF LINEAR HISTOGRAM, PRINT INFORMATION IN UPPER
C     RIGHT CORNER
C
      CALL SYMB(8.0,6.0,.15,NEG,0.0,1)
      CALL NUMB(8.8,6.0,.15,NUM(NBINS+1),0.0,-1)
      CALL SYMB(8.0,5.5,.15,POS,0.0, )
      CALL NUMB(8.8,5.5,.15,NUM(NBINS+2),0.0,-1)
      IF(NORM.NE.1)GO TO 715
C
C     IF NORMALIZED, PRINT MAX VALUE
C
      CALL SYMB(8.0,5.0,.15,IMAX,0.0,1)
      CALL NUMB(8.8,5.0,.15,MAX,0.0,-1)
  715 CALL URITE
      WRITE(LU,725)
  725 FORMAT(" MORE RUNS?")
      READ(LU,730)NRUN
  730 FORMAT(A2)
      IF(NRUN.NE.2HYE)GO TO 750
      IRUN=1
      GO TO 1
  750 CALL CLOSE(ID7)
   35 FORMAT(E16.8)
      END
```

APPENDIX E

PERTURBATION MODEL FOR FLUCTUATION ERROR

For this deviation we assume a sinusoidal signal

$$S(t) = a \sin (\omega_s t)$$

and filtered zero-mean noise n(t) with signal power to noise power ratio

$$S/N = a^2/2 \langle n^2(t) \rangle \gg 1$$

where < > denotes long-time or statistical average. We make the condition that the measurement is not accepted if a signal zero crossing is missed or if the noise adds one. These events are very low probability for large S/N and are assumed to be detected and omitted.

The Nth positive going zero crossing of the signal occurs at time t_0 where

$$t_0 = NT_s = \frac{2\pi N}{\omega_s}$$

The actual beginning and ending positive-going zero crossings of the composite signal r(t) occur at $t_1 \approx 0$ and at $t_2 \approx t_0$. The estimated signal period is thus

$$\hat{T}_s = \frac{t_2 - t_1}{N}$$

as opposed to the exact value $T_s = t_0/N$.

For small errors, it is just as useful to determine the statistics of the period measurement errors as it is to invert first and determine frequency measurement errors. Thus the error in period is

$$\varepsilon_T = \frac{(t_2-t_0)-(t_1-0)}{N} = \frac{t_2-t_1-t_0}{N}$$

The times of the zero crossings satisfy the following equations

$$a \sin \omega t_1 + n(t_1) = 0$$

$$a \sin \omega(t_2-t_0) + n(t_2) = 0$$

where we have made use of the fact that t_0 is an integral number of periods of S(t) with the result that Sin ωt_2 - sin $\omega(t_2-t_0)$.

The quantities t_1 and t_2-t_0 are both very small by assumption. Thus we may expand the equations for t_1 and t_2 by a Taylor series about 0 and t_0 and keep only the first two terms to obtain:

$$0 + a \left.\frac{d(\sin \omega t)}{dt}\right|_{t=0} t_1 + n(0) + \left.\frac{dn}{dt}\right|_{t=0}^{t_1} = 0$$

i.e.,

$$a\, \omega t_1 + n(0) + n'(0)t_1 \approx 0$$

$$a\, \omega(t_2-t_0) + n(t_0) + n'(t_0)(t_2-t_0) = 0$$

Solving for t_1 and t_2 gives

$$t_1 \approx \frac{-n(0)}{a\omega + n'(0)}$$

$$t_2 \approx t_0 - \frac{n(t_0)}{a\omega + n'(t_0)}$$

and thus

$$\varepsilon_N = \frac{1}{N}\left(\frac{n(0)}{a\omega + n'(0)} - \frac{n(t_0)}{a\omega + n'(t_0)}\right)$$

Thus far we have made no noise assumptions except that n(t) was small and the errors are small. The n' terms in the denominator will make the exact evaluation of ε_N somewhat tedious even if n(t) is zero-mean Gaussian noise, so for now we will assume the slope of the waveform at the zero-crossing locations is nearly equal to that of the signal alone, with the vertical displacement due to noise being adequate for finding the horizontal displacement.* For this very simplified case,

$$\varepsilon_N \approx \frac{1}{N}\left(\frac{n(0)}{a\omega} - \frac{n(t_0)}{a\omega}\right)$$

With all the approximations made, the first and second order statistics become

$$\langle\varepsilon_N\rangle = \frac{1}{N}\left(\frac{\langle n(0)\rangle}{a\omega} - \frac{\langle n(t_0)\rangle}{a\omega} = 0-0\right)$$

$$\langle\varepsilon_N^2\rangle = \frac{1}{N^2a^2\omega^2}\left(\langle n^2(0)\rangle + \langle n^2(t_0)\rangle - 2\langle n(0)n(t_0)\rangle\right)$$

---

* If a tracking filter is used with bandwidth only slightly larger than the signal bandwidth, and if S/N >> 1, this condition will hold.

If n(t) is assumed to possess an autocorrelation function

$$R_{nn}(t_1,t_2) = \langle n(t_1)n(t_2)\rangle$$

then

$$\langle \epsilon_N^2 \rangle = \frac{2}{N^2 a^2 \omega^2} \left[R_{nn}(0,0) + R_{nn}(t_0,t_0) - 2R_{nn}(0,t_0)\right]$$

We will approximate the noise as being statistically stationary (even though it is not) with noise power $R_{nn}(0)$ determined by the local mean optical power incident on the photodetector (the value of the background plus the pedestal). The autocorrelation function $R_{nn}(\tau)$ will also exist, and

$$\langle \epsilon_N^2 \rangle = \frac{2}{N^2 a^2 \omega^2} \left[R_{nn}(0) - R_{nn}(t_0)\right]$$

Now $R_{nn}(\tau)$ is an inverse Fourier transform of the magnitude square of the noise filter frequency characteristic; we see that if the filter were an infinitely narrow one centered at ω, the autocorrelation $R_{nn}(\tau)$ would be periodic with $R_{nn}(t_0) = R_{nn}(0)$ and there would be zero fluctuation error. This is obviously not possible; if we knew the frequency, there would not be anything to do. Generally, the filter bandwidth exceeds the signal bandwidth, and the noise then becomes uncorrelated in less time than the width of a single signal burst. If the counter is set to count for approximately this number of cycles, $R_{nn}(t_0) \simeq 0$ and the error is the sum of the errors at each end independently:

$$\langle \epsilon_N^2 \rangle \approx \frac{2\langle n^2(t)\rangle}{N^2 a^2 \omega^2}$$

The rms signal period error is thus

$$\sqrt{\epsilon_N^2} = \frac{1}{\omega N}\sqrt{\frac{\langle n^2\rangle}{a^2/2}} = \frac{1}{\omega N}\sqrt{\frac{1}{S/N}}$$

If we normalize this result by dividing by the correct signal period, we obtain

$$\sigma_T = \frac{1}{\omega TN}\sqrt{\frac{1}{S/N}} = \frac{1}{2\pi N\sqrt{S/N}}$$

For small errors, the same fractional error is made in the frequency estimates if the inversions are errorless.

The formula which has been derived uses many approximations. It should only be valid for low-noise, high accuracy cases. We do not know how the nonstationarity limits this.

APPENDIX F

EXPERIMENTAL CONFIRMATION OF NOISE ERROR THEORY

Laboratory experiments concerning photon noise limitations of LV burst-counter processor accuracy were conducted during the period June 15, 1977, to July 7, 1977. The tests were conducted with signals produced by a photomultiplier tube illuminated by a light emitting diode driven by the sum of DC current plus the output of a precision stable sine wave oscillator. The purpose was to verify small-error theory with high signal-to-noise ratio signals.

EQUIPMENT

Figures F-1 and F-2 are schematic diagrams of the experimental equipment. The signal source was a 100 KHz crystal oscillator with a divide by 2^N option for 50 KHz, 25 KHz, 12.5 KHz, and 6.25 KHz. A bandpass filter was included to remove harmonics other than the fundamental sine wave. The oscillator had absolute accuracy of 0.0025 percent with drift stability better than $1:10^5$. This signal was passed through a variable attenuator and added to a DC level. This was followed by an LED driver amplifier. The light emitting diode (LED) was chosen to have a linear light output versus drive current input to avoid sine wave distortion with high visibility signals. A calibrated variable optical attenuator was located between the LED and the entrance pin hole of a photomultiplier tube housing assembly.

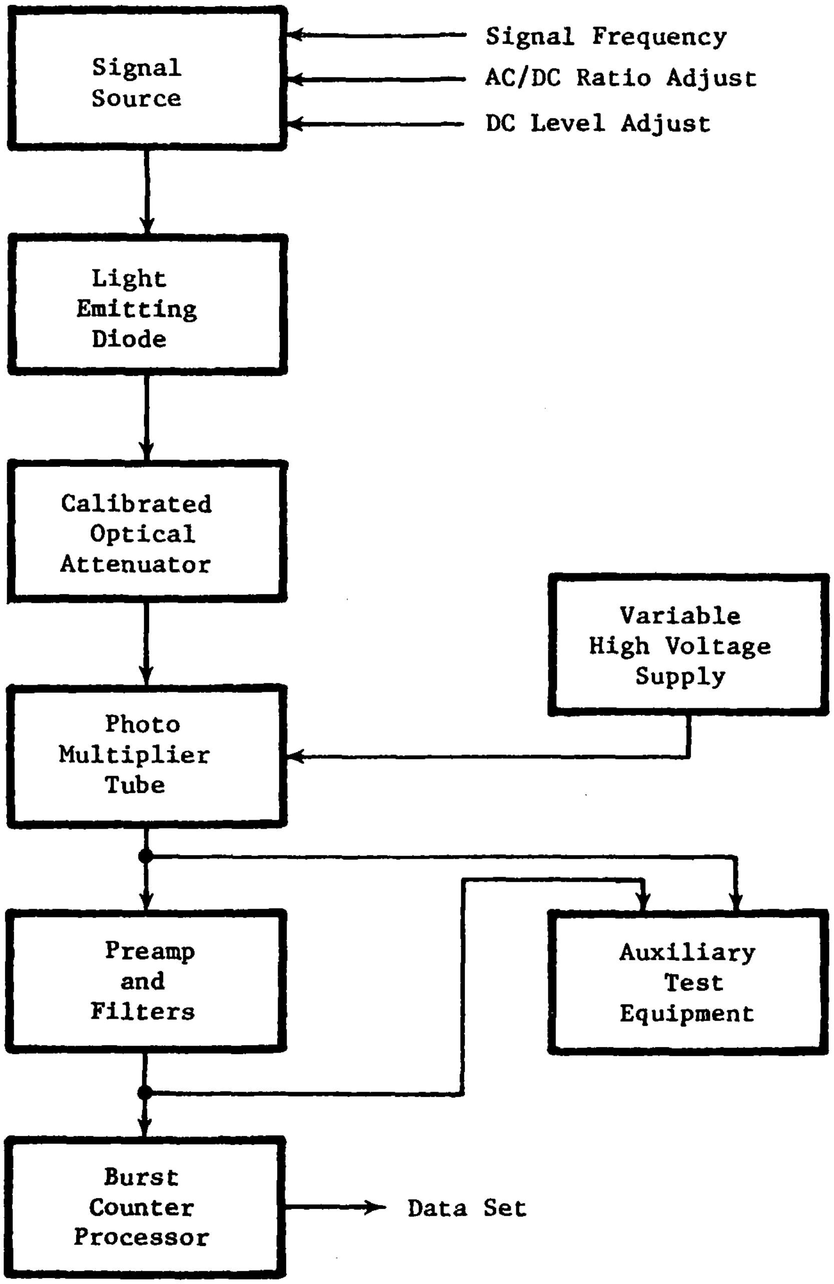

Figure F-1. Schematic Diagram of Equipment for Experiment.

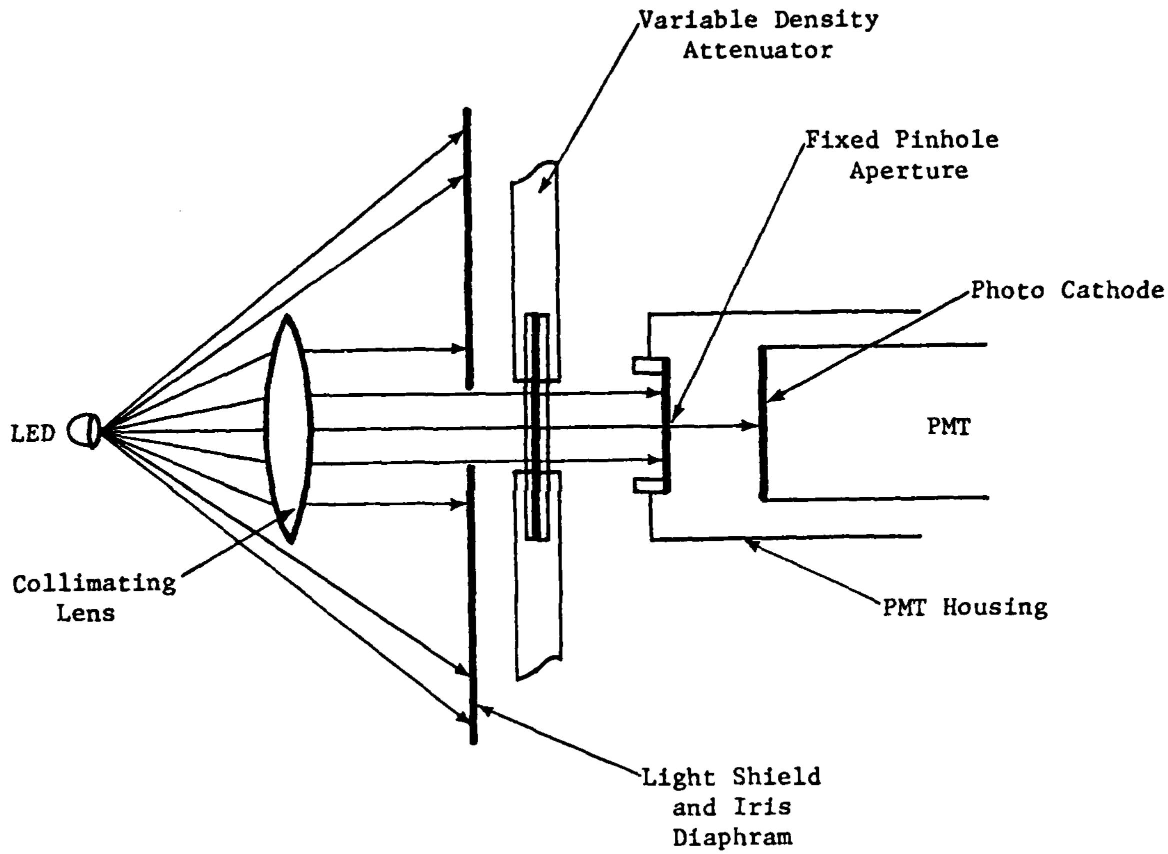

Figure F-2. Optical Arrangement for Lab Experiment. (Components Mounted on Optical Bench in Fixed Geometry)

The apparatus which was used is illustrated in the copy of a photograph in Figure F-3. The divide by 2^N option was not used. All experiments were performed with a fixed 100 KHz signal, accurate to better than $1:10^5$. When the LED drive signal was applied directly to the counter processor, the reading was 100.0 KHz with an uncertainty less than $\pm(0.5/625)\times 100$ KHz.* The precision of the processor used was limited to 10 bits (1:1024) readout of a 22-bit counter.

In Figure F-3, from left to right, the electronic equipment is as follows: Macrodyne Model 2096-2 processor and 2096-5 output unit (large cabinet), LED binary display for Macrodyne computer interface output, hand calculator on printer for conversion of binary outputs, camera (not part of experiment), CR 21213 power meter display (top), signal source power supply (middle), power designs high-voltage supply (bottom), SDL precision signal source (top), Krohn-hite Model 3200 variable band-pass filter (middle), HP 3400A RMS voltmeter (bottom left), SDL band-pass filter for rejecting harmonics in precision source (bottom right). On the optical bench we show from left to right: Sensor head for CR power meter, PMT housing, focussing lens, NRC 925B optical attenuator (calibrated with power meter to 2 db increments), lens, LED mounted in end of a plastic rod for support.

---

* For the Macrodyne processor used, the reading is $f = \frac{64\times 500\times 10^6}{N\times 2^9}$. For N = 625, f = 100,000 KHz.

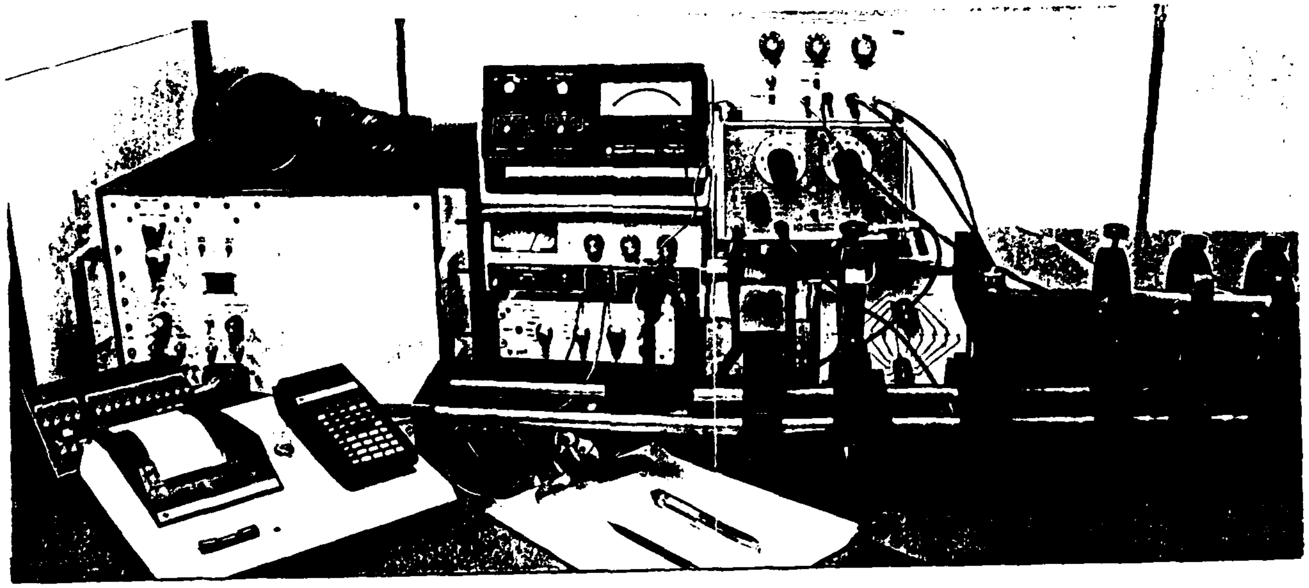

Figure F-3. Laboratory Equipment Used to Verify Signal-to-Noise Ratio Theory.

PROCEDURE

The power meter head and PMT housing each had identical .052" apertures and were interchanged before and after the experiment. The average optical power (centered at 5650 Å) from the TI-211 LED source was measured to be 0.075×10^{-6} watts with the variable optical attenuator at zero db (unity). This measurement was repeated before and after the experiment without change of the reading. The load resistance for the RCA 931A PMT was set at 10,000 ohms after computing that the low-pass rolloff frequency for the combined RC load was approximately 0.4 MHz. The ratio of the peak-to-peak AC current to the DC current applied to the LED source was measured to be 1.4 to 5.3. A check was made over all ranges of the experiment to show that the noise produced at the output of the Krohn-hite filter (following the PMT and preamp) was negligible when the LED source was turned off.

Before beginning the data collection, a check over all ranges was made to select a suitable threshold voltage setting for the Macrodyne processor. A potentiometer setting of 30 mv worked well in combination with an rms input voltage of 50 mv. The procedure adopted was to vary the PMT current gain at each optical attenuation level to bring the total rms signal plus noise (in the pass band of the filter) to 50 mv and then turn the AC modulation off and read the rms value of the shot noise alone (produced by the DC value of the light source only). This procedure was modified at the lowest light level by using an additional 10x preamp (in the Macrodyne processor) and reading 5 mv rms signal plus noise. This was necessary to avoid exceeding the high voltage limits on the PMT. This changing the mechanism of gain does not alter the results of first order theory.

For each value of the bandpass filter settings and the optical attenuator settings, 10 independent binary outputs from the Macrodyne processor were read and converted to decimal. The values read centered approximately on 625 (see previous footnote) with scatter due to the effects of noise.

This total procedure was performed for one setting of the bandpass filter centered on the signal (80 KHz - 125 KHz). The experiment was repeated on another day after plotting the normalized rms deviation of the first test on the same page with the theoretical predictions. In the second performance of the experiment, the filter bandwidths were chosen similar to those typical of commercial burst counters (4:1 frequency spread of filter) with the 100 KHz signal located at the ends and the middle of these pages (LOW: 30 - 120 KHz, MED: 40 - 160 KHz, HIGH: 80 - 320 KHz). Also, the readings were taken with a centered bandpass typical of a potential tracking counter (TRACK: 80 - 120 KHz) and the same bandwidth as MED "slipped" to the end (SLIP: 80 - 200 KHz). See Figures F-4 through F-8.

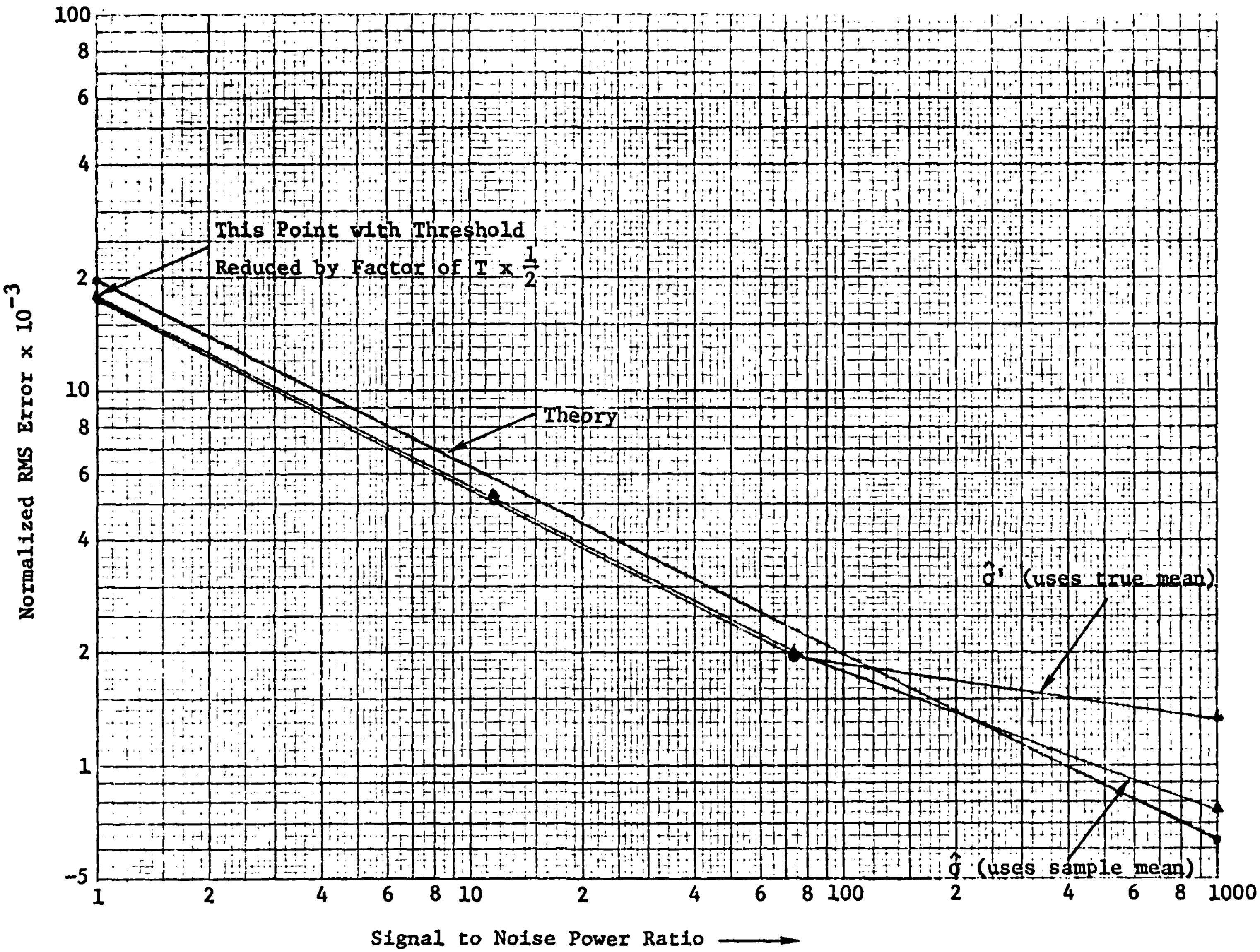

Figure F-4. Plotted Data from Experiment #0.

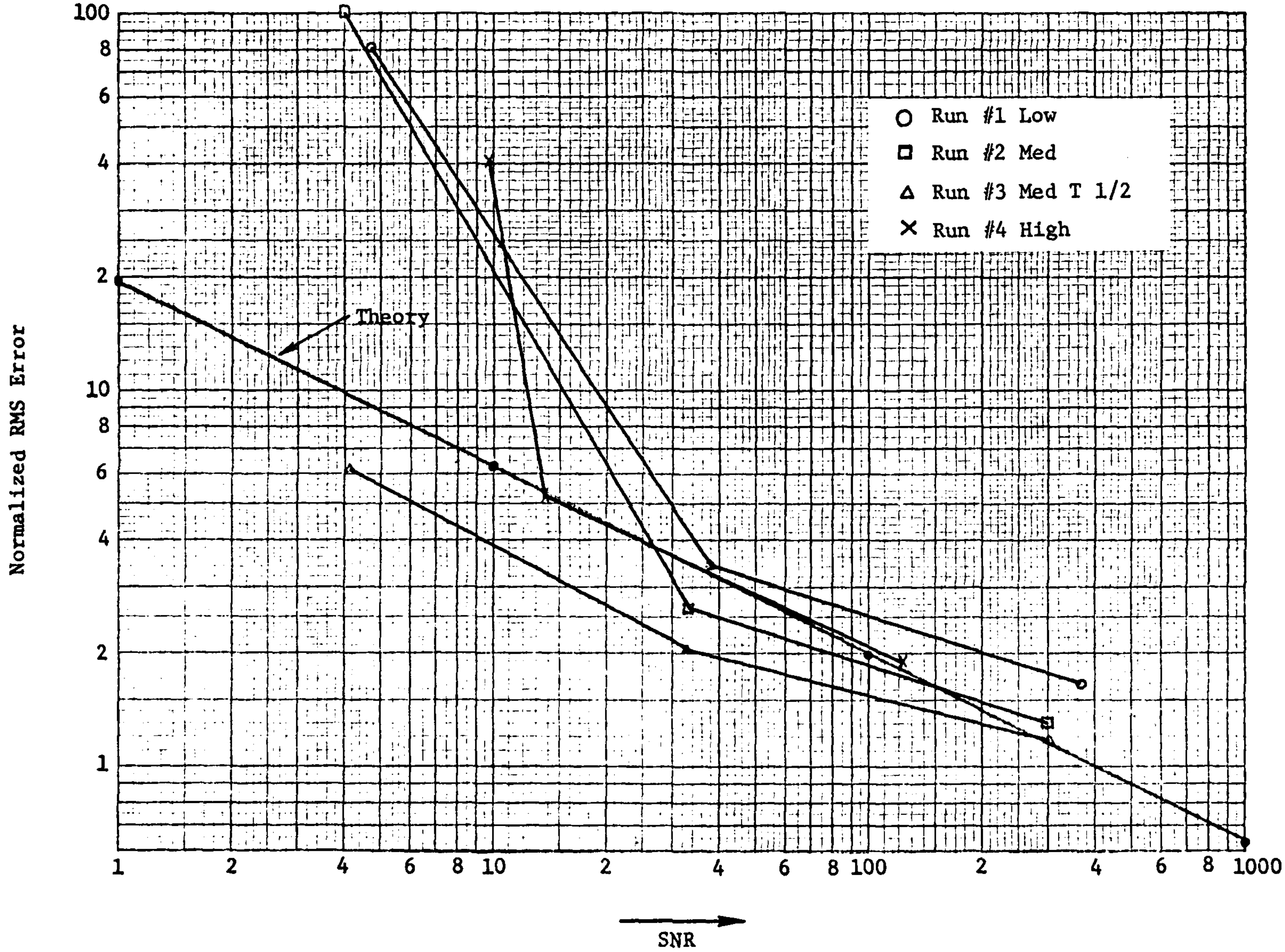

Figure F-5. Normalized RMS Error vs. SNR: Experimental and Theoretical.

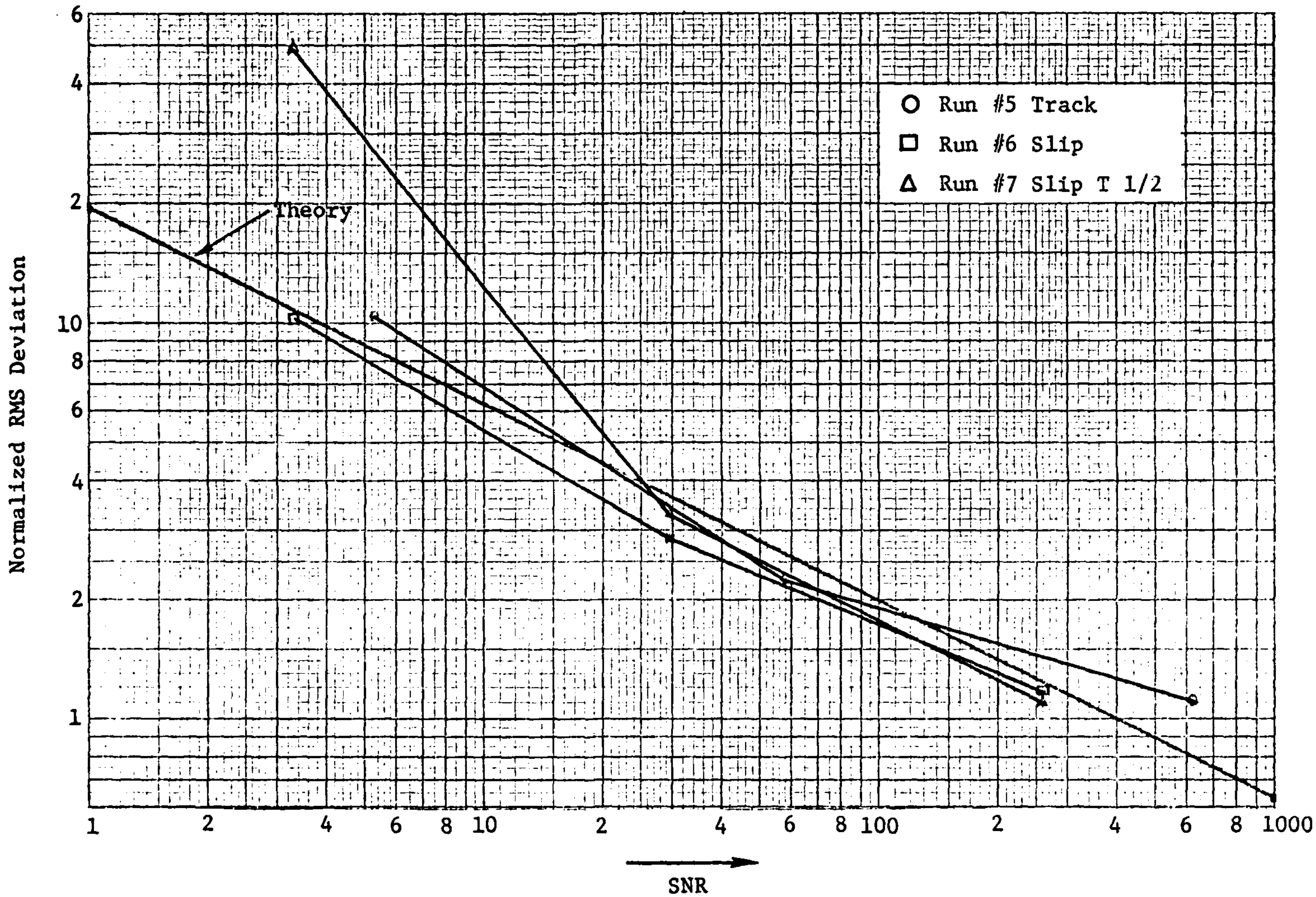

Figure F-6. Normalized RMS Error vs. SNR: Experimental and Theoretical.

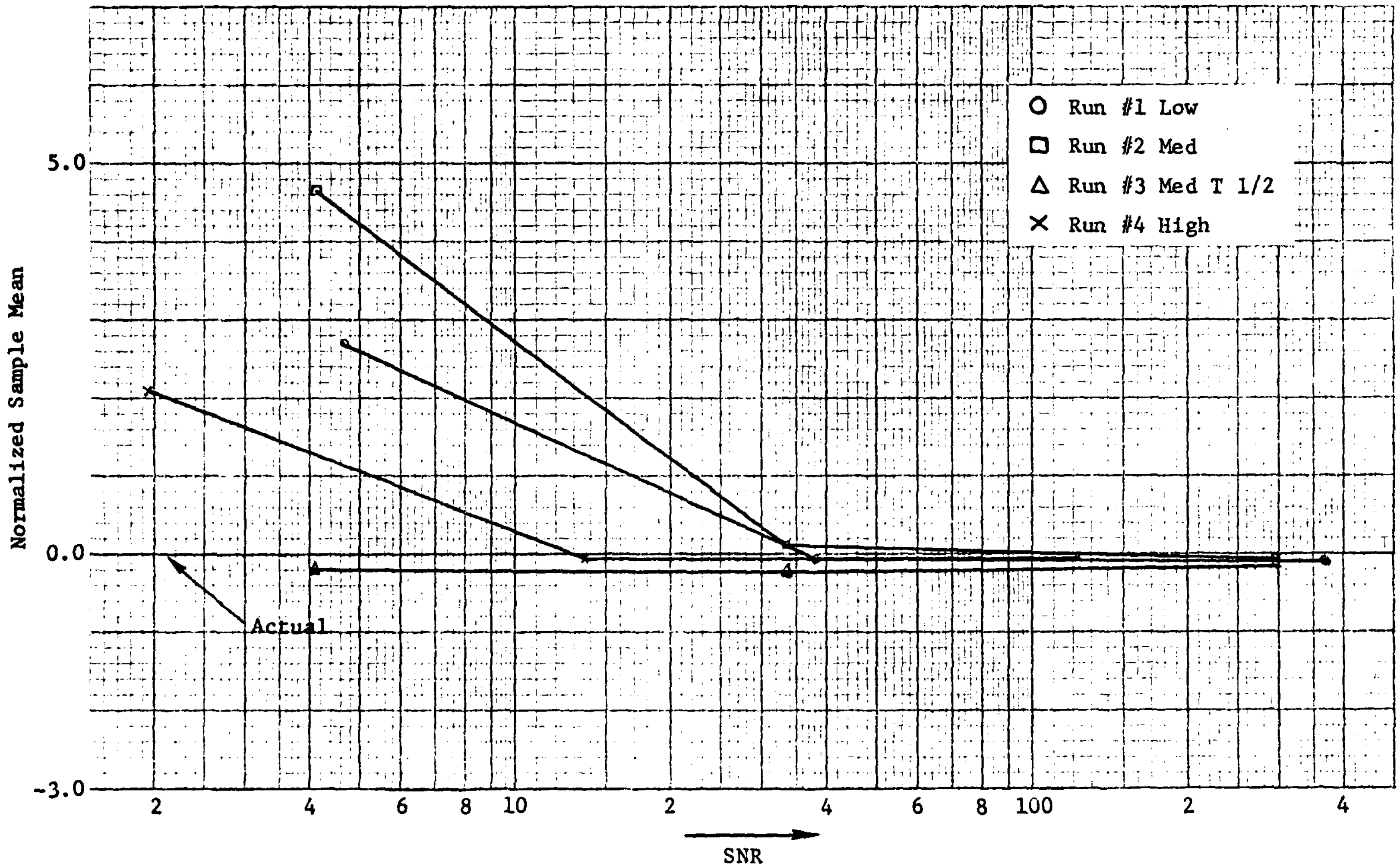

Figure F-7. Normalized Error of the Absolute Mean Measurement.

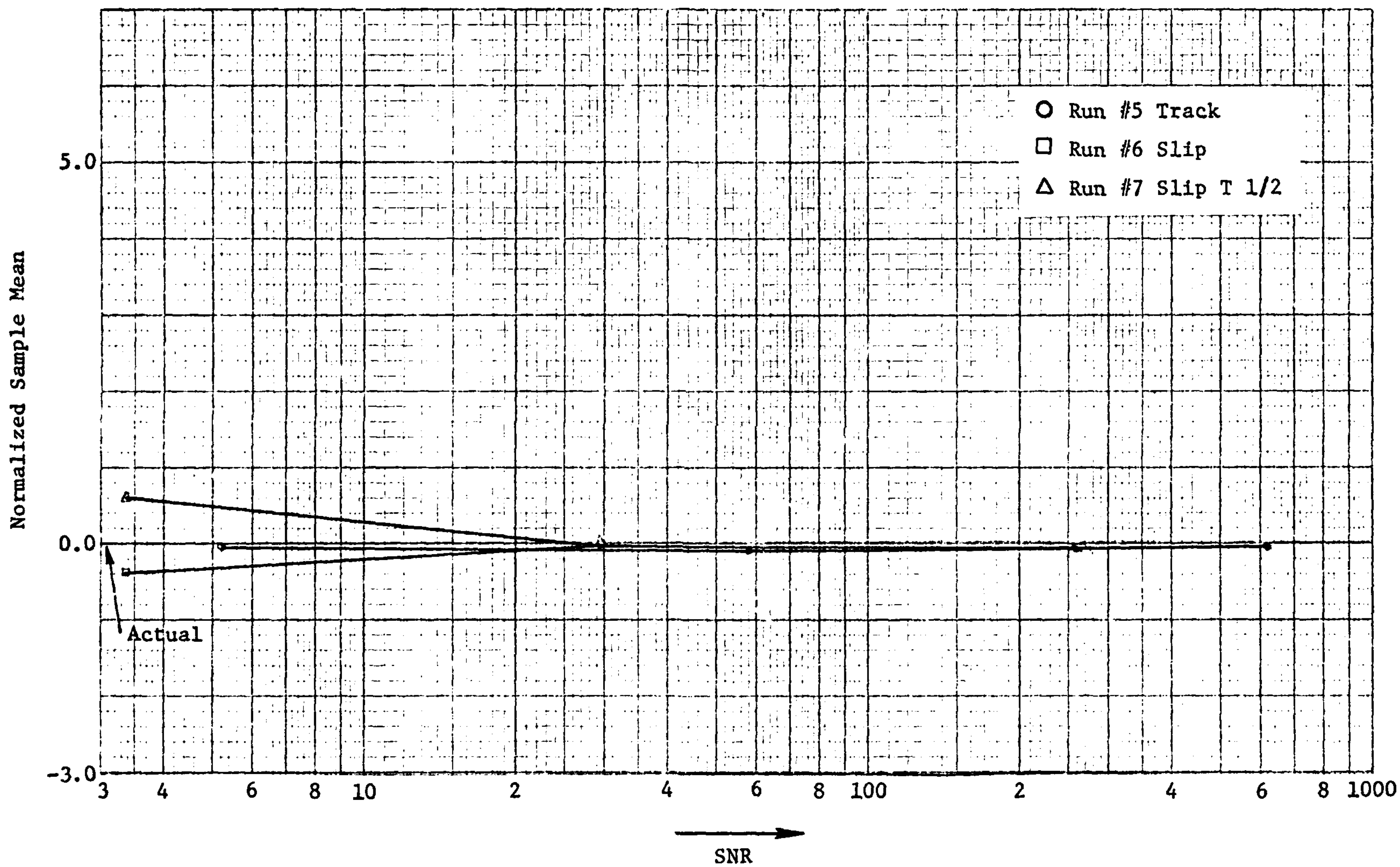

Figure F-8. Normalized Error of the Absolute Mean Measurement.

RESULTS

In all cases, the normalized sample mean $\hat{F}$ and rms deviation $\hat{\sigma}$ was computed as:

$$\hat{F} = \frac{1}{10} \sum_{1}^{10} F_i \qquad \hat{\sigma} = \sqrt{\frac{1}{9} \sum_{1}^{10} (F_i - \hat{F})^2}$$

The results were normalized and plotted graphically versus signal to noise ratio as

$$\delta F = \frac{(\hat{F} - \bar{F})}{\bar{F}}$$

and $\hat{\sigma}/\bar{F}$ where $\bar{F}$ is 625*. Our theoretical expression for rms error derived in Appendix E was also plotted along with the experiment results.

INTERPRETATION

The first experiment with pass band 80 KHz - 125 KHz duplicates the assumptions of the theoretical derivation as does the TRACK data from the second experiment. We find that the theoretical expression is indeed well supported by the results. On the low signal-to-noise ratio (less than 10) end of the data there is no reason why the theory should continue to be valid. We note that in general it doesn't;

---

* All computations were performed on the digital period readings ($\bar{F}$ = 625) rather than on the frequencies obtained by inversion. For small errors, there is negligible loss of accuracy in this procedure.

but with a lower threshold setting (which was arbitrary in the first place), the theory is supported down to a signal-to-noise ratio of unity for the Macrodyne processor with double threshold logic which rejects data with skips and extra zero-crossings. It is our opinion that the perturbation theory would not be supported at such low signal-to-noise ratios without an excellent *error rejection* circuit.*

On the high signal-to-noise ratio end there is the disturbing tendency of all the standard deviation results to exceed the theory. We wish to project these results down to lower error levels, so this is questionable. We observe, however, that the readout of the Macrodyne counter is obtained by <u>truncating</u> all the bits below the 10 (out of the 22-bit counter) which have been selected. Thus, the slightest negative error causes the exact number 625 to be read as 624. This shows up in the high signal-to-noise ratio data where typically 9 out of 10 readings are 624's and 625's split equally (without the truncation we would expect about eight 625's with a 626 and a 624.)

We believe that the truncation effect will show up as an rms deviation due to digitization precision at a level on the order of $0.5/625 = 0.8 \times 10^{-3}$. The theory predicts 0.7×10^{-3} at SNR = 1000. Adding the mean square deviations and taking the square root of the

---

* Our own results show that a certain amount of luck is required in threshold setting at these levels.

results is not necessarily valid in this case, but it would predict a minimum obtainable rms deviation of about 1×10^{-3} at the SNR = 1000 level. We conclude that the theory is substantiated as much as is possible until a processor is modified to produce more bits in the output readings.

The data may or may not substantiate the notion of mean bias due to the "pulling" towards the noise band center. A quick glance at the results indicates that considerably more data than 10 readings per setting are required to reduce the rms deviation enough to produce a useful confidence level.

The results of computing the normalized deviation of the mean from the known frequency are included for completness. They do indicate absolute accuracies of better than 0.1 percent were obtained in our laboratory experiment. However, the procedure of reading the binary output of the Macrodyne processor by hand without a computer interface was too tedious for us to obtain sufficient data for the deviations of the means to have useful confidence levels.

SIGNAL-TO-NOISE RATIO CALCULATIONS FOR EXPERIMENT

The signal-to-noise ratios (SNR) were actually measured to avoid relying on predictions based on difficult to measure parameters. However, we also obtained data for predicting the SNR in order to determine how useful certain formulas are. Theory gives the following:

$$i_c(t) = i_{ac}(t) + i_{dc} + i_n(t) \quad , \quad \langle i_{ac} \rangle = \langle i_n \rangle = 0$$

$$\langle i_c(t) \rangle = \frac{\langle P(t) \rangle \eta_c e}{h\nu} = \frac{P_o \eta_c e}{h\nu}$$

where P(t) consists of a steady component P_o and a sinusoidal component $P_s \sin \omega t$. The normalized signal power is

$$\langle i_{ac}^{\,2}(t) \rangle = \frac{P_s^{\,2}}{2} \frac{\eta_c^{\,2} e^2}{(h\nu)^2}$$

When $i_{ac}(t)$ is present, then $\langle i_n^{\,2}(t) \rangle$ is a function of time. As an approximate theory, we assume that it is the value of $\langle i_n^{\,2}(t) \rangle$ when $i_{ac}(t) = 0$ which is important.* The noise is thus evaluated using the steady part of the optical power as

$$\langle i_n^{\,2}(t) \rangle = 2e\,B\left(\frac{P_o \eta_c e}{h\nu}\right)$$

The signal to noise ratio at the cathode is thus

$$\text{SNR} \; \frac{P_s^{\,2} \eta_c}{4P_o B h\nu} = \frac{1}{4}\left(\frac{P_s}{P_o}\right)^2 \left(\frac{P_o \eta_c}{B h\nu}\right)$$

The expression is thus reduced to the product of a modulation index factor and the usual expression for the detection of steady light. If the modulation is 100 percent, this reduces to the usual expression

---

* Although phase shifts due to filters can invalidate this assumption.

of $P_o \eta_c / 4Bh\nu$. Now in addition, we add factors less than unity for various real PMT effects:

F_1 = dynode collection efficiency (0.5 - 1.0)

F_2 = dynode gain variance factor (0.5 - 1.0)

F_3 = cathode sensitivity fatigue factor (0 - 1.0)

F_4 = discrepancy in manufacturer "typical" specifications

and we have

$$SNR = \frac{F_1 F_2 F_3 F_4}{4} \left(\frac{P_s}{P_o}\right)^2 \left(\frac{P_o \eta_c}{Bh\nu}\right)$$

We anticipate that for the RCA 931A, F_1 and $F_2 \approx 0.5$. The fatigue factor and discrepancy factors are unknown so we use 0.5 as an estimate arbitrarily. For our experiment the ratio of (P_s/P_o) as measured by the LED drive current was $(0.7/5.3)^2 = 0.0174$. The measured value of P_o was 0.075×10^{-6} watts. We thus predict for the case of no optical attenuation:

$$SNR = \frac{(0.5)(0.5)(0.5)}{4} (0.0174) \left(\frac{(0.075 \times 10^{-6})(0.026)}{(45\ \text{KHz})(3.5 \times 10^{-19})}\right) = 673.$$

Here the cathode quantum efficiency was obtained for the typical spec on the peak cathode responsivity, S_c, by multiplying by the relative spectral response at 5650 Å and using the formula:

$$\eta = \frac{S_c h\nu}{e}$$

We note that the measured value of SNR was 1000 during the first experiments (no attenuation) and decreased to 624 when the experiment was repeated. This seems to indicate that the cathode was being fatigued by operating the tube at a level high enough to obtain a signal-to-noise ratio of 1000 with the modulation index as low as it was.

We conclude that signal-to-noise ratios may easily differ by factors of four or more (for the worst) if careful selection of high-quality tubes is not made. Furthermore, a reliability study of the fatigue of tubes may be required if they are to be operated at very high signal-to-noise ratio (and thus total current) levels. The use of a tracking filter to obtain the required signal-to-noise ratios at lower power (and count) levels due to reduced bandwidth would be helpful in this regard.

APPENDIX G

MID TERM BASELINE SYSTEM

SUMMARY

Purpose

The purpose of this discussion is to indicate that an accuracy of $1:10^4$ is feasible for a near term LV system for operation in clear ocean water at a range of 2 meters. This discussion is based upon the results given in the following subsections for photon noise errors and the simulation of multiparticle errors. The multiparticle error results are sensitive to the choice of particle size, index and number density, but parametric cases for particle models are not given here. The details of the optical system follow this summary of results.

Particle Model

For the purposes of this assessment, we have used the Kullenberg Pacific Deep model for number density. Our interpretation of this data yields a cumulative distribution which is of the form (diameter) exp (-2.65) with 2000 particles per cc greater in diameter than $1x10^{-6}$ m. We have used the large particle index of refraction 1.03 - j0.01 from Brown and Gordon as the index of refraction for all scatterers. (This is unrealizable as discussed in the report body.)

Data Rate Imposed by Photon Noise

Our error formula can be simplified by assuming for now that eight cycles of signal will be counted. The formula than gives the rms error as

$$\tau = \frac{1}{50\sqrt{S/N}}$$

We will assume that for short range, large SNR single-particle signals, the background light is negligible and the noise is dominated by the shot noise from the single-particle signals. Then we can make the approximation

$$SNR \approx \frac{\lambda(t)}{2B}$$

where B is the bandwidth and where $\lambda(t)$ is the pedestal photoelectron rate*.†

Now given a burst with 19 fringes within the $1/e^2$ width, we may deduce that a threshold must be lower than the peak by a factor

$$\exp\left[-2(4/8.5)^2\right] = 0.64 \approx 0.5$$

Therefore, we may write

---

* Also assumes fringe visibility = unity, i.e., equal power beams with fringe spacing much larger than the particle diameter.

† Since this mid term assessment was performed, we have concluded that $\lambda(t)/4B$ is a more realistic SNR expression than $\lambda(t)/2B$. These results have not been corrected for this more conservative view.

$$\mathrm{SNR} \geq \frac{0.5\ \lambda_p}{2B}$$

where λ_p is the peak rate which is twice the threshold.

In order to obtain a single-particle signal with normalized error σ less than or equal to X, then we solve

$$X = \frac{1}{50 \sqrt{\frac{0.5\ \lambda_p}{2B}}}$$

as the bound and obtain $\sigma \leq X$ when

$$\lambda_p \geq \frac{B}{625\ X^2}$$

Now photon noise errors are independent. If we average the measurements over one meter, small scale turbulence effects will be removed* by averaging, as will photon noise errors. For example, if 10 measurements are made per meter (100/sec at 10 m/sec), then the rms error of the 10 measurement average (0.1 sec sample rate) is the single-particle error reduced by $1/\sqrt{10}$. The error level depends on the signal to noise ratio (and thus particle peak rate) as the inverse of the square root. Thus, if we reduce the peak photoelectron

---

* An issue of performance not handled yet is the level of small scale turbulence which must be averaged away.

rate by a factor of 10 and increase the burst occurrence rate by a factor of 10, the short-time-average error level due to photon noise remains constant while the error due to small scale turbulence are reduced. We can see this in Table G-1.

We observe that the table may not be extended to lower values because of several reasons. The primary ones are the high probability of violating the signal-limited shot noise assumption at lower peak rates; the overlap of signals to produce excessive multiparticle errors; and the invalidity of the error theory at lower values of signal to noise ratio.

The "simulated rate" column in Table G-1 was obtained by reading the rate of occurrence of bursts with peak rate greater than the value in the corresponding top column*. All of these rates are low enough to assume essentially single-particle signals (of the given magnitude or larger) with the presence of an average of about 13 smaller signals present at any given time. The last line is questionable, but the remaining lines of the table are at signal-to-noise ratios of 400 or more and should produce a high percentage of validated measurements from a counter processor. The table thus indicates that the desired accuracy for 0.1 sec averages could be obtained with any of the three threshold settings: 3.2×10^9, 3.2×10^8, or 3.2×10^7. Background light induced photon noise and multiparticle efforts are more likely to be a problem at the lower threshold settings.

---

* From Figure G-4 following.

Error For 0.1 sec Average	Single Particle Error	λ_p †	Simulated Rate † $> \lambda_p$	Required Data Rate	
10^{-4}	10^{-4}	6.4×10^9	280	10/sec	
10^{-4}	3.16×10^{-4}	6.4×10^8	1100	100/sec	
10^{-4}	10^{-3}	6.4×10^7	2900	1000/sec	
10^{-4}	3.16×10^{-3}	6.4×10^6	5400	10^4/sec ↓	Inadequate SNR

Table G-1. Requirements on Peak Photoelectron Rate and Validated Burst Data Rate for Bandwidth = 40 KHz.

---

† Since this mid term assessment was performed, we have concluded that $\lambda(t)/4B$ is a more realistic SNR expression than $\lambda(t)/2B$. These results have not been corrected for this more conservative view.

Multiparticle Effects

In order to assess the multiparticle effects, we have plotted histograms of the frequency estimates made by the processor and noted the data rate obtained for three threshold settings: 3.2×10^9, 3.2×10^8, and 3.2×10^7. These thresholds are shown in the three plots of the signal at different scales in the following material. The results are shown by histograms and summarized in Table G-2.

SOFTWARE TEST: OPTIC

The primary output of OPTIC is a set of signal amplitudes expressed in mean peak photoelectron rate values and a calculation of the mean rate of arrival of these signals. We have also included an output file which separately lists the particle diameter, the differential mie scattering cross section (at 180°), the random probe volume entry multiplier, the optical power to the detector and the mean peak photoelectron rate.* This file allows us to observe the component factors for checkout.

Table G-3 is a list of the parameters selected to exercise OPTIC for purposes of the midterm exam. The parameters are with minor exceptions (as noted) the same as those used in the test case of our proposal. These parameters are also shown as the first portion of

* This redundant file of PKRT has been replaced by SNR = PKRT/4B in the final version reported in Appendix C.

Threshold Peak Rate	Validated Data Rate*	RMS Error Single Particle	0.1 sec Average Error
3.2×10^9	280	4.2×10^{-5}	7.9×10^{-6}
3.2×10^8	1100	5.54×10^{-5}	5.2×10^{-6}
3.2×10^7	2900	1.31×10^{-4}	7.7×10^{-6}
3.2×10^6	5400	0.0146	6×10^{-4} ↓ Inadequate SNR

* From Output of COMP.

Table G-2. Error Due to Multiparticle Effects (Bipolar Test Included).

Table G-3. Trial System Parameters.

$V = 10$ m/sec		Velocity
$R = 2$m		Range
$w_t = 1\text{x}10^{-3}$ m		Transmitter beam radius
$\theta = \frac{d}{R} = 0.015$ radians		Beam angle intersection
$d = 30\text{x}10^{-3}$		Transmitter beam separation
$A_c = \pi[(0.06)^2-(0.03)^2]$ $= 0.00848\ m^2$		Receiver collecting area (5 inch diameter)
$T = 0.3$		Transceiver transmission efficiency
$P_o = 0.4$ watts		0.8 watt laser split to form two 0.4 watt sections
$\phi = 0.015$ rad		Off axis view angle of receiver due to observation disc
$\gamma = 1.0$	Excluded from final version of OPTIC	Elliptical beam compression factor
$F_B = 0$	Excluded from final version of OPTIC	Bragg cell frequency
$\lambda_o = 0.488\text{x}10^{-6}$		Free-space wavelength of laser
$\eta = 0.05$		Effective quantum efficiency (0.2 divided by practical factors of 4 -- to be studied further -- was 0.2 in proposal)
$C = 0.1/m$		Water attenuation coefficient

Table G-3. Trial System Parameters (Cont'd).

$n_o = 1.03 - j0.01$	Relative index of refraction of particles
$n = 1.33$	Index of refraction of water
$N = 2000 \times 10^6$	Number of particles*/m^3 greater in diameter than y_o
$y_o = 1.0 \times 10^{-6}$ m	Lower cutoff of size distribution
$b = 3.65$	Negative slope of particle diameter probability density

---

* Cumulative:

$$N > y = 2000\left(\frac{y}{1.0 \times 10^{-6}}\right)^{-2.65} \times 10^6/m^3 \quad , \quad 1.0 \times 10^{-6} \leq y \leq 20\ \mu m$$

the output file printout reproduced as Figure G-1. Figure G-2 is a plot of a histogram for 1000 scatterers of the diameters realized. This is a differential distribution. The figure also includes the expected value of the histogram. Figure G-3 is the same information in cumulative log-log form. Figure G-4 is a log-sort cumulative histogram of the resulting values of peak photoelectron rate. The values are the rate of occurrence of signal bursts with peak photoelectron rate greater than the abscissa value. The number of fringes, the mean signal frequency, and mean time between burst centers are shown on the printout. The data in Figure G-4 is used for photon noise considerations in the summary.

The proposal used $r_0^3/\sin(\theta/2)$ as the definition of the volume of the optical probe. This was used to compute the rate of signal bursts. We have decided after additional consideration that a more appropriate measure of rate is that given in the definition of OPTIC as

$$\lambda_b = N_0 V (2r_0)^2/\phi$$

where N_0 = total number of particles*/m^3, V is the velocity, r_0 is the $1/e^2$ intensity beam radius, and ϕ is the off-axis viewing angle. Implicit in this formulation are the facts that we assure the cross-over region is viewed off axis with a slit equal in width to the

---

* N_0 is the number greater than the lower cutoff of the model.

```
 OPTIC OUTPUT
  14  LINES OF HEADER INFORMATION
CREATION DATE:   200  1977         TIME:    18    0    23
N(PARTICLE)=  1.0300  -.0100 N(MEDIUM)=  1.330E 0    23
FREE SPACE WAVELENGTH= .4880E-06    ANGLE BETWEEN BEAMS= .1500E-01
RANGE TO BEAM CROSS OVER= .2000E+01    1/E**2 BEAM RADIUS=1.0000E-03
LOWER CUTOFF SIZE= .1000E-05          TOTAL # OF PARTICLES= .2000E+10
OFF AXIS VIEWING ANG= .1500E-01  TRANSMISSION EFFICIENCY= .3000E+00
ELLIP BEAM EXPANS FACTOR= .1000E+01   RECEIVER COLLECTION AREA= .8480E-02
ATTENUATION COEFF=1.0000E-01    LASER POWER= .4000E+00
CATHODE QUANTUM EFFIC.= .5000E-01       BRAGG CELL OFFSET FREQ= .0000E+00
B COEFF. IN NEG. POWER LAW DIST.= .3650E+01     # OF FACTORS GENERATED= 1000
VELOCITY=1.0000E+01
FREQUENCY=    .40880769E+06
NUMBER OF FRINGES= .1910E+02
BURST SEPARATION=    .34364048E-05
 1.00000000E+03    .10000000E+01
  .72838828E+04
  .11340846E+05
  .17535387E+05
  .42040752E+04
  .55365635E+04
  .25577278E+06
  .65722047E+05
  .56334516E+05
  .10015182E+05
  .47211437E+05
  .39123726E+04
  .43773625E+05
  .62326578E+05
  .62360625E+05
  .22235058E+04
  .59693145E+04
  .50633721E+04
  .40335602E+05
  .16732801E+05
  .16331138E+04
  .14577242E+05
  .77589639E+04
  .53442680E+05
  .37369033E+04
  .14684645E+07
  .20971023E+05
  .97064737E+06
  .13320234E+05
  .55015258E+05
  .37735383E+05
```

Signal Period = $1/f_s$ = 2.446 x 10^{-6} sec

$1/e^2$ Burst Width = 19.1 fringes x $1/f_s$ = 46.72 μsec

Burst Separation = 3.44 μsec

No. of Particles in $1/e^2$
Probe Volume at Once = 45.27/3.49 μsec ≈ 13.6

Total Burst Rate = 291,000

DT = $1/(f_s*17.314159)$ = 1.412796 x 10^{-7}

$T_{max} \approx 0.34364 \times 10^{-2}$ = 24,323 DT values

Figure G-1. Output Files OPTIC
a. Primary File Used by SIGNAL.

OPTIC OUTPUT--TABLE OF VALUES
CREATION DATE: 200 1977 TIME: 16 0 23

DIAMETER	SIGMA	FACT	PC	PKRT
.1021E-05	.3341E-16	.7565E+00	.5932E-13	.7284E+04
.1102E-05	.9512E-16	.4966E+00	.9398E-13	.1134E+05
.1109E-05	.9782E-16	.7338E+00	.1428E-12	.1754E+05
.1061E-05	.1057E-15	.1628E+00	.3424E-13	.4204E+04
.1174E-05	.2302E-16	.9845E+00	.4509E-13	.5537E+04
.3112E-05	.1053E-14	.3976E+00	.2091E-11	.2568E+06
.2125E-05	.9667E-15	.2843E+00	.5433E-12	.6672E+05
.2231E-05	.2691E-15	.8910E+00	.4771E-12	.5858E+05
.1113E-05	.6425E-16	.6380E+00	.8156E-13	.1002E+05
.2713E-05	.9878E-15	.1956E+00	.3845E-12	.4721E+05
.1188E-05	.5308E-16	.3017E+00	.3186E-13	.3912E+04
.1237E-05	.1934E-15	.9264E+00	.3565E-12	.4378E+05
.2436E-05	.4190E-15	.6088E+00	.5076E-12	.6233E+05
.1937E-05	.4601E-15	.5547E+00	.5078E-12	.6236E+05
.1004E-05	.1457E-16	.6245E+00	.1811E-13	.2224E+04
.1039E-05	.1903E-15	.2437E+00	.4861E-13	.5969E+04
.1028E-05	.5173E-16	.4011E+00	.4128E-13	.5069E+04
.1434E-05	.2531E-15	.6612E+00	.3330E-12	.4090E+05
.1060E-05	.1050E-15	.6546E+00	.1368E-12	.1679E+05
.1153E-05	.1338E-16	.5014E+00	.1335E-13	.1639E+04
.1102E-05	.9554E-16	.6219E+00	.1187E-12	.1458E+05
.1068E-05	.1111E-15	.2858E+00	.6318E-13	.7759E+04
.1427E-05	.2636E-15	.9230E+00	.4841E-12	.5944E+05
.1016E-05	.3211E-16	.4840E+00	.3092E-13	.3797E+04
.4046E-05	.6271E-14	.9584E+00	.1196E-10	.1468E+07
.1240E-05	.1977E-15	.4341E+00	.1708E-12	.2097E+05
.5366E-05	.1718E-13	.2312E+00	.7904E-11	.9706E+06
.1650E-05	.9987E-16	.8164E+00	.1622E-12	.1992E+05
.2353E-05	.5601E-15	.4020E+00	.4480E-12	.5502E+05
.1438E-05	.2422E-15	.6378E+00	.3073E-12	.3774E+05

-more on disc-

Figure G-1. Output Files OPTIC (Continued)
b. Diagnostic File: Diameter, Differential Cross Section, Probe Volume Entry Factor, Optical Power to Detector, Peak Photoelectron Rate.

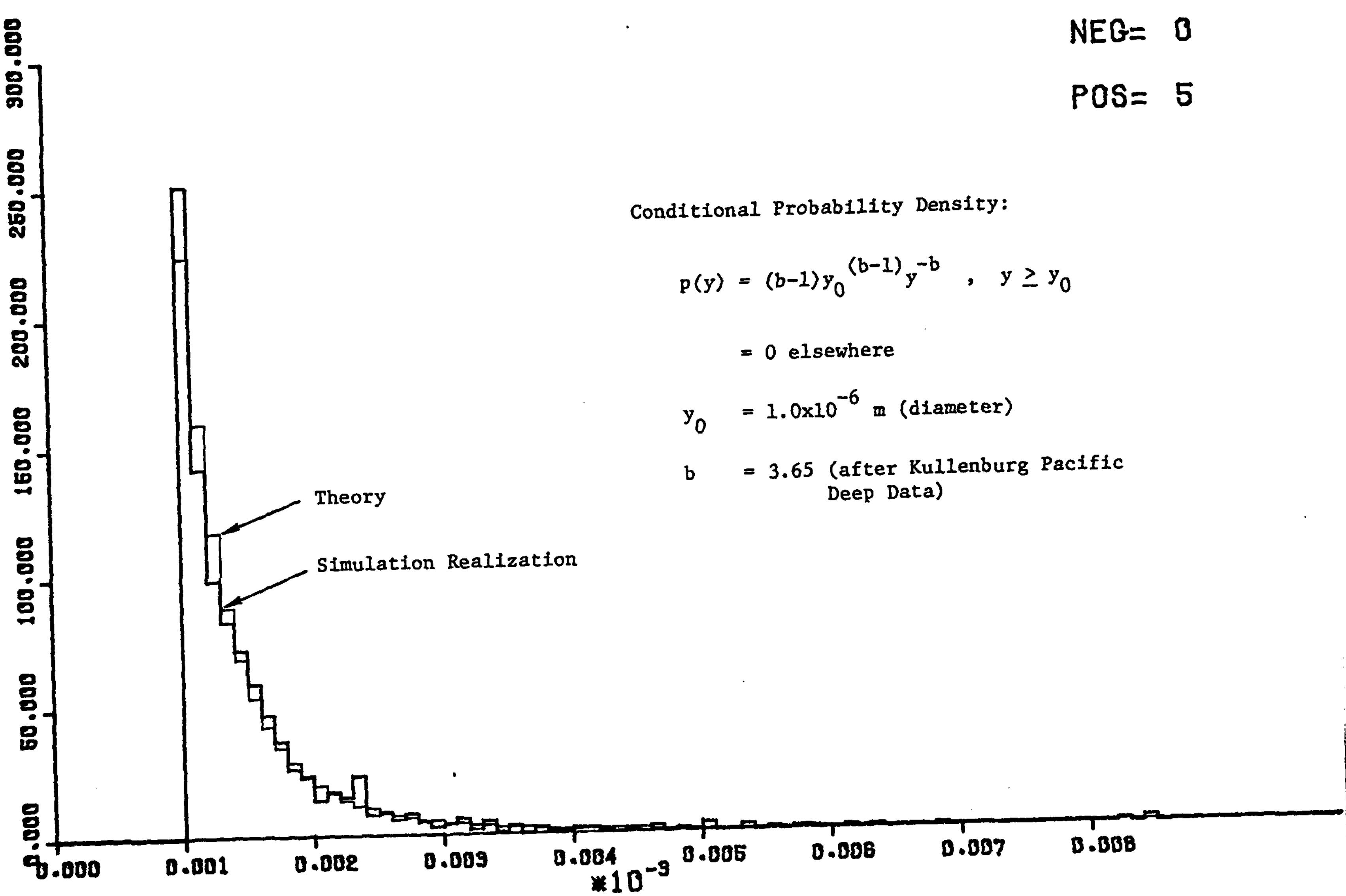

Figure G-2. Histogram of 1000 Realizations of Random Particle Diameters.

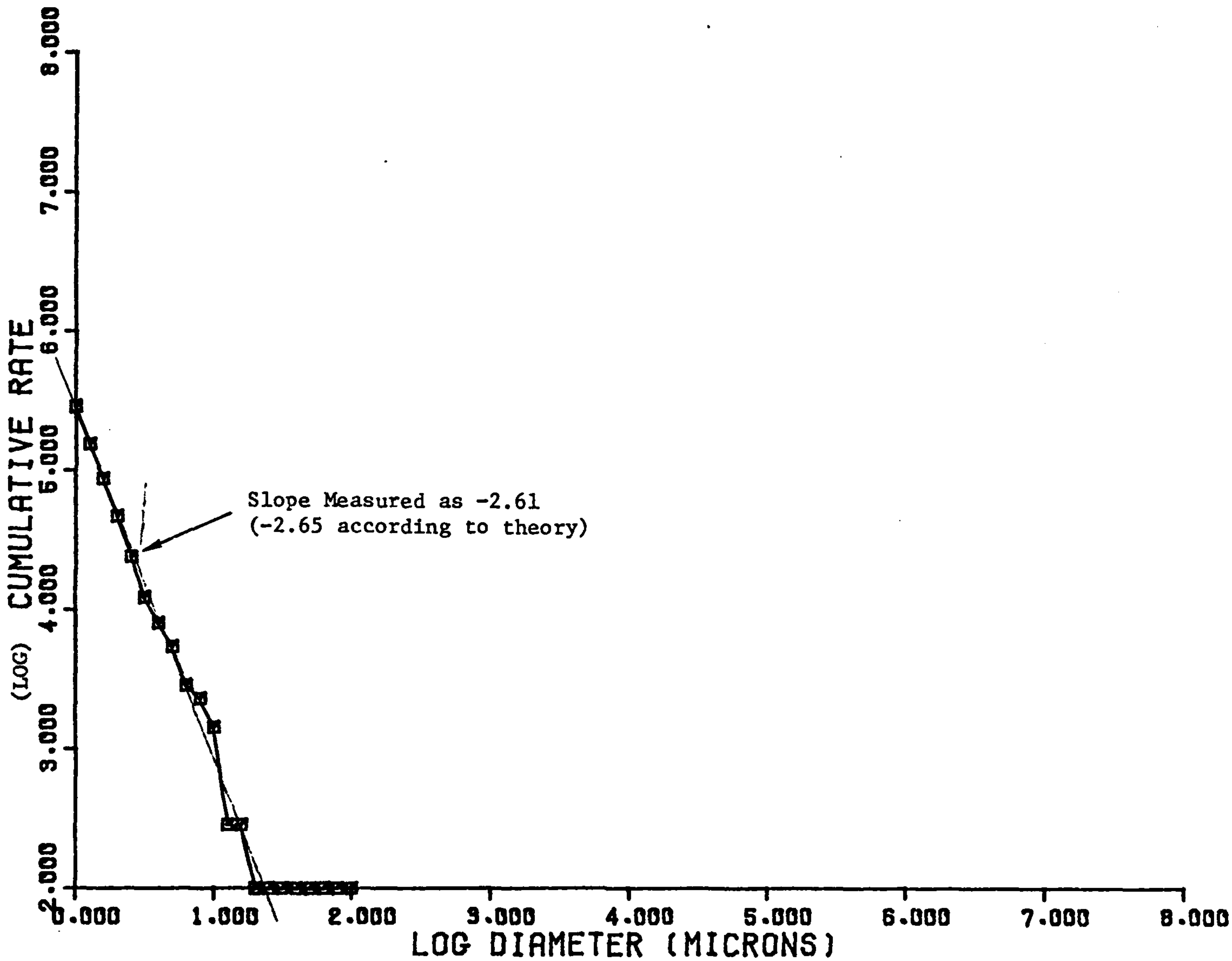

Figure G-3. Cumulative Log-Log Plot of Rate of Simulated Particle Diameters.

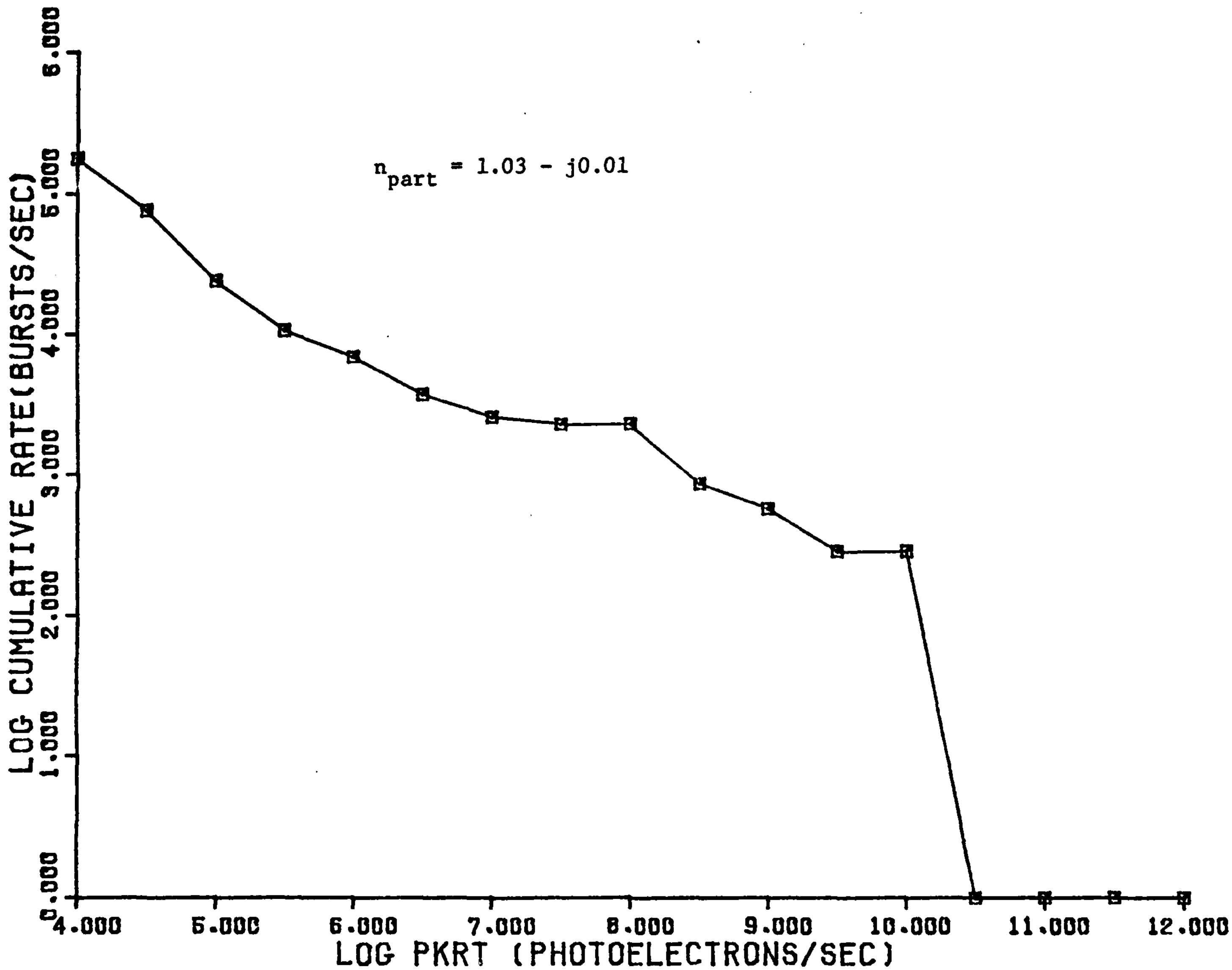

Figure G-4. Cumulative Rate of Signals with PKRT > X.

image of the cross-over beam $1/e^2$ intensity diameter, and that a Gaussian amplitude multiplier is used with a uniform random probe volume entry location. This new procedure results in a burst rate λ_b which is approximately four times larger than the procedure of assuming that the volume is $r^3/\sin(\theta/2)$ used in the proposal. Furthermore, we have included particle sizes down to 1×10^{-6} m diameter (2000/cc) instead of only going down to 1000/cc of 1.25×10^{-6} m particles. Thus, the total burst rate for 10 m/sec is eight times larger than in the proposal calculations and the rate due to the 10 nmeter particles is four times larger.

SIGNAL

At the present time we wish to assess the effects of multiparticle error independently of photon noise effects. We are also presently limited in our ability to correctly include the photon noise effects as direct simulation due to the fact that the FILTER program used previously in our NASA work is inadequate for this project and no time is available for replacing it with an appropriate filter. We have solved this problem by removing the generation of the low-pass pedestal portion of the signals in SIGNAL and eliminating the step of simulating the photon noise. Thus, SIGNAL now simulates a perfectly filtered signal (not achievable in real life) whose only physical error source is multiparticle overlap effects. In order to assess the errors produced by such effects, as opposed to whatever residual error level is inherent in the simulation with the specified digitization precision and other simulation parameters, we have executed SIGNAL with both a poisson random arrival of the bursts and also as a periodic, non-overlapping set of signals. In each case, the frequency of the burst has been chosen to be random with Gaussian probability density centered at the mean frequency computed by OPTIC and with a standard deviation of 0.0001. Figure G-5 is a normalized histogram of the difference between the actual burst frequencies and the assumed (input) mean frequency (the difference) divided by the input mean frequency. This figure should be compared with the histogram of the measurements indicated by COUNT in the next section.

Figure G-6 is a collection of plots of the output file of SIGNAL. We have selected several scale factors to allow observation of the signals from the perspective of a variety of threshold levels. This is a more experiential view of a small subset of the data summarized in Figure G-4. In these figures the time scale has been compressed by periodically skipping points which are actually used in the succeeding programs. The compression factor is the ratio of the total number of points within the time interval shown to the number actually plotted.

COUNT - COMP

The output of COUNT is a set of time measurements and message errors. At present the best overview of performance is obtained by

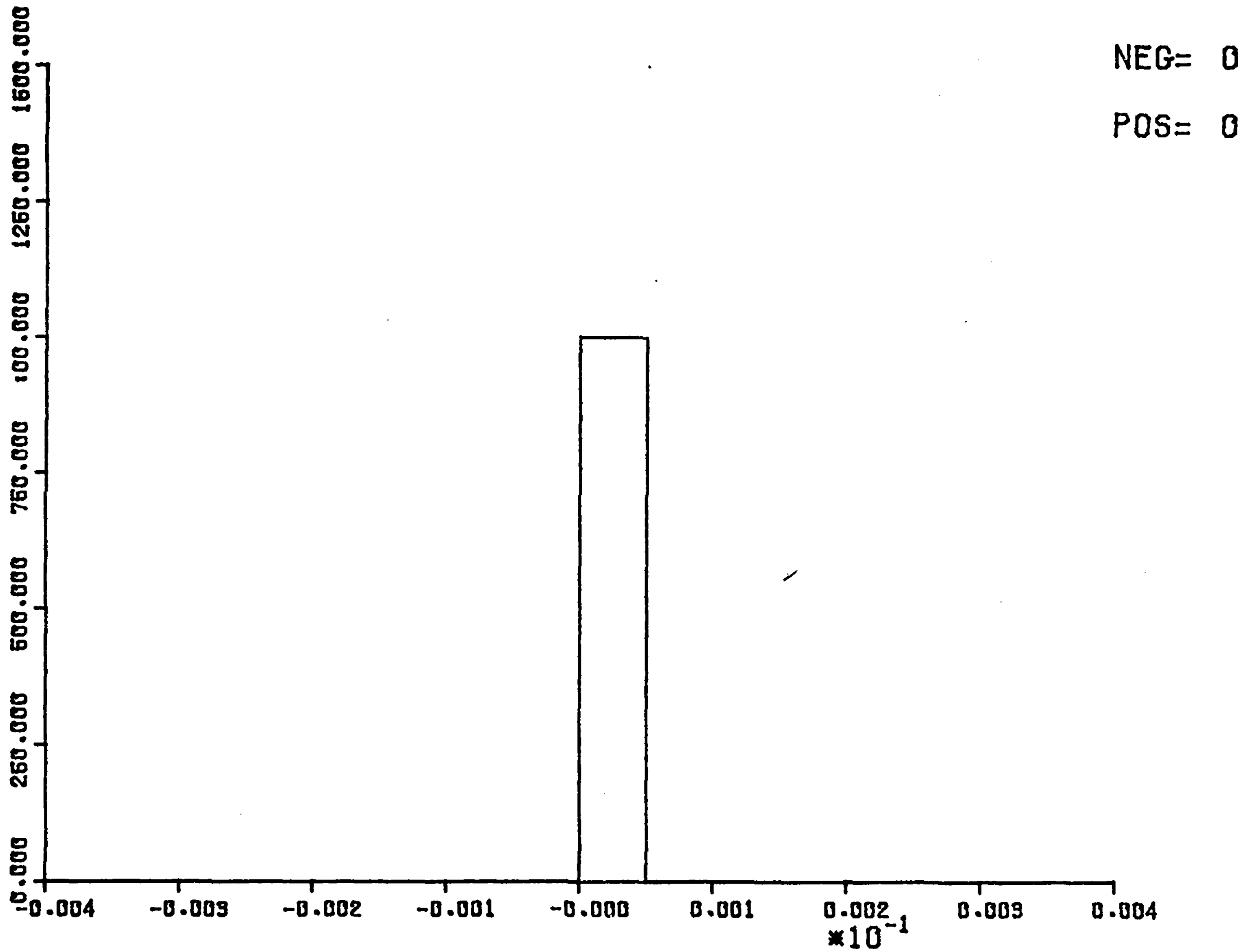

Figure G-5. Histogram of Input Frequencies from Signal (Cont'd)
a) 1000 Frequencies All Equal to Mean for Sea Simulation.

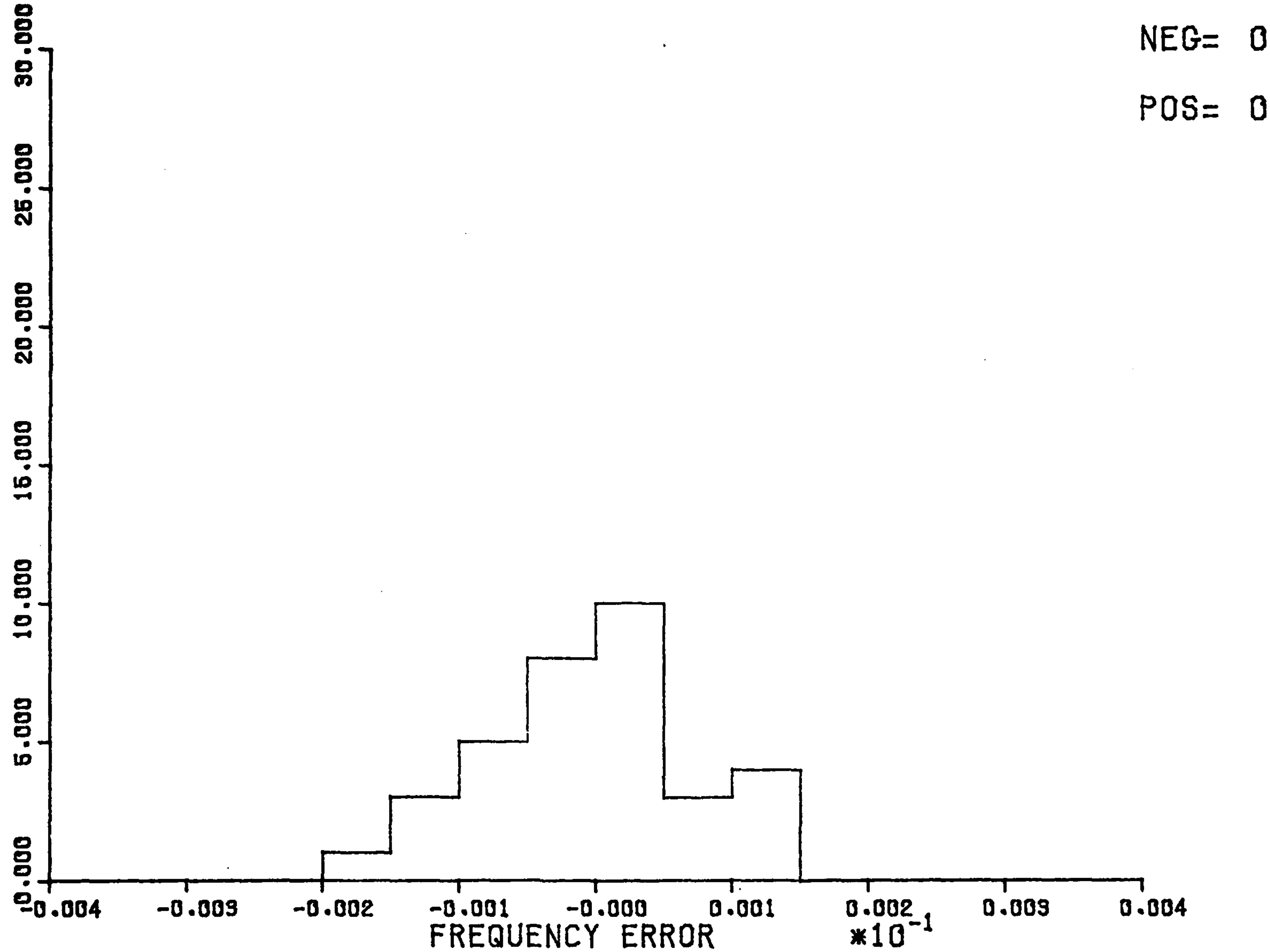

Figure G-5. Histogram of Input Frequencies from Signal (Cont'd)
b) 34 Frequencies for Test Case.

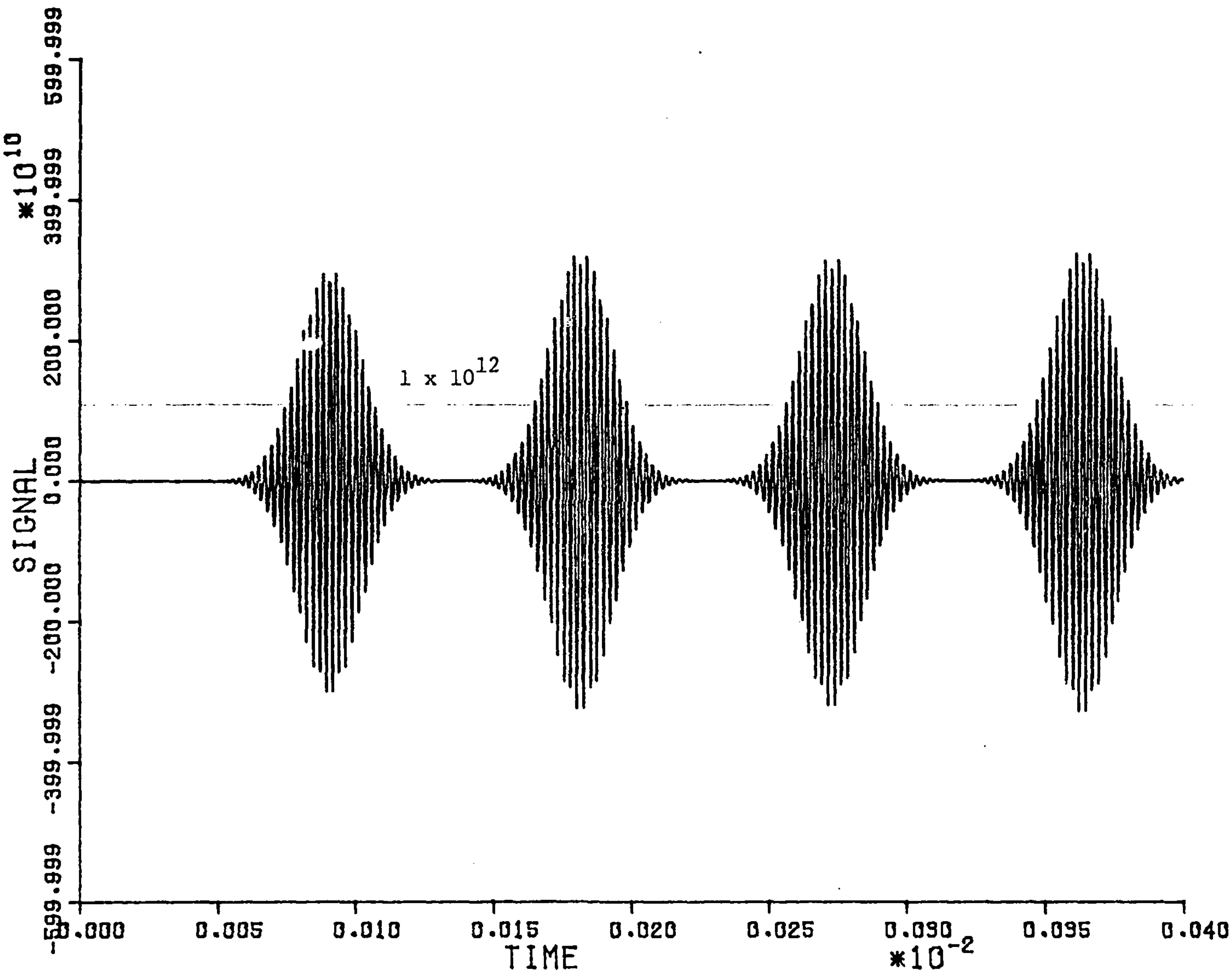

Figure G-6. Plots of Simulated Signal
a) Uniform Spacing Test Case.

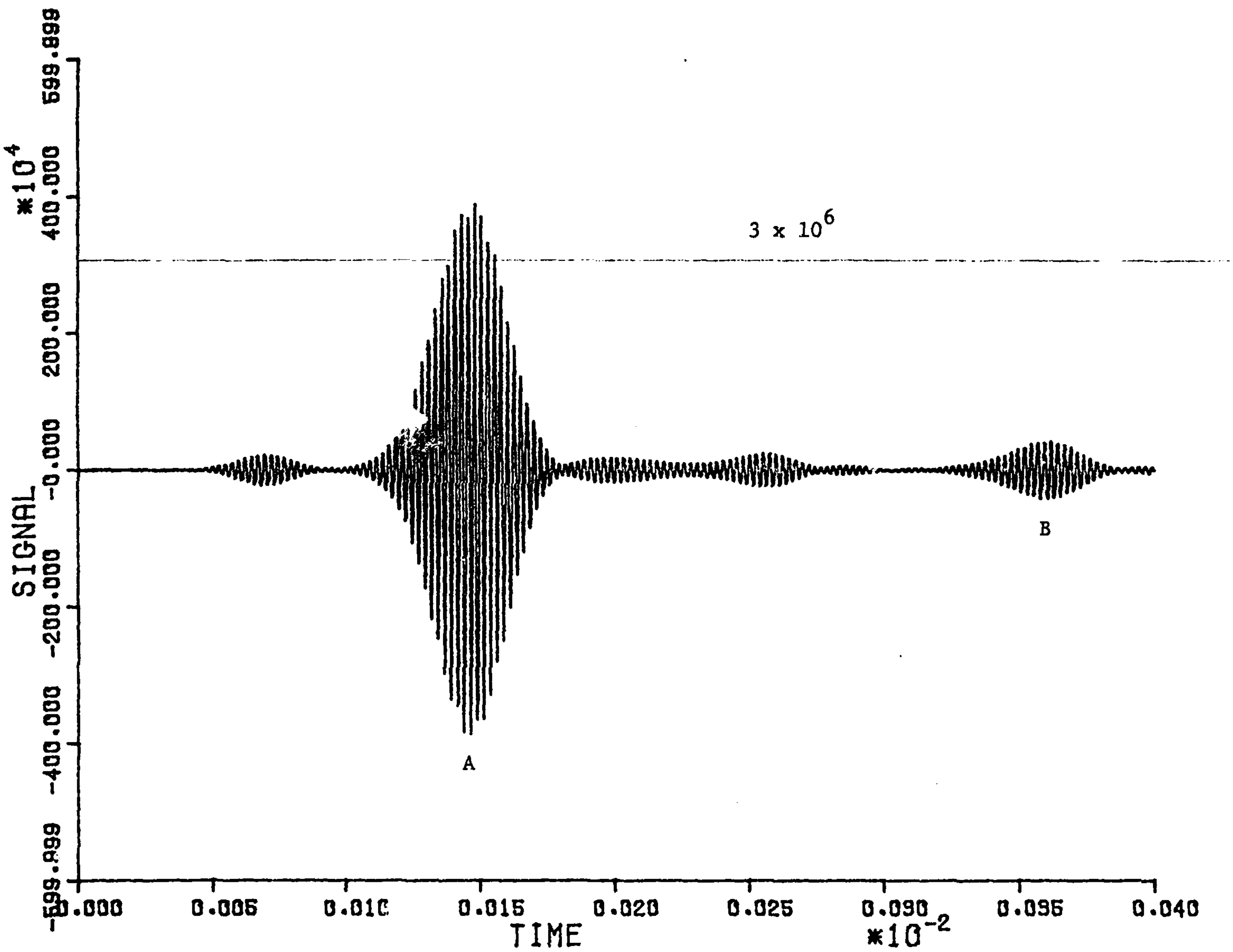

Figure G-6. Plots of Simulated Signal (Cont'd)
b) Every 2nd Point, 2×10^6 Vertical Scale.

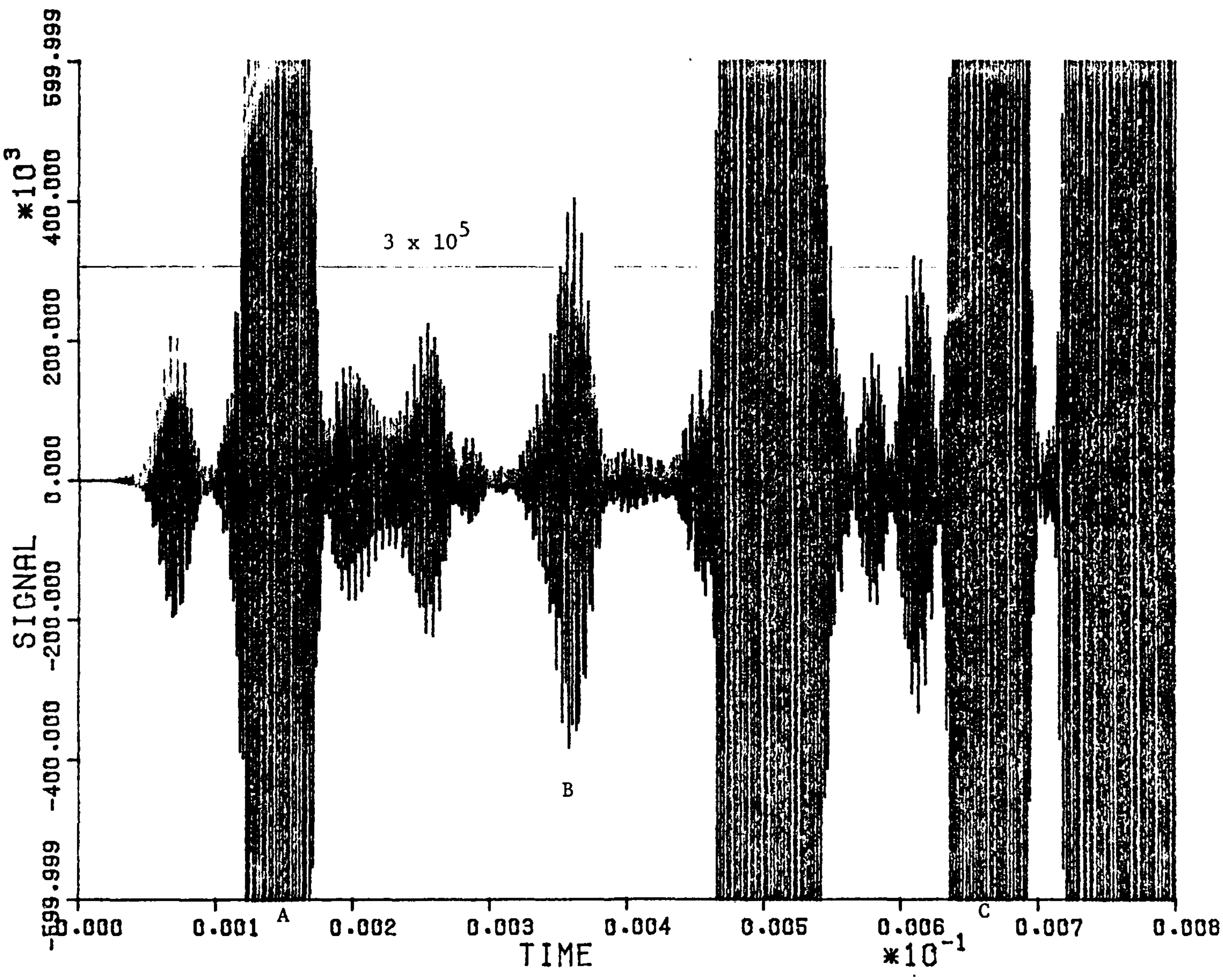

Figure G-6. Plots of Simulated Signal (Cont'd)
c) Every 5th Point, 2 x 10^5 Vertical Scale.

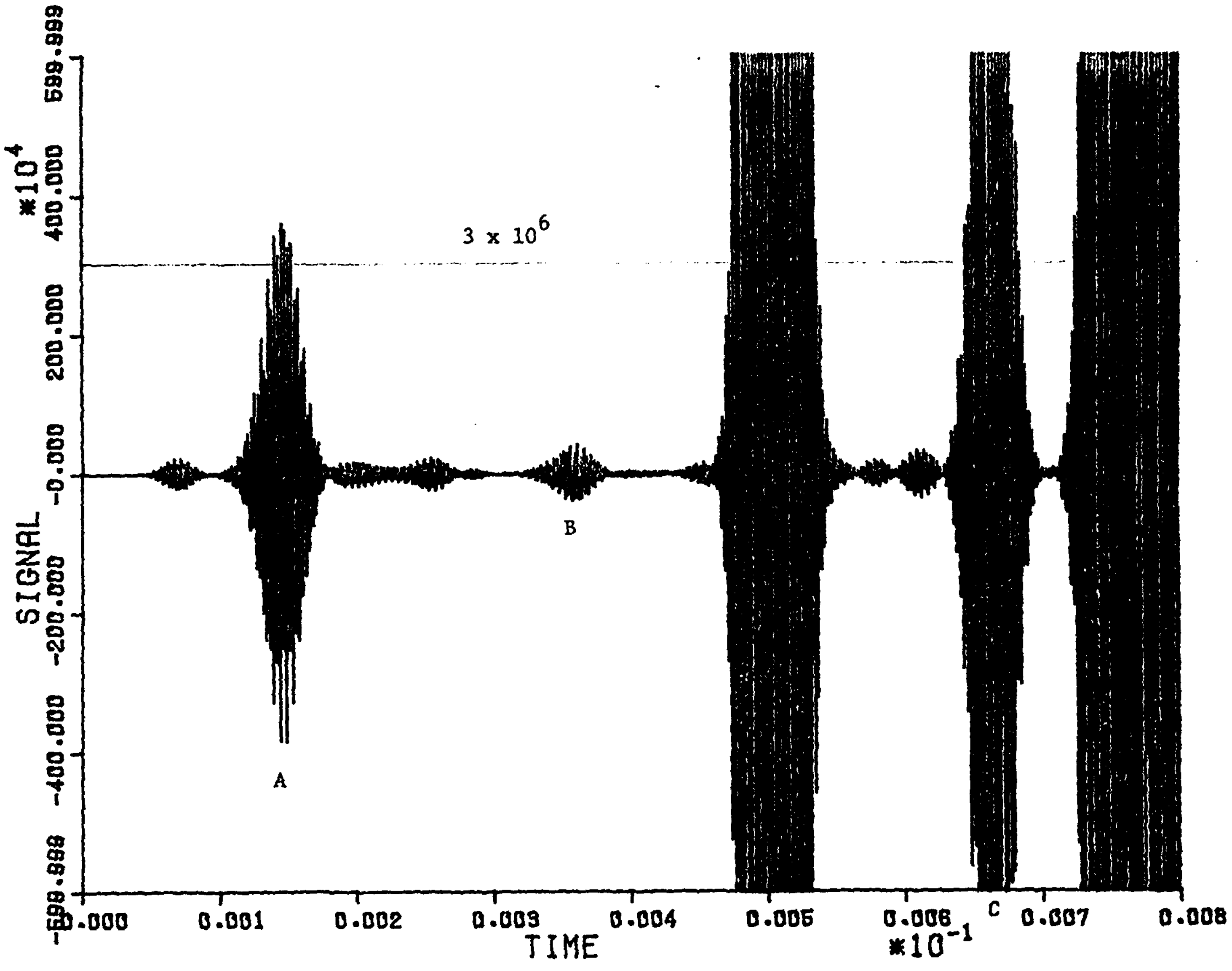

Figure G-6. Plots of Simulated Signal (Cont'd)
d) Every 5th Point, 2×10^6 Vertical Scale.

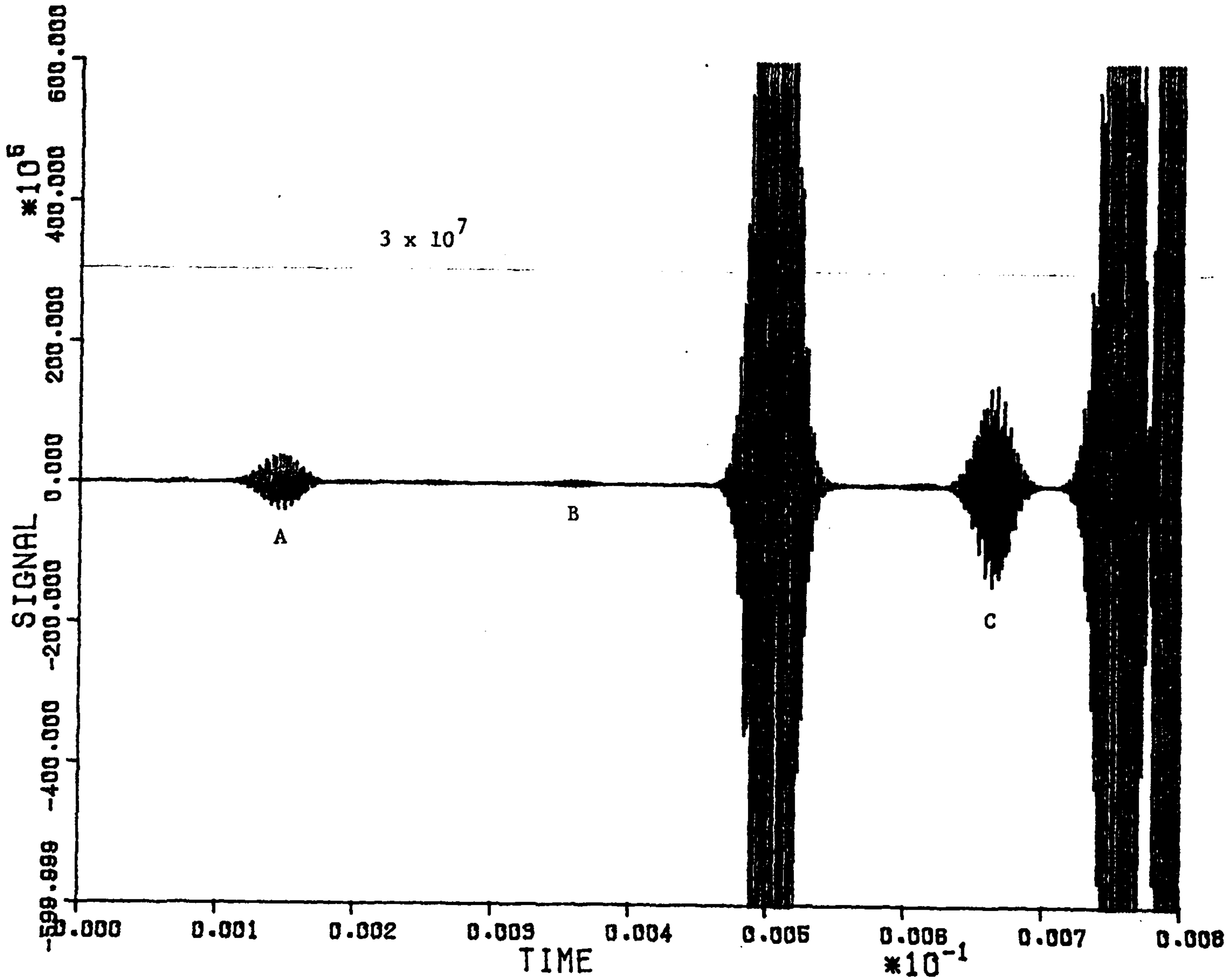

Figure G-6. Plots of Simulated Signal (Cont'd)
e) Every 5th Point, 2×10^7 Vertical Scale.

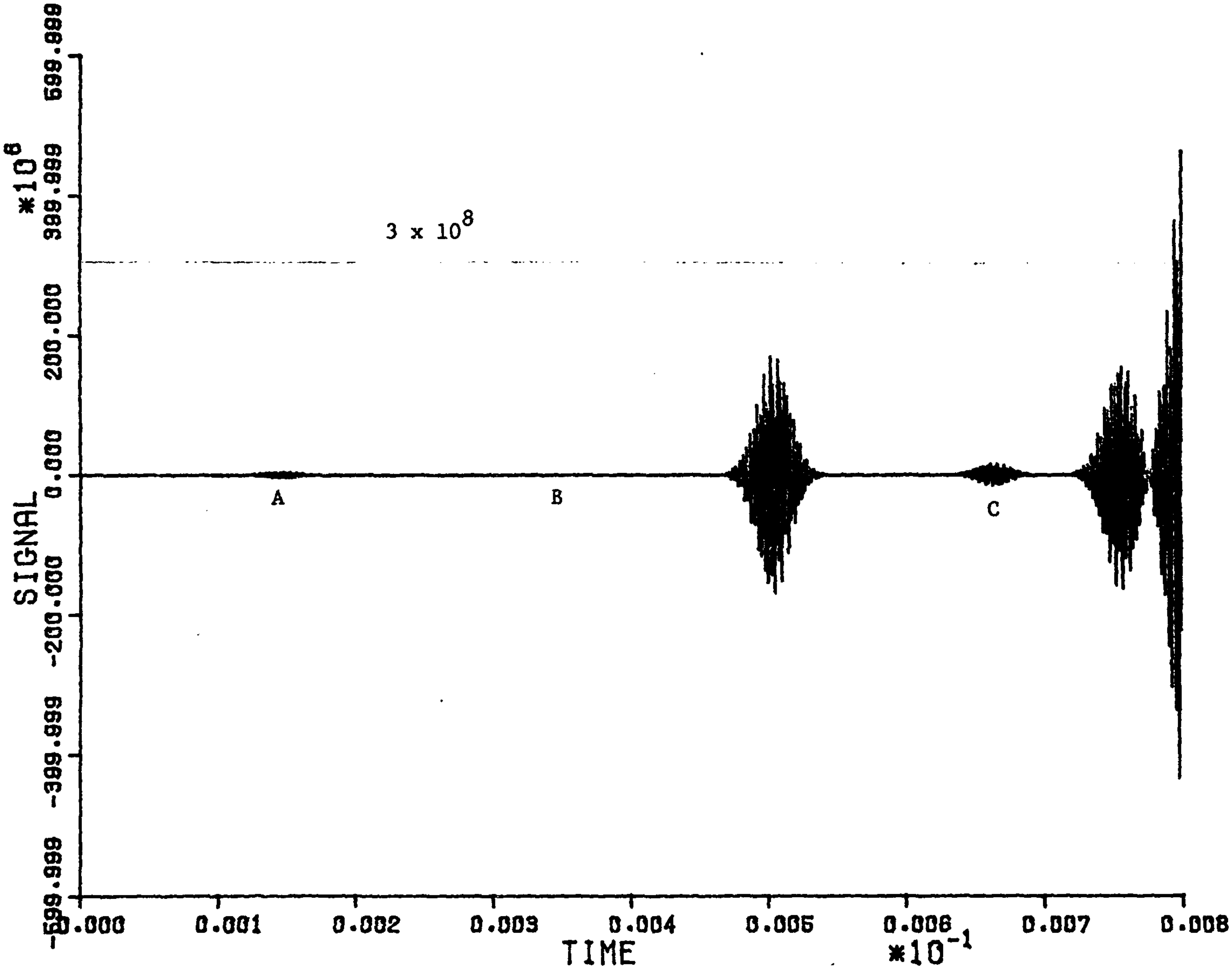

Figure G-6. Plots of Simulated Signal (Cont'd)
f) Every 5th Point, 2×10^8 Vertical Scale.

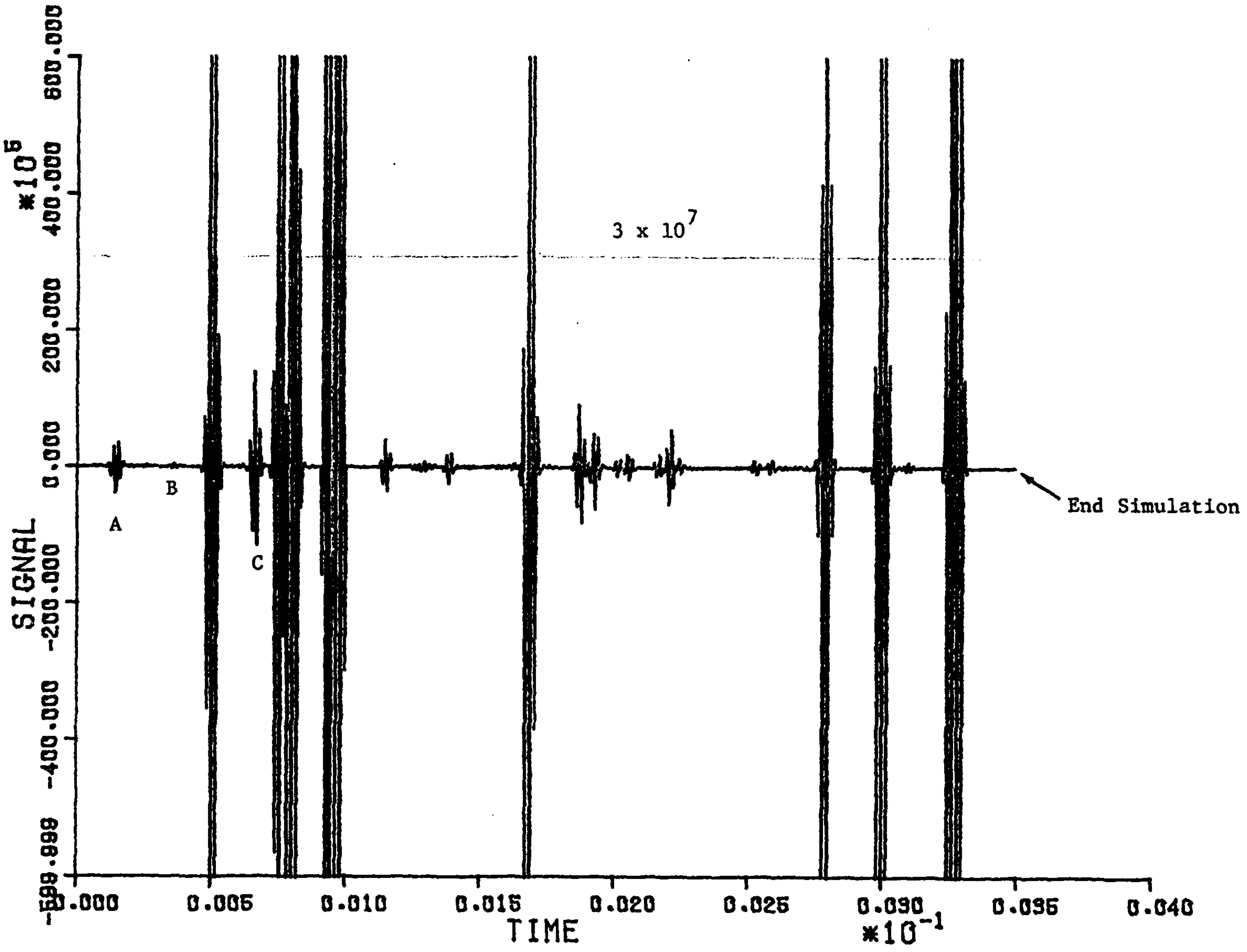

Figure G-6. Plots of Simulated Signal (Cont'd)
g) Every 20th Point, 2 x 10^7 Vertical Scale.

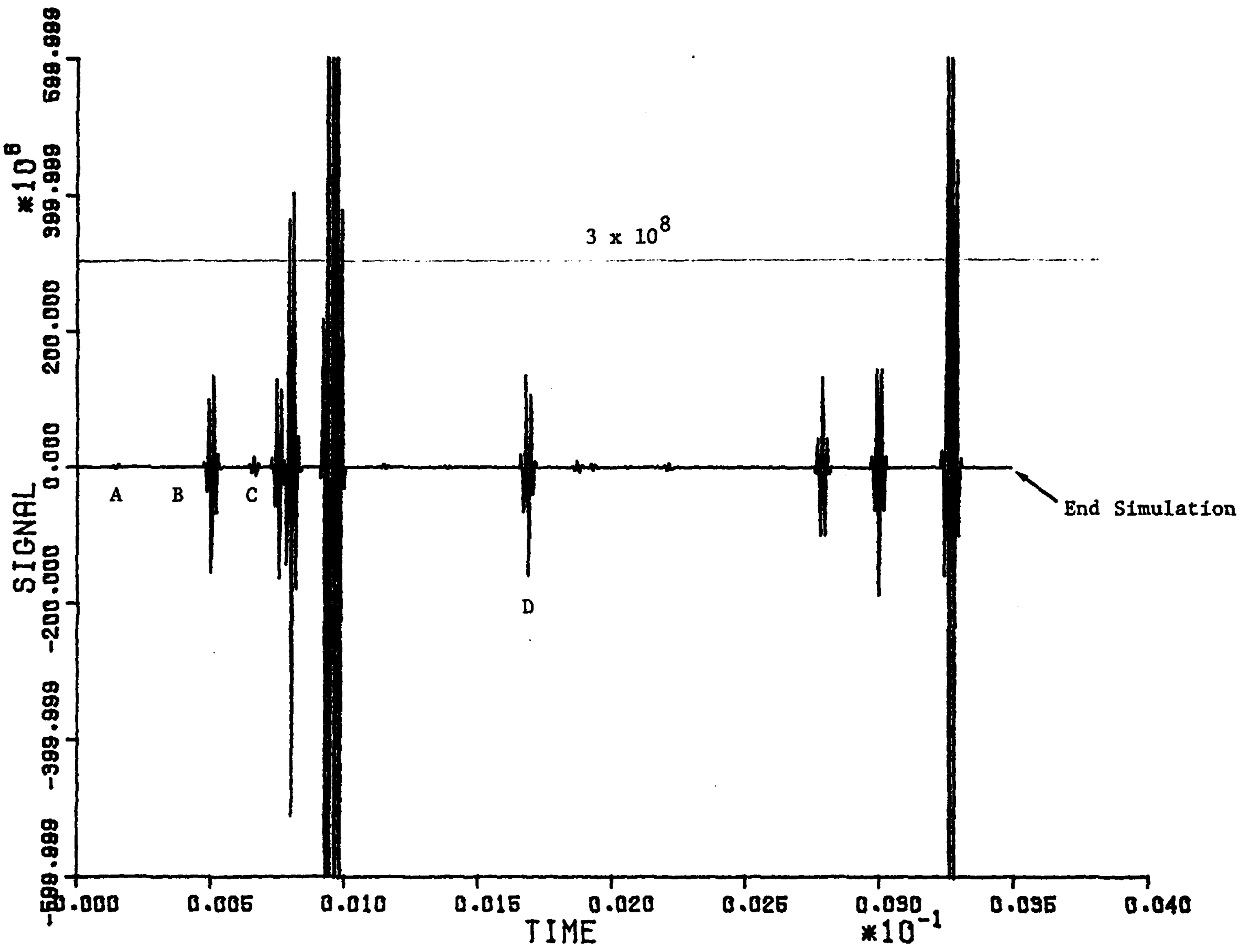

Figure G-6. Plots of Simulated Signal (Cont'd)
h) Every 20th Point, 2×10^8 Vertical Scale.

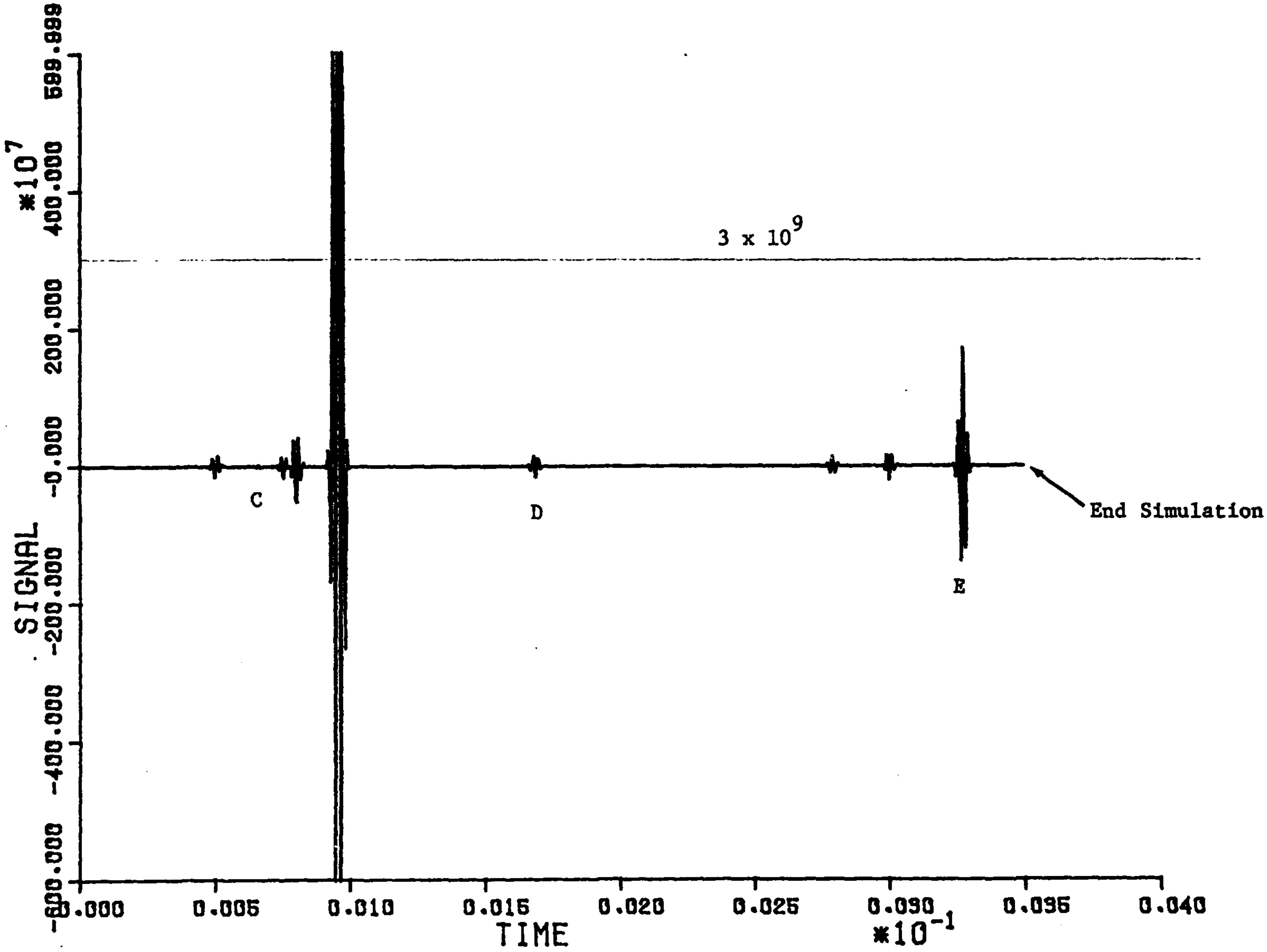

Figure G-6. Plots of Simulated Signal (Cont'd)
i) Every 20th Point, 2 x 10^9 Vertical Scale.

using COMP to take these measurements, throw out the ones with error messages, just as a processor would do, and form a histogram of the frequency deviations which occur.

Figure G-7 is a histogram plot of 32 values of frequency estimate from the test case of SIGNL. This test case was designed to determine if the interpolation error and computer round-off error were sufficiently small to be less than $1:10^4$. The seemingly obvious approach of making the input test frequency constant and observing the output deviation was not used because we wanted to avoid any singularities that could arise from having periodic bursts and periodic sampling. Thus, the amplitude and the frequency of the test signals shown in G-5(b) and G-6(a) are slightly random. Comparison of Figure G-7 with G-5(b) indicates the desired accuracy level was achieved.

Figure G-8 shows the results of multiparticle error versus threshold for the baseline case. The results shown in Figure G-8 were summarized in Table G-2 in the summary.

REPEATABILITY TEST

The simulations reported in this report were all performed with a 1000 particle signal sample. The runs reported have more than filled up a 15 Mbyte disc which holds 3.75 million 32-bit words. Nevertheless, due to the negligible contribution of many of the smaller scattering particles, the number of signals simulated at

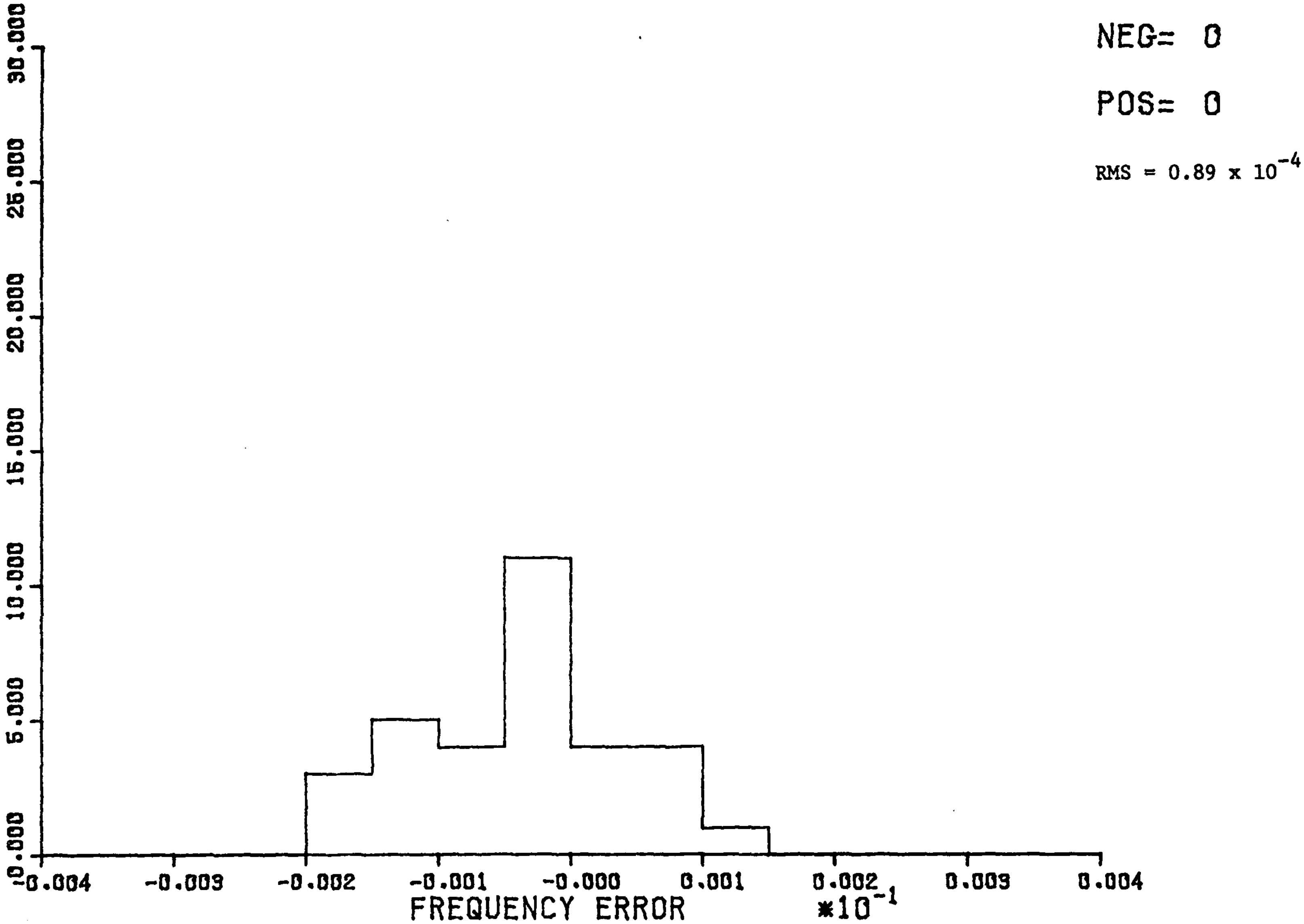

Figure G-7. Output of COMP for 34 Burst Test Case (32 Results Out).

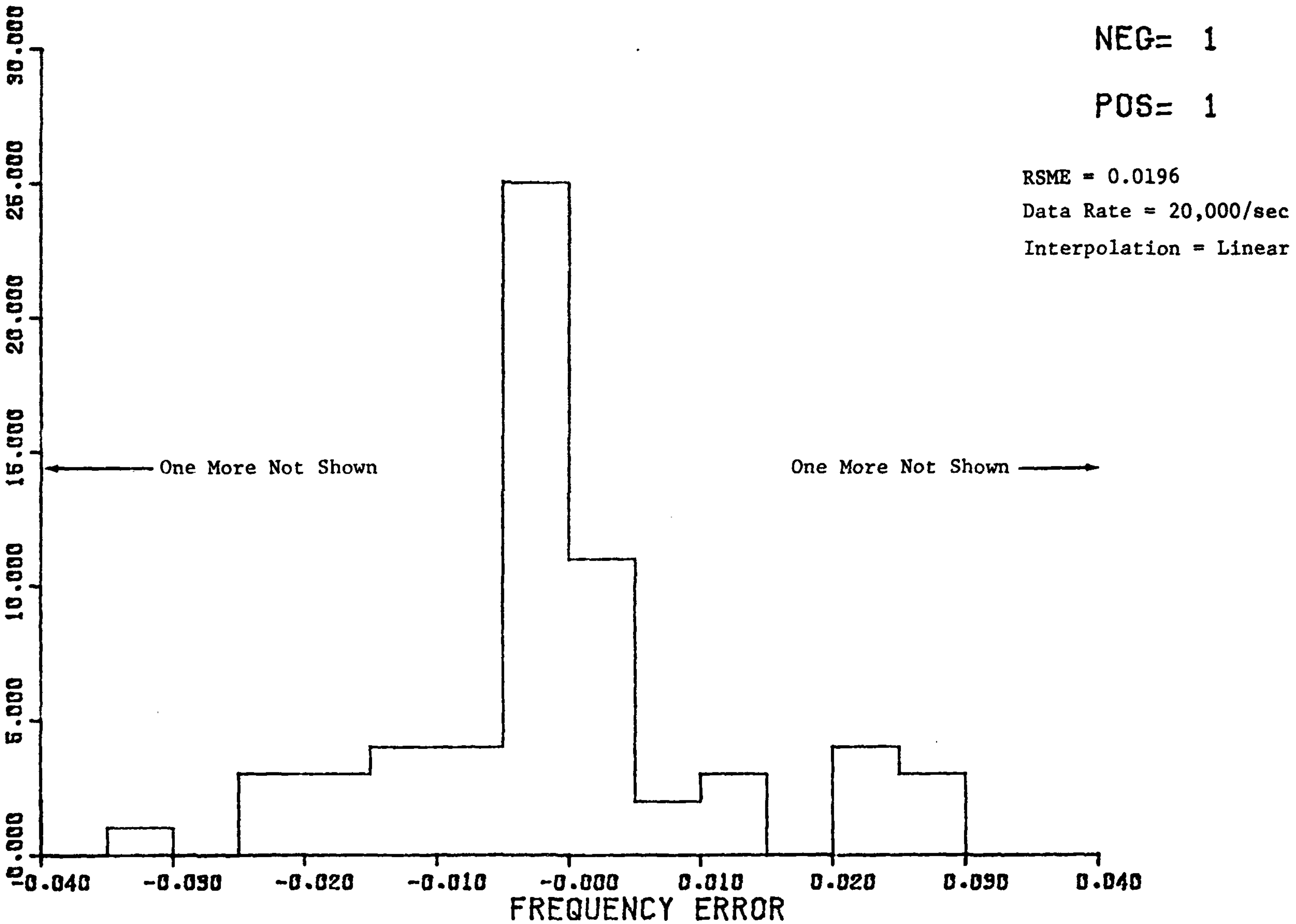

Figure G-8. Histogram of Frequency Deviation
a) Threshold = 3.0×10^4, Bipolar Test Included.

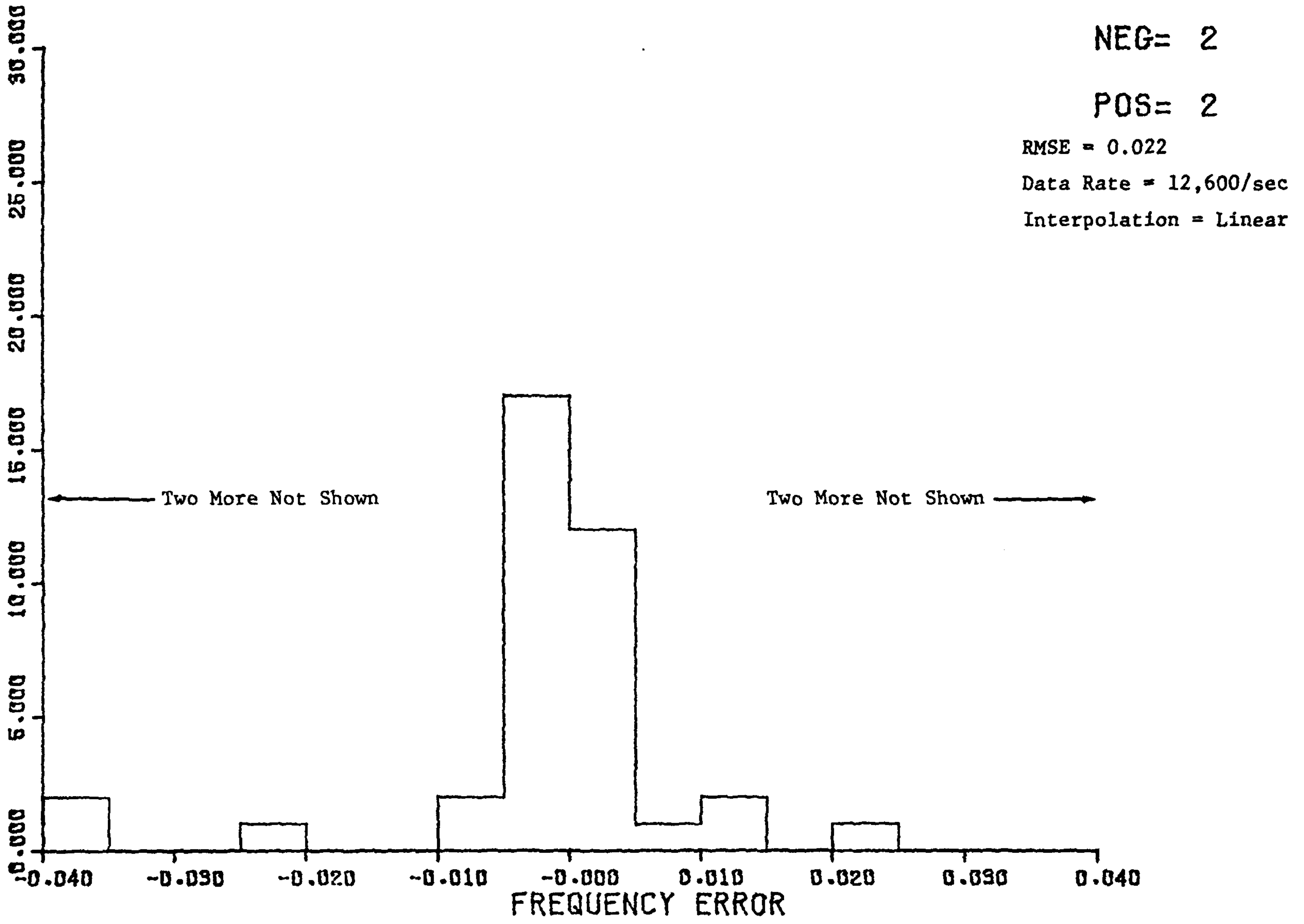

Figure G-8. Histogram of Frequency Deviation (Cont'd)
b) Threshold = 3.0×10^5, No Bipolar Error Rejection.

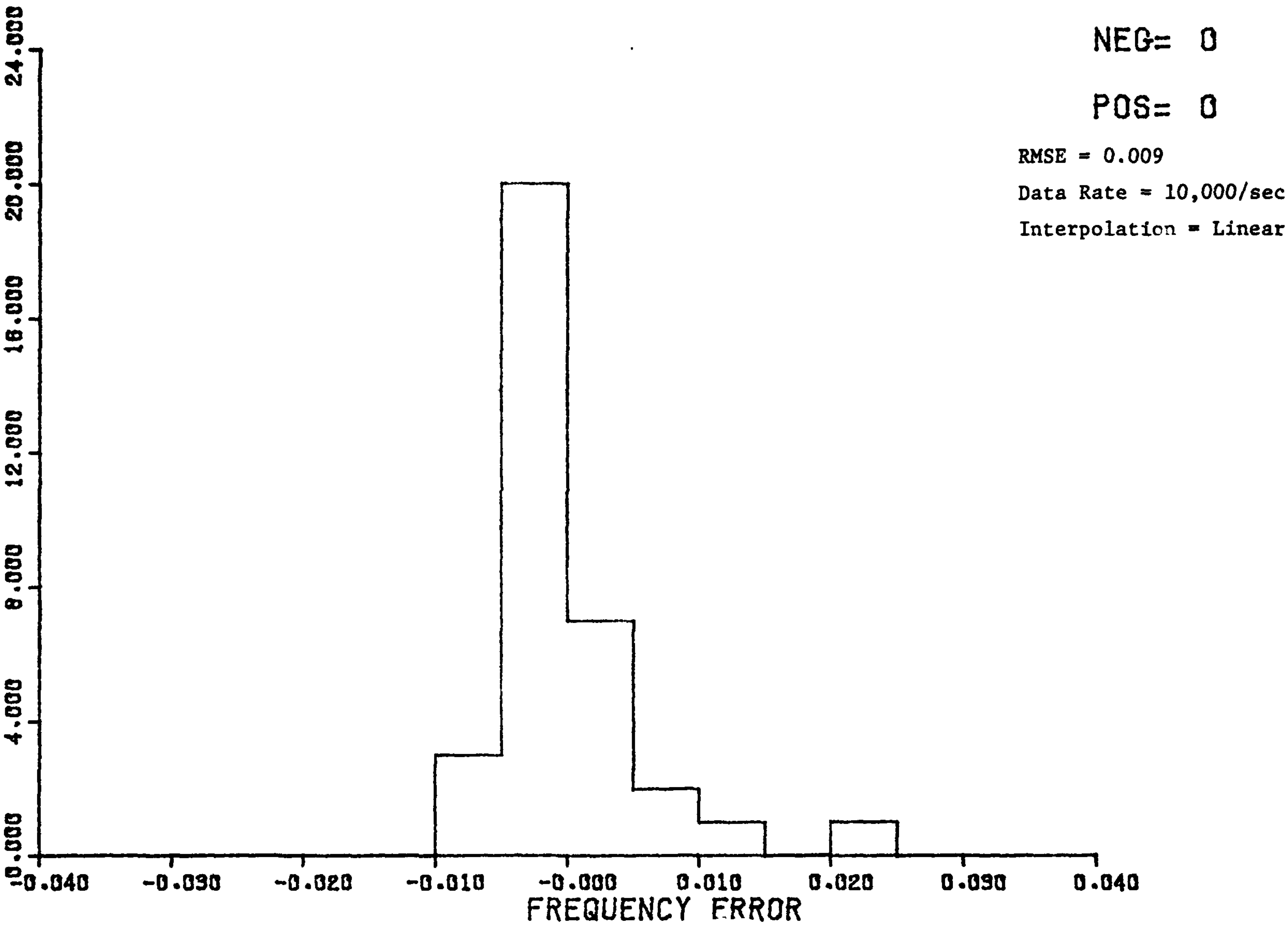

Figure G-8. Histogram of Frequency Deviati (Con'd)
c) Threshold = 3.0 x 10^5, Bipolar Test Included.

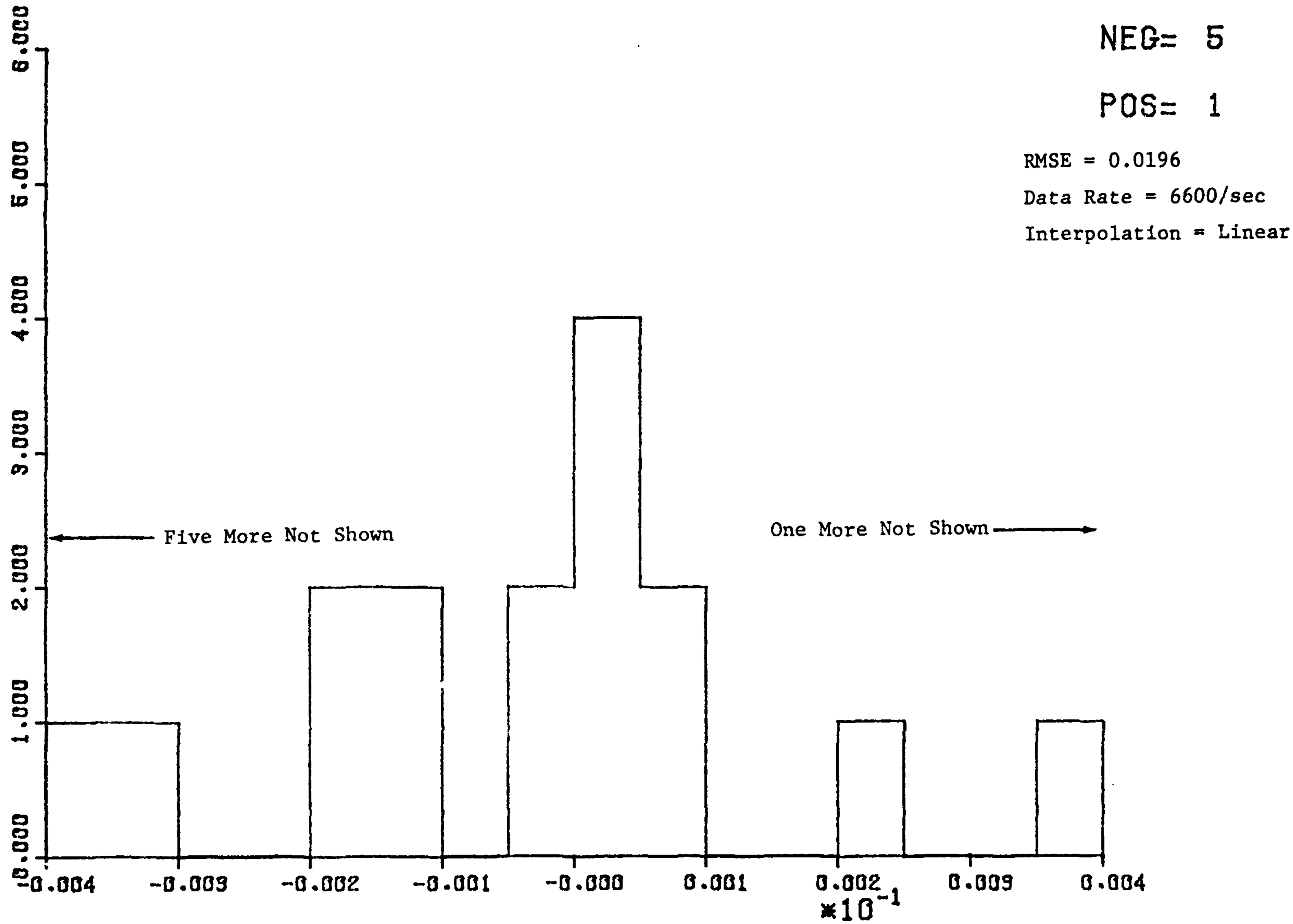

Figure G-8. Histogram of Frequency Deviation (Cont'd)
d) Threshold = 3×10^6, No Bipolar Error Rejection.

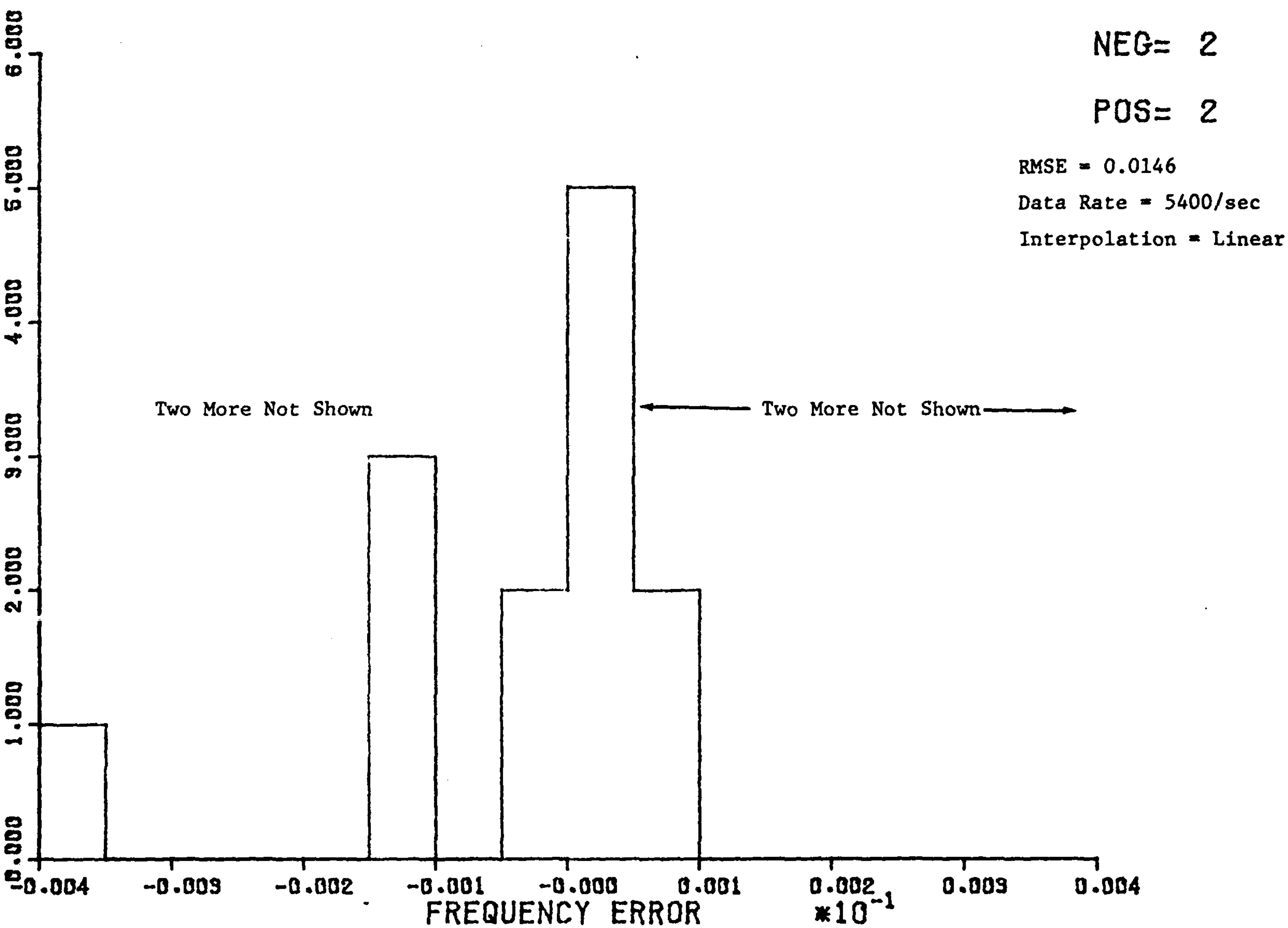

Figure G-8. Histogram of Frequency Deviation (Cont'd)
e) Threshold = 3×10^6, Bipolar Test Included.

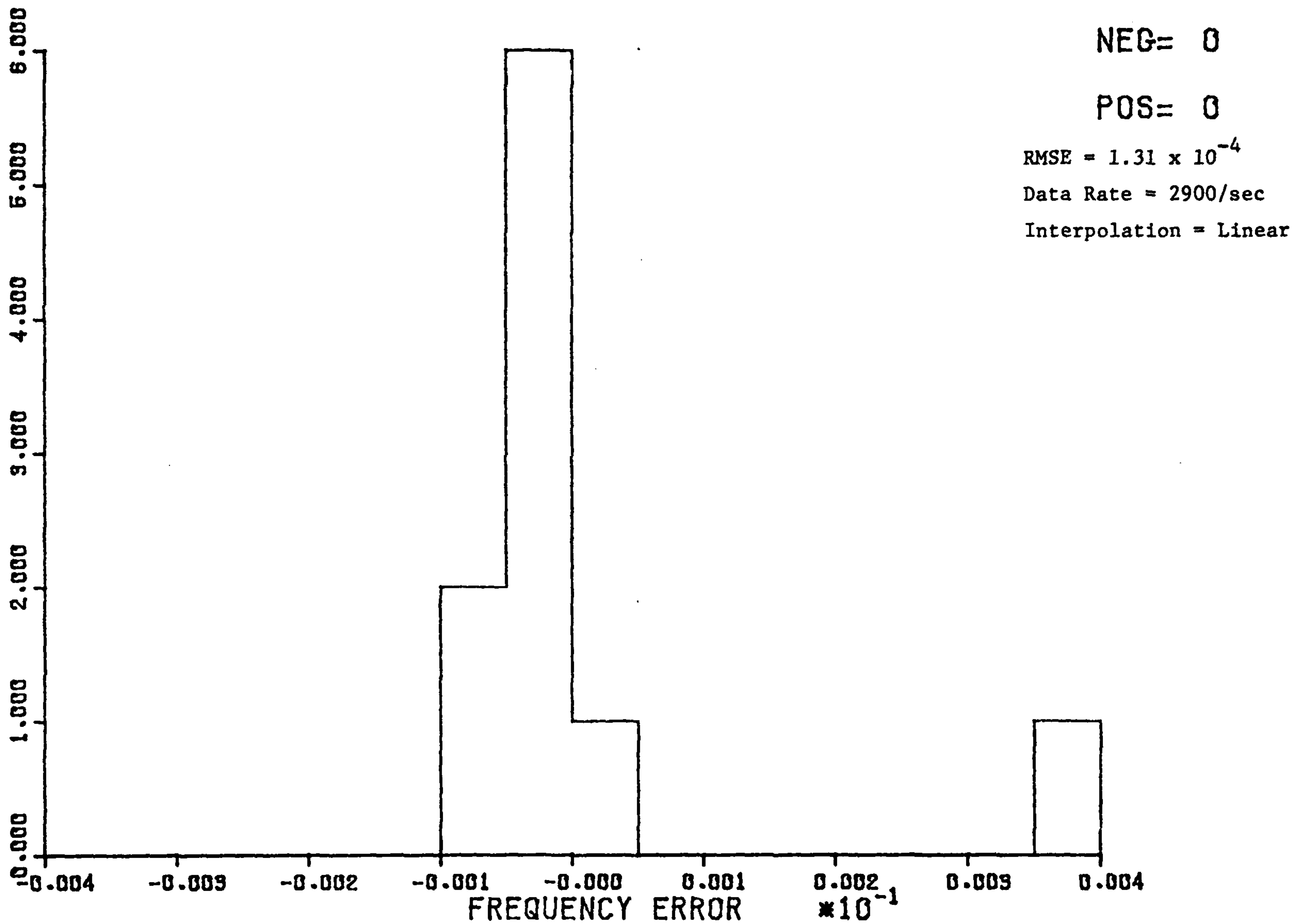

Figure G-8. Histogram of Frequency Deviation (Cont'd)
f) Threshold = 3×10^7, Bipolar Test Included.

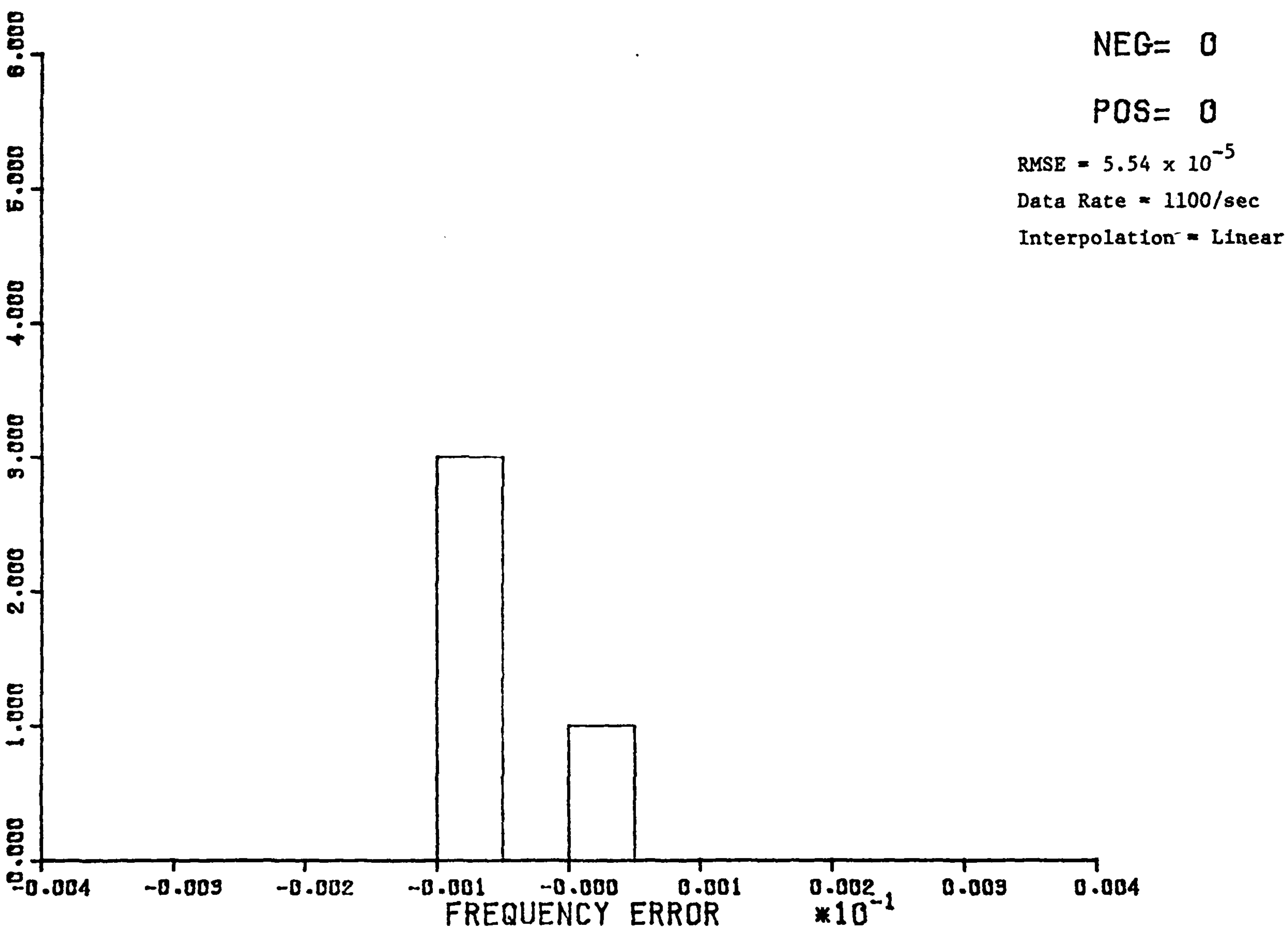

Figure G-8. Histogram of Frequency Deviation (Cont'd)
g) Threshold = 3×10^8, Bipolar Test Included.

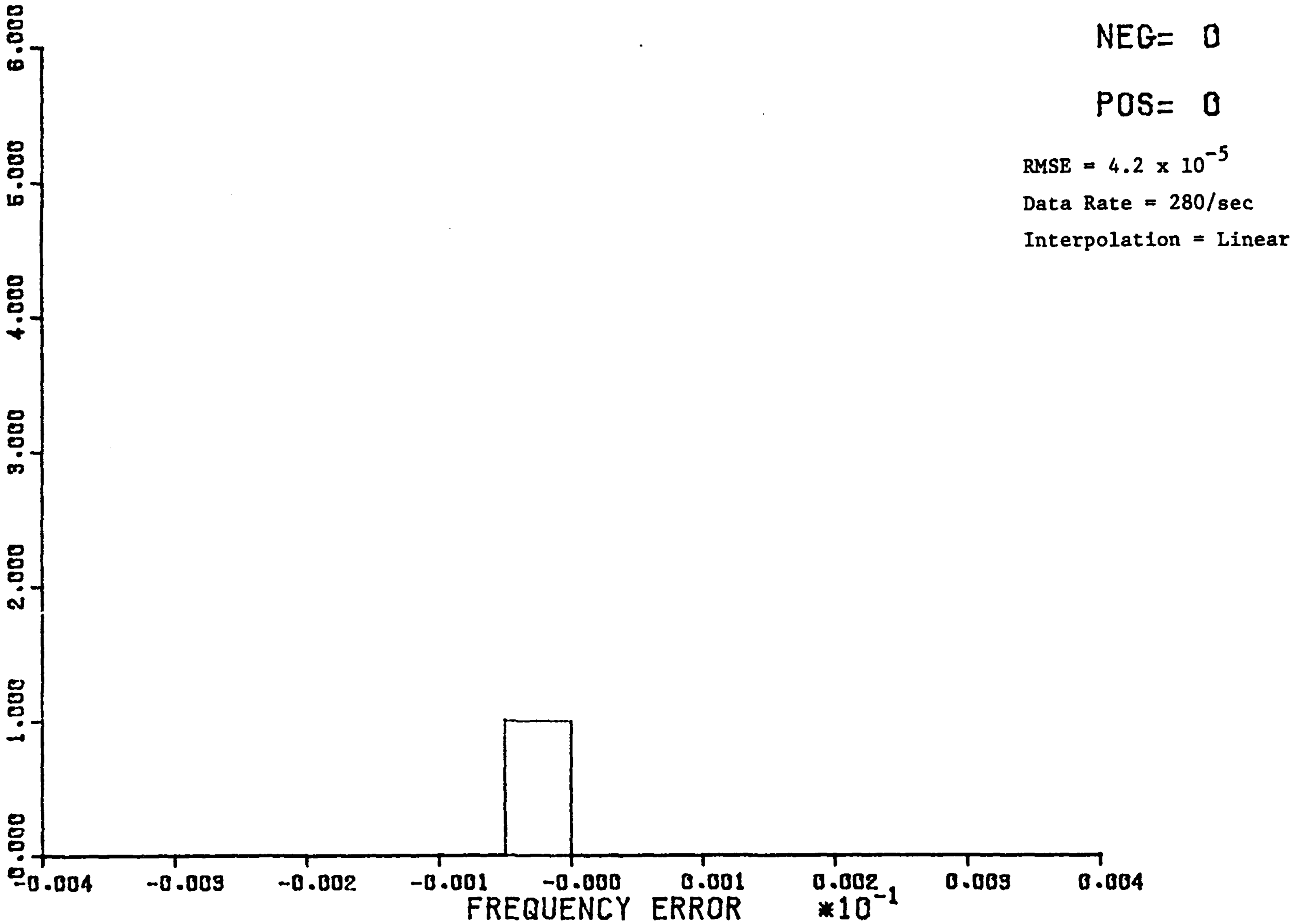

Figure G-8. Histogram of Frequency Deviation (Cont'd)
h) Threshold = 3×10^9, Bipolar Test Included.

peak photo-electron rates high enough to produce large SNR signals is fairly low. Because of this, the numbers reported in Tables G-1 and G-2 are subject to statistical fluctuation. In this section we consider this statistical variability by comparison.

First, the statistical realization of particle diameters has already been presented. Figures G-2 and G-3 compare a histogram of the actual particle diameters realized with the intended theoretical probability density and cumulative probability.

We do not have a theoretical expression for the histograms of realized signal amplitudes. Thus, in order to provide a comparison, we have repeated the entire mid term case for a second 1000 particles randomly realized independently with respect to the mid term case. The results of this repetition are presented in the Figures G-9 through G-13. They may be compared with the corresponding figures above (as indicated on each figure).

Best Available Copy

```
OPTIC OUTPUT
 19  LINES OF HEADER INFORMATION
CREATION DATE    236  1977          TIME       13   38   53
N(PARTICLE)=  1.0300   -.0100 N(MEDIUM)=   1.3300
FREE SPACE WAVELENGTH= .4880E-06    ANGLE BETWEEN BEAMS= .1500E-01
RANGE TO BEAM CROSS OVER= .2000E+01   1/E**2 BEAM RADIUS=1.0000E-03
LOWER CUTOFF SIZE= .1000E-05        UPPER CUTOFF SIZE= .1300E-04
OFF AXIS VIEWING ANG= .1500E-01  TRANSMISSION EFFICIENCY= .3000E+00
ELLIP BEAM EXPANS FACTOR= .1000E+01   RECEIVER COLLECTION AREA= .8480E-02
ATTENUATION COEFF=1.0000E-01   LASER POWER= .4000E+00
CATHODE QUANTUM EFFIC.= .5000E-01         BRAGG CELL OFFSET FREQ= .0000E+00
B COEFF. IN NEG. POWER LAW DIST.= .3650E+01  # OF FACTORS GENERATED= 1000
VELOCITY=1.0000E+01     TOTAL # OF PARTICLES= .2000E+10
FREQ(FRINGE)=     .40880769E+06      SIGNAL PERIOD(FRINGE)= .24461376E-05
MODE=1 (1=FRINGE,2=REF BEAM)       MIE LOOP LIMIT=  200
BURST SEPARATION=     .34364048E-05    BURST RATE=   .29100181E+06
1/E**2 BURST WIDTH= .4672E-04      BANDWIDTH= .2140E+05
GAIN CONSTANT(INCLUDES EXP(-2CR))= .4974E+04 EXP(-2CR)= .6703E+00
P*G= .1990E+04   # OF PARTICLES IN 1/E**2 VOLUME= .1360E-02
# OF FRINGES=     .19098953E+02
T=    .34364047E-02        DT=    .14127363E-06
 1.00000000E+03  .10000000E+01
  .16612085E+04
  .84441465E+04
  .96727285E+04
  .11937144E+05
  .27880767E+04
  .19234395E+05
  .11914629E+04
  .38117486E+04
  .18128023E+03
  .17435816E+05
  .46812471E+04
  .31323562E+05
  .19363477E+03
  .22713641E+06
  .93114734E+05
  .18803088E+04
  .88879141E+04
  .33133394E-04
  .31333898E-03
  .12564226E+04
  .16229805E-03
  .38312617E+05
  .23303920E+03
  .98220633E+05
  .10213375E+03
  .38801707E-03
  .41300287E-03
  .10733409E-03
  .22772036E+04
```

Figure G-9. (a) Output Files OPTIC - Second Set. Compare with Figure G-1(a).

OPTIC OUTPUT--TABLE OF VALUES
CREATION DATE 236 1977 TIME 13 38 53

DIAMETER	SIGMA	FACT	PC	AMP
.1152E-05	.1369E-16	.4966E+00	.1333E-13	.1661E+04
.1569E-05	.2123E-15	.1628E-00	.6876E-13	.8444E+04
.1345E-05	.3966E-16	.3976E+00	.7877E-13	.9673E+04
.2334E-05	.5484E-15	.6910E+00	.9721E-12	.1194E+06
.1122E-05	.5834E-16	.1936E+00	.2279E-13	.2788E+04
.1046E-05	.6498E-16	.9264E+00	.1366E-12	.1923E+05
.1685E-05	.9529E-17	.5347E+00	.1032E-13	.1251E+04
.1119E-05	.6469E-16	.2437E+00	.3137E-13	.3852E+04
.1069E-05	.1122E-15	.5612E+00	.1476E-12	.1813E+05
.1639E-05	.1422E-15	.5014E+00	.1419E-12	.1743E-05
.1116E-05	.6588E-16	.2858E+00	.3747E-13	.4601E+04
.1413E-05	.2649E-15	.4840E+00	.2551E-12	.3132E+05
.1234E-05	.1883E-15	.4341E+00	.1626E-12	.1997E-05
.2697E-05	.1139E-14	.8164E+00	.1851E-11	.2273E+06
.1963E-05	.6150E-15	.6378E+00	.7803E-12	.9582E+05
.1018E-05	.3469E-16	.2230E+00	.1539E-13	.1890E+04
.1339E-05	.3096E-16	.9104E+00	.3609E-13	.6888E+04
.1004E-05	.1445E-16	.5189E-00	.1492E-13	.1832E+04
.2514E-05	.6462E-15	.1373E+00	.1766E-12	.2168E+05
.1017E-05	.3217E-16	.1611E+00	.1031E-13	.1266E+04
.1287E-05	.1341E-15	.4973E+00	.1327E-12	.1630E-05
.1595E-05	.2522E-15	.5277E+00	.2648E-12	.3251E+05
.1113E-04	.3239E-11	.1821E+00	.1898E-08	.2330E+09
.1046E-05	.8500E-16	.9255E+00	.1567E-13	.1922E+05
.1721E-05	.7139E-16	.9873E+00	.1402E-12	.1722E+05
.1229E-05	.1784E-15	.7481E+00	.2650E-12	.3260E-05
.2232E-05	.2709E-13	.6280E+00	.3834E-1[illegible]	.4[illegible]E-05
.3179E-05	.2762E-14	.2332E+00	.280[illegible]E-1[illegible]	.1073E-05
.1150E-05	.2206E-1[illegible]	.9957E-00	.2422E-1[illegible]	.2273E-04
.1572E-05	.1214E-16	.8869E+00	.2093E-13	.2570E+04
.2308E-05	.1800E-15	.7016E+00	.2712E-12	.3665E+05
.1171E-05	.1911E-16	.3774E+00	.1433E-13	.1763E+04
.1324E-05	.2960E-16	.3133E+00	.1857E-13	.2280E+04
.1723E-05	.6128E-16	.9704E-00	.1568E-12	.1323E+05
.2467E-05	.7481E-15	.3717E-00	.4044E-12	.4966E+05
.1779E-05	.3036E-15	.1436E+00	.8680E-1[illegible]	.1066E-05
.1946E-05	.3403E-15	.2113E+00	.2271E-12	.2733E+05
.1642E-05	.4282E-16	.7178E+00	.6116E-13	.7510E+04
.1901E-05	.1362E-15	.4632E+00	.1255E-12	.1541E+05
.1461E-05	.1037E-15	.9576E+00	.2966E-12	.3642E+05
.1064E-05	.1132E-15	.9786E-00	.2203E-12	.2706E+05
.1136E-05	.3196E-16	.9181E+00	.5842E-13	.7174E+04
.2207E-05	.3422E-15	.4036E+00	.2749E-12	.3373E+05
[illegible]	.1319E-16	.5223E+00	.2153E-1[illegible]	.2650E-04
[illegible]	.2273E-15	.5287E+00	.2392E-12	.2937E-05
[illegible]	.2331E-13	.3560E+00	.1994E-1[illegible]	.2450E-0[illegible]
[illegible]	.2388E-15	.4013E+00	.1866E-12	.2337E-05
[illegible]	.5218E-16	.4236E+00	.4396E-13	.5401E-04

Figure G-9. (b) Output Files OPTIC - Second Set (Cont'd). Compare with Figure G-1(b).

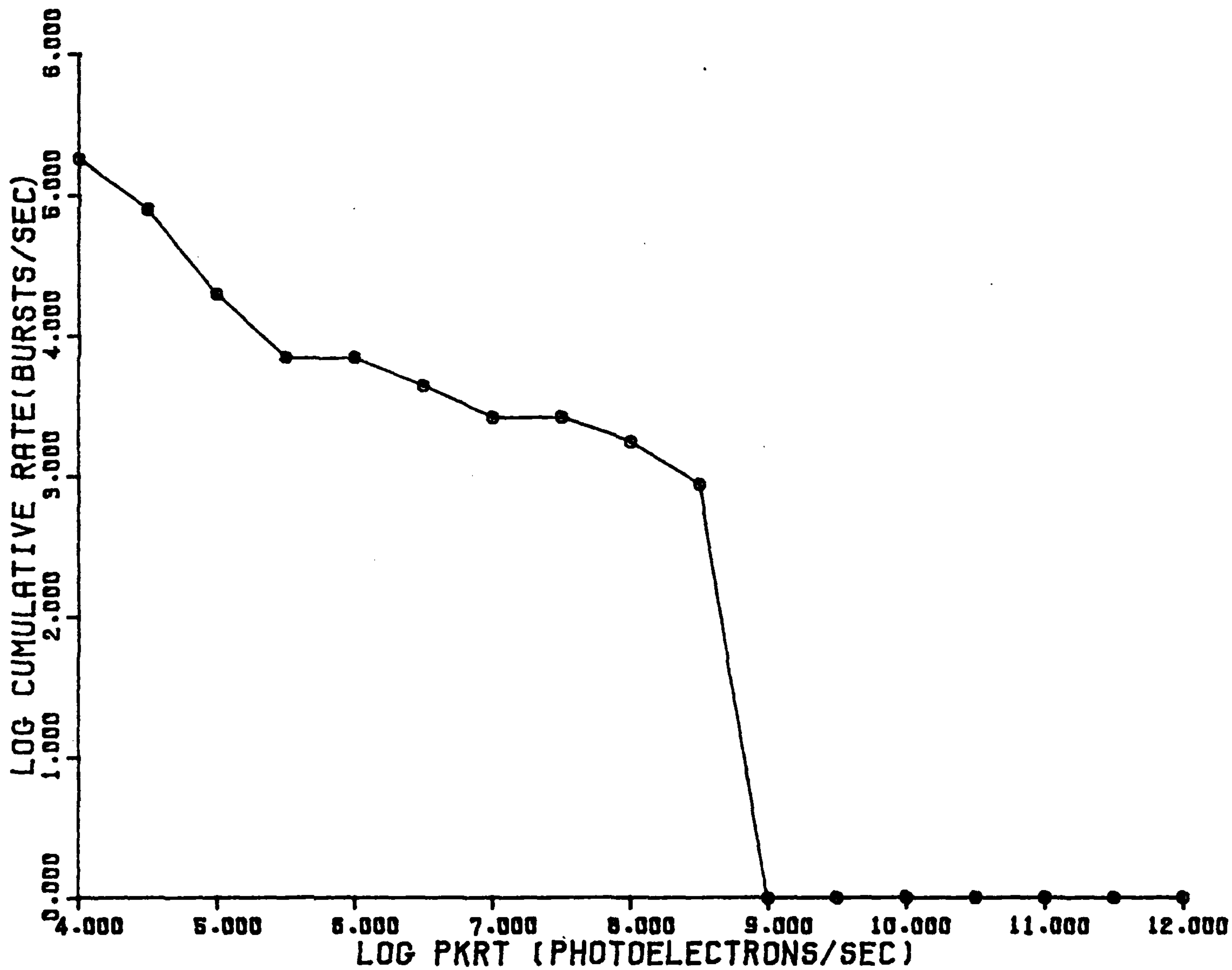

Figure G-10. Cumulative Rate of Signals with PKRT > X (Second 1000). Compare with Figure G-4.

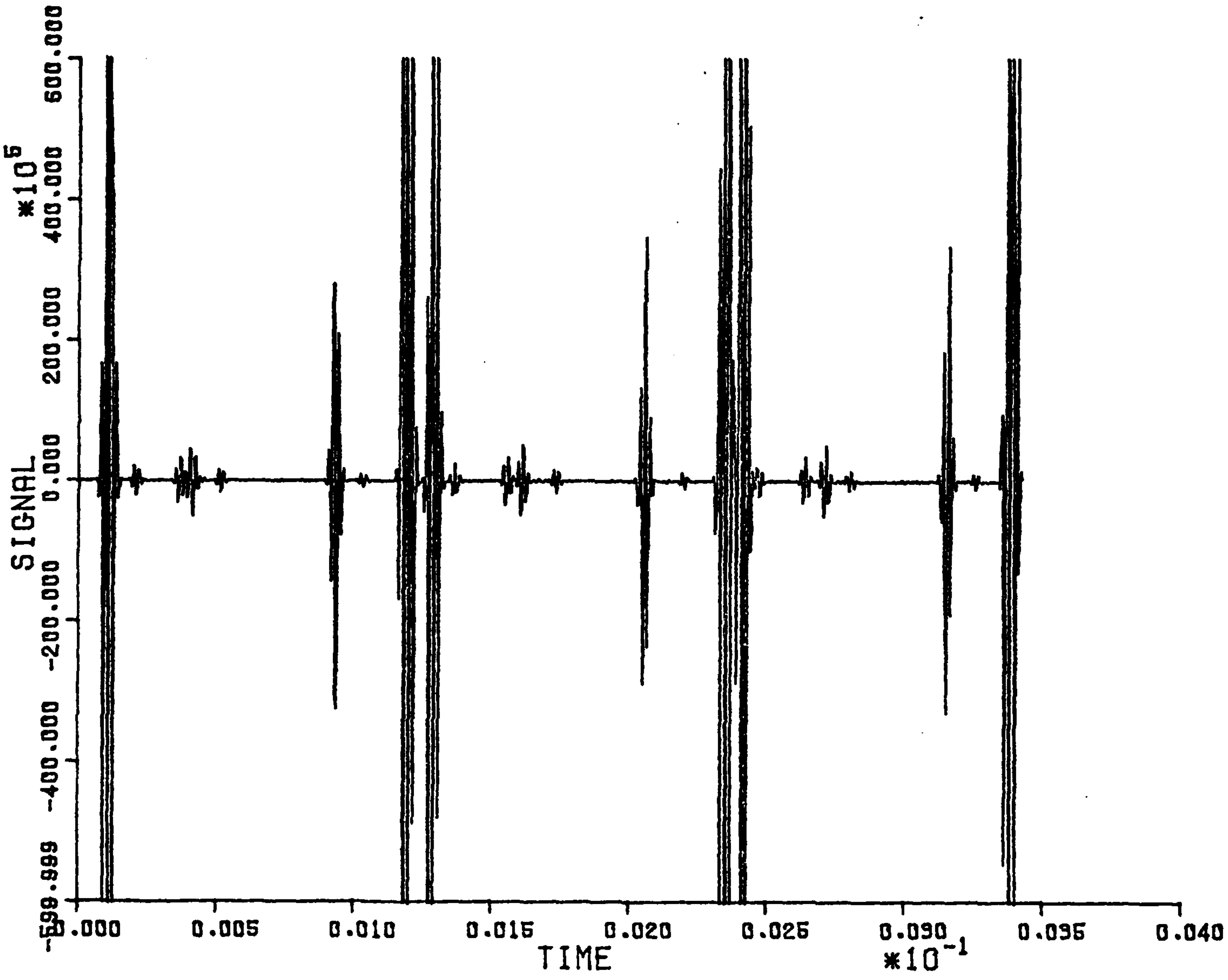

Figure G-11. Plot of Simulated Signal: Every 20th Point, $2x10^7$ Vertical Scale. Compare with Figure G-6(g).

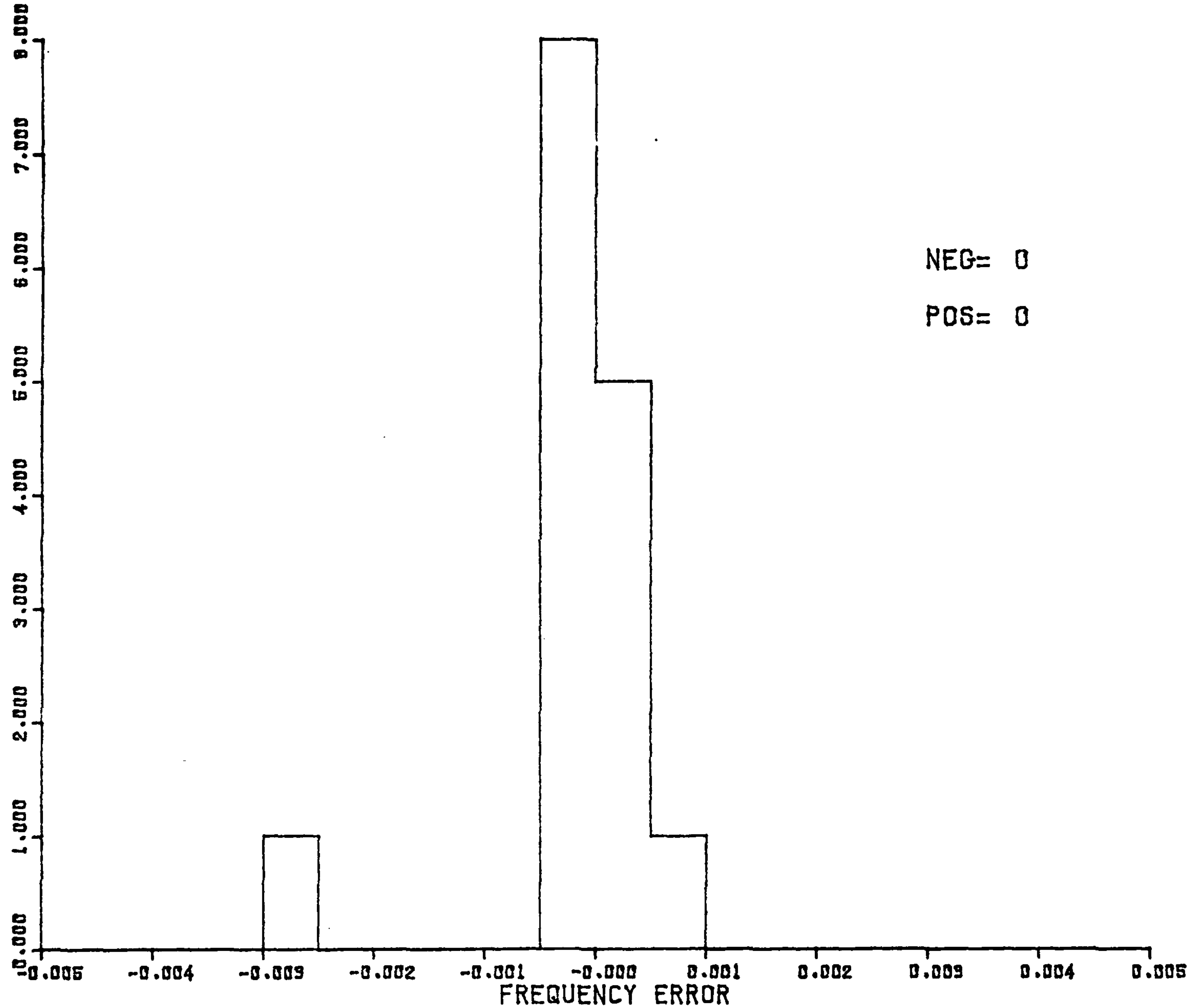

Figure G-12. Histogram of Frequency Deviation: Threshold = $3x10^6$, Bipolar Test Included. Compare with Figure G-8(e).

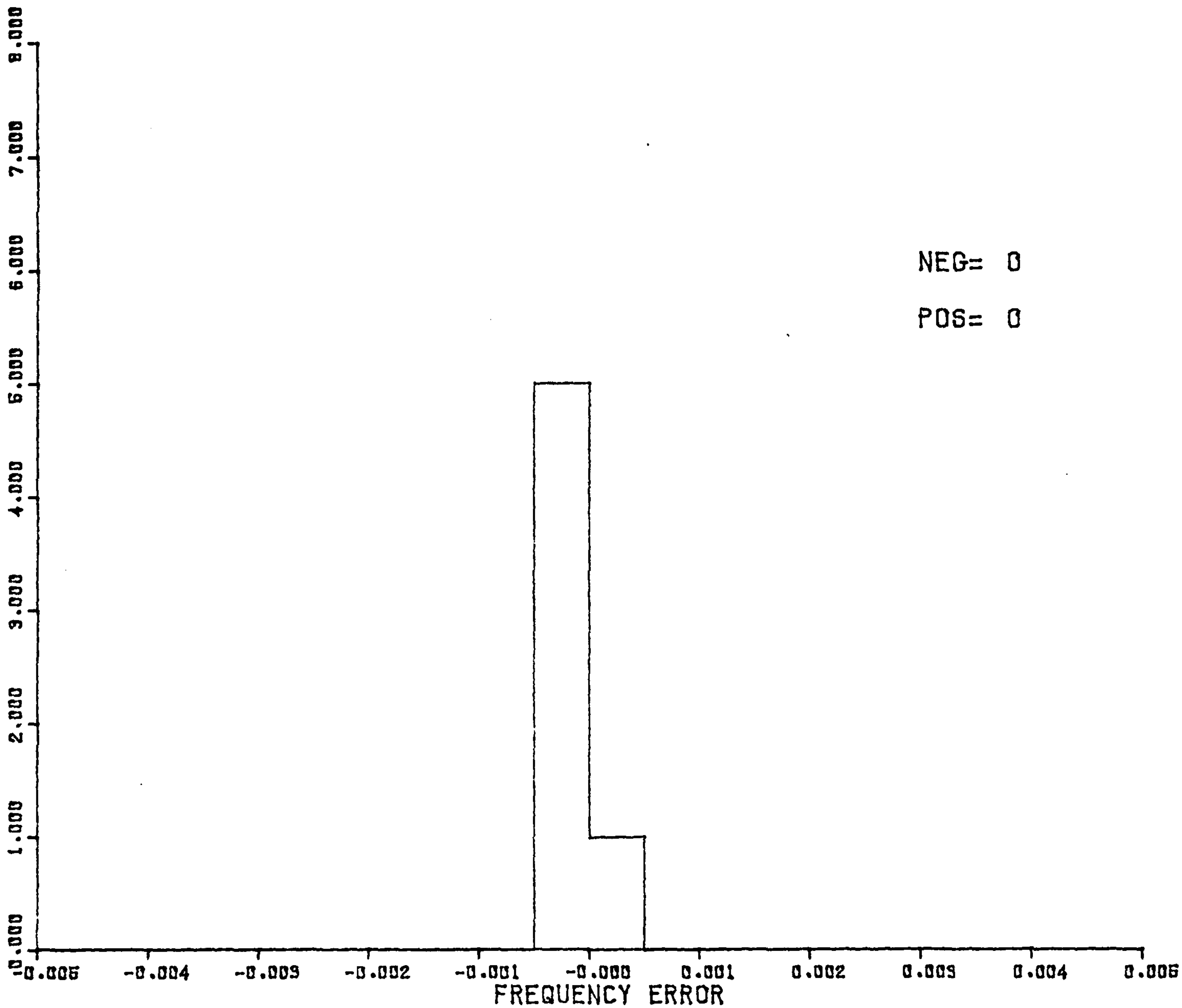

Figure G-13. Histogram of Frequency Deviation: Threshold = $3x10^7$, Bipolar Test Included. Compare with Figure G-8(f).

APPENDIX H

PARAMETRIC COMPUTER DESIGN STUDY: THREE-METER RANGE

The programs OPTIC, SIGNAL, HISTO, PLOT, COMP, and COUNT have all been executed for eight sets of system parameters for a 3-meter fringe laser velocimeter system. The optical parameters were chosen to simultaneously satisfy several practical relationships. These include the fact that for backscatter systems the fringes should not be smaller than the particles being observed; and for a non-Bragg cell system with a count of 8 processors, more than 8 cycles, (15-20) are desired. The eight cases were obtained by permutation of the following three parameters:

I: Optics scaled up by 1.5 from the 2 meter baseline.
II: Optics with transmitter beam diameters increased by factor of 2.5 with beam separation increased by factor of 2.

A: 2000 scatterers/cc $\geq$ 1 micrometer diameter.
B: 20,000 scatterers/cc $\geq$ 1 micrometer diameter.

1: $n = 1.03+j0.0$
2: $n = 1.15+j0.0$

The eight cases there have designations of IA1, IA2, IB1, IB2, IIA1, IIA2, IIB1, IIB2. The entire set of parameters for the runs is given in Table H-1.

The results of running OPTIC are described by the header information and the sample peak rate printout reproduced as Figures H-1(a) through H-1(h) by the cumulative log histograms of

Table H-1. Parameters for 3 Meter Design Study.

$V = 10$ m/sec	Velocity
$R = 3$ m	Range
$w_t =$ I: 1.5×10^{-3} m II: 3.75×10^{-3} m	Transmitter beam radius
$\theta = \frac{d}{R} =$ I: 0.015 radians II: 0.03 radians	Beam angle intersection
$d =$ I: 45×10^{-3}	Transmitter beam separation (19 fringes)
II: 90×10^{-3}	Transmitter beam separation (16 fringes)
$A_c =$ I: $\pi[(0.09)^2-(0.045)^2]$ $= 0.019$ m^2 II: $\pi[(0.09)^2-(0.055)^2]$ $= 0.016$ m^2	Receiver collecting area ($\approx$7.5 inch diameter)
$T = 0.5$	Transceiver transmission efficiency
$P_o = 1.0$ watt	2.0 watt laser split to form two 1.0 watt sections
$\phi =$ I: 0.015 rad II: 0.018 rad	Off axis view angle of receiver due to observation disc
$\lambda_o = 0.488\times10^{-6}$	Free-space wavelength of laser
$\eta = 0.2$	Effective quantum efficiency
$C = 0.1$/m	Water attenuation coefficient

Table H-1. Parameters for 3 Meter Design Study (Cont'd).

n_o = 1: 1.03+j0.0 2: 1.15+j0.0	Relative index of refraction of particles
$n = 1.33$	Index of refraction of water
N = A: 2000×10^{6} B: $20{,}000 \times 10^{6}$	Number of particles*/m^3 greater in diameter than y_o
$y_o = 1.0 \times 10^{-6}$ m	Lower cutoff of size distribution
$b = 3.65$	Negative slope of particle diameter probability density
$y_{max} = 20 \times 10^{-6}$ m	

---

* Cumulative:

$$N > y = 2000 \left(\frac{y}{1.0 \times 10^{-6}}\right)^{-2.65} \times 10^{6}/m^{3} \quad , \quad 1.0 \times 10^{-6} \leq y \leq 20\ \mu m$$

Best Available Copy

```
OPTIC OUTPUT
  19  LINES OF HEADER INFORMATION
CREATION DATE    227  1977         TIME    10    1   40
N(PARTICLE)=  1.0300   .0000 N(MEDIUM)=  1.3300
FREE SPACE WAVELENGTH= .4880E-06    ANGLE BETWEEN BEAMS= .1500E-01
RANGE TO BEAM CROSS OVER= .3000E+01   1/E**2 BEAM RADIUS= .1500E-02
LOWER CUTOFF SIZE= .1000E-05      UPPER CUTOFF SIZE= .2000E-04
OFF AXIS VIEWING ANG= .1500E-01  TRANSMISSION EFFICIENCY= .5000E+00
ELLIP BEAM EXPANS FACTOR= .1000E+01   RECEIVER COLLECTION AREA= .1900E-01
ATTENUATION COEFF=1.0000E-01   LASER POWER= .1000E+01
CATHODE QUANTUM EFFIC.= .2000E+00     BRAGG CELL OFFSET FREQ= .0000E+00
B COEFF. IN NEG. POWER LAW DIST.= .3630E+01  # OF FACTORS GENERATED= 1000
VELOCITY=1.0000E+01    TOTAL # OF PARTICLES= .2000E+10
FREQ(FRINGE)=    .40880769E+06    SIGNAL PERIOD(FRINGE)=    .24461378E-05
MODE=1 (1=FRINGE,2=REF.BEAM)     MIE LOOP LIMIT=  200
BURST SEPARATION=    .34364048E-05    BURST RATE=    .29100181E+06
1/E**2 BURST WIDTH= .4672E-04    BANDWIDTH= .2140E+05
GAIN CONSTANT(INCLUDES EXP(-2CR))= .6759E+04 EXP(-2CR)= .5488E+00
P*G= .6759E+04    # OF PARTICLES IN 1/E**2 VOLUME= .1360E+02
# OF FRINGES=  .19098943E+02
T=    .34364047E-02      DT=    .14127963E-06
 1.00000000E+03    10000000E+01
  .17214316E+05
  .10546661E+06
  .16093432E+05
  .39173506E+06
  .93080937E+05
  .18338910E+07
  .11591914E+06
  .90688086E+04
  .70245094E+05
  .51534156E-03
  .16192172E+06
  .38374700E+06
  .50640631E+06
  .18525127E+07
  .67812828E+05
  .10833606E+05
  .31709731E-04
  .34870223E+06
  .18872172E+05
  .12115206E+06
  .73876766E+05
  .11658409E+06
  .21648831E+06
  .24932910E+05
  .39133756E+05
  .13346275E+05
  .82734631E+05
  .34240969E+06
  .44393392E+05
  .36114150E+06
  .67932484E+05
  .50383164E+05
  .26996660E+04
  .17481289E+05
  .91213281E+04
  .14865137E+06
  .62276891E+05
  .87024156E+05
  .54129516E+05
```

Figure H-1. OPTIC Printout
(a) Case IA1.

```
OPTIC OUTPUT
 13  LINES OF HEADER INFORMATION
CREATION DATE   227  1977          TIME      10   37   48
N(PARTICLE)=  1.1500   .0000 N(MEDIUM)=  1.3300
FREE SPACE WAVELENGTH= .4880E-06    ANGLE BETWEEN BEAMS= .1500E-01
RANGE TO BEAM CROSS OVER= .3000E+01    1/E**2 BEAM RADIUS= .1500E-03
LOWER CUTOFF SIZE= .1000E-05        UPPER CUTOFF SIZE= .2000E-04
OFF AXIS VIEWING ANG= .1500E-01  TRANSMISSION EFFICIENCY= .5000E+00
ELLIP BEAM EXPANS FACTOR= .1000E+01   RECEIVER COLLECTION AREA= .1900E-01
ATTENUATION COEFF=1.0000E-01    LASER POWER= .1000E+01
CATHODE QUANTUM EFFIC.= .2000E+00         BRAGG CELL OFFSET FREQ= .0000E+00
B COEFF. IN NEG. POWER LAW DIST.= .3650E+01  # OF FACTORS GENERATED= 1000
VELOCITY=1.0000E+01    TOTAL # OF PARTICLES= .2000E+10
FREQ(FRINGE)=    .40880769E+06    SIGNAL PERIOD(FRINGE)=    .24461378E-05
MODE=1 (1=FRINGE,2=REF.BEAM)      MIE LOOP LIMIT=  200
BURST SEPARATION=    .34364048E-05    BURST RATE=    .29100181E+06
1/E**2 BURST WIDTH= .4672E-04    BANDWIDTH= .2140E+05
GAIN CONSTANT(INCLUDES EXP(-2CR))= .6759E+04 EXP(-2CR)= .5488E+00
P*G= .6759E+04   # OF PARTICLES IN 1/E**2 VOLUME= .1360E+02
# OF FRINGES=    .19098949E+02
T=    .34364047E-02      DT=    .14127963E-06
 1.00000000E+03    .10000000E+01
   .78518587E+06
   .39996570E+07
   .64772150E+07
   .49579992E+08
   .10610004E+08
   .16388585E+07
   .33159852E+08
   .14302377E+07
   .20441107E+07
   .17097984E+06
   .66270680E+07
   .41788216E+08
   .53028736E+09
   .61486858E+10
   .34029768E+08
   .33180285E+07
   .35885350E+07
   .23398320E+08
   .65305780E+07
   .15678867E+07
   .14550342E+08
   .94942187E+06
   .10650222E+07
   .51532050E+06
   .48127890E+07
   .34299728E+08
   .33552244E+08
   .11407816E+09
   .27979305E+07
   .36738312E+08
   .35277304E+08
   .35095536E+08
   .77719940E+07
   .14707738E+08
   .10435262E+08
   .23169792E+08
   .70744070E+07
   .21190264E+08
   .18515260E+07
```

Figure H-1. OPTIC Printout
(b) Case IA2.

```
OPTIC OUTPUT
 19  LINES OF HEADER INFORMATION
CREATION DATE    227  1977          TIME      10   42    2
N(PARTICLE)=  1.0300    .0000 N(MEDIUM)=  1.3300
FREE SPACE WAVELENGTH=  .4880E-06    ANGLE BETWEEN BEAMS=  .1500E-01
RANGE TO BEAM CROSS OVER= .3000E+01   1/E**2 BEAM RADIUS= .1500E-02
LOWER CUTOFF SIZE= .1000E-05      UPPER CUTOFF SIZE= .2000E-04
OFF AXIS VIEWING ANG= .1500E-01  TRANSMISSION EFFICIENCY= .5000E+00
ELLIP BEAM EXPANS FACTOR= .1000E+01   RECEIVER COLLECTION AREA= .1900E-01
ATTENUATION COEFF=1.0000E-01    LASER POWER= .1000E+01
CATHODE QUANTUM EFFIC.= .2000E+00       BRAGG CELL OFFSET FREQ= .0000E+00
B COEFF. IN NEG. POWER LAW DIST.= .3650E+01  # OF FACTORS GENERATED= 1000
VELOCITY=1.0000E+01     TOTAL # OF PARTICLES= .2000E+11
FREQ(FRINGE)=    .40880769E+06    SIGNAL PERIOD(FRINGE)=    .24461378E-05
MODE=1 (1=FRINGE,2=REF.BEAM)      MIE LOOP LIMIT=  200
BURST SEPARATION=    .34364035E-06    BURST RATE=    .29100190E+07
1/E**2 BURST WIDTH= .4672E-04    BANDWIDTH= .2140E+05
GAIN CONSTANT(INCLUDES EXP(-2CR))= .6759E+04 EXP(-2CR)= .5488E+00
F*G= .6759E+04   # OF PARTICLES IN 1/E**2 VOLUME= .1360E+03
 # OF FRINGES=    .19098943E-02
T=     .34364033E-03        DT=    .14127963E-06
  1.00000000E+03    .10000000E+01
   .17214316E+05
   .10546661E+06
   .16093432E+05
   .39173306E+06
   .93080937E+05
   .18338910E+05
   .11591914E+06
   .90688086E+04
   .70245094E+05
   .51534136E+05
   .16132172E+06
   .33974700E+06
   .50640631E+06
   .18323127E+07
   .67312826E+05
   .10888606E+06
   .31709731E+04
   .34670223E+05
   .39872172E+05
   .12115206E+06
   .73876766E+05
   .11638409E+06
   .21649831E+06
   .24932910E+03
   .33188758E+05
   .13346275E+05
   .82734691E+05
   .72340969E+06
   .44939992E+05
   .36114130E+06
   .67992484E+05
   .30733164E+03
   .26996660E+04
   .17481289E+03
   .91317281E+04
   .14665137E+06
   .62278891E+05
   .87024136E+03
   .54112316E+05
```

Figure H-1. OPTIC Printout
(c) Case IB1.

```
OPTIC OUTPUT
 19  LINES OF HEADER INFORMATION
CREATION DATE:   227  1977          TIME:   10   43   49
N(PARTICLE)=  1.1500   .0000 N(MEDIUM)=  1.3300
FREE SPACE WAVELENGTH=  4880E-06    ANGLE BETWEEN BEAMS= .1500E-01
RANGE TO BEAM CROSS OVER= .3000E+01   1/E**2 BEAM RADIUS=  .1500E-02
LOWER CUTOFF SIZE= .1000E-03       UPPER CUTOFF SIZE=  2000E-04
OFF AXIS VIEWING ANG= .1500E-01  TRANSMISSION EFFICIENCY= .5000E+00
ELLIP BEAM EXPANS FACTOR= .1000E+01   RECEIVER COLLECTION AREA= .1900E-01
ATTENUATION COEFF=1.0000E-01    LASER POWER= .1000E-01
CATHODE QUANTUM EFFIC.=  2000E+00        BRAGG CELL OFFSET FREQ= .0000E+00
B COEFF. IN NEG. POWER LAW DIST.= .3650E+01  # OF FACTORS GENERATED= 1000
VELOCITY=1.0000E+01     TOTAL # OF PARTICLES= .2000E+11
FREQ(FRINGE)=    .40880769E+06    SIGNAL PERIOD(FRINGE)=   .24461378E-05
MODE=1 (1=FRINGE,2=REF.BEAM)      MIE LOOP LIMIT=  200
BURST SEPARATION=    .34364035E-06    BURST RATE=     29100190E+07
1/E**2 BURST WIDTH= .4672E-04    BANDWIDTH= .2140E+05
GAIN CONSTANT(INCLUDES EXP(-2CR))= .6759E+04 EXP(-2CR)= .5488E+00
P*Q= .6759E+04   # OF PARTICLES IN 1/E**2 VOLUME= .1360E+03
# OF FRINGES=    .19098549E+02
T=    .34364033E-03      DT=   .14127363E-06
 1.00000000E+03    .10000000E+01
  .78518587E+06
  .39996570E+07
  .64772150E+07
  .49579992E+08
  .10610004E+08
  .16388585E+07
  .33159832E+08
  .14302377E+07
  .28441107E-07
  .17097984E+06
  .66270680E+07
  .41788216E+08
  .33028736E+09
  .61486858E+10
  .34029768E-08
  .33158086E+07
  .33883330E-07
  .27793320E-08
  .55305730E-07
  .15678667E-07
  .14530342E+08
  .24942187E+06
  .10630322E+07
  .51532050E+06
  .48127390E-07
  .14129728E+05
  .77732244E-08
  .11407816E+07
  .27979905E-07
  .55736312E+08
  .33277304E+08
  .33090536E+08
  .77711940E-07
  .14707738E+06
  .16473262E-06
  .23187792E+08
  .70744070E-07
  .21190264E+08
  .18513260E-07
```

Figure H-1. OPTIC Printout
(d) Case IB2.

```
OPTIC OUTPUT
 19  LINES OF HEADER INFORMATION
CREATION DATE    227  1977          TIME      10    48   38
N(PARTICLE)=  1.0300    .0000 N(MEDIUM)=  1.3300
FREE SPACE WAVELENGTH=  .4880E-06     ANGLE BETWEEN BEAMS= .3000E-01
RANGE TO BEAM CROSS OVER= .3000E+01    1/E**2 BEAM RADIUS= .3750E-02
LOWER CUTOFF SIZE=  .1000E-05       UPPER CUTOFF SIZE=  .2000E-04
OFF AXIS VIEWING ANG= .1800E-01  TRANSMISSION EFFICIENCY=  .5000E+00
ELLIP BEAM EXPANS FACTOR=  .1000E+01   RECEIVER COLLECTION AREA= .1600E-01
ATTENUATION COEFF=1.0000E-01    LASER POWER=  .1000E+01
CATHODE QUANTUM EFFIC.=  .2000E+00       BRAGG CELL OFFSET FREQ=  .0000E+00
B COEFF  IN NEG. POWER LAW DIST.=  .3650E+01   # OF FACTORS GENERATED= 1000
VELOCITY=1.0000E+01     TOTAL # OF PARTICLES=  .2000E+10
FREQ(FRINGE)=     .81759237E+06    SIGNAL PERIOD(FRINGE)=     .12231035E-05
MODE=1 (1=FRINGE 2=REF.BEAM)      MIE LOOP LIMIT=  200
BURST SEPARATION=     .25773097E-04     BURST RATE=      .38800148E+05
1/E**2 BURST WIDTH= .1869E-04     BANDWIDTH= .5351E+05
GAIN CONSTANT(INCLUDES EXP(-2CR))= .3557E+05 EXP(-2CR)= .5488E+00
P*G= .3557E+05    # OF PARTICLES IN 1/E**2 VOLUME= .7251E+00
# OF FRINGES=     .15280024E+02
T=     .25773097E-01     DT=    .70641694E-07
  1.00000000E+03    .10000000E+01
   .90601891E+05
   .55308887E+06
   .64702484E+05
   .20617690E+07
   .46580094E+06
   .96320828E+05
   .61010225E+06
   .47730635E+07
   .36271134E+06
   .37123306E+06
   .85111162E+06
   .30147260E+07
   .22553030E+07
   .37708820E+07
   .35571050E+06
   .57706600E+06
   .16653575E+05
   .15757875E+07
   .10110662E+06
   .63754400E+06
   .38662512E+06
   .61150200E+06
   .11394150E+07
   .13173144E+06
   .20625712E+06
   .70240734E+07
   .43771100E+06
   .15021410E+07
   .23511106E+06
   .15507493E+07
   .35755606E+06
   .26317323E+06
   .14208303E+05
   .52007016E+05
   .48007109E+05
   .71237762E+06
   .32778450E+06
   .45558712E+06
   .28415287E+06
```

Figure H-1. OPTIC Printout
(e) Case IIA1.

```
OPTIC OUTPUT
 19  LINES OF HEADER INFORMATION
CREATION DATE    227  1977          TIME     10   30   43
N(PARTICLE)=  1.1500   .0000 N(MEDIUM)=  1.3300
FREE SPACE WAVELENGTH=  .4880E-06      ANGLE BETWEEN BEAMS= .3000E-01
RANGE TO BEAM CROSS OVER=  .3000E+01   1/E**2 BEAM RADIUS= .3750E-03
LOWER CUTOFF SIZE= .1000E-05         UPPER CUTOFF SIZE=  .2000E-04
OFF AXIS VIEWING ANG= .1600E-01  TRANSMISSION EFFICIENCY=  .5000E+00
ELLIP BEAM EXPANS FACTOR=  .1000E+01   RECEIVER COLLECTION AREA= .1600E-01
ATTENUATION COEFF=1.0000E-01    LASER POWER=  .1000E+01
CATHODE QUANTUM EFFIC.= .2000E+00        BRAGG CELL OFFSET FREQ= .0000E+00
S COEFF. IN NEG. POWER LAW DIST.= .3650E+01  # OF FACTORS GENERATED= 1000
VELOCITY=1.0000E+01    TOTAL # OF PARTICLES=  .3000E+10
FREQ(FRINGE)=   .81759237E+06    SIGNAL PERIOD(FRINGE)=    .12231035E-05
MODE=1 (1=FRINGE,2=REF.BEAM)      MIE LOOP LIMIT=  200
BURST SEPARATION=    .25773097E-04    BURST RATE=    .38800148E+05
1/E**2 BURST WIDTH= .1869E-04    BANDWIDTH=  .5351E+05
GAIN CONSTANT(INCLUDES EXP(-2CR))= .3357E+05 EXP(-2CR)= .5488E+00
P*G= .3357E+05   # OF PARTICLES IN 1/E**2 VOLUME= .7251E+00
# OF FRINGES=    .15280034E+02
T=    .25773097E-01     DT=    .70641804E-07
 1.00000000E+03    .10000000E+01
   .41325675E+07
   .21050880E+08
   .34090696E+08
   .26094794E+09
   .55842272E+08
   .86255940E+07
   .17432598E+09
   .77275850E+07
   .10758306E+08
   .69953600E+06
   .34879392E+08
   .21993853E+09
   .27909934E+10
   .32361583E+11
   .17910448E+09
   .17453332E+08
   .23413420E+08
   .12714938E+09
   .36476824E+09
   .81720550E+07
   .75380944E+08
   .49969700E+07
   .34053950E+07
   .27122300E+07
   .23770532E+09
   .12759362E+09
   .17553836E+09
   .20841237E+09
   .14726304E+08
   .15336006E+09
   .16587153E+09
   .16471362E+09
   .46901128E+08
   .77409360E+09
   .34423368E+09
   .12205164E+09
   .37233816E+08
   .11127798E+09
   .37448980E+07
```

Figure H-1. OPTIC Printout
(f) Case IIA2.

```
OPTIC OUTPUT
 19  LINES OF HEADER INFORMATION
CREATION DATE    227  1977          TIME       10   32   49
N(PARTICLE)=  1.0300    .0000 N(MEDIUM)=  1.3300
FREE SPACE WAVELENGTH= .4880E-06     ANGLE BETWEEN BEAMS= .3000E-01
RANGE TO BEAM CROSS OVER= .3000E+01    1/E**2 BEAM RADIUS= .3750E-02
LOWER CUTOFF SIZE= .1000E-05        UPPER CUTOFF SIZE= .2000E-04
OFF AXIS VIEWING ANG= .1800E-01  TRANSMISSION EFFICIENCY= .5000E+00
ELLIP BEAM EXPANS FACTOR= .1000E+01    RECEIVER COLLECTION AREA= .1600E-01
ATTENUATION COEFF=1.0000E-01    LASER POWER= .1000E+01
CATHODE QUANTUM EFFIC.= .2000E+00        BRAGG CELL OFFSET FREQ= .0000E+00
B COEFF  IN NEG. POWER LAW DIST.= .3650E+01  # OF FACTORS GENERATED= 1000
VELOCITY=1.0000E+01     TOTAL # OF PARTICLES= .2000E+11
FREQ(FRINGE)=    .81759237E+06     SIGNAL PERIOD(FRINGE)=    .1223103 3E-05
MODE=1 (1=FRINGE 2=REF.BEAM)      MIE LOOP LIMIT=  200
BURST SEPARATION=    .25773097E-05     BURST RATE=    .38800150E+06
1/E**2 BURST WIDTH= .1869E-04     BANDWIDTH= .5351E+05
GAIN CONSTANT(INCLUDES EXP(-2CR))= .3557E+05 EXP(-2CR)= .5488E+00
P*G= .3557E+05   # OF PARTICLES IN 1/E**2 VOLUME= .7251E+01
# OF FRINGES=    .15280024E+02
T=     .25773095E-02      DT=    .70641504E-07
 1.00000000E+03    .10000000E+01
  .90601891E+05
  .33309887E+06
  .84701484E+05
  .20617690E+07
  .46390094E+06
  .96320828E+07
  .61610225E+06
  .47770695E+05
  .36771184E+06
  .17133706E+06
  .83221162E+06
  .10157260E+07
  .26573030E+07
  .97509920E+07
  .35671050E+06
  .57326600E+06
  .18683375E+07
  .33737375E+07
  .10439052E+06
  .33764400E+06
  .38882612E+06
  .61762800E+06
  .11341500E+07
  .13133144E+06
  .20625712E+06
  .70343734E+07
  .45771100E+06
  .15021610E+07
  .23611068E+06
  .16807493E+07
  .33735606E+06
  .26317525E+06
  .14103503E+05
  .82007016E+05
  .46207109E+05
  .71337762E+06
  .31774450E+06
  .43802312E+06
  .23453287E+06
```

Figure H-1. OPTIC Printout
(g) Case IIB1.

```
OPTIC OUTPUT
 19  LINES OF HEADER INFORMATION
CREATION DATE:   227  1977          TIME:     10   54   31
N(PARTICLE)=  1.1500    .0000 N(MEDIUM)=  1.3300
FREE SPACE WAVELENGTH=  .4880E-06     ANGLE BETWEEN BEAMS= .3000E-01
RANGE TO BEAM CROSS OVER= .3000E+01   1/E**2 BEAM RADIUS= .3750E-02
LOWER CUTOFF SIZE= .1000E-05       UPPER CUTOFF SIZE= .2000E-04
OFF AXIS VIEWING ANG= .1800E-01  TRANSMISSION EFFICIENCY= .5000E+00
ELLIF BEAM EXPANS FACTOR= .1000E+01   RECEIVER COLLECTION AREA= .1600E-01
ATTENUATION COEFF=1.0000E-01     LASER POWER= .1000E+01
CATHODE QUANTUM EFFIC.=  .2000E+00         BRAGG CELL OFFSET FREQ= .0000E+00
B COEFF. IN NEG. POWER LAW DIST.= .3650E+01  # OF FACTORS GENERATED= 1000
VELOCITY=1.0000E+01    TOTAL # OF PARTICLES= .2000E+11
FREQ(FRINGE)=   .81759237E-06    SIGNAL PERIOD(FRINGE)=    .12231035E-05
MODE=1 (1=FRINGE,2=REF.BEAM)       MIE LOOP LIMIT=  200
BURST SEPARATION=    .25773037E-05     BURST RATE=    .38800150E-06
1/E**2 BURST WIDTH= .1569E-04     BANDWIDTH= .5351E+05
GAIN CONSTANT(INCLUDES EXP(-2CR))=  .3557E+05 EXP(-2CR)= .5488E+00
P*G= .3557E+05   # OF PARTICLES IN 1/E**2 VOLUME= .7251E+01
# OF FRINGES=     .15280024E+03
T=    .25773035E-02       DT=    .70641804E-07
 1.00000000E+03    .10000000E+01
   .41323673E+07
   .21050880E+06
   .34090696E+08
   .26094734E+09
   .35842272E+08
   .86255940E+07
   .17432398E+09
   .75275850E+07
   .10758506E+06
   .83535000E+06
   .34873392E+08
   .21993653E+09
   .37409934E+10
   .32351563E+11
   .79104443E+07
   .17433352E+08
   .33434302E+09
   .13149338E+09
   .33479324E+08
   .82320350E+07
   .75380944E+08
   .43353700E+07
   .56033950E+07
   .27122200E+07
   .23370332E+08
   .12753362E+09
   .75578366E+09
   .60041293E+09
   .47263042E+08
   .19336006E+09
   .13367135E+09
   .15471382E+09
   .40501128E+08
   .77483360E+08
   .54223568E+09
   .12251184E+09
   .37233816E+08
   .  .52778E+09
   .37443980E+07
```

Figure H-1. OPTIC Printout
(h) Case IIB2.

peak photoelectron rate in Figures H-2(a) through H-2(h), and by the resulting signal simulations in Figures H-3(a) through H-3(h). The histograms and rms error obtained when the signals were applied to the simulated burst-counter with the Macrodyne bipolar test are illustrated by Figures H-4(a) through H-4(k). These are the result of using programs COUNT, COMP, HISTO and PLOT.

In three cases we ran COUNT and COMP for two different thresholds. The last three cases in Figure H-4 show that when the threshold is set high enough, low multiparticle errors result even in the multiparticle case.

The results indicate that in a practical system, an adaptive threshold will be required to obtain only the larger signals. The results also indicate that even with optimized optics, the n = 1.03+j0.0 particles provide only marginal signals for very high accuracy work. However, it is still probable that when larger particles in the 10-100 micrometer range are included, the results will be adequate. More than adequate signals will always result from the inorganic particles with index in the 1.15-1.20 range.

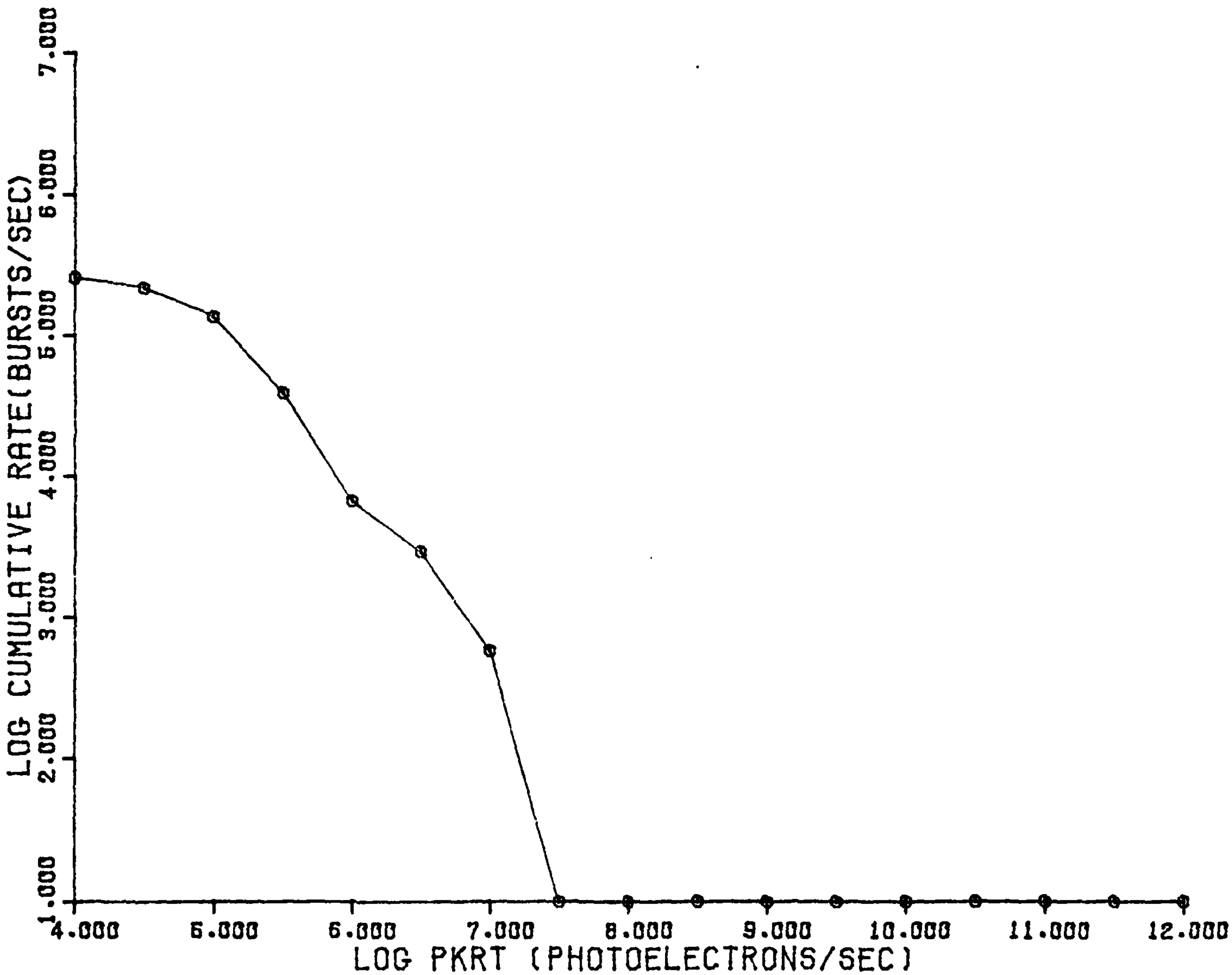

Figure H-2. Peak Rate Histogram
(a) Case IA1.

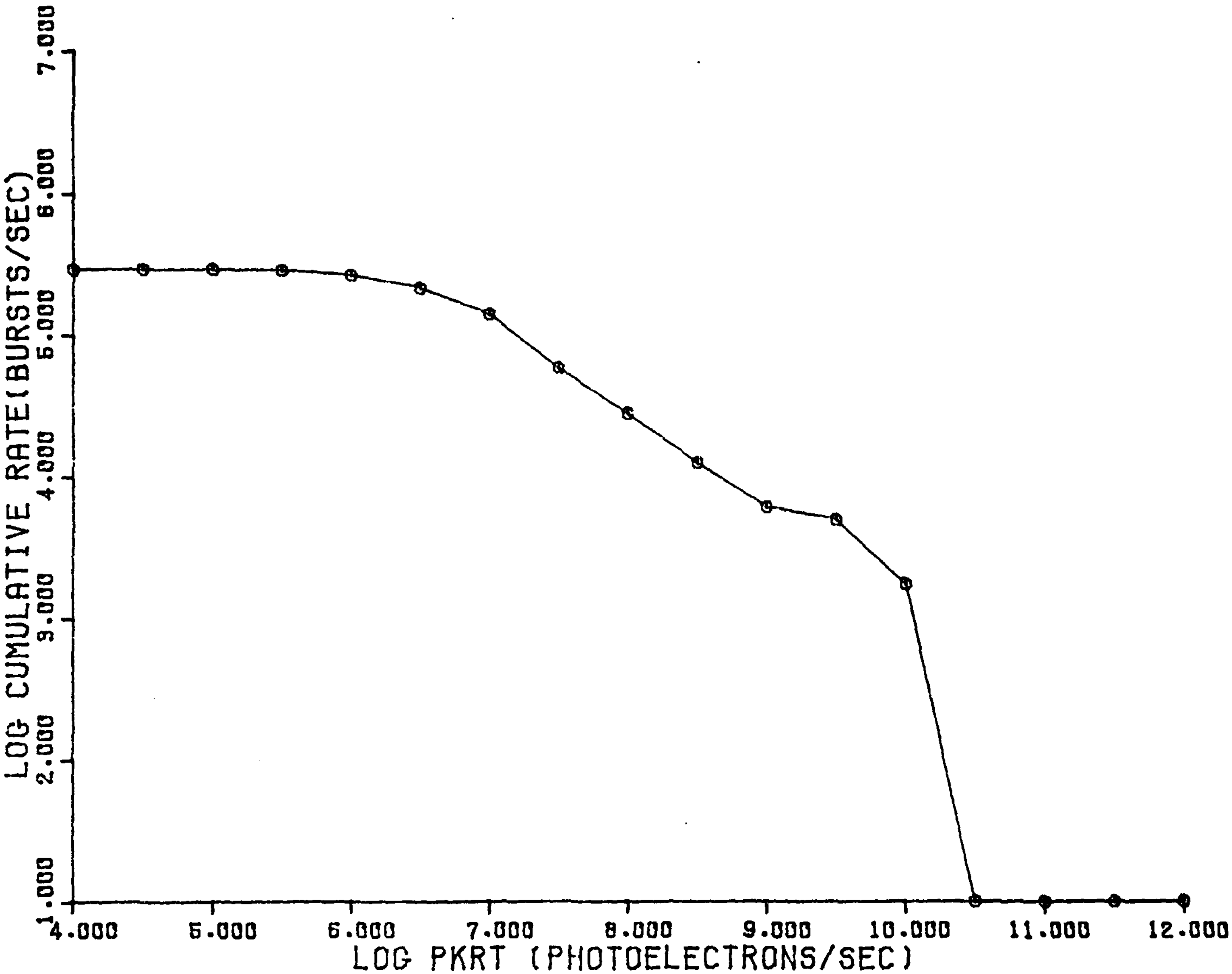

Figure H-2. Peak Rate Histogram (Cont'd)
(b) Case IA2.

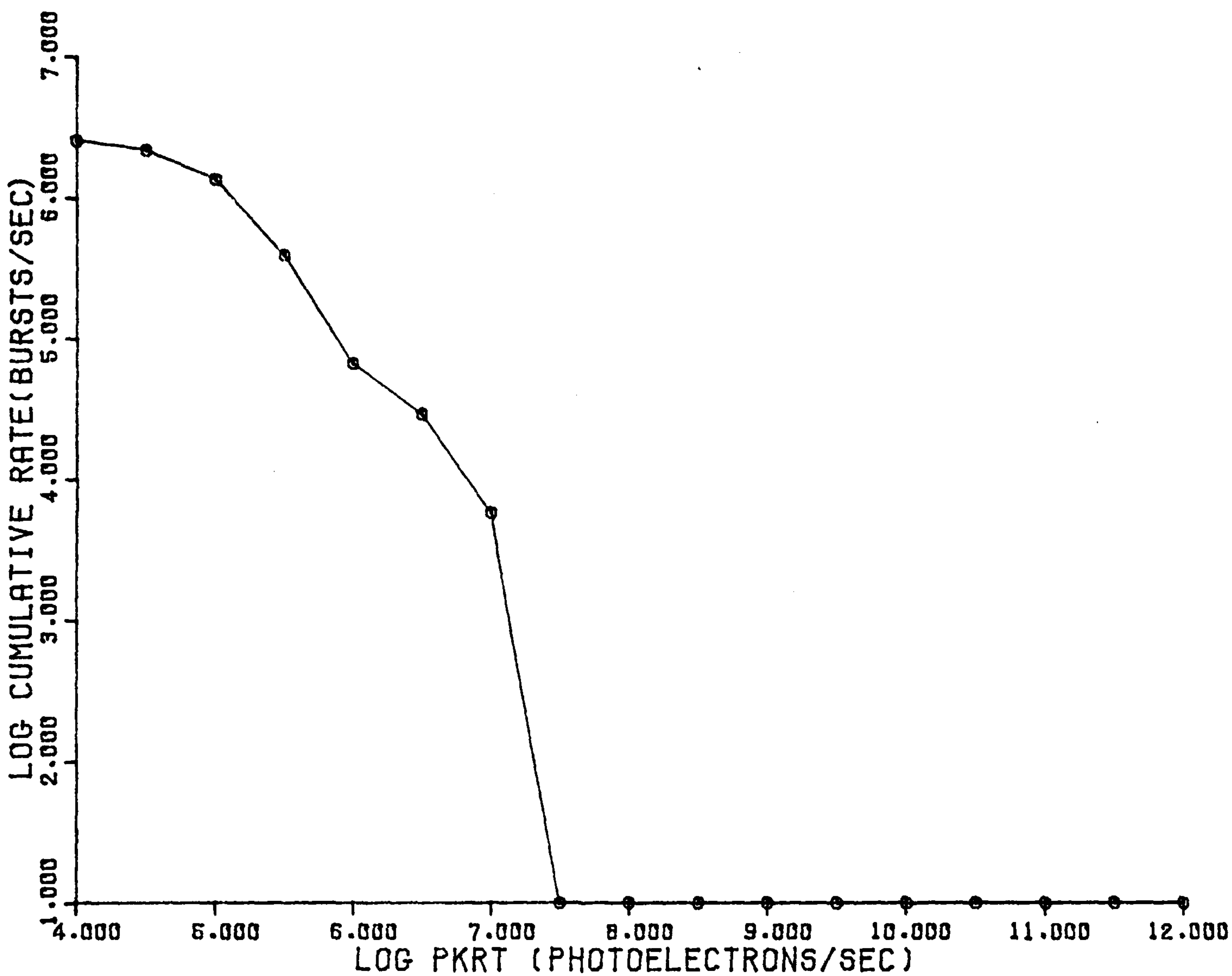

Figure H-2. Peak Rate Histogram (Cont'd)
(c) Case IB1.

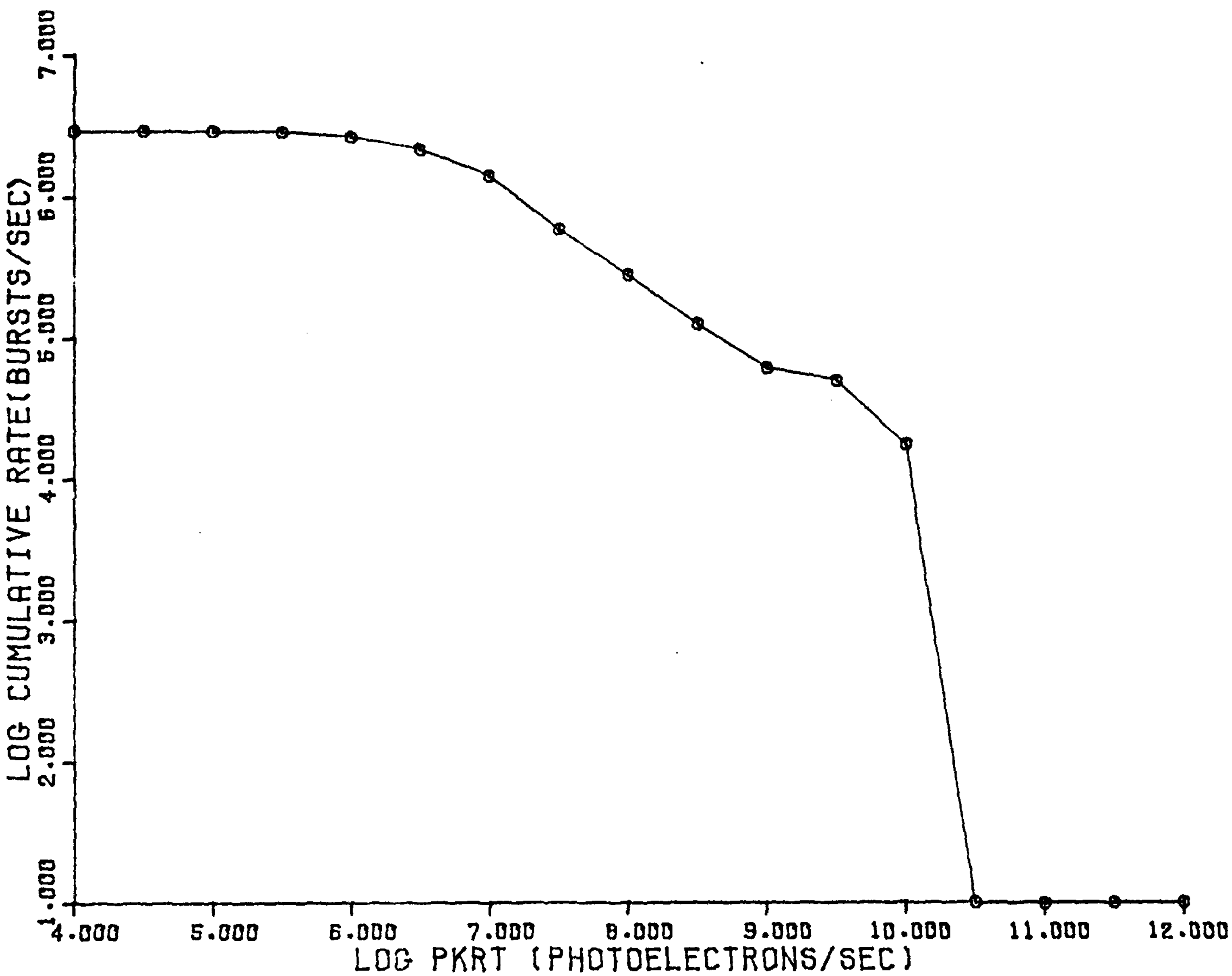

Figure H-2. Peak Rate Histogram (Cont'd)
(d) Case IB2.

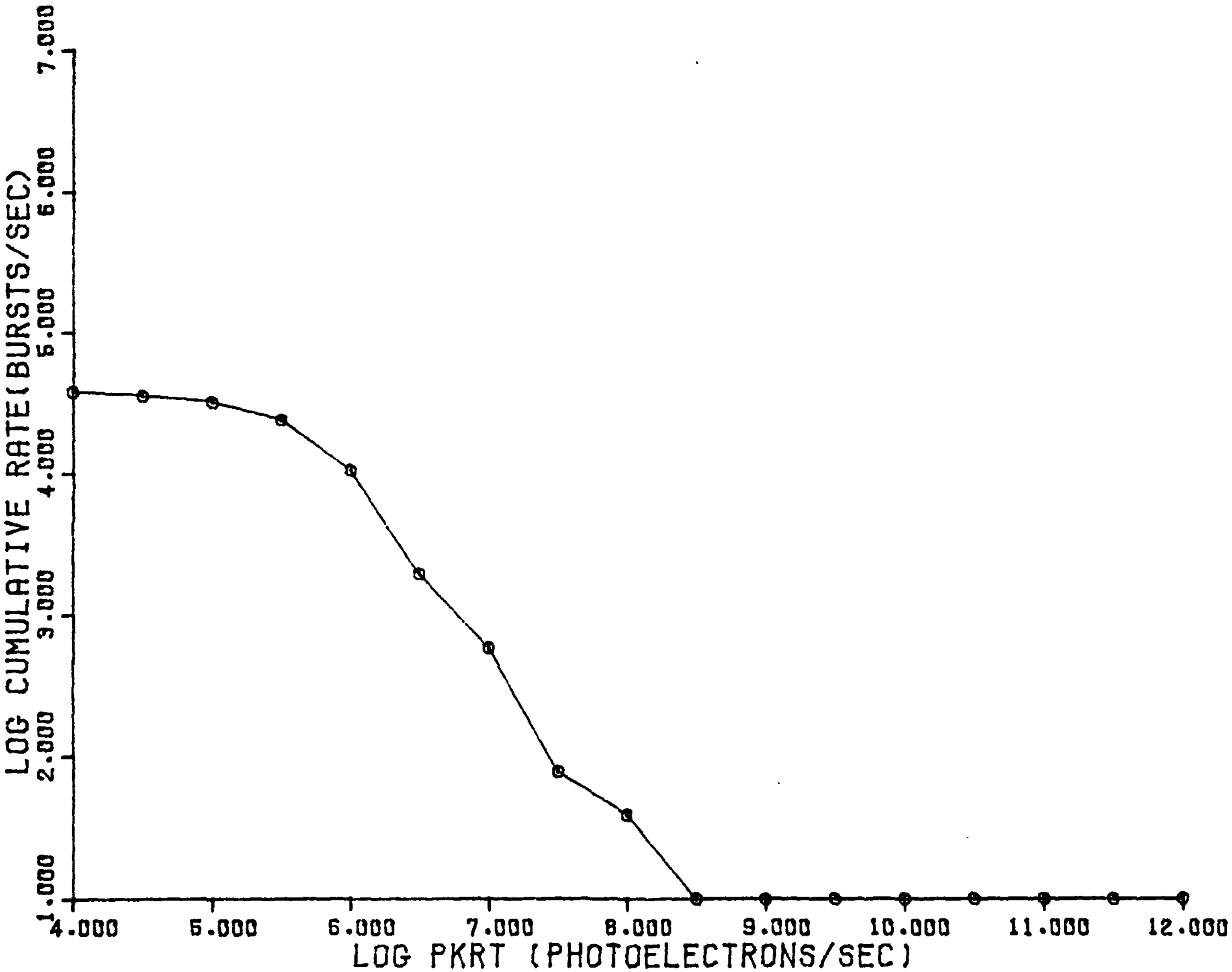

Figure H-2. Peak Rate Histogram (Cont'd)
(e) Case IIA1.

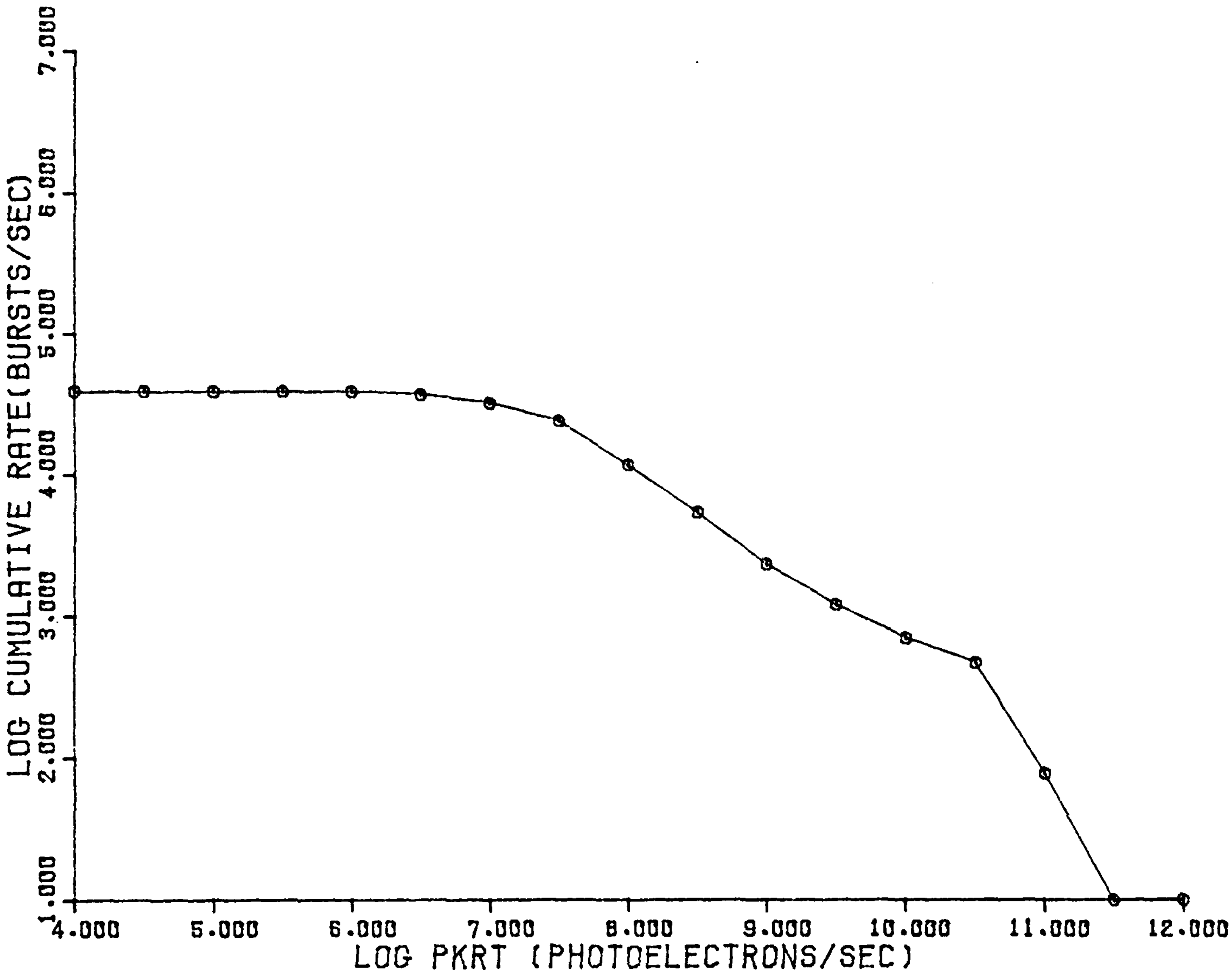

Figure H-2. Peak Rate Histogram (Cont'd)
(f) Case IIA2.

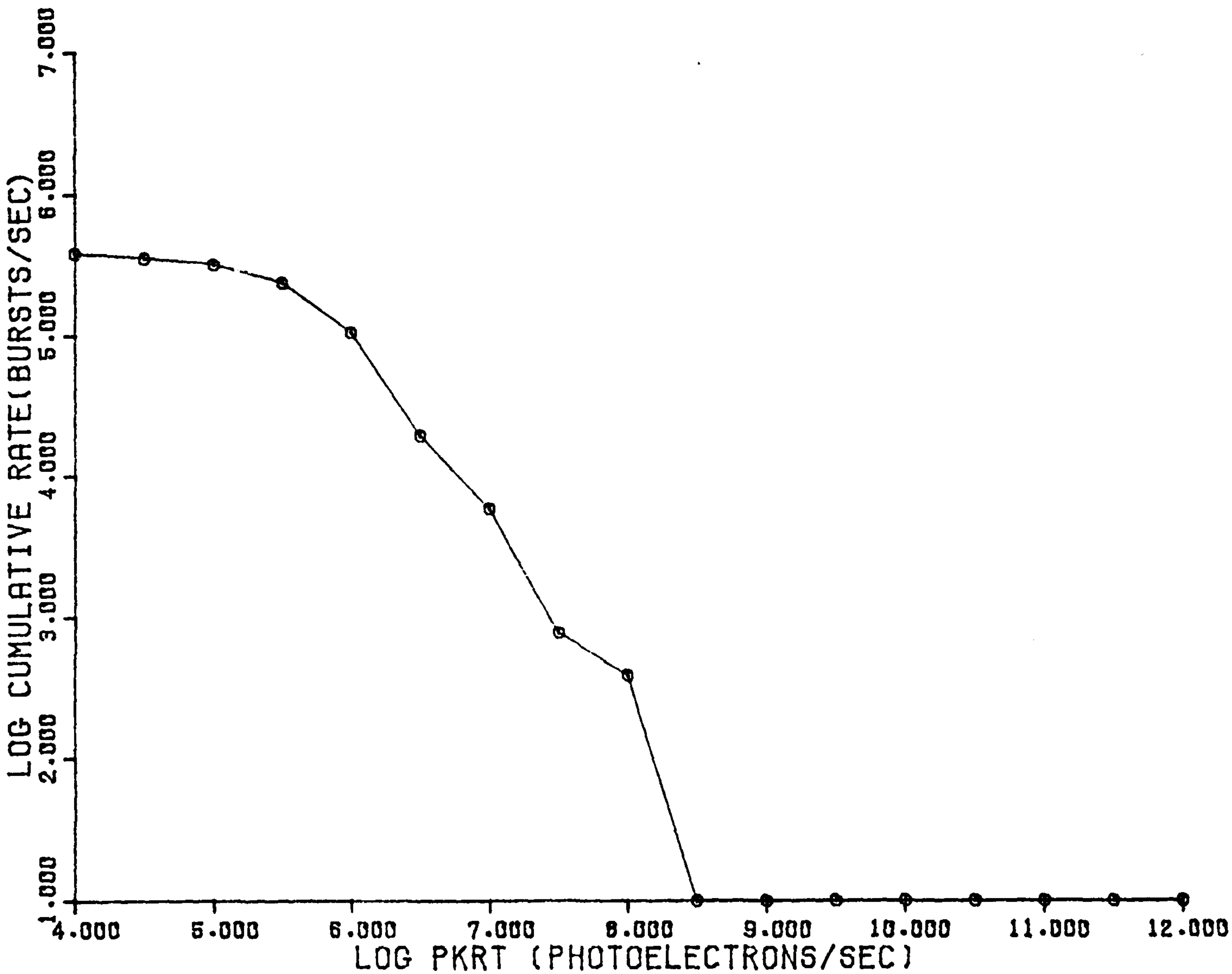

Figure H-2. Peak Rate Histogram (Cont'd)
(g) Case IIB1.

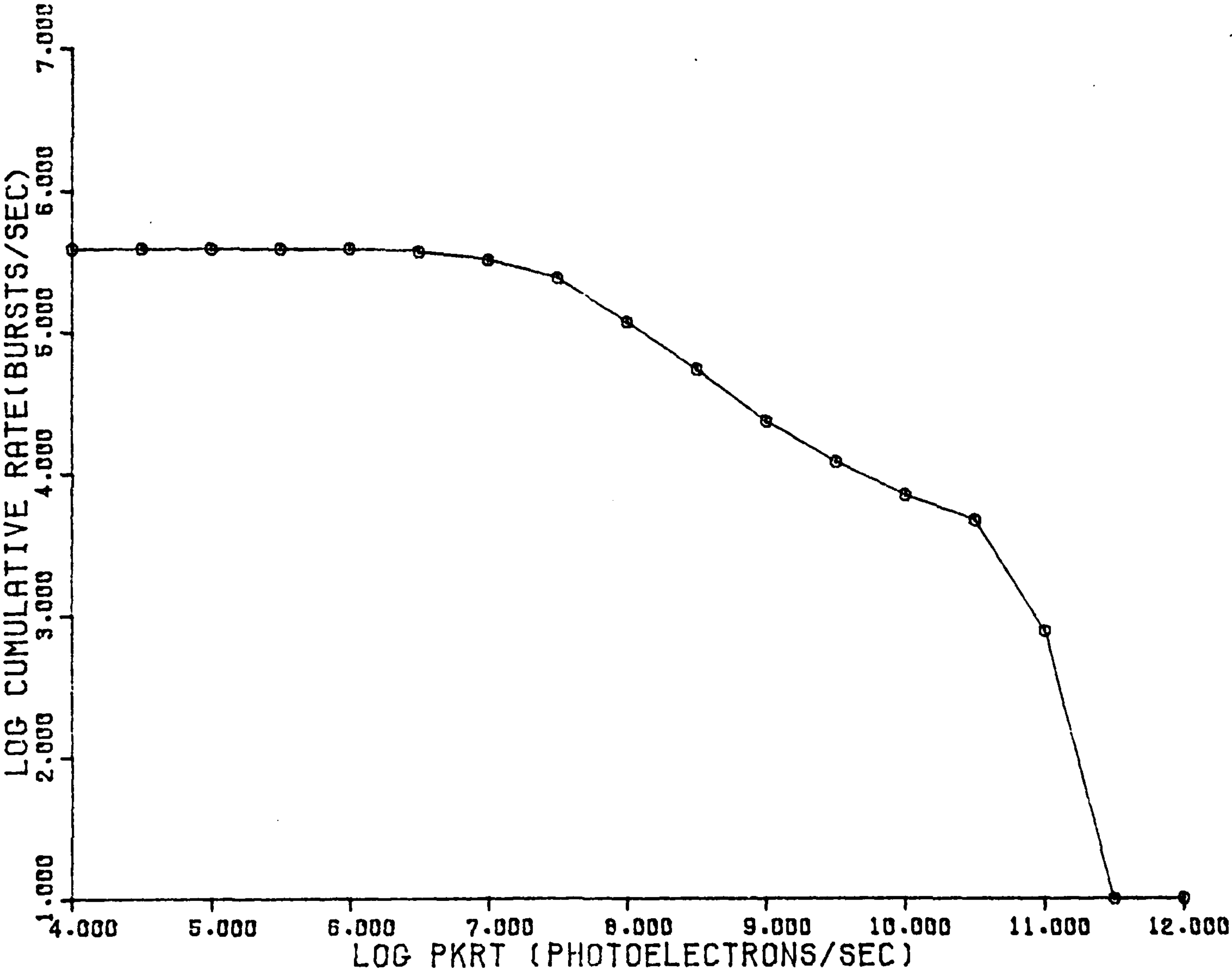

Figure H-2. Peak Rate Histogram (Cont'd)
(h) Case IIB2.

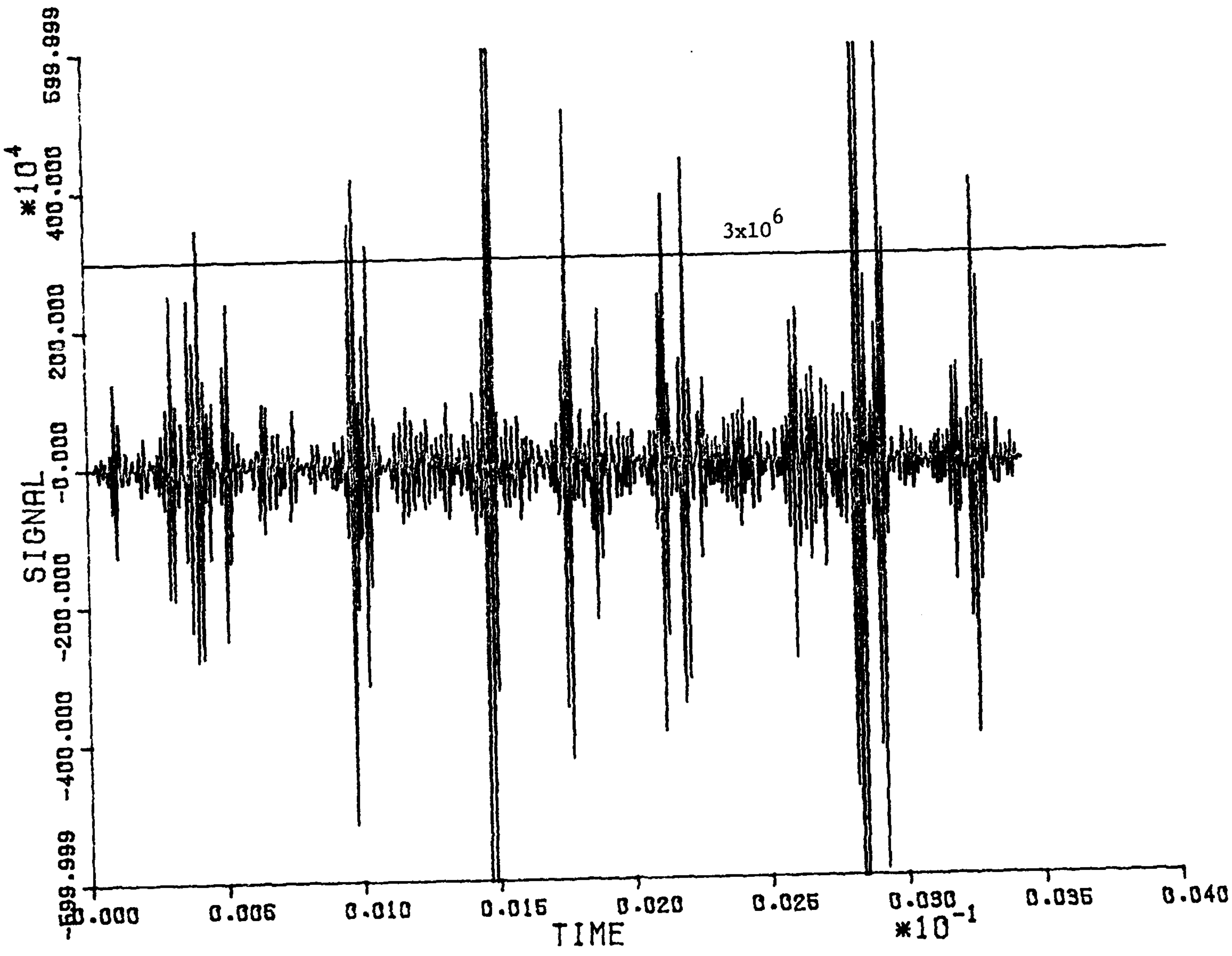

Figure H-3. SIGNAL Simulations
(a) Case IA1.

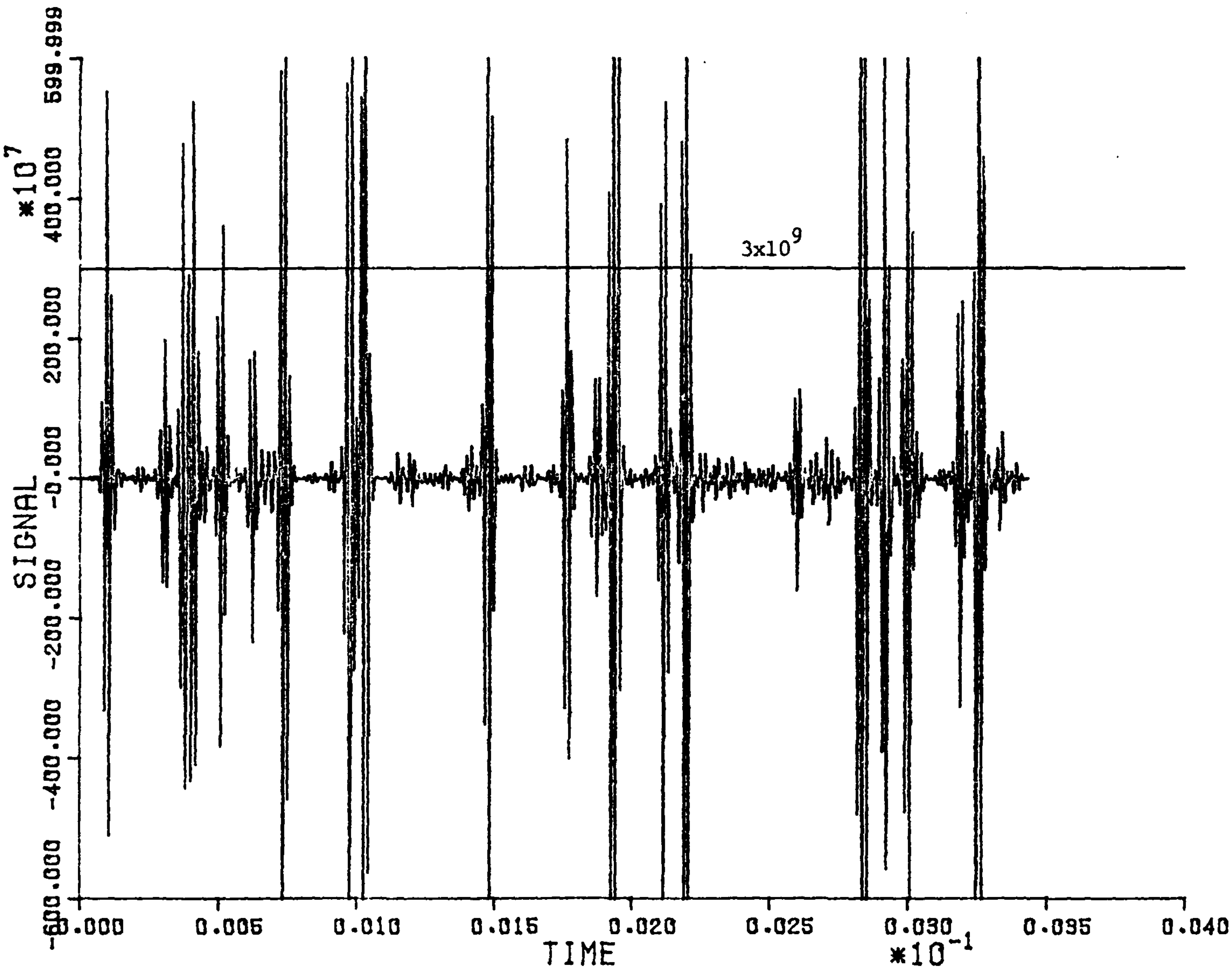

Figure H-3. SIGNAL Simulations (Cont'd)
(b) Case IA2.

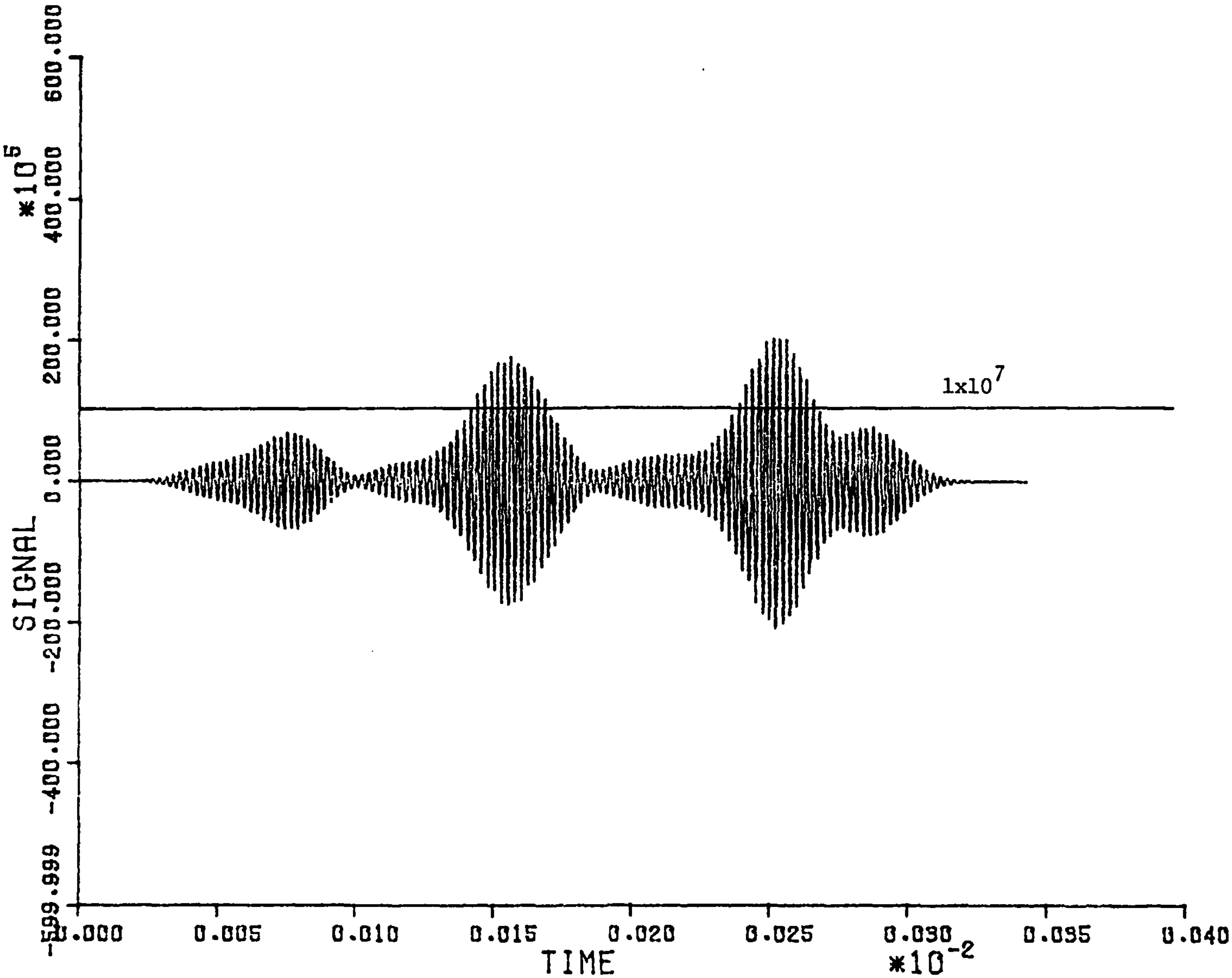

Figure H-3. SIGNAL Simulations (Cont'd)
(c) Case IB1.

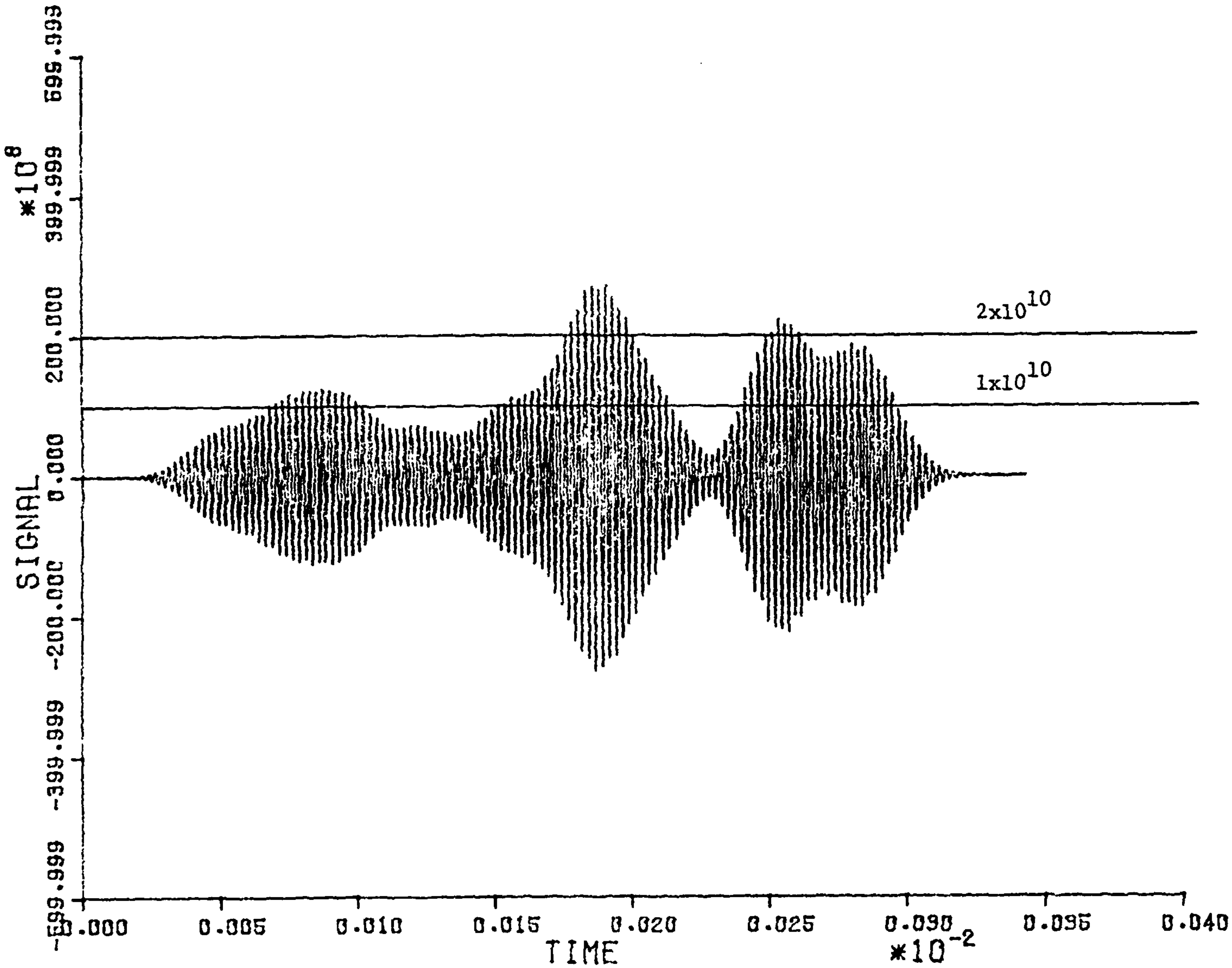

Figure H-3. SIGNAL Simulations (Cont'd)
(d) Case IB2.

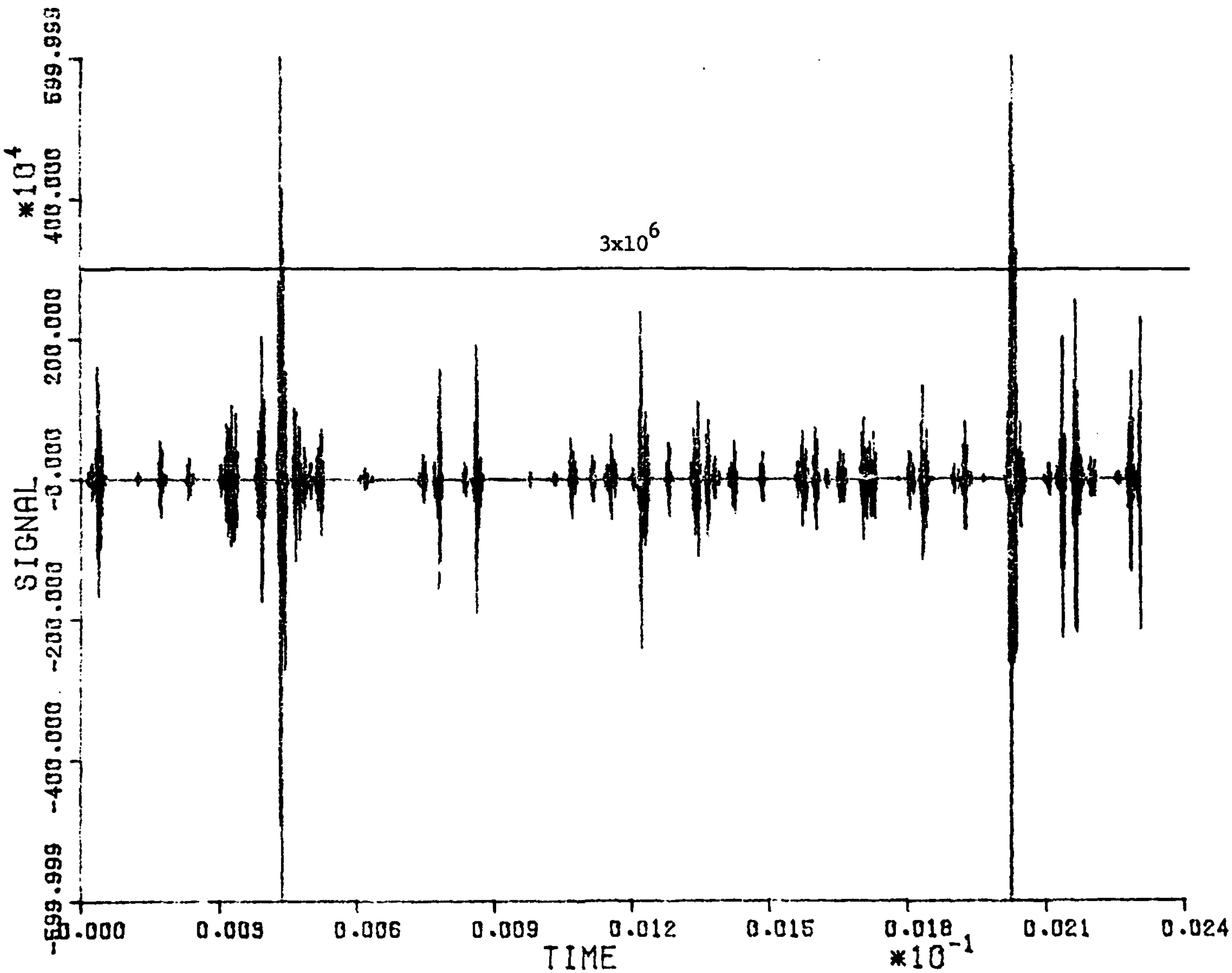

Figure H-3. SIGNAL Simulations (Cont'd)
(e) Case IIA1.

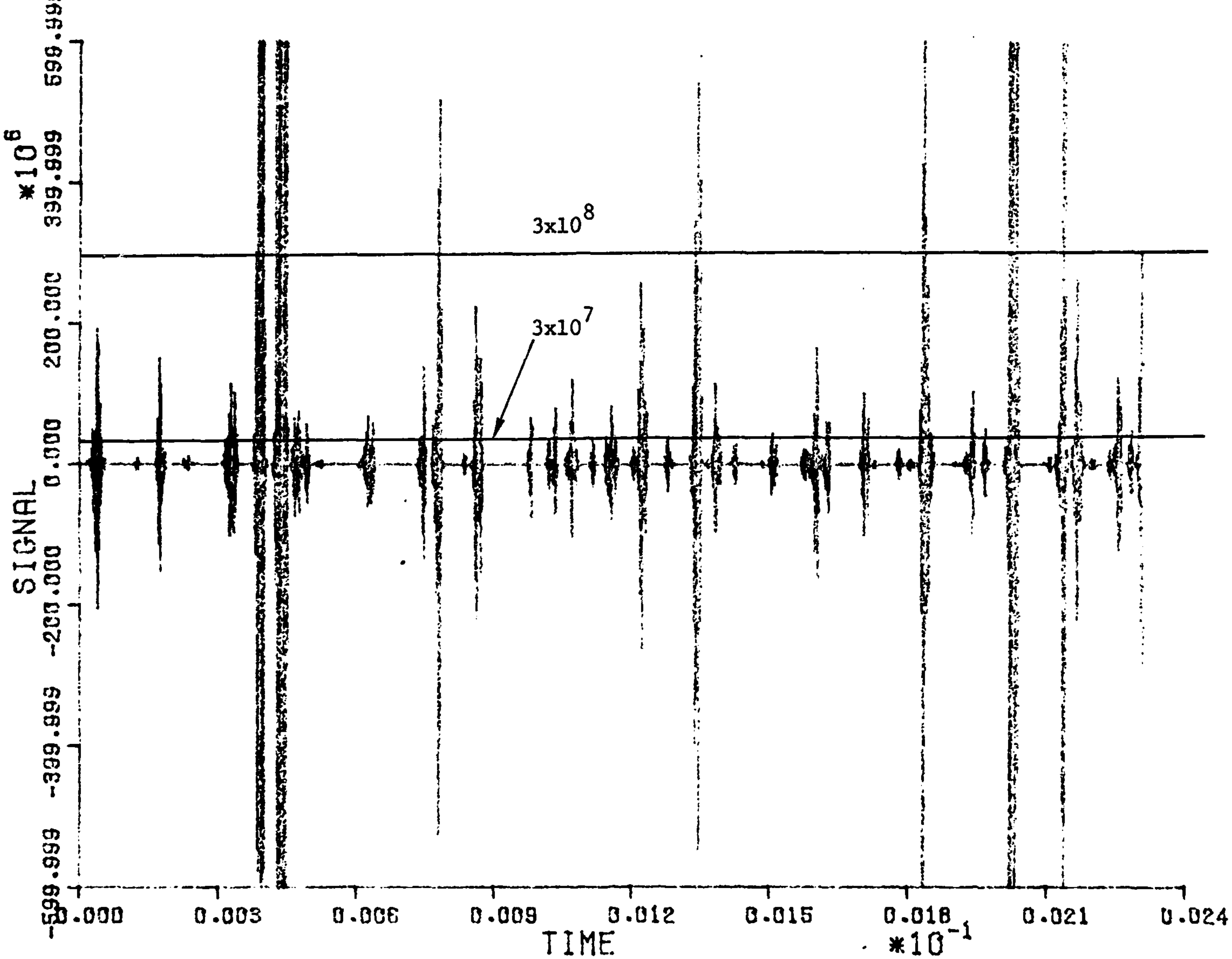

Figure H-3. SIGNAL Simulations (Cont'd)
(f) Case IIA2.

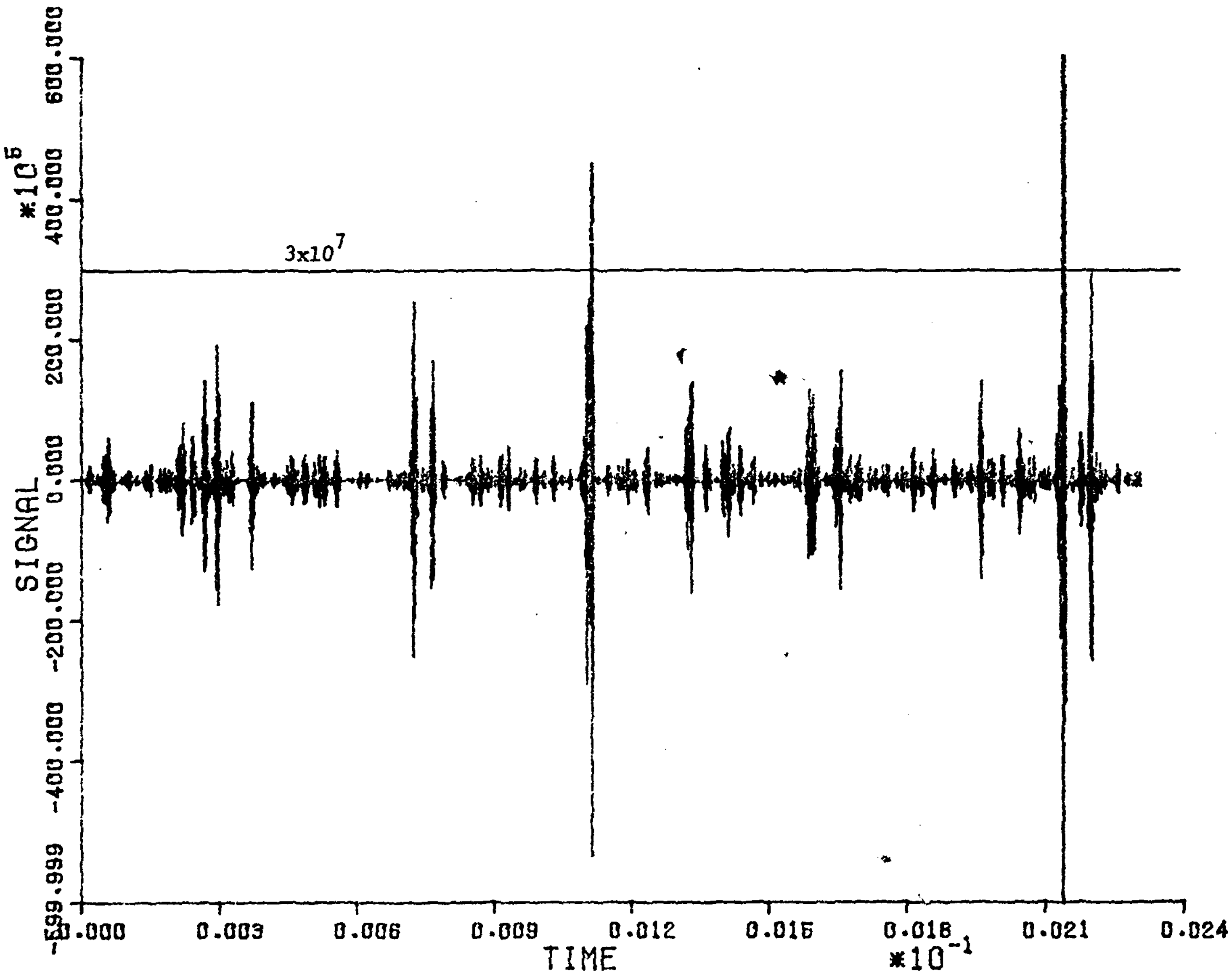

Figure H-3. SIGNAL Simulations (Cont'd)
(g) Case IIB1.

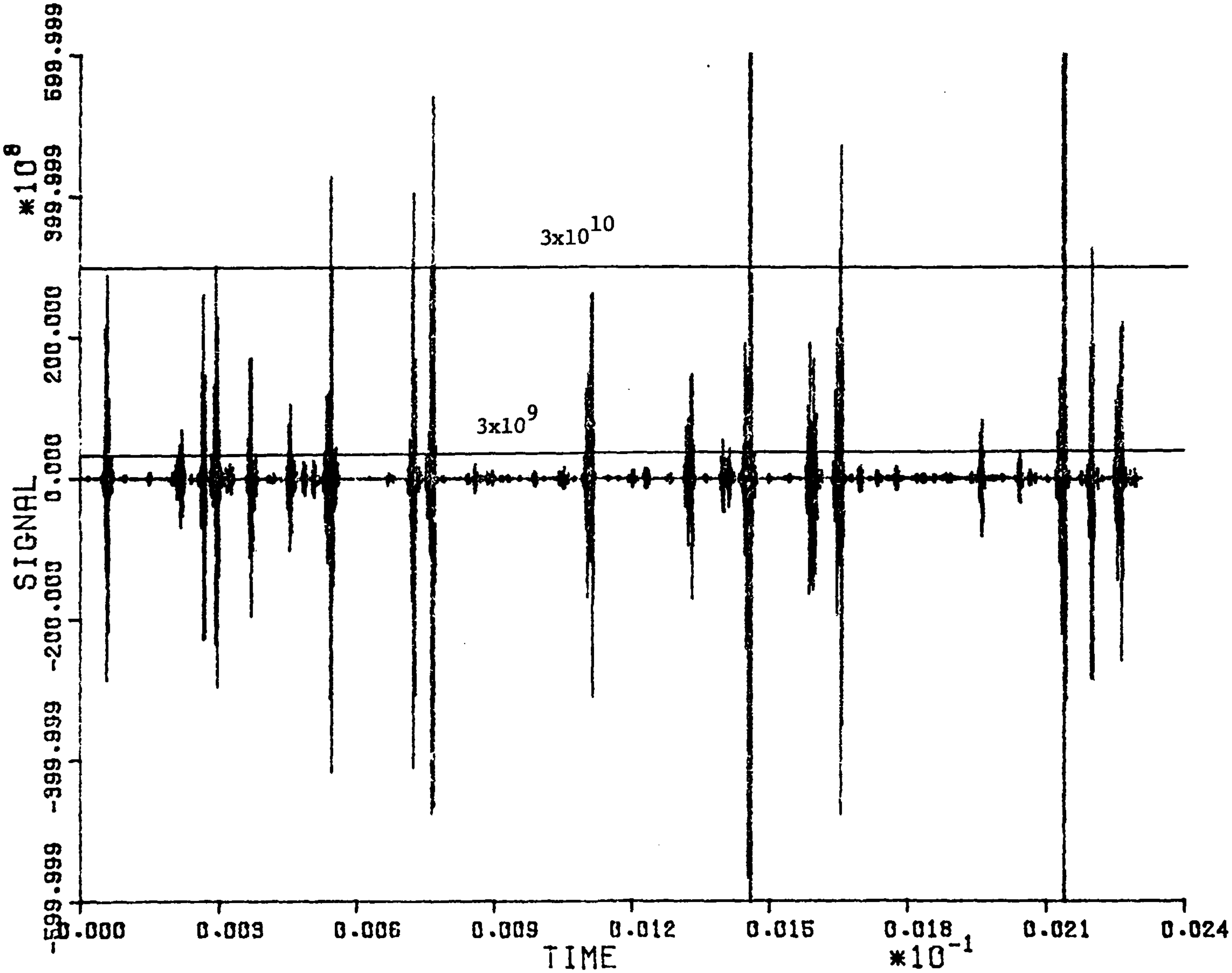

Figure H-3. SIGNAL Simulations (Cont'd)
(h) Case IIB2.

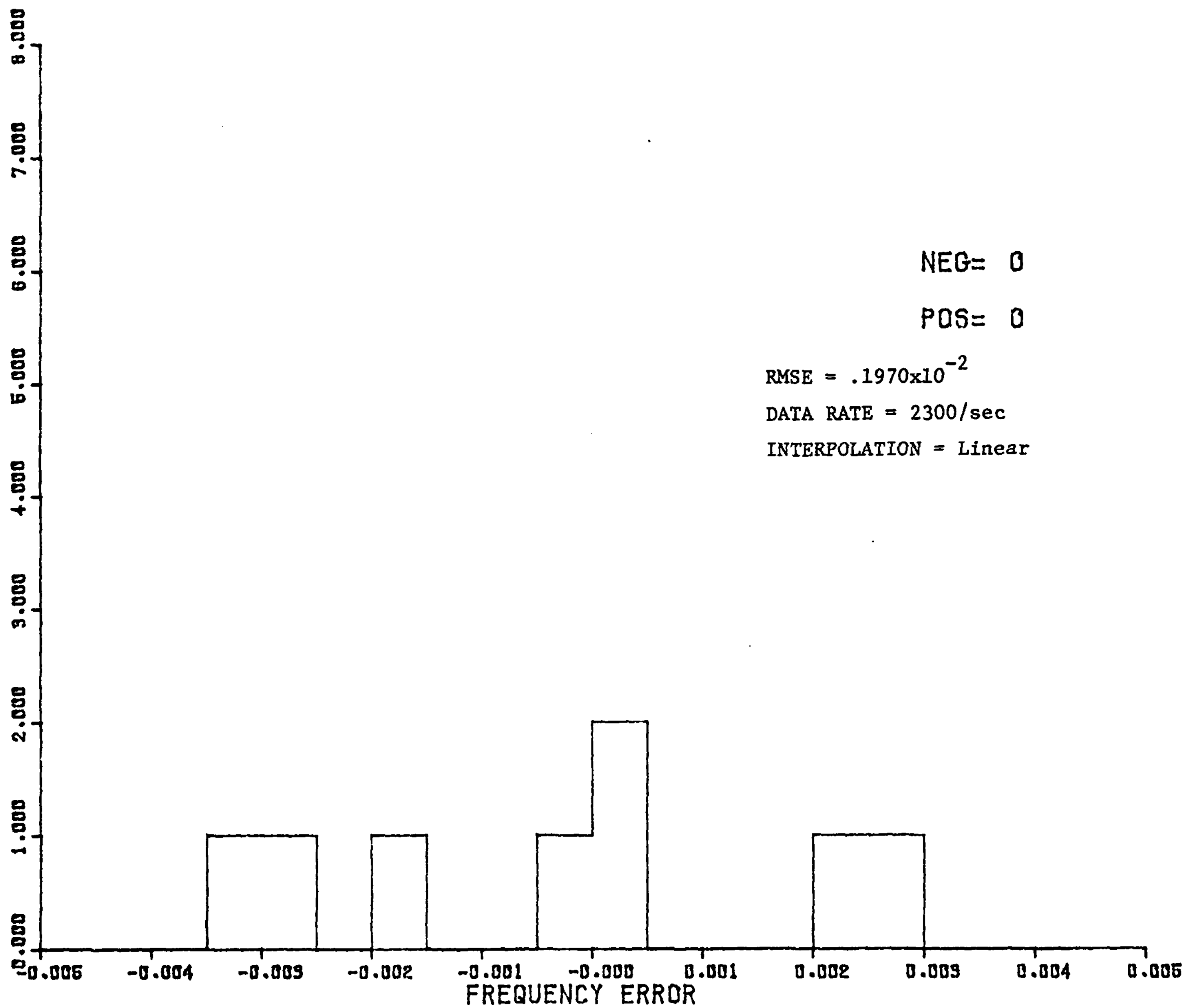

Figure H-4. Histograms of Error
(a) Case IA1.

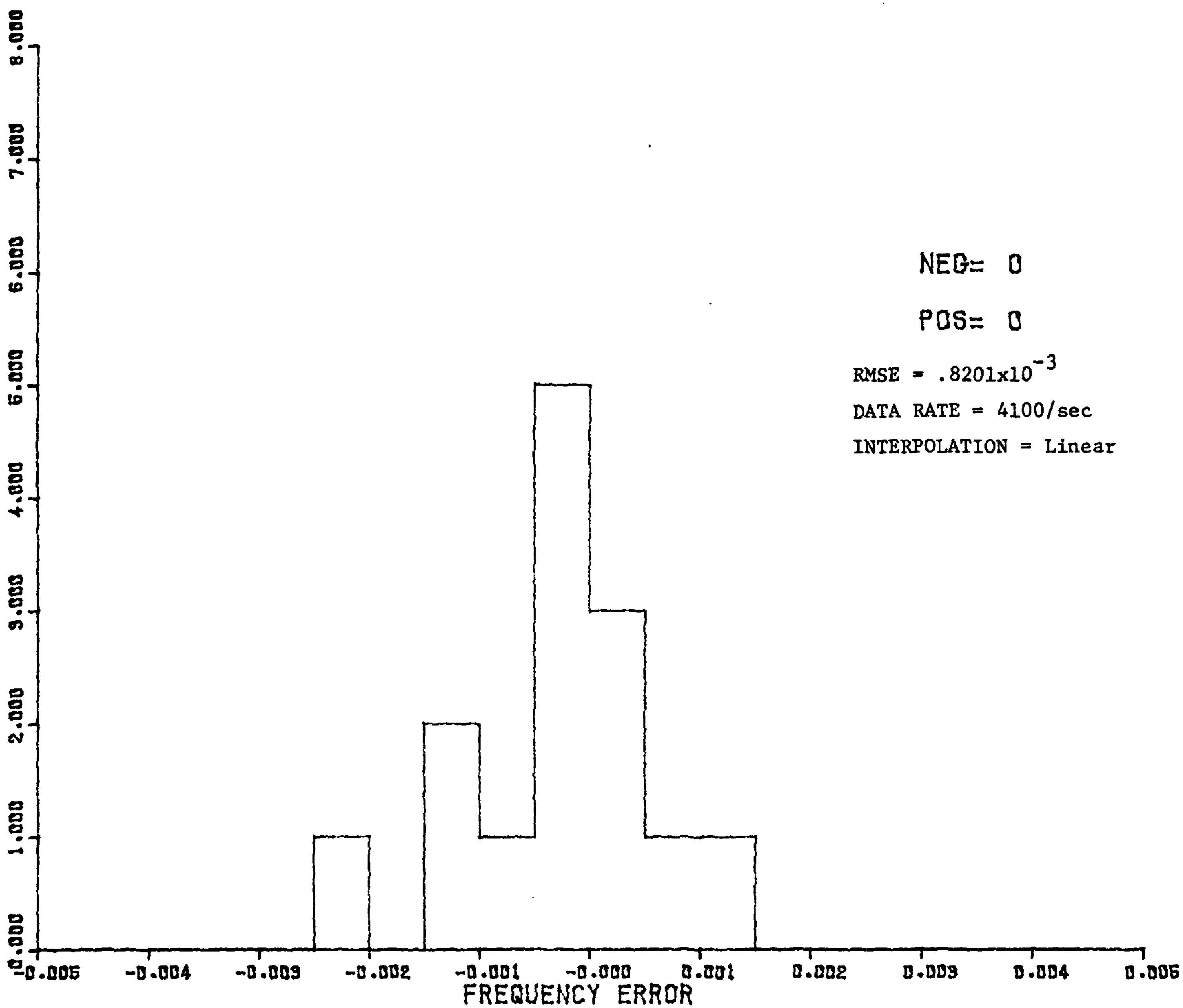

Figure H-4. Histograms of Error (Cont'd)
(b) Case IA2.

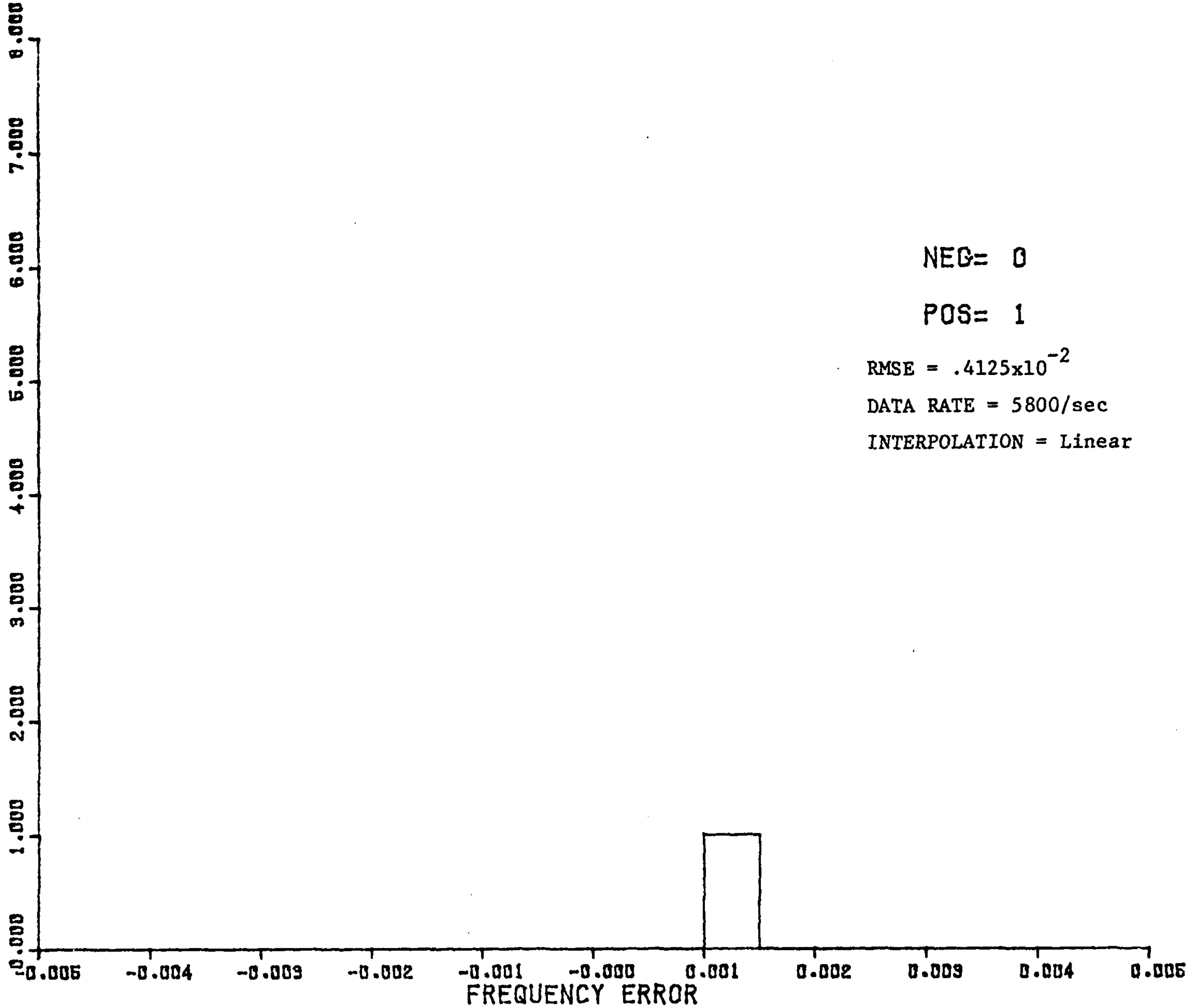

Figure H-4. Histograms of Error (Cont'd)
(c) Case IB1.

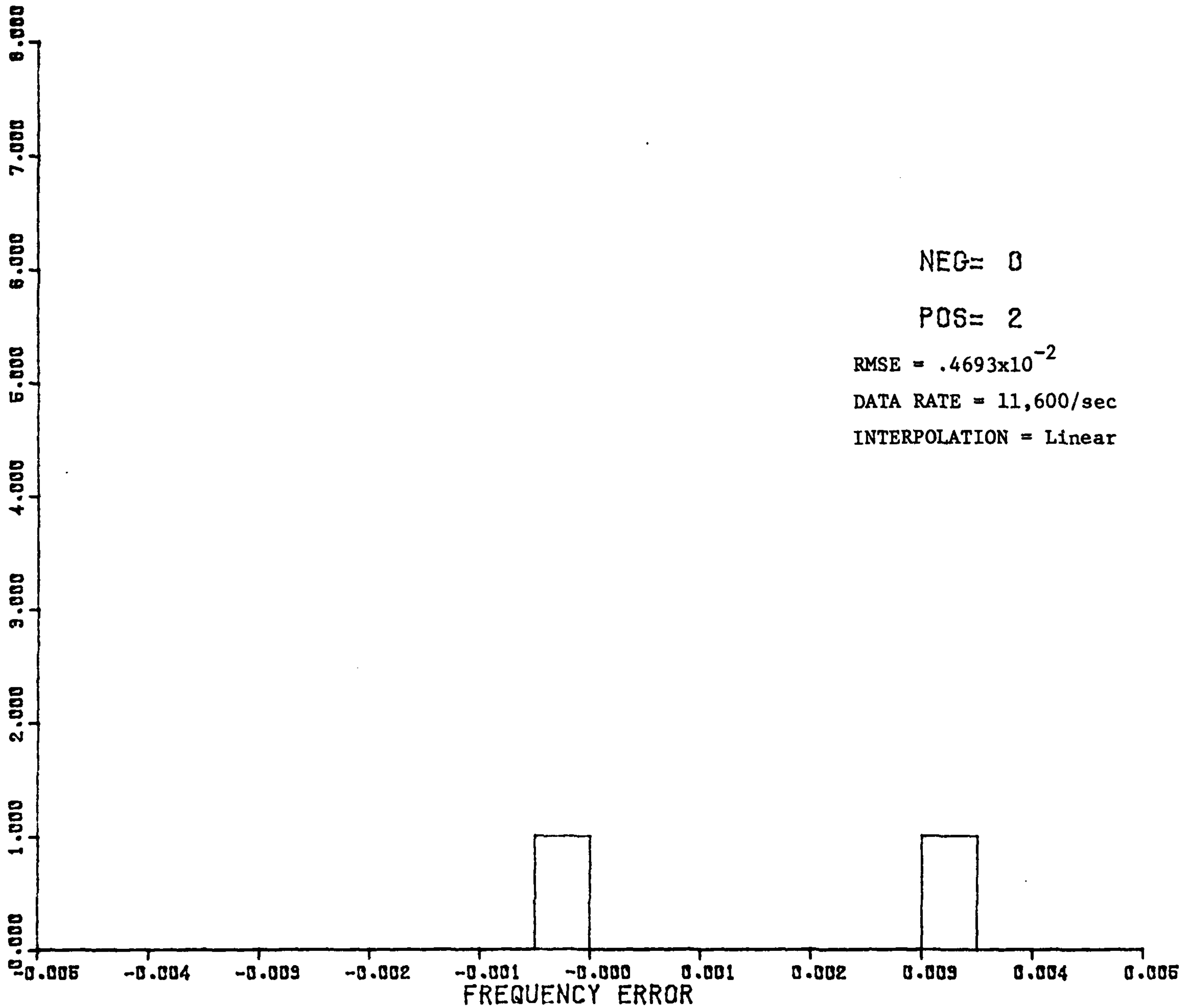

Figure H-4. Histograms of Error (Cont'd)
(d) Case IB2.

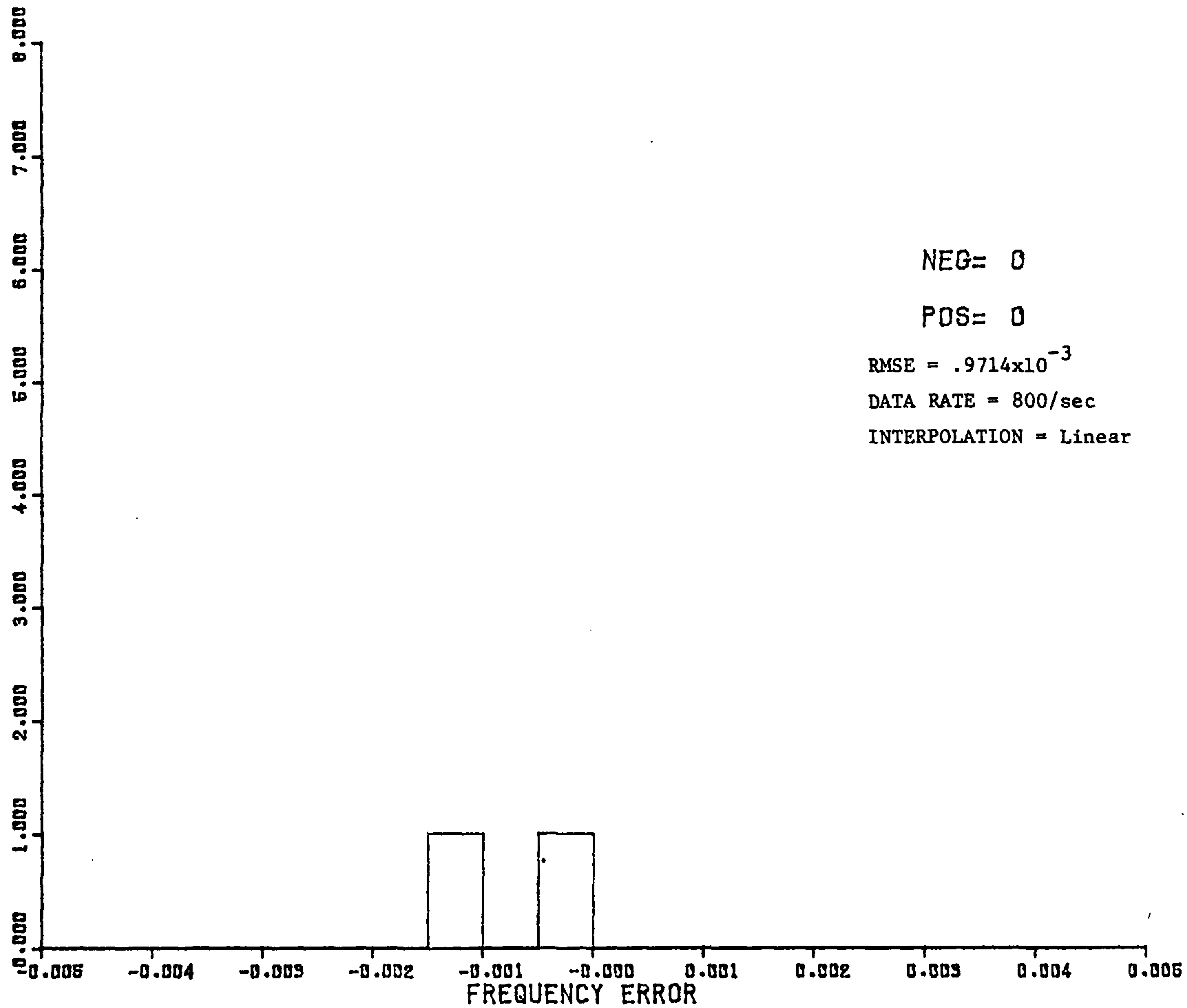

Figure H-4. Histograms of Error (Cont'd)
(e) Case IIA1.

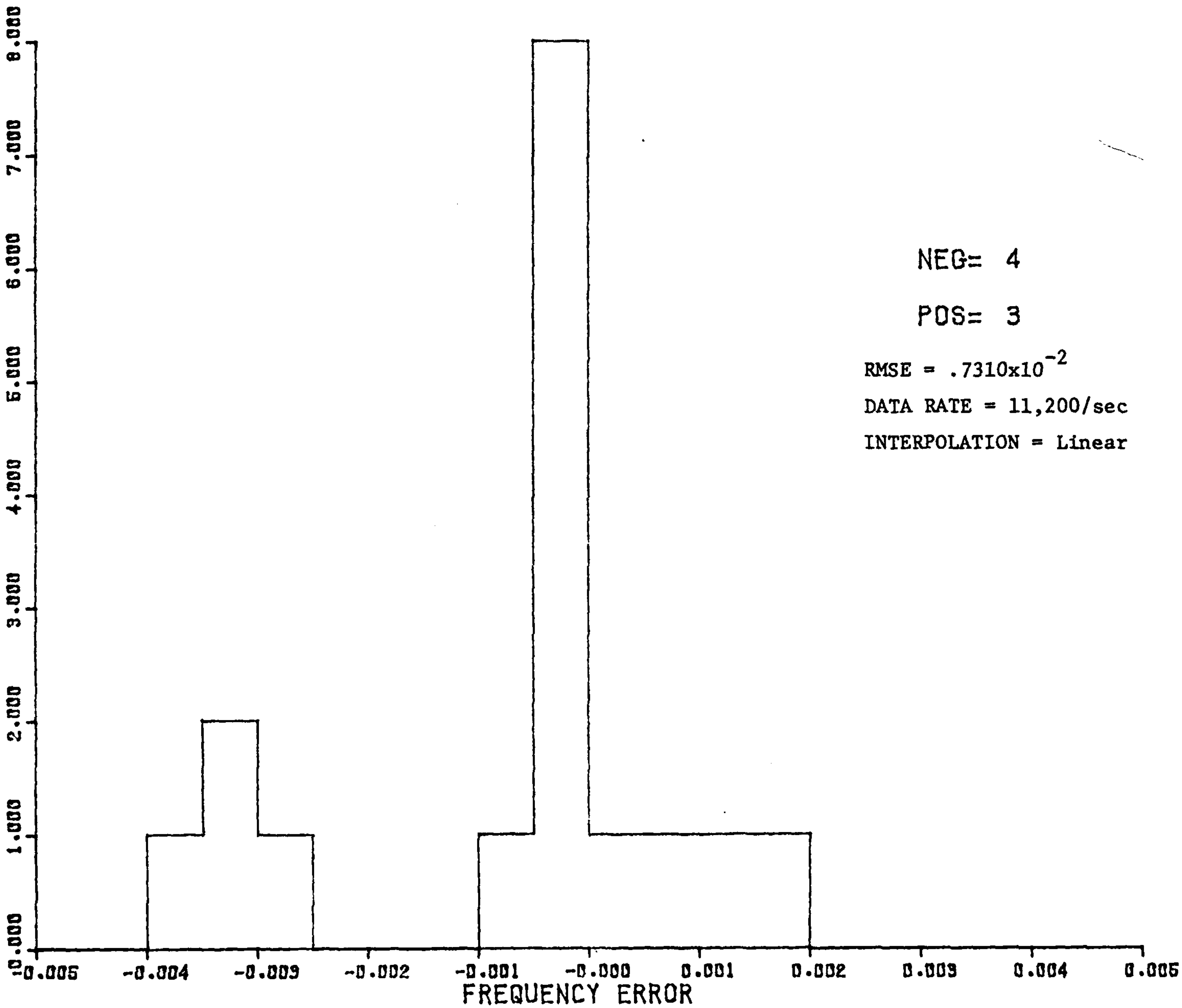

Figure H-4. Histograms of Error (Cont'd)
(f) Case IIA2.

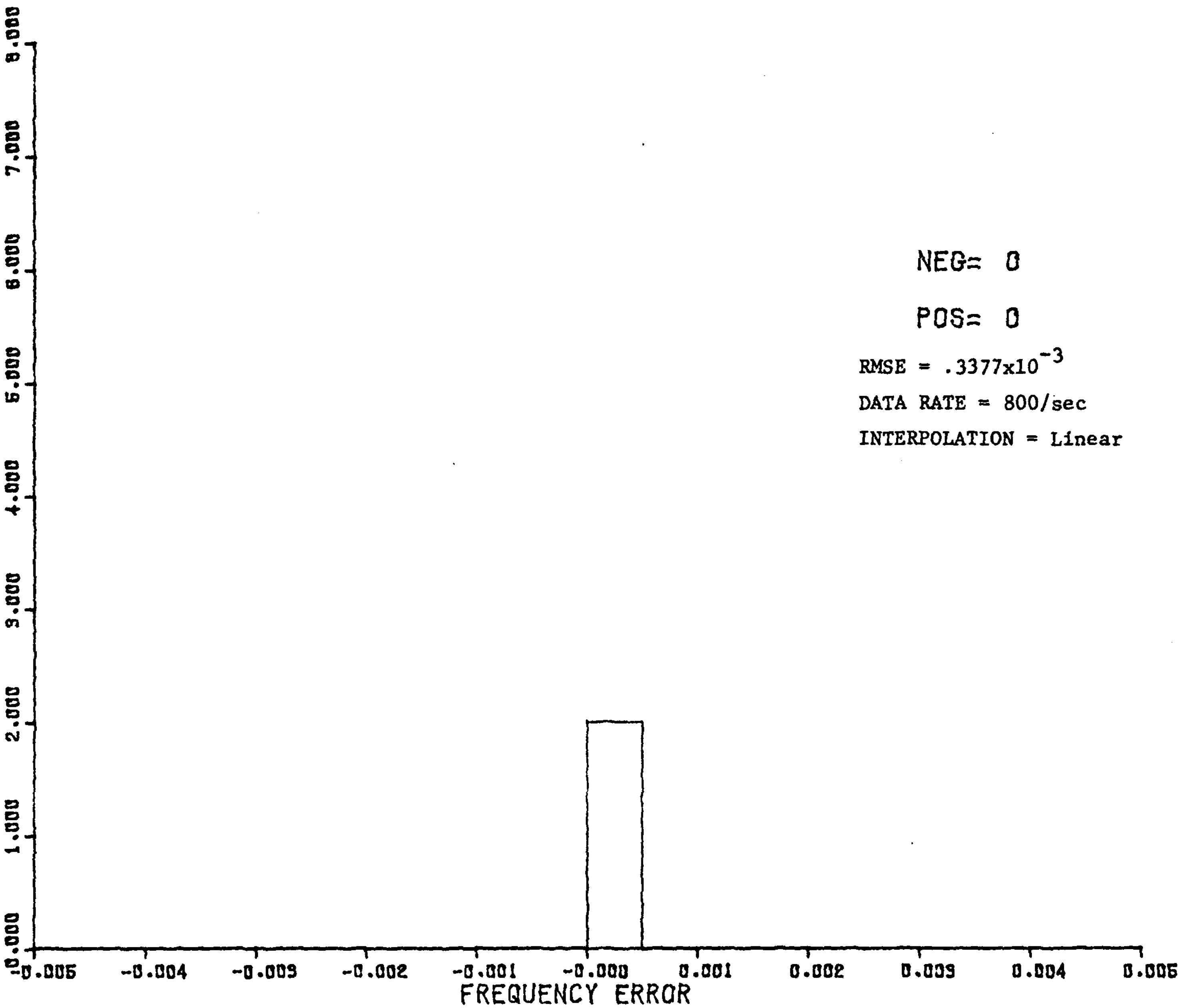

Figure H-4. Histograms of Error (Cont'd)
(g) Case IIB1.

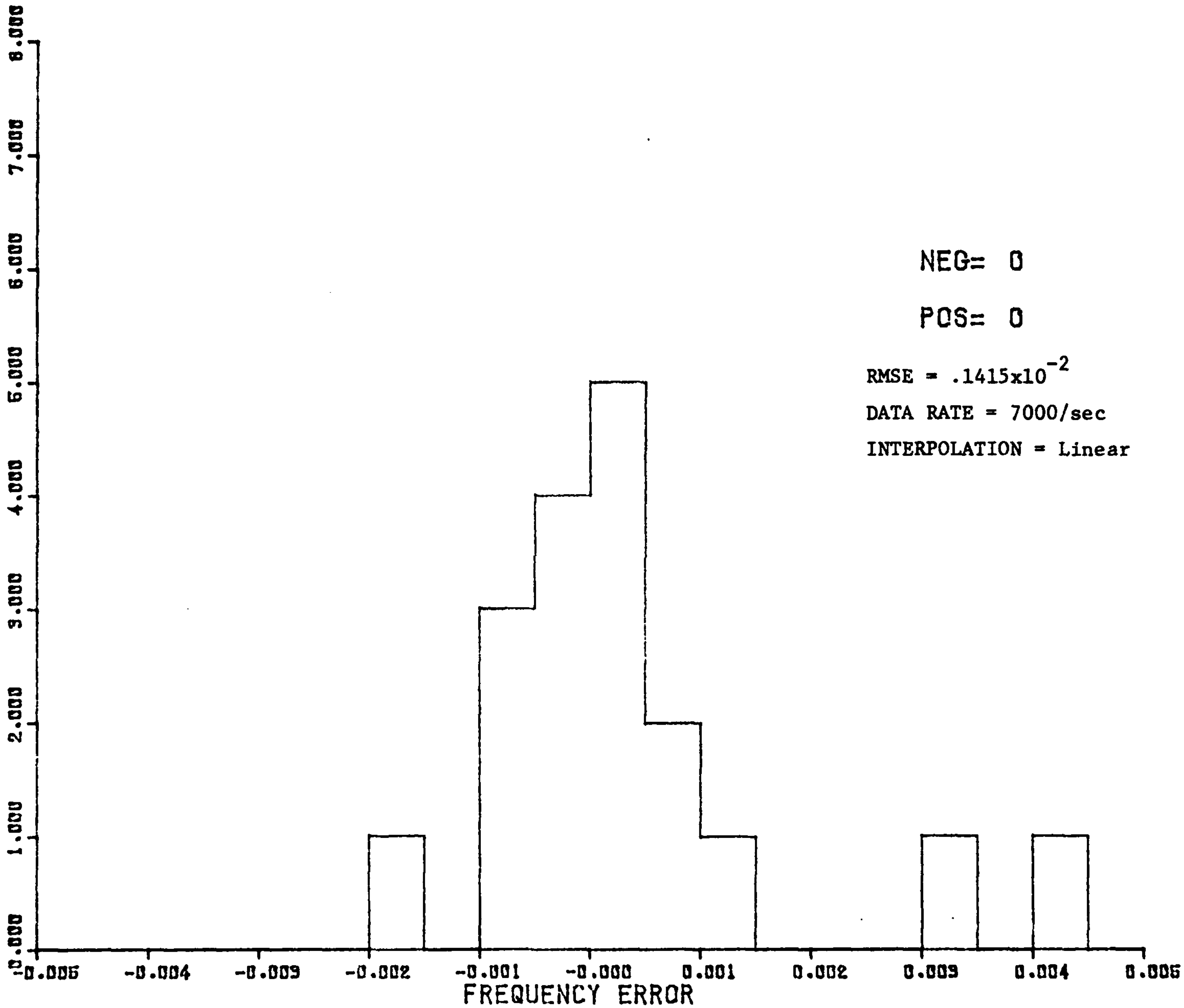

Figure H-4. Histograms of Error (Cont'd)
(h) Case IIB2.

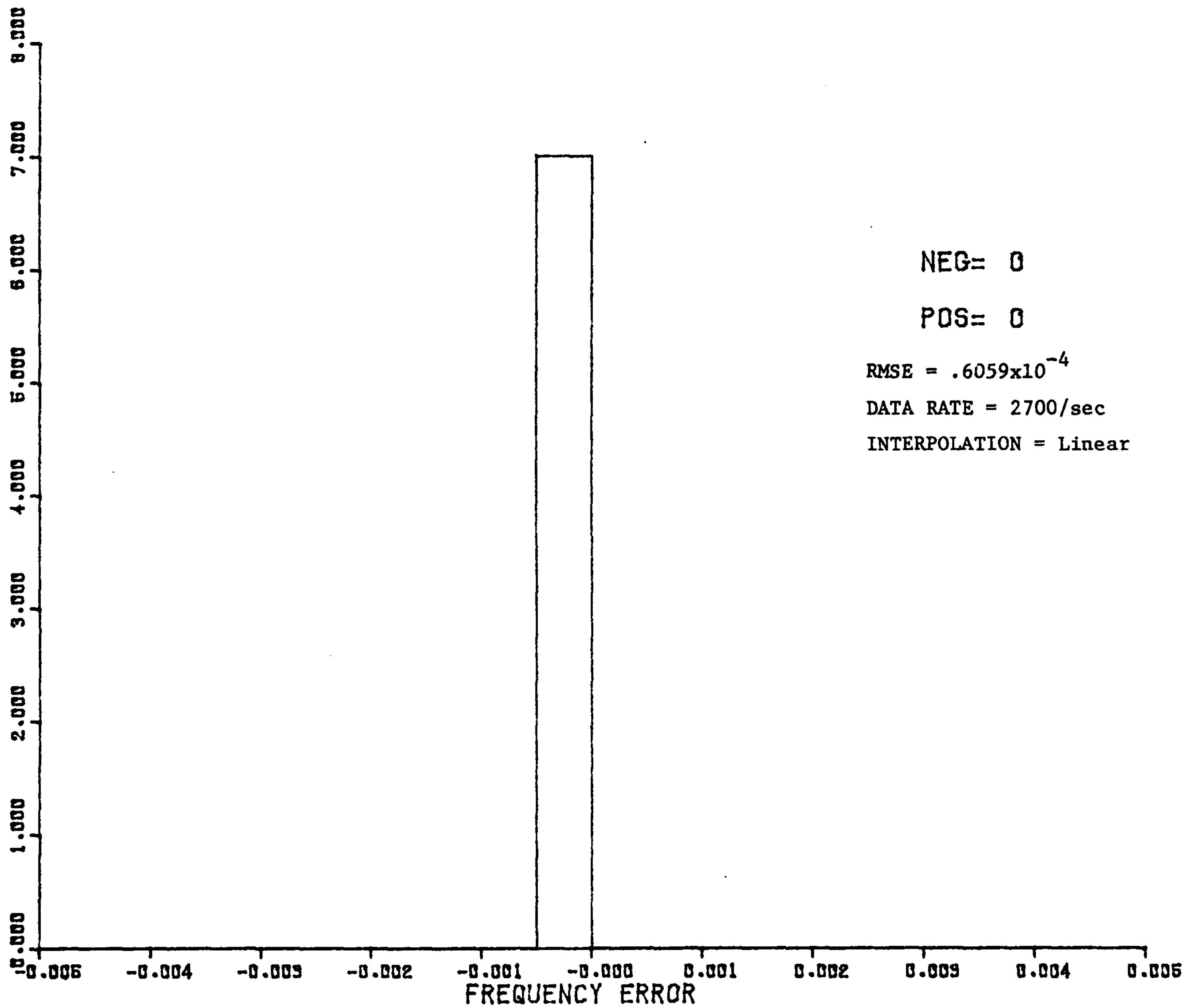

Figure H-4. Histograms of Error (Cont'd)
(i) Case IIA2 (Run 2).

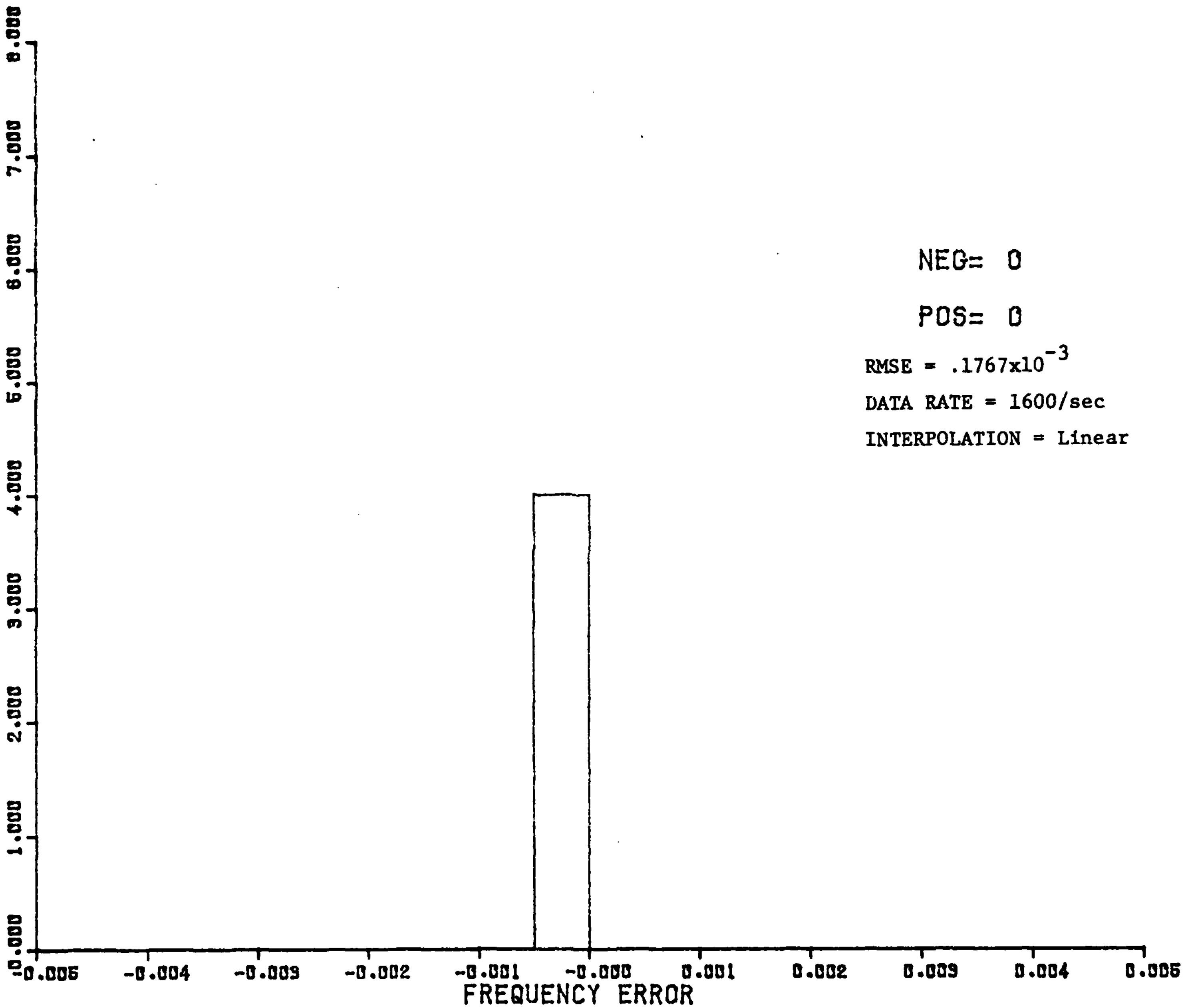

Figure H-4. Histograms of Error (Cont'd)
(j) Case IIB2 (Run 2).

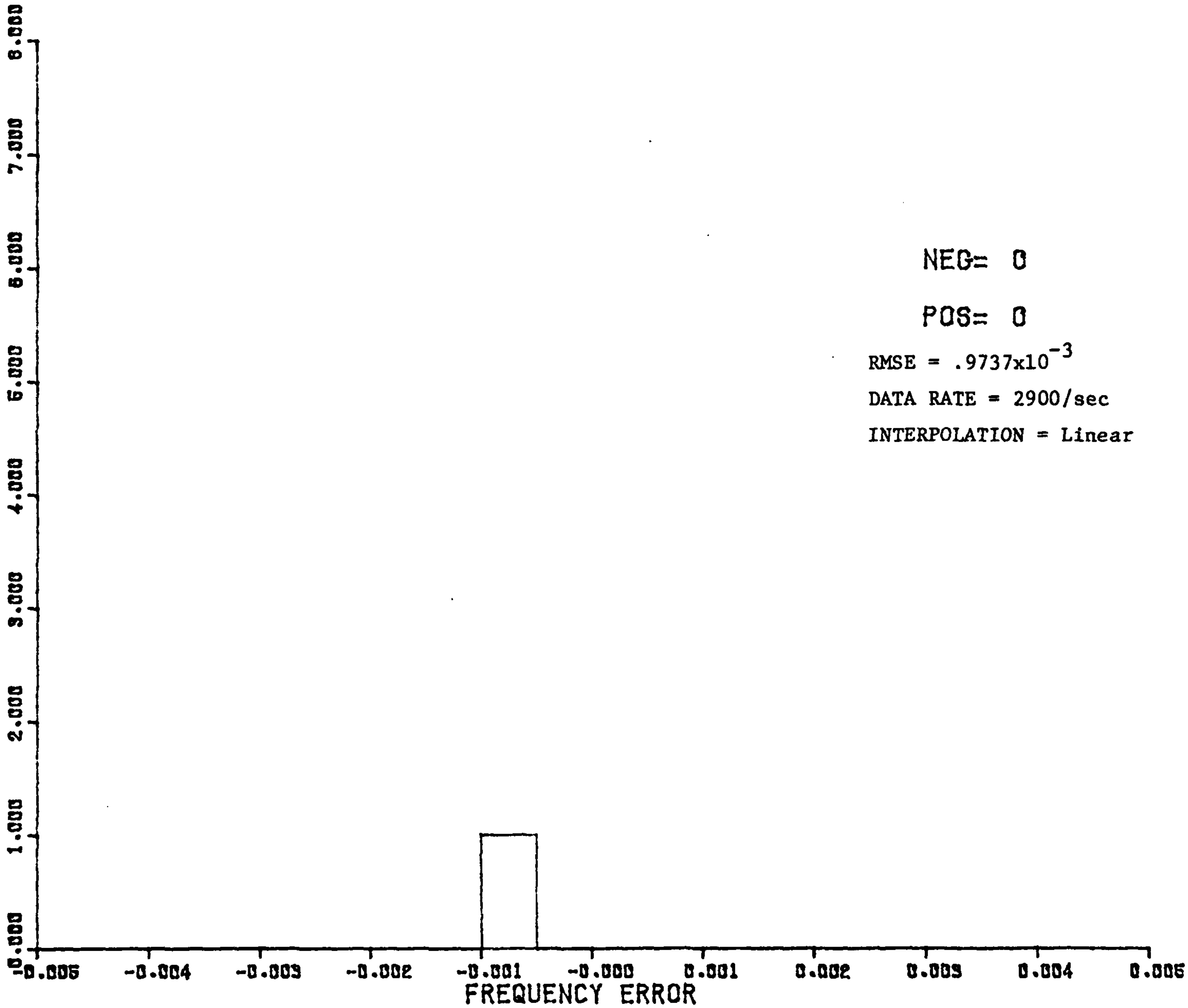

Figure H-4. Histograms of Error (Cont'd)
(k) Case IB2 (Run 2).

APPENDIX I

EXCERPTS FROM "PROPOSAL TO THE ADVANCED RESEARCH PROJECTS AGENCY FOR DEVELOPMENT OF A SYSTEM FOR INTERNAL WAVE MEASUREMENT," BY WILLIAM STACHNIK, 5 JANUARY 1977

FACILITIES AT NOSC AND SCRIPPS
PROVIDED BY DR. MIKE REICHMAN, NOSC, JUNE 8, 1977

NRL MTF EQUIPMENT
DR. VINCE DEL GROSSO
APRIL 13, 1977

Draft Proposal prepared by W. Stachnik, Submarine
Electro-Optical Systems Division of the
Naval Underwater Systems Center

PROPOSAL FOR PROVIDING INTERNAL WAVE MEASURING INSTRUMENTATION

Work prepared under Project Courageous has indicated that many of the basic requirements of the ARPA program are within reach. The primary cause for hesitancy in giving a more positive support of the approach lies in the optical propagation requirements necessary for high-accuracy velocity sensing.

Also important in the feasibility of the approach is the nature of individual particle backscatter and how widely different individual scattering functions will affect the Doppler signal.

If the above areas of critical concern were completely independent of the optical aperture size and optical speed, one would be inclined to place an LDV system into seawater as soon as possible and take note of the results. Unfortunately, such independence does not exist and results obtained with one configuration will not be readily transferred to the next.

The above argument does not consider whether the oceanic-particle scattering functions found are typical or what distributions of scattering functions are present.

This proposal is addressed to the ARPA goal of obtaining internal wave measuring instrumentation that is economical, effective and available within a two-year period, but obtaining these goals will require an investigation of the areas presented above and additional areas to be presented later.

NUSC wishes to contribute in a significant way to the expanded organization that will be necessary to carry out this task. As part of this contribution, NUSC offers its facilities, its experienced staff and the valuable associations that it has made with the technical-scientific community. The following material summarizes NUSC's resources. The two most important facilities are described below:

I. The AUTEC Test Range in the Bahamian Chain of Islands

This facility possesses clear ocean water whose optical properties are well documented—a result of the Deep-Look and Look-Sea programs. The facility also possesses a pleasant Mediterranean-like climate which allows year-round testing. Extensive shop, diving and communications facilities exist at AUTEC. These facilities have as one of their primary uses the support of torpedo programs such as the Mark 48. Significant in the later phases of this program will be the submarine traffic that exists there, for AUTEC is the acoustical test range and torpedo firing test range for the Atlantic-based Navy.

II. NUSC Oceanographic Van and Optical-Oceanographic Instrumentation.

This complex of equipment is capable of being fitted onto practically any ocean-going vessel. It can be transported by cargo plane, rail or truck to the port of departure. Since it is self-contained, the equipment does not suffer the usual consequences of repeated assembling and dismanteling. The full complement of equipment is listed in Appendix I, but the most significant features are the following:

- A twenty meter optical bench that provides high accuracy attenuation coefficient determinations.

- An onboard computer that calibrates equipment, processes and records data and allows computer codes to be generated as needed at sea.

Other contributions to be made to the ARPA program involve new instrumentation and techniques:

I. NUSC/TRIADIC Microstructure Measuring Instrumentation

Special microstructure instrumentation has been fabricated for NUSC by the TRIADIC Corporation. This instrumentation will provide both density and optical refractive index information besides giving the statistics of index variations. The unique aspects of this equipment is its ability to sense high frequency, small scale refractive phenomena.

II. Ocean Water Simulation and Quantification Equipment

Ocean water has many properties that affect system performance. It is, however, perishable. In order to execute significant tests of either system breadboard configurations or systems ready for sea-trials, reasonable simulations of seawater should be utilized and methods of checking the simulations available. This Laboratory has just completed three months of simulations and has developed both the techniques and instrumentation necessary.

The final contribution to point out is the staff available at NUSC. The author does not intend that individuals listed here replace those that have already made significant contributions to the ARPA program. It is merely a way of indicating, in a specific way, the staff we can draw upon for consultations when many specialized inputs are necessary.

A. Brooks/C. ... - consultants on natural seawater particulates (biologists)

P. Cable - consultant on internal wave behavior (physicist)

W. Huntley - LDV electronics (electrical engineer)

R. Randall - seawater simulations (physicist)

F. Replogle - hydrospheric propagation (physicist)

W. Stachnik - optical oceanography, propagation and systems (physicist)

The work performed by these individuals in previous and ongoing projects spans many important hydro-optical areas:

- Deep-Sea Optical Transmission
- Integrated Laser Beam Spread Analysis

- Correspondence of Point and Beam Spread Functions
- Underwater Viewing Systems
- LDV Analysis and Test
- Underwater Optical Communications
- Underwater Solar Light Measurement
- Deep-Sea Current Measurement
- Deep-Sea Nephelometer Measurements

The above material has intended to show the contributions that this Laboratory can make to the ARPA task. It is difficult to numerically express their value and be certain of the objectivity of the estimate but an estimate has been attempted in Appendix II, not because the resulting dollar figures have great significance, but that the topics listed serve to generate further discussion and more accurate assessments.

Program for Internal Wave Measurement (IWM)

The flow chart of the following page describes the major considerations in IWM development. The chart begins with areas already addressed in Project Courageous and indicates their fundamental applicability. The chart continues to show regions of overlap--where similar considerations are necessary in each pursuit, and where coordinated efforts can conserve sponsoring resources. The last region represents those areas that are unique to the ARPA work. This area of uniqueness may occur earlier in the chart than presently shown. The support for this point can be found in the SDL portion of this proposal.

Instrumentation Development Flow Chart

(Applicable to the measurement of small and large scale turbulent phenomena)

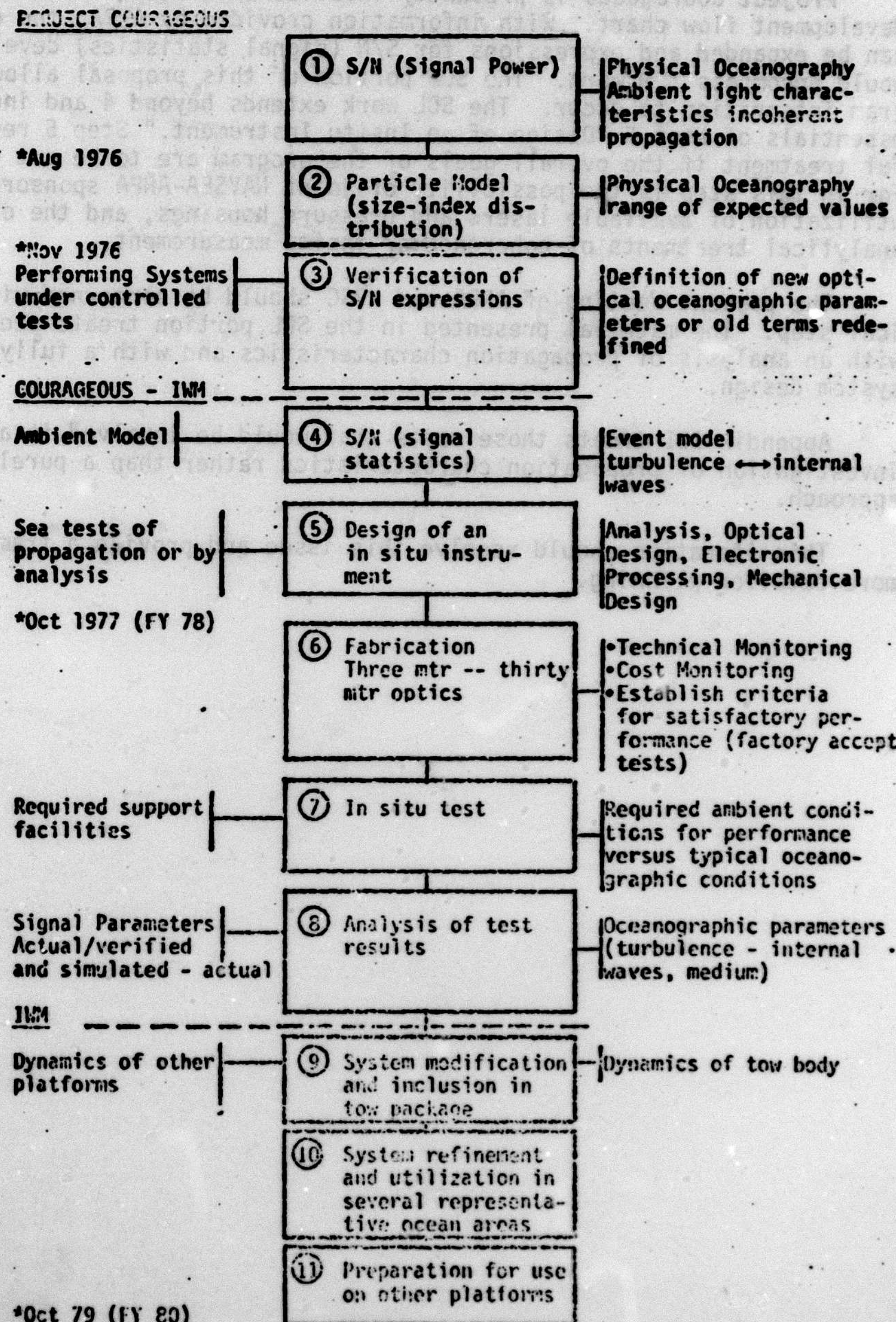

Program for Fiscal 77 (1 Jan 1977 - 1 Oct 1977)

Project Courageous is presently involved with steps 3 and 4 on the development flow chart. With information provided by ARPA, the event model can be expanded and expressions for S/N (signal statistics) developed that would encompass IMM work. The SDL portion of this proposal allows this program integration to occur. The SDL work extends beyond 4 and includes the essentials of step 5 "Design of an Insitu Instrument." Step 5 requires careful treatment if the overall goals of the program are to be met economically. For in this step is the possibility of joint NAVSEA-ARPA sponsorship, the utilization of available lasers and pressure housings, and the choice between analytical treatments of coherence or insitu measurement.

The present meeting of ARPA and NUSC should be concerned with this critical step. The material presented in the SDL portion treats steps 4 and 5 with an analysis of propagation characteristics and with a fully analyzed system design.

Appendix III treats those costs that would be involved in a sea-test investigation of propagation characteristics rather than a purely analytical approach.

This iteration should resolve this issue and provide a framework for more detailed planning.

APPENDIX I

NUSC Optical-Oceanographic Equipment

- 20 Meter Optical Bench
- 20 Meter Transmissometer
- Image Orthicon Underwater Television System
- Spectra Pritchart Underwater Photometer
- RCA LD2101 Underwater Laser System
- 100 Watt CW Argon-Ion Laser
- Salinometer/Quartz Thermometer
- Current Speed and Direction System
- Pulsed Insitu Absorption Meter
- Marine Illuminance Meter
- M-225 Cine Camera
- 200 mm Data Camera
- 50 Gallon Clean Water Tank
- 550 Gallon Clean Water Tank
- 1000 Ft Cable Winches
- Cintra Radiometers
- Underwater Light Sources (Thallium Iodide)
- Spectraphysics 5 Watt Underwater Laser System
- Lensless Camera/Vidicon System
- ITF Meter
- On-Line Data Processing Computer
- Relative Irradiance Meter

APPENDIX II

Evaluation of Facilities

AUTEC	
Prior quantification of water parameters	>50k
Facilities adjacent to clear ocean water (save in transit time)	>20k
Facilities allowing heavy machine work to be performed	≥10k
	>80k
NUSC Oceanographic Van	
Development of 20 meter optical bench	100k
Development of ITF instrumentation	200k
Lensless Camera/Vidicon Camera	50k
Oceanographic instrumentation (abs temp, salinity, current speed, direction, bench depth, etc.)	100k
Oceanographic van (Incl. computer, HF radio communication, oscilloscope complement, etc	500k
	950k
Microstructure Instrumentation	
Purchase Cost	14k
Staff experience with ocean-optical measurements with respect to Laser Doppler Velocimetry	138k

Previous Staff Active Experience in Ocean Optics

2. W. Huntley - 1 year
3. R. Polley - 15 years
4. R. Randall - 2 years
5. F. Replogle - 20 years
6. W. Stachnik - 12 years
7. M. Green - 5 years

Additional Notes on NOSC Facilities

Dr. Mike Reichman, NOSC, June 8, 1977

HYDROMECHANICS LAB

- Water Tunnel (see brochure) (omitted from report)
  - standard, variable-speed flow, well-characterized
  - LDA side-by-side with hot film probe measurements
  - could use approximately 1 meter for propagation/accuracy experiments
  - controlled particulate

- LDA
  - TSI Series 900 with accompanying Model 1076 True RMS voltmeter
  - 15 mw laser, Bragg cell
  - Optics for 100, 250, 600, 1000 mm forward/back scatter
  - complete traversing capability, resolution to 0.001"

- Static Tank
  - 5' x 8' by 6' high visualization tank
  - optical grade plexiglas sides
  - develop circulating cell for low velocity environment
  - can filter and reseed
  - best for basic propagation experiments

- Accessory Equipment
  - Nicolett 444A spectrum analyzer w/Tektronix digital plotter

- Cost
  - funded research or $200/day minimum (single person, no materials) to outside contractor on a not-to-interfer basis

NOSC OCEANOGRAPHIC RESEARCH TOWER (See brochure) (omitted from report)

- Site has fundamental instrumentation, then equipped specially for each experiment either by user or NOSC
  - concurrent thermistor array measurements with
    - (i) 100 channel data lagger or
    - (ii) computer controlled data logging w/plotting and/or conversion capability

- Large boom to be installed in approximately 1 month, will handle 6000 lbs.
- Tower moves a bit with the ocean swell, amount is to be measured in July 77, could continue to do same
- Two type packages could be used
  - (i) dipped, free falling from boom
  - (ii) track mounted, can clamp for rigidity
- Easy access, 1 boat/day, from Mission Beach
- Can accommodate 6 people overnight for long term measurement
- Scheduling
  - 15 people can be handled nicely
  - can always work things in, at least short tasks

- Cost
  - minimum of $400/day
  - somewhat dependent on operation

FLIP (See brochure) (omitted from report)

- Scripps-owned
  - *expensive if not "piggy-back" experiments*
- General character
  - 4 cm heave in 4-5' waves
  - < 1 m heave in 30' waves
  - 27 second natural period
  - boom capability of 700 lbs., 60 ft. long, many other booms available

RELEVANT NOSC CAPABILITY

- Instrumentation Group
  - start-to-finish instrumentation support
  - computer aided data collection/analysis. (HP-2100)

- Deep-Sea Package Design
  - multitude of submerged packages (CURV, MNV, RUWS, etc.)
  - cable handling requirements well known

- Electro Optics Expertise
  - BAYSIDE (Formerly NUC)
  - specialized in ocean operation

- have current experiments in
  - (i) bottom viewing/mapping
  - (ii) laser propagation
- limited laboratory capability

—— TOPSIDE (Formerly NELC) ——

- underwater optics as applied to communications
- completely equipped lab (lasers, optics, ass't. hardware)
- have done at-sea experiments

• Extensive Ocean Data Base Available
  - gathered as portion of biological studies and underwater vehicle technologies programs.

MISCELLANEOUS

• Inertial Navigation Package, LTN 51 (Litton Industries)
  - suitable accuracy for motion compensation measurements, .007^{o}/hr
  - on hand, at Scripps, available for loan
  - needs recalibration, $10K approximately, Litton unofficial quote
  - special 110 vac, 400 Hz power supply available

NRL MTF EQUIPMENT
APRIL 13, 1977

This appendix includes three selected pages from a 1975 paper by Vincent Del Grosso of NRL. The paper describes laboratory MTF equipment with reported sensitivity of 25 microradians (1/(40,000 lines per radian)).

Dr. Del Grosso is presently preparing ocean-going equipment for October 1977 with a path length of 1 meter. The new equipment is planned to perform scans at a rate of 1 per 0.2 sec. with a possible resolution of up to 1,000,000 cycles per radian*. No reports were available as of Dr. Mayo's visit with Dr. Del Grosso on April 13, 1977.

---

* Present lab model is still 40,000 lines/radian. The figure of 1 microradian resolution was "possible" but not planned.

Reprinted from Vol. 64—Ocean Optics.
Palos Verdes Estates, California 90274 USA

MODULATION TRANSFER FUNCTION OF WATER

V. A. Del Grosso

Naval Research Laboratory
Washington, D.C. 20375

Abstract

Particulate matter of the sizes, concentrations, and refractive indices found in situ renders the Optical Transfer Function of water a real quantity. Modulation Transfer Function (MTF) is measured in vitro by spatial filtering of the projected image of a slit in the Fourier Transform plane. Analysis is by Moire' fringes with a smooth and continuous variation of spatial frequency (nominally 0-40,000 cycles/radian) obtained by counter-rotating Ronchi rulings. The analogue of convolution of impulse responses is tested as the cascadability in a scattering medium of true sinusoidal MTF's. Coulter Counter techniques are used to measure differential particulate count in 15 channels up to 100 μm. Experimental data for various ranges and particle distributions are compared to theoretical predictions based on volume scattering functions (VSF) obtained by Mie scattering calculations and the Fourier transform conversion relating MTF and VSF first obtained by Willard Wells. The equipment is being repackaged for in-situ measurements to accompany forthcoming flood-illuminated SEGAIP (SELF GATED IN-WATER PHOTOGRAPHY) trials.

Introduction

Before heroic[1,2] measures may be justified to pass the primary limit[3-6] of backscatter for artificially illuminated in-water optical viewing systems, adequate knowledge of the ultimate limit[7] attributable to the image degradation and accompanying photon loss of small angle forward scattering is essential. Since adequate pictures[8-10] have been obtained at a 20 m range over a 90 degree field by the LIBEC or light behind the camera technique, determination of the image carrying ability of water is the obvious task before investing in expensive schemes to increase range and/or coverage. And the most satisfactory specification of this image transmission ability is via the Optical Transfer Function (OTF)[11].

This concept of the sinusoidal response derivable as the Fourier transform of an impulse response or spread function requires isoplanatism or stationarity as well as linear superposition or linearity. The first condition is not met in turbulent conditions so familiar to astronomers but will be shown to hold for scattering from particulate matter. The second condition is met by most optical systems and will similarly be shown satisfied by in-water imaging with suspended particles. It will further be shown that, following the precepts of Mie scattering theory, the intensity is the linear parameter for the resultant non-coherent process. This is fortuitous since the cascadability[12] of individual OTF's applies only if there are no intermediate partial coherence effects.

Even for initially coherent waves, non-coherent imaging is the result since we are in the far field of a scatterer where the scattering cross-section holds and power is added irrespective of phase for this random interference of a large number of waves of random phase from many particles.

Optical Transfer Function

A blurred image g(x, y) is formed by the convolution of the object f(x, y) with the spread function h(x, y) as

$$g(x', y') = \iint_{-\infty}^{\infty} f(x, y) h(x' - x, y' - y)\, dx dy$$

or

$$g = f * h$$

which in the spatial Fourier transform domain becomes

$$G(u, v) = F(u, v) H(u, v)$$

as a (usually) complex function of the spatial frequencies u, v and where

$$F(u, v) = \iint_{-\infty}^{\infty} f(x, y) \exp\left[2\pi i(ux + vy)\right] dx dy.$$

The transfer function is the Fourier transform of the spread function as

$$H(u, v) = \iint h(x, y) \exp\left[-i(ux + vy)\right] dx dy$$

and also the autocorrelation of the pupil function f(s, t) as wave gratings that are more easily and accurately made. The original three bar targets were soon increased to 15 or so to permit establishment of a steady state frequency for each pattern at a constant scan velocity. Usually 10 or so such patterns were employed. It was originally believed that the resultant square wave response had to be converted to the pertinent sine wave response by calculation[18], but it was soon realized that the sinusoidal response could more easily be obtained by electronic filtering[19].

Apart from these direct instruments yielding MTF's at discrete frequencies there are two continuous frequency devices available. One[20] employs a radial grating and crossed slits moved along a radius to vary frequency at constant rotation, while the other[21] employs crossed Ronchi rulings rotated at varying speed to produce Moire fringes aligned with a projected slit. This latter not only passes more illumination from a given source, and utilizes a larger aperture, but results in a triangular pattern more easily filtered to sinusoidal response[22]. The rationale of measurement is that a Fourier transform is performed on the spread function by imaging the slit object onto the Moire pattern. The frequency of the pattern is made to vary linearly with time by driving the counterrotating Ronchi rulings with a sine-cosine motor such that the sine of the angle between them is proportional to time. The imaging is done through an objective lens confocal with a microscope objective. The line spread function of the water is represented by the intensity distribution across the image of the slit scanned by the analyzer. A photomultiplier collects the transmitted light and, after suitable filtering to obtain sine wave response, produces an ac signal whose time base is proportional to the spatial frequency and whose amplitude is proportional to the integral of the product of the line spread function and the sine wave of varying spatial frequency which is the MTF. In its fast mode a scan is completed in 0.2 sec, repeated every three seconds, and displayed on an oscilloscope. A slow mode for x-y plotting requires 3 minutes/scan.

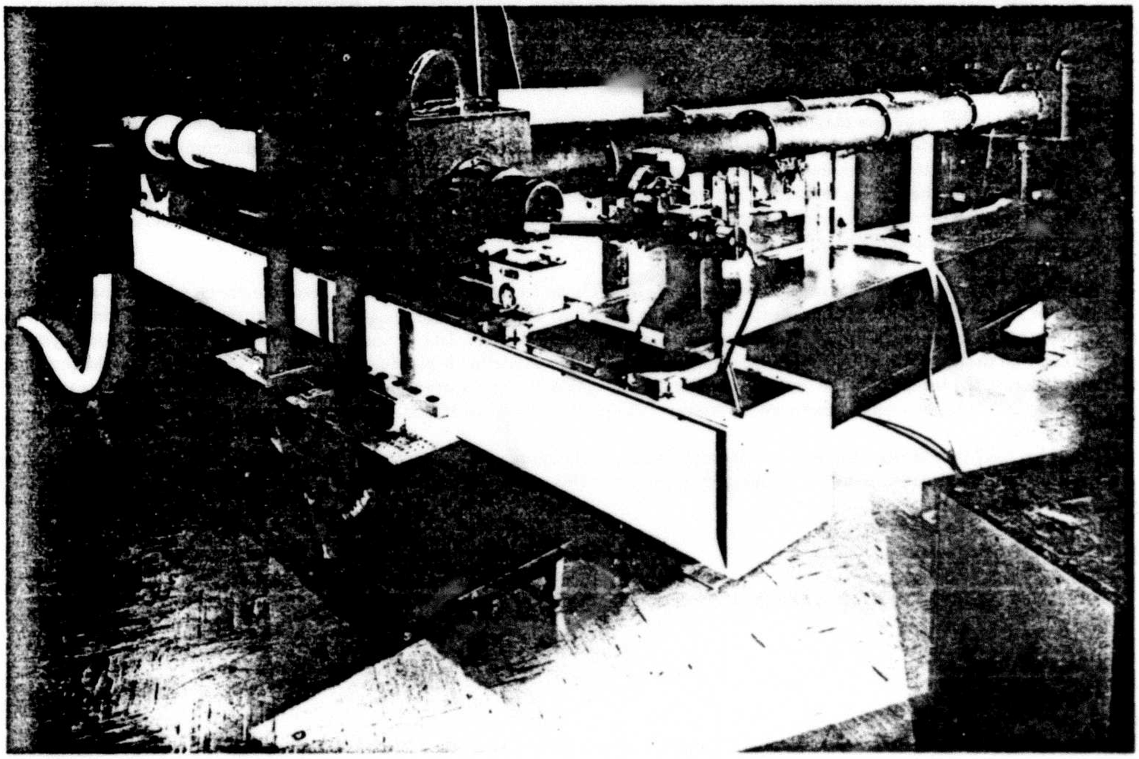

Fig. 1. Laboratory Set-up for Measurement of MTF of Water.

The equipment is shown in Fig. 1. Basically there is an optical bench 3.6 m long, carrying the analyzer to the right consisting of microscope objective, rotating Ronchi rulings, temporal wavelength filter (all measurements were made in a 30 nm band centered at 480 nm) and photomultiplier. To the left of this assembly is the imaging or decollimating lens which in large part determines the MTF of the system. Basically we are measuring the MTF of this lens and noting how the response is modified by various water paths. The total response divided by the system response is the MTF of the water path if cascadability holds—and of course this may be checked for various path lengths or ranges to determine whether the MTF of water is itself cascadable. Proceeding to the left on the optical bench there is next a black-teflon lined tank with optical windows adjustable to perpendicularity with the axis of the optical bench. The direct light path between these windows is 1 m. Finally, working backwards through the basic system there is an 230 cm long, 4" diameter collimator which is used to project the image of a 4 μm slit illuminated through opal glass and a condenser system by a 250 w tungsten halogen quartz lamp in a dichroic-coated elliptical reflector (EMM-EKS). This lamp is operated from a stabilized supply. The large hose is used for cooling the lamp while at the same time minimizing vibrations. The optical bench plus the entire water path is mounted on a 6 m long vibration isolated table. Another 1 m tank is located at the other end of the table and joined to the first tank by 8" diameter black-teflon lined tubes. These tubes are in 1 meter and half-meter lengths permitting ranges from 1 to 11 meters in 1 m steps. Four mirrors are used to properly direct the collimated beam and baffles are inserted in the tubes at strategic locations to minimize wall reflections. The projecting collimator has been auto-collimated at 480 nm and the physical location of the 30 cm decollimator is optimized for maximum system response at the same temporal wavelength.

by the pre-calculations the dominance of the larger particle sizes on narrow angle scattering and MTF is corroborated. And, although not demonstrated here, the VSF at very small angles is calculable from the experimental MTF. In the pre-calculations VSF was calculated for each particle distribution and number density first, then transformed to MTF, and then inverse transformed back to VSF with excellent agreement for angles between 0 and 0.05 radians and good agreement to 0.1 radians.

References

1. Heckman, Jr., P. J., "Underwater Range Gated Photography," SPIE Underwater Photo-Optics Seminar Proceedings, Santa Barbara, CA, Oct. 1966.

2. Angelbeck, A. W., "Application of a Laser Scanning and Imaging System to Underwater Viewing," SPIE Underwater Photo-Optics Seminar Proceedings, Santa Barbara, CA, Oct. 1966.

3. Mertens, L. E., In-Water Photography—Theory and Practice, Wiley-Interscience, John Wiley and Sons, N.Y., 1970.

4. Duntley, S. Q., "Light in the Sea," Jour. Opt. Soc. Amer. 53, 214 (1963).

5. Duntley, S. Q., "Underwater Visibility and Photography," in: Optical Aspects of Oceanography, Jerlov, N.G., and E. S. Nielsen, Eds., Academic Press, N.Y., 1974.

6. Duntley, S. Q., "Principles of Underwater Lighting," SPIE Underwater Photo-Optics Seminar Proceedings, Santa Barbara, CA, Oct. 1966.

7. Wells, W. H., "Loss of Resolution in Water as a Result of Multiple Small-Angle Scattering," Jour. Opt. Soc. Amer. 59, 686 (1969).

8. Brundage, W. L., "Large Scale Photographs from the Rift Valley in the Project FAMOUS Area," Proceedings of the Geol. Soc. of Amer., Abstracts with Programs, 6, No. 7, 761 (Oct. 1974).

9. Ballard, R. D., "Photography from a Submersible During Project "FAMOUS" Oceanus 18, 31 (1975).

10. Phillips, J. D.; Fleming, H. S.; and Brundage, W. L., "Multi Narrow-Beam Array Sonar and Large Area Photography in the Mid-Atlantic Ridge Median Valley 36° N," Int. Assoc. for the Phys. Sci. of the Ocean (IAPSO) General Assembly Symposium Proceedings, Aug. 1975 (preprint).

11. Barnes, K. R., The Optical Transfer Function, American Elsevier Pub. Co., Inc., N.Y., 1971.

12. DeVelis, J. B., and Parrent, G. B., Jr., "Transfer Functions for Cascaded Optical Systems," Jour. Opt. Soc. Amer. 59, (1967).

13. Moore, R., and Slaymaker, F. H., "Comparison of OTF Data Obtained from Edge Scan and Interferometric Measurements," SPIE Image Assessment and Specification Seminar Proceedings, Rochester, N.Y., May 1974.

14. Funk, C. J., "Multiple Scattering Calculations of Light Propagation in Ocean Water," Applied Optics 2, 301 (1973).

15. Yura, H. T., "Small-Angle Scattering of Light by Ocean Water," Applied Optics 10, (1971).

16. Arnush, D., "Underwater Light-Beam Propagation in the Small-Angle Scattering Approximation," Jour. Opt. Soc. Amer. 62, 1109 (1972).

17. Optical Society of America. Topical Meeting on Optical Propagation Through Turbulence; University of Colorado, Boulder, Co., July 9-11, 1974.

18. Coltman, J. W., "The Specification of Imaging Properties by Response to a Sine Wave Input," Jour. Opt. Soc. Amer. 44, 468 (1954).

19. Murata, K., in: Progress in Optics 5, E. Wolf, Ed., N. Holland Pub. Co., Amsterdam, 1966.

20. Rosenbruch, K. J., "Trends in the Development of OTF Measuring Equipments," SPIE Image Assessment and Specification Seminar Proceedings, Rochester, N.Y., May 1974.

21. Bouma, J. A., "Improvement in MTF-Measurement of I.I. Systems," SPIE Image Assessment and Specification Seminar Proceedings, Rochester, N.Y., May 1974.

22. Debergerová, L. and Daberger, J., "Some Experience with the Use of a Moiré Test Pattern in the Measurement of the Optical Transfer Function," SPIE Image Assessment and Specification Seminar Proceedings, Rochester, N.Y., May 1974.

23. Jerlov, N. G., Optical Oceanography, Elsevier Pub. Co., N.Y., 1968.

24. Van de Hulst, H. C., Light Scattering by Small Particles, John Wiley & Sons, Inc., N.Y., 1957.

25. Bader, H., "The Hyperbolic Distribution of Particle Sizes," Jour. Geophys. Res., 75, 2822 (1970).

26. Kullenberg, G., "Observed and Computed Scattering Functions," in: Optical Aspects of Oceanography, Jerlov, N. G., and Nielsen, E. S., Eds., Academic Press, N.Y., 1974.

27. Cited in Ref. 26.

28. Ochakovsky, Y. E., "On the Dependence of the Total Attenuation Coefficient Upon Suspension in the Sea," U.S. Dept. Commerce, Joint Publ. Res. Ser. Report 36, 16 (1966).

29. Cited in Ref. 26.

30. Morel, A., "Optical Properties of Pure Water and Pure Sea Water," in: Optical Aspects of Oceanography, Jerlov, N. G. and Nielsen, E. S. Eds., Academic Press, N.Y., 1974.